



The Faculty of Engineering  
Department of Architecture and the Built Environment  
*Institute of Building Technology*  
*Institute of Sustainable Energy Technology*

# *Investigations of Novel Heat Pump Systems for Low Carbon Homes*

By

**Blaise Mempouo**

*M Sc (Hon) Renewable Energy*  
*B Eng (Hon) Mechanical Engineering*

*Thesis submitted to the University of Nottingham For the degree of Doctor of Philosophy*

**January 2011**

# Contents

List of Tables .....	xvi
Nomenclature .....	xviii
Abstract .....	xxii
Published Papers as a Result of the PhD Project .....	xxiv
Acknowledgements .....	xxv
<b>CHAPTER 1 - INTRODUCTION .....</b>	<b>1</b>
1. Introduction.....	2
1.1 Statement of the problems .....	2
1.2 Objective and scope of the project.....	6
1.2.1 Scopes .....	7
1.3 Novelty and timeliness of the project .....	8
1.4 Methodology approach: .....	10
1.5 Structure of the thesis: .....	11
<b>CHAPTER 2 - BACKGROUND AND OVERVIEW OF HEAT PUMP AND PERFORMANCES.....</b>	<b>16</b>
2. Background of the research .....	17
2.1 Climate Change, Global Warming and Domestic Energy Consumption.....	17
2.2 Carbon Footprint.....	19
2.3 Patterns of energy consumption in building .....	22
2.4 Energy Performance Certificates .....	23
2.5 The Code for Sustainable Homes .....	24
2.6 Technology/fuels to provide space and/or water heating for residential buildings .....	27
2.7 Overview of the Heat Pump and Performances .....	31
2.7.1 Heat pump.....	31
2.7.2 Classification of heat pump technology.....	32
2.7.3 Heat source for heat pump .....	33

2.7.4	Heat pump theory.....	38
2.7.5	Ideal Vapor-Compression Cycle.....	39
2.7.6	Heat pumps' working fluids.....	42
2.7.6.1	The impact of the working fluids .....	42
2.7.6.2	Side 1: Primary Refrigerant.....	44
2.7.6.3	Side 2: secondary refrigerants, water or water/antifreeze .....	46
2.8	Coefficient Of Performance (COP) .....	46
2.8.1	Carnot heat pump COP:.....	46
2.8.2	The effectiveness of a heat pump : .....	49
2.8.3	Primary energy ratio (PER) .....	49
2.8.4	Seasonal performance factor (SPF) .....	50
2.9	Factors affecting heat pumps' performances .....	51
2.9.1	Factors Affecting the COP of Air Source Heat Pumps.....	51
2.9.1.1	Effect of defrost cycle.....	51
2.9.1.2	Losses due to starting and stopping .....	52
2.9.1.3	Losses at part load.....	52
2.9.1.4	Heat exchanger between condenser and evaporator .....	52
2.9.1.5	Vapour density / volumetric capacity .....	53
2.9.1.6	Seasonal temperatures - variability with external temperature....	53
2.9.1.7	Mixture of refrigerant fluids .....	53
2.9.1.8	Effect of maximum temperature (tests with different temperatures)	53
2.9.1.9	Effect of vapour at the entrance to the evaporator .....	54
2.9.1.10	Motor efficiency of the heat pump.....	54
2.9.2	Factors Affecting the COP of Ground Source Heat Pumps.....	54
	Conclusion - Chapter 2 .....	61
	<b>CHAPTER 3 - LITERATURE REVIEW .....</b>	<b>65</b>
3.	Overview of past works to improve COP of Heat Pump Systems .....	66
3.1	Past work on Technologies to Improve the COP of ASHP .....	66

3.2	Past work on technologies to improve the COP of GSHP.....	76
3.2.1.1	Ground heat exchangers.....	78
	Conclusion - Chapter 3 .....	81

**CHAPTER 4 - NUMERICAL AND EXPERIMENTAL ANALYSIS ON THE PERFORMANCES OF A NOVEL DIRECT EXPANSION SOLAR HEAT PUMP (DX-SHP)..... 84**

4	INTRODUCTION.....	85
4.1	DX-SHP System Description.....	85
4.2	Equipments and Instrumentation .....	87
4.2.1	Experimentation heat source.....	88
4.2.2	Solar collector (evaporator) .....	88
4.2.3	Compressor .....	90
4.2.4	Condenser ( <i>flat plate heat exchanger</i> ).....	91
4.2.5	Thermostatic Expansion Valve (TXV) .....	92
4.3	Mathematical Model and Simulation of the DX-SHP System.....	95
4.3.1	Assumptions.....	95
4.3.2	EES Software.....	96
4.3.3	Unglazed Solar Collector/evaporator Model: .....	97
4.3.4	Compressor Model:.....	103
4.3.5	Condenser Model:.....	104
4.4	Analytical Results of the DX-SHP: .....	106
4.4.1	The effect of the collector/evaporator and condenser temperatures on the Heat pump COP.....	107
4.4.2	The effect of the collector/evaporator and condenser temperatures on the compressor power consumption .....	108
4.4.3	The effect of the collector/evaporator and condenser temperatures on the heat gain at the condenser .....	109
4.4.4	The effect of the collector/evaporator Area on the COP of the heat pump..	110
4.4.5	The effect of the pitch between refrigerant's serpentine tubes of the collector/evaporator on the COP of the heat pump .....	111

4.4.6	The effect of the diameter of the refrigerant's tubes of the collector/evaporator on the COP of the heat pump .....	112
4.5	Experimental Study of the DX-SHP System .....	113
4.5.1	Methodology .....	113
4.5.2	Experimental Procedure.....	113
4.5.3	Experimental set-up .....	116
4.5.4	Data acquisition and Processing System.....	117
4.5.5	Experimental uncertainty .....	118
4.5.6	Measuring Equipments .....	120
4.5.6.1	Measuring the Temperatures, solar radiation and relative humidity.....	120
4.5.6.2	Measuring the Pressures .....	122
4.5.6.3	Measuring ambient temperature and relative humidity .....	123
4.5.6.4	Measuring water mass flow rate .....	123
4.5.6.5	Measuring the compressor power consumption.....	124
4.5.6.6	Second temperatures control.....	124
4.5.6.7	Measuring the simulated solar radiation .....	125
4.6	Analysis .....	125
4.7	Experimental results and discussion .....	126
4.7.1	Performance investigation of DX-SHP at solar radiation of 200W/m <sup>2</sup> .....	127
4.7.2	Performance investigation of DX-SHP at solar radiation of 400W/m <sup>2</sup> .....	130
4.7.3	Performance investigation of DX-SHP at solar radiation of 600W/m <sup>2</sup> .....	133
4.7.4	Performance investigation of DX-SHP at solar radiation of 800W/m <sup>2</sup> .....	136
4.8	Theoretical results Vs Experimental results: .....	140
4.8.1	The effectiveness of the DX-STSHP: .....	144
4.9	Conclusion - Chapter 4 .....	145
4.10	Further Works .....	146
4.10.1	DX-Solar roof Heat Pump .....	146

**CHAPTER 5 - NUMERICAL AND EXPERIMENTAL ANALYSIS ON PERFORMANCE OF A NOVEL DIRECT- EXPANSION PHOTOVOLTAIC/HEAT-PIPE - HEAT PUMP SYSTEM..... 149**

5.	INTRODUCTION .....	150
----	--------------------	-----

5.1	Brief background of this work .....	150
5.2	PV/hp-HP system description .....	153
5.1	Mathematical model and simulation of the DX-PV/hp-HP system .....	156
5.1.1	EES Software .....	157
5.1.2	PV/hp evaporator Models .....	157
5.1.2.1	Vacuum glass tube model .....	157
5.1.2.2	PV module model .....	159
5.1.2.3	Aluminium sheet model .....	160
5.1.2.4	Refrigerant's Copper tube model .....	161
5.1.2.5	Refrigerant in the panel model .....	162
5.1.3	Compressor model .....	162
5.1.4	Expansion valve model .....	163
5.1.5	Condenser model .....	163
5.1.6	Coefficient of performance (COP) .....	164
5.2	Numerical results and discussion .....	165
5.2.2	Solar radiation and ambient temperature .....	165
5.2.3	Temperatures at different layers .....	166
5.2.4	Thermal performance of PV/hp evaporator .....	167
5.2.5	Electrical performance of PV evaporator .....	168
5.2.6	COP and condenser capacity .....	169
5.3	Preliminary experimental study of the DX-STC/HP system .....	170
5.3.1	Methodology .....	170
5.3.2	Layout of the testing rig set-up .....	171
5.3.3	Equipments and Instrumentation .....	173
5.3.3.1	Solar collector (evaporator) .....	173
5.3.7.1	Compressor .....	174
5.3.8	Condenser (flat plate heat exchanger) .....	174
5.3.9	Thermostatic Expansion Valve (TXV) .....	175
5.3.10	Experimental Procedure .....	177
5.3.11	Data acquisition and processing system .....	178
5.4	Preliminary experimental results and discussion .....	179
5.5	Conclusion - Chapter 5 .....	181
5.6	Further Works .....	183
5.6.1	Propose research on PV/hp roof modules .....	183

**CHAPTER 6 - SMALL SCALE TESTING OF A NOVEL SOLAR ROOF/COLLECTORS ASSISTED QUICK RECOVERY OF THE GROUND SURROUNDING ENERGY PILES IN SUMMER..... 185**

6	INTRODUCTION .....	186
6.1	Brief background of this work .....	186
6.2	CASE STUDY.....	192
6.2.1	The Foundation piles and heat pump .....	192
6.2.2	The Solar roof collector .....	195
6.3	Heat Transfer between Solar-roof/collector and Water/glycol mixture.....	199
6.4	Heat Transfer Budget and Geothermal Situation of the Soil Battery.....	202
6.5	Local geology of the ground at the experiment side .....	206
6.6	Heat transfer between water/glycol and energy pile (concrete)/soil.....	211
6.7	Method .....	213
6.8	RESULTS AND DISCUSSION .....	216
6.8.1	Metal tiles roof/collector and energy piles, Circuit 3.....	216
6.8.2	Concrete tiles roof/collector and energy piles, Circuit 4.....	219
6.8.3	Solar roofs/collectors temperature gain .....	222
6.8.4	Solar roof/collectors Vs Reverse operation of a heat pump.....	224
6.9	Conclusion Chapter 6.....	225
6.10	Further Works .....	228
6.10.1	Renewable Heat for Ground Heat Recharge.....	228

**CHAPTER 7 - A FIELD TRIAL OF THE GROUND-SOURCE HEAT PUMP PERFORMANCE ENHANCED WITH THE EARTH CHARGING BY MEANS OF SOLAR –AIR COLLECTORS..... 232**

7.	INTRODUCTION .....	233
7.1	THE FIELD TRIAL DESCRIPTION.....	234
7.1.1	The Building .....	234
7.1.2	The heating system .....	236
7.1.3	Solar –air Source Panels (Sunboxes) on the south wall of the house .....	239
7.1.4	SAGS-HP Operation Modes .....	241
7.1.5	Modes and Status Control.....	244
7.2	Method.....	245

7.2.1 Measured Parameters .....	246
<b>7.3 RESULTS AND DISCUSSION</b> .....	<b>247</b>
7.4 Conclusion Chapter 7.....	257
<b>CHAPTER 8 - GENERAL DISCUSSION</b> .....	<b>259</b>
8. General discussion .....	260
8.1 Seasonal thermal storage.....	264
8.2 Environmental Impact.....	266
8.3 Economics analysis .....	268
<b>CHAPTER 9 - CONCLUSION AND FURTHER WORKS</b> .....	<b>271</b>
9 General Conclusions .....	272
9.1 Further works .....	273
References .....	274
Appendix.....	281

## List of Figures

<i>Figure 1.1: Variations in temperature of air, the River Glomma and shallow groundwater at a site in Norway, throughout one year (BRE, 2005) .....</i>	<i>5</i>
<i>Figure 1.2: The chart illustrates the link between chapters of thesis .....</i>	<i>12</i>
<i>Figure 2.3: Breakdown of UK energy consumption per sector (Bureau of Energy Efficiency, 2006) .....</i>	<i>18</i>
<i>Figure 2. 4: This pie chart above shows the main elements which make up the total of a typical person's carbon footprint in the developed world (Home of Carbon Management, 2011). .....</i>	<i>21</i>
<i>Figure 2.5: Carbon footprint evaluation boundary (BP, 2007) .....</i>	<i>22</i>
<i>Figure 2.6: Breakdown of buildings energy consumption (Grubb &amp; Ellis, 2007) .....</i>	<i>23</i>
<b>Figure 2. 7 :</b> <i>Heat pumps achieve lower carbon-dioxide emissions than other forms of heating with ground-source heat pumps performing best of all (WYATT, 2004). .....</i>	<i>30</i>
<i>Figure 2. 8: Four main components of the Refrigerant Loop of a Heat Pump</i>	<i>32</i>
<i>Figure2. 9: Thermodynamic model of heat pump vapour compression cycle ...</i>	<i>39</i>
<i>Figure 2.10: Thermodynamic model of heat pump vapour compression cycle.</i>	<i>40</i>
<i>Figure 2.11: The annual variation of the ground temperature at a site in Newcastle, UK, throughout years (Kuang, Sumathy, &amp; Wang, 2003).....</i>	<i>56</i>
<i>Figure 2.12: Ground temperature at 5m and 10m depth at a site in Burton-on-Trent, UK, throughout two years (Wood C. J., 2009) .....</i>	<i>57</i>
<i>Figure 2.13: Long term thermal cycle across its entire pile depth due to the heat extraction for two heating seasons at a site in Burton-on-Trent, UK (Wood C. J., 2009).....</i>	<i>59</i>
<i>Figure 2.14: Schematic graph of annual decline in ground temperature in Burton-on-Trent, UK, throughout 5 years of heating seasons.....</i>	<i>60</i>
<i>Figure 3.15: Direct expansion solar collector/evaporator heat pump.....</i>	<i>67</i>
<i>Figure 3.16: Conventional heat pump with solar-preheated water cylinder ....</i>	<i>68</i>
<i>Figure 3. 17: Conventional heat pump with solar-preheated water cylinder ...</i>	<i>68</i>
<i>Figure 3.18: Multifunction heat pump.....</i>	<i>69</i>
<i>Figure 3. 19: Schematic diagram of the DX-SAHP water heater [63]. .....</i>	<i>70</i>

<i>Figure 3.20: A prototype DX-SAHP water heater: (a) outdoor; (b) indoor.</i> (Kuang, Sumathy, & Wang, 2003) .....	71
<i>Figure 3. 21: Heat pump using dual heat sources in parallel arrangement for evaporation</i> (Ito & Miura, 2000). .....	72
<i>Figure 3.22: Schematic of DX-SAHP system</i> (Chaturvedi, Chen, & Kheireddne, 1996) .....	73
<i>Figure 3.23: Schematic diagram of heat-pump assisted solar-dryer and water heater</i> (Hawlader, Chou, Jahangeer, Rahman, & Eugene Lau, 2003).....	74
<i>Figure 3. 24: The schematic diagram of the simulated SAS-HPWH</i> (Guoying, Xiaosong, & Shiming, 2006). .....	75
<i>Figure 3. 25: Schematic of system circuit</i> (Li, Wang, Wu, & Xu, 2007). .....	76
<i>Figure 3.26: Schematic view of a solar-assisted domestic hot water tank integrated GCHP system</i> (Trilliant-Berdal, Souyri, & Fraise, 2006) .....	77
<i>Figure 3. 27: Three ways of installation GCHE</i> .....	79
<i>Figure 4. 28: Schematic Diagram of the DX-SHP System</i> .....	86
<i>Figure 4.29: Schematic Diagram of the Refrigerant Loop of the Experimental Test Rig</i> .....	87
<i>Figure 4. 30: The twenty one 500W sun lights simulator and the regulator switch</i> .....	88
<i>Figure 4. 31: The metal flat-plate collectors/evaporator and the schematic diagram of it structure</i> .....	90
<i>Figure 4.32: Compressor and Heat exchanger</i> .....	91
<i>Figure 4. 33: Heat Exchanger (Condenser), SWEP: B8x10H/IP</i> .....	92
<i>Figure 4. 34: Thermostatic Expansion Valve (TXV)</i> .....	93
<i>Figure 4. 35: Refrigerant receiver, AIRMENDER, capacity of 1.5 litres</i> .....	94
<i>Figure 4. 36: Liquid Line Filter and a Sight Glass</i> .....	94
<i>Figure 4. 37: Schematic Diagram of the Heat Flow in the flat plate solar collector/evaporator.</i> .....	98
<i>Figure 4. 38: The thermal network of the metal flat-plate collectors/evaporator.</i> .....	99
<i>Figure 4. 39: Schematic diagram of the Contraflow Flat plate L-line type heat exchanger</i> .....	104

<i>Figure 4.40: Condensing and Evaporating Temperatures Vs Heat Pump COP</i>	107
<i>Figure 4.41: Condensing and Evaporating Temperatures Vs Compressor power consumption</i>	108
<i>Figure 4.42: Condensing and Evaporating Temperatures Vs Heat gain at the Condenser</i>	109
<i>Figure 4. 43: Evaporator Area Vs Heat Pump COP</i>	110
<i>Figure 4.44: Pitch of the refrigerant /evaporator tubes Vs COP</i>	111
<i>Figure 4. 45: Diameter of the Collector/Evaporator' tubes Vs COP</i>	112
<i>Figure 4.46: Picture of the DX-SHP under experimental Set-up</i>	116
<i>Figure 4. 47: Simulated solar radiations on the experimental rig</i>	116
<i>Figure 4.48: Data Taker DT500 series 3 and expansion channel connected in the Experimental Rig</i>	118
<i>Figure 4.49: Data logger wiring on the Experimental Test Rig</i>	119
<i>Figure 4.50: Illustration of the temperature sensors of the test rig</i>	121
<i>Figure4. 51: GP Pressure transducer</i>	122
<i>Figure 4. 52: Digital temperature and humidity meter</i>	123
<i>Figure 4.53: Water flow meter</i>	123
<i>Figure 4. 54: The single phase watt hour meter</i>	124
<i>Figure 4. 55: A digital thermometer, Digitron T208</i>	124
<i>Figure 4. 56: Kipp &amp; Zonen, CM11 Pyranometer</i>	125
<i>Figure 4. 57: Test results obtained on August, 25, space heating mode, with 35oC water temperature at the condenser at 200W/m<sup>2</sup></i>	127
<i>Figure 4. 58: The effects the collector/evaporator inlet temperature (T<sub>evp i</sub>) on the COP of the heat pump, the heat rate gain at the condenser, and the compressor energy consumption at 200W/m<sup>2</sup></i>	128
<i>Figure4. 59: Test results obtained on August, 25, space heating mode, with 35oC water temperature at the condenser at 200W/m<sup>2</sup></i>	129
<i>Figure 4. 60: Heat gain at condenser, the COP Vs temperature change across the condenser at 400W/m<sup>2</sup></i>	130
<i>Figure 4. 61: Test results obtained on August, 25, space heating mode, with 35oC water temperature at the condenser at 400W/m<sup>2</sup></i>	131

<i>Figure 4. 62: Test results obtained on August, 26, space heating mode, with 35oC water temperature at the condenser at 400W/m<sup>2</sup> .....</i>	132
<i>Figure 4. 63: The effects the collector/evaporator inlet temperature (T<sub>evp i</sub>) on the COP of the heat pump, the heat rate gain at the condenser, and the compressor energy consumption at 600W/m<sup>2</sup> .....</i>	133
<i>Figure 4. 64: Test results obtained on August, 21, space heating mode, with 35oC water temperature at the condenser at 600W/m<sup>2</sup> .....</i>	134
<i>Figure 4. 65: Test results obtained on August, 21, space heating mode, with 35oC water temperature at the condenser at 600W/m<sup>2</sup> .....</i>	135
<i>Figure4. 66: The effects the collector/evaporator inlet temperature (T<sub>evp i</sub>) on the COP of the heat pump, the heat rate gain at the condenser, and the compressor energy consumption at simulated radiation 800W/m<sup>2</sup> .....</i>	137
<i>Figure 4. 67: The effects the COP of the heat pump, the heat rate gain at the condenser and the compressor energy consumption with time at 800W/m<sup>2</sup> .....</i>	138
<i>Figure 4. 68: Test results obtained on August, 24<sup>th</sup> space heating mode, with 35° C water temperature at the condenser at 800W/m<sup>2</sup> .....</i>	139
<i>Figure 4. 69: Summary of Theoretical Performance Vs Experimental Performance .....</i>	143
<i>Figure 4. 70: Effectiveness of DX-SHP compare to conventional one .....</i>	144
<i>Figure 4. 71: Illustration of the development of the evaporator as a roof module .....</i>	147
<i>Figure 4. 72: A solar collector with a transparent cover as an evaporator of a DX-ASHPS .....</i>	148
<i>Figure 4. 73: illustration of the solar collector/evaporator integrated in the roof as an evaporator of the DX-ASHPS.....</i>	148
<i>Figure 5.74: Schematic diagram of the DX-PV/hpS-Heat pump system .....</i>	154
<i>Figure 5.75: PV/heat pipe Evaporator panel .....</i>	155
<i>Figure 5.76: A cross-sectional view of vacuum glass tube.....</i>	155
<i>Figure 5.77: The thermal network of the Internal Vacuum glass tube .....</i>	157
<i>Figure 5.78: The thermal network of the PV module .....</i>	159
<i>Figure 5.79: The thermal network of the Aluminium sheet .....</i>	160
<i>Figure 5.80: The thermal network of the Refrigerant's copper tube.....</i>	161

<i>Figure 5.81: The monthly average solar radiation (30°) and ambient temperatures .....</i>	165
<i>Figure 5.82: The temperatures at different layers.....</i>	166
<i>Figure 5.83: The monthly average thermal efficiency and heat gain of evaporator.....</i>	167
<i>Figure 5. 84: The monthly average electrical efficiency and output of PV evaporator.....</i>	168
<i>Figure 5.85: The monthly average COP and condenser capacity of PV/hp heat pump system .....</i>	169
<i>Figure 5.86: The sep-up pictures of the preliminary test rig of DX-PV/hp -HP .....</i>	171
<i>Figure 5.87: Simulated solar radiations on the collector/evaporator without vacuum tubes.....</i>	172
<i>Figure 5. 88: Heat Exchanger (Condenser), SWEP: B8x10H/1P .....</i>	175
<i>Figure 5. 89: Thermostatic Expansion Valve (TXV, Danfoss) .....</i>	176
<i>Figure 5. 90: Refrigerant receiver, AIRMENDER, capacity of 1.5 litres .....</i>	177
<i>Figure 5. 91: Liquid Line Filter.....</i>	177
<i>Figure 5.92: Preliminary results of PV/hp- heat pump testing .....</i>	180
<i>Figure 5.93: The testing average COP and condenser capacity of PV/hp- heat pump.....</i>	181
<i>Figure 5. 94 : Schematic of the PV/hp roof modules: Flat plate PV/hp structure, Evacuated tube (rectangle or circle) PV/hp structure .....</i>	184
<i>Figure 5. 95: The PV/hp roof module based heat pump system .....</i>	184
<i>Figure 6. 96: Concept 1-Solar roof/collector using concrete tiles .....</i>	190
<i>Figure 6. 97: Concept 2-Solar roof/collector using Metal tiles .....</i>	190
<i>Figure 6. 98: Concept 3-Solar roof/collector integrated with evacuated tubes .....</i>	191
<i>Figure 6. 99: Pile Foundation and thermocouple array layout (Wood C. J., 2009). .....</i>	193
<i>Figure 6. 100: Schematic of a ground source heat pump with energy piles and simulated loads .....</i>	194
<i>Figure 6.101: Set-up of the piled Foundation of a detached two storeys House .....</i>	194

<i>Figure 6.102: Piled Foundation of a detached two storeys House .....</i>	195
<i>Figure 6. 103: The basic schematic diagram of the Case Study 2- Solar roof for ground heat recharging (Inter-seasonal heat storage).....</i>	197
<i>Figure 6. 104: Aluminium sheet and water/glycol pipe under the metal tiles .</i>	197
<i>Figure 6. 105: Solar roof thermal collector under construction, at the experiment side .....</i>	198
<i>Figure 6.106: Heat transport from ambient air/solar radiation to heat carried fluid (water/glycol mixture) within the absorber pipe of the solar roof/collector.....</i>	200
<i>Figure 6. 107: Heat Budget of the Soil Battery .....</i>	204
<i>Figure 6. 108: Heat transfer and geothermal situation of the Soil Battery during winter and summer.....</i>	205
<i>Figure 6.109: The set-up of the thermal response testing to determine thermal conductivity value of the concrete pile.....</i>	209
<i>Figure 6.110: The set-up of the thermal response testing to determine thermal conductivity value of the concrete pile.....</i>	211
<i>Figure 6.111: Schematic diagram of the Wiring of the Data Logger DT500..</i>	214
<i>Figure 6. 112: The relation of energy injected in the ground, ambient air temperatures and the Time for the metal tile roof/collectors loop (Circuit 3) .....</i>	217
<i>Figure 6. 113: The relation of energy injected in the ground and the PWET for metal tile roof/collectors loop (Circuit 3).....</i>	219
<i>Figure 6. 114: The relation of energy injected in the ground, ambient air temperatures and the Time for the concrete tile roof/collectors loop (Circuit 4).....</i>	221
<i>Figure 6. 115: The relation of energy injected in the ground and the PWET for concrete tile roof/collectors loop (Circuit 4) .....</i>	222
<i>Figure 6.116: The relation of the temperature gain at the solar roofs/collectors with the ambient temperatures.....</i>	224
<i>Figure 6. 117: Renewable Heat Energy and Soil Battery Concept .....</i>	229
<i>Figure 6. 118: Renewable Heat Energy and Soil Battery Concept in 2D .....</i>	230
<i>Figure 6.119: Renewable Heat Energy and Soil Battery Concept in 2D for 10 Unit Developments.....</i>	231

<i>Figure 7.120: Case Study House with the SUNBOXES-Ground Hybrid Source Heat Pump (13% DHW and 87 % space heating).....</i>	235
<i>Figure 7. 121: Hot Water Tank Integrated Heat Pump (Enerfina, 2008) .....</i>	237
<i>Figure 7.122: The basic schematic diagram of the field trial, the House with the Sunboxes-combined with the GSHP .....</i>	238
<i>Figure 7. 123: Drilling of the boreholes to a nominal depth of 48 metres.....</i>	239
<i>Figure 7. 124: Concept diagram of the sunboxes on the south wall .....</i>	240
<i>Figure 7. 125: Schematic diagram of the GSHP's performance testing with SUNBOXES in working Mode 1, Ground source only .....</i>	242
<i>Figure 7. 126: Schematic diagram of the GSHP's performance testing in working Mode 2, SUNBOXES-Ground Hybrid Source .....</i>	243
<i>Figure 7.127: Schematic diagram of the GSHP's performance testing with SUNBOXES in working Mode 3, Charging .....</i>	244
<i>Figure 7.128: Schematic diagram of the Wiring of the Data Logger DT500..</i>	246
<i>Figure 7.129: The relation of energy injected in the ground and the time.....</i>	249
<i>Figure7.130: The relation of energy injected in the ground and Sunboxe air temperatures .....</i>	249
<i>Figure 7.131: The relation between the energy gain at the evaporator, COP and the temperature of glycol /water at the evaporator .....</i>	251
<i>Figure 7.132: The relation between the energy gain at the evaporator, COP and the temperature of glycol /water at the evaporator. ....</i>	252
<i>Figure 7. 133: The relation between the COP and the compressor power consumption with time in winter. ....</i>	256

## List of Tables

<i>Table 2.1 : The Kyoto protocol's Greenhouse gases (IPCC, 2007) .....</i>	20
<i>Table 2.2: Levels in the Code of sustainable Homes (Communities and Local Government, 2008) .....</i>	26
<i>Table 2. 3: Nine varieties of heating system for residential buildings .....</i>	27
<i>Table 2. 4: Typical delivery temperatures for various building heating distribution systems (Energetics , 2007) .....</i>	30
<i>Table 2. 5: Classification of heat pumps for heating of buildings.....</i>	33
<i>Table 2.6: Characteristics of heat sources for heat pump (CUBE &amp; Fritz, 1981) .....</i>	36
<i>Table 2 7: The desired properties of refrigerants' heat pump.....</i>	45
<i>Table 3. 8: Typical arrangements of Ground Coupled heat pumps (ground heat exchanger).....</i>	79
<i>Table 3. 9: Main relevant recent studies conducted on heating only heat-pump systems .....</i>	82
<i>Table 4. 10: Specification of main equipments in the DX-SHP system .....</i>	86
<i>Table 4. 11: Sensor uncertainty .....</i>	119
<i>Table 4. 12: The most commonly used temperature sensors and their properties (Technology Pico, 2001).....</i>	120
<i>Table 4. 13: Specification of the pressure transducer .....</i>	123
<i>Table 4.14: Specifications of Digital temperature.....</i>	123
<i>Table 4. 15: Specifications of the digital thermometer .....</i>	124
<i>Table 4. 16: Specifications of the CM11 Pyranometer .....</i>	125
<i>Table4. 17: Summary results of the performance testing of DX-SHP .....</i>	143
<i>Table 4. 18: Effectiveness of the DX-SHP .....</i>	144
<i>Table 5. 19: Specification of main equipments in the DX-STSHP system .....</i>	154
<i>Table 5.20: Characteristic dimensions of PV evaporator panel (mm).....</i>	156
<i>Table 5. 21: Performance of DX-PV/hp-HP at Space heating-only Mode (Water 35oC).....</i>	179
<i>Table 6.22: Summary of the technical data for this experiment .....</i>	198
<i>Table 6. 23: Results of the moisture content analysis of the soil around the piles .....</i>	207

<i>Table 6. 24: test results of the ground density of the energy pile location .....</i>	210
<i>Table6. 25: Summary results of two weeks testing from 6 July to 19 July 2010 .....</i>	226
<i>Table 7. 26: Building construction materials .....</i>	236
<i>Table7. 27: Summary of the experimental results .....</i>	255

## NOMENCLATURE

- $W_C$ : Electrical energy input at the heat pump compressor, W;  
 $Q_E$ : Energy collected at the evaporator, W;  
 $Q_C$ : Energy collected at the condenser, W;  
 $T_{High}$ : High temperature at heat pump condenser side, K;  
 $T_{Low}$ : Low temperature at heat pump evaporator side, K;  
 $W_{Power\ Generation}$ : Average efficiency of electric power generation for power supply to heat pump, W;  
 $\eta_{power\ generation}$ : Average efficiency of Power Generation for electric heat pump;  
 $T_{evp}$ : Collector/evaporator temperature of the heat pump, K;  
 $Q_{evp}$ : heat gain at the evaporator of the heat pump or energy extracted by the collector, W;  
 $T_a$ : Ambient temperature, K;  
 $Q_l$ : Rate of heat loss to the ambient of the room by convection and radiation, W/s;  
 $U_l$ : Collector overall heat transfer coefficient, W/m<sup>2</sup>K;  
 $T_p$ : Collector surface temperature, K;  
 $S$ : Incident solar absorbed by the collector, W/m<sup>2</sup>;  
 $A_c$ : Area of the collector/evaporator, m<sup>2</sup>;  
 $I$ : Intensity of the solar radiation in W/m<sup>2</sup>;  
 $\alpha$ : Collector absorption rate, %;  
 $F'$ : Collector efficiency factor;  
 $\bar{T}$ : Mean refrigerant temperature in the collector/evaporator;  
 $F$ : Fin efficiency factor of the collector plate/evaporator;  
 $W$ : Pitch between the serpentine tubes of the collector, m;  
 $D$ : Diameter of the refrigerant tube, m;  
 $\delta_m$ : Thickness of the collector/evaporator flat plate, m;  
 $k_m$ : Thermal conductivity of the collector/evaporator flat plate, W/mK;  
 $h_{fi}$ : Fin tubes internal heat transfer coefficient of two-phase flow in horizontal tubes;  
 $J$ : Dimensional constant, with a value 7785;  
 $\Delta x$ : Change in quality of the refrigerant from collector/evaporator inlet to exit;  
 $U_L$ : Collector overall heat loss coefficient, W/m<sup>2</sup>K;  
 $U_t$ : Top of the collector heat loss coefficients, W/m<sup>2</sup>K;  
 $U_b$ : Bottom of the collector heat loss coefficients, W/m<sup>2</sup>K;  
 $h_c$ : Convection coefficient heat loss due to wind, W/m<sup>2</sup>K;  
 $h_r$ : Heat transfer coefficient heat loss by radiation, W/m<sup>2</sup>K;  
 $V$ : Wind speed, m/s;  
 $T_{sky}$ : Sky temperature, K;  
 $\epsilon$ : Emissivity of the collector, %;  
 $\sigma$ : Stefan –Boltzmann constant, Wm<sup>-2</sup>K<sup>-4</sup>;  
 $\dot{m}_r$ : Refrigerant fluid mass flow rate, Kg/s;  
 $h_4$ : Enthalpy change of the refrigerant at the inlet of the collector/evaporator, J/kg;  
 $h_1$ : Enthalpy change of the refrigerant at the exit of the collector/evaporator, J/kg;

$h_2$  : Enthalpy change of the refrigerant at the outlet of the compressor, J/kg;  
 $\eta_v$  : Volumetric efficiency of the compressor;  
 $v_1$  : Specific volume at the inlet of the compressor, m<sup>3</sup>/kg;  
 $V_d$  : Displacement volume for a reciprocating-type compressor;  
 $\eta_v$  : Volumetric efficiency;  
 $\eta_{comp}$  : General efficiency of the compressor;  
 $W_{oi}$  : Total ideal input electric power to the compressor, W;  
 $T_{rei}$  : Inlet refrigerant temperature, K;  
 $T_{wcond}$  : Cold water temperature at the heat exchanger, K;  
 $Q_{rcond}$  : Heat gain from the refrigerant side of the heat exchanger, W;  
 $Q_{wcond}$  : Heat gain from the water side of the heat exchanger, W;  
 $\dot{m}_w$  : Mass flow rate of the water, Kg/s;  
 $C_p$  : Specific heat coefficient of the water, J/kg K;  
 $C$  : Specific heat coefficient of the refrigerant, J/kg K;  
 $T_{co}$  : Temperatures of the water at the exit of the heat exchanger, K;  
 $T_{ci}$  : Temperatures of the water at the inlet of the heat exchanger, K;  
 $eff_{DX-STSHP}$  : the effectiveness of the DX-SHP system;  
 $\beta_g$  : Absorptance of the vacuum glass tube, %;  
 $G$  : Solar radiation, W/m<sup>2</sup>;  
 $A_g$  : Outer surface area of the vacuum glass tube, m<sup>2</sup>  
 $A_p$  : Area of the PV module, m<sup>2</sup>;  
 $A_{al}$  : Area in m<sup>2</sup> of the aluminum sheet, , m<sup>2</sup>;  
 $\epsilon_p$  : Emittance of the PV module, %;  
 $T_p$  : Temperature in K of the PV module, K;  
 $T_g$  : Temperature in K of the vacuum glass tube, K;  
 $T_{sky}$  : Background sky temperature, K;  
 $q_{r,p-g}$  : Heat flux radiation from the PV module to the vacuum glass tube, W/m<sup>2</sup>;  
 $q_{r,al-g}$  : Heat flux radiation from the aluminum sheet PV module to the vacuum glass tube,  
 $q_{r,g-sky}$  : Heat flux radiation from the vacuum glass tube to sky, W/m<sup>2</sup>;  
 $\alpha_{g-a}$  : Convexional heat transfer coefficient between the vacuum glass and ambient air, W/m<sup>2</sup>K  
 $(\beta\tau)_c$  : Effective absorptance of the solar cells, %  
 $(\beta\tau)_p$  : Effective absorptance of the solar cells base plate, %  
 $\tau_a$  : Transmittance of the vacuum glass tube “g”  
 $\tau_p$  : Transmittance of the PV module “p”  
 $\epsilon_{al}$  : Emittance of the aluminium plate, %;  
 $T_{al}$  : Temperature of the aluminium plate, K;  
 $\cdot u_{wind}$  : Wind velocity, m/s;  
 $u_{mean}$  : Mean velocity of laminar flow, m/s

Re : Reynolds number,;  
 u : Mean velocity, m/s;  
 d: Pipe diameter, m;  
 $\nu$  : Kinematic viscosity, m<sup>2</sup>/s;  
 $\eta$  : Dynamic viscosity, kg/ms  
 Q: volumetric flow rate, m<sup>3</sup>/s;  
 $\dot{Q}_s$ : Heat flux, W;  
 $\dot{q}$ : Heat flux density, W/m<sup>2</sup>;  
 C: Circumference of the energy pile , m;  
 $l_{pile}$ : Energy pile length, m;  
 $n_{pipes}$ : Quantity of absorber pipe; (unity);  
 $\alpha$ : Heat transfer coefficient,  $\frac{W}{m^2k}$ ;  
 c: Specific heat capacity, Ws/kgk;  
 $\dot{m}$ : mass flow rate,  $\frac{kg}{s}$ ;  
 T: Temperature, °C;

### Subscripts

a                    ambience or air  
 av                   averaged value  
 evp                  evaporator  
 comp                compressor  
 cond                 condenser  
 wcond              water condenser  
 rcond               refrigeration condenser  
 i                     inlet  
 o                     outlet  
 rad                  radiator  
 st                    storage tank  
 w                    water  
 “al”: Aluminum sheet;  
 “g” : Vacuum glass tube;  
 “p”: PV module;  
 “a”: Ambient air ;  
 “c”; Solar cell;

COP: Coefficient of Performance;  
 PWET : Pile-Water-Equilibrium Temperature;  
 SCPF : Soil Charging Performance Factor;  
 DHW : Domestic Hot Water;  
 SAGS-HP: Solar-Air-Ground Source’ Heat Pump  
 GSHP: Ground Source Heat Pump  
 GWET : Ground-Water-Equilibrium Temperature

Ch: Data logger channel

## **Measured Parameters**

### **Temperatures**

Temperature of the refrigerant inlet at the evaporator

Temperature of the refrigerant at the compressor inlet

Temperature of the refrigerant at the compressor outlet

Temperature of the refrigerant at heat exchanger outlet

Supply water temperature to the radiator

Temperature of the water at heat exchanger inlet

Return water temperature from the radiator or heat distribution system

Temperature of the water at the top part of the heat storage tank

### **Pressures**

- **Evaporation pressures**

Evaporator /solar collector inlet pressure

Compressor inlet/outlet pressure

- **Condenser pressures (Refrigerant side)**

Compressor outlet pressure (**P<sub>co</sub>**)

Heat exchanger outlet pressure (**P<sub>eri</sub>**)

### **Power**

Power input to the compressor (**W<sub>c</sub>**)

Power input to the fan (**W<sub>f</sub>**)

Power input to the water circulation pump (**W<sub>cp</sub>**)

### **Mass Flow**

Mass Flow rate of the water (**m<sub>w</sub>**)

### **Solar Radiation**

Measure solar radiation (200W/m<sup>2</sup> – 1200 W/m<sup>2</sup>)

### **Calculated Parameters**

Heat rate gain at the condenser

Heat Collected at the Evaporator

Coefficient of performance of the heat pump

Coefficient of performance of the overall system

# Abstract

*The European standard EN15450 states that the Coefficient of Performance (COP) target range for a Ground Source Heat Pump (GSHP) installation should lie within the range of 3.5 to 4.5; when used for heating a building, and a typical Air-Source Heat Pump (ASHP) has a COP of 2.0 to 3.0 at the beginning of the heating season and then decrease gradually as the ambient air becomes cooler, whereas a typical GSHP is in the range of 3.5 –4.0, also at the beginning of the heating season and then decrease gradually as heat is drawn from the ground. For these reasons, in the middle of winter, when the COP drop, the heat pumps can generally only be considered as a ‘pre-heating’ method for producing higher temperature heat such as domestic hot water. In addition soil presents certain difficulties, due to the high cost of drilling to position coils in the ground compare to air source, although frost formation on the evaporator in winter limits also limit the use of air source. Though technology advances or are needed to overcome those issues.*

*The aims of this project, therefore, were firstly to reduce the drilling length of the ground heat exchanger of the ground source heat pumps and to maintain high COPs of the air and ground source heat pumps from beginning to the end of the heating season; and secondly to develop a viable alternative evaporator for air source heat pumps to reduce frost formation during winter. These were achieved; the first aim through the combination of ground loops with solar-air panels or solar roof/collectors roof to ground heat exchangers loops to reduce the length of the boreholes, and to reduce the freezing effects around the boreholes, hence increase or maintain a constant temperature during heating season. The second aim was also achieved through development and validation of novel air source heat pump evaporator, using Direct Expansion (DX) black flat plate absorber or/and vacuum tubes for frost reduction.*

*In this thesis, in order to achieve the above aims; four aspects of investigations have been independently investigated as following:*

- 1- Preliminary investigation on Direct Expansion (DX) Solar Source Heat Pump system.
- 2- Investigation on the performance of the DX- PV/heat pipe heat pump system to reduce frost and enhance the COP of the air source heat pumps,
- 3- A small scale testing on the heat injection on energy piles for residential buildings for earth charging by means of solar roof/collectors
- 4- A field trial testing of the performance of the combination of solar-air thermal collectors with conventional GSHP with shorter ground heat exchangers (48m deep) to charge the ground and reduce freezing effects around the piles after heating cycle.

*From the simulation results, the novel PV/hp-HP system has a COP ranging from 4.65 to 6.16 with an average of 5.35. The condenser capacity ranging from 33 to 174 W would provide the heat source for space heating and domestic hot water. The energy performance of the novel PV/hp-heat pump was not as good as expected due to the low solar radiation. It should be much better in some low latitude locations with better solar radiation.*

*The results of this thesis have shown that the length of ground source boreholes could be considerably reduce by about 60% compare to conventional boreholes using a combination of solar-air collectors with the GSHP and the average COP of 3.7 was achieved.*

## **PUBLISHED PAPERS AS A RESULT OF THE PhD PROJECT**

**Mempouo, B.** Riffat S.B. and Cooper E. (2010), *Preliminary Performance Analysis of a Novel Direct Expansion Solar Thermal Source Heat Pump (DX-STSHP)*, SET2010 - 9<sup>th</sup> International Conference on Sustainable Energy Technologies, Shanghai, China

**Mempouo, B.** Riffat S.B. and Nicholson-Cole, D. (2010) *Experimental Analysis of the Ground-Source Heat Pump Performance Enhanced with the Earth Charging by Means of Solar Thermal Collectors*, SET2010 - 9<sup>th</sup> International Conferences on Sustainable Energy Technologies, Shanghai, China

**Mempouo, B.** Riffat S.B. and Cooper E. (2010), *A Review of Window Technologies and the Code for Sustainable Homes in the UK*, Proceeding of the SET2009 - 8<sup>th</sup> International Conference on Sustainable Energy Technologies, Aachen, Germany

**Mempouo, B.** Riffat S.B. and Cooper E. (2010), *Novel Window Technologies and the Code for Sustainable Homes in the UK*, The International Journal of Low-Carbon Technologies 2010; doi: 10.1093/ijlct/ctq013

Chen, H. **Mempouo, B.** and Riffat S.B. (2010), *Numerical study on the energy performance of a novel PV/T heat pump system*, accepted to be published in the proceeding and presented at the SET2010 - 9<sup>th</sup> International Conference on Sustainable Energy Technologies, Shanghai, China

Y. Fu, **B. Mempouo**, J. Zhu, S. B. Riffat (2010), *Basic Analysis of High Performance Air Source Heat Pump Using PCM Storage Tank and No Frost Evaporator*, accepted to be published in the proceeding and presented at the SET2010 - 9<sup>th</sup> International Conference on Sustainable Energy Technologies, Shanghai, China

## Acknowledgements

*At a PhD project have been carrying out at the Department of Architecture and Built Environment. This report was the result of the three years long reading and investigation that have been performed at the Institute of Building Technology/Institute of Sustainable Energy Technology in the Sustainable Research Building. The work in this report started in the earlier February 2008.*

*I would to take this opportunity to thanks those who make these first and second years possible. I gratefully acknowledged the support of the Engineering and Physical Science Research Council (EPSRC) and Roger Bullivant Ltd for fund the work described in this report; Professor Saffa Riffat for the tremendous help he provided both technical and academically, it is a privilege to be your student; Dr Edward Cooper for the outstanding academic and morale help provided; Amante-Roberts Zeny for her times and assistance; Christopher Wood, All the technicians at the school' s workshop and finally my family for their understanding and moral support.*

*Many thanks go to my family for being there for me when I needed them the most and for their understanding and encouragement. Thank you especially to my encouraging wife, Mbouayie F. Eugenie and my lovely Son, Mempouo Giancarlo for their constant moral support and also my parents for their patience, help and support throughout my studies.*

## **CHAPTER 1 - INTRODUCTION**

---

## **1. Introduction**

In a typical UK family house, the energy used for space and Domestic Hot Water Heating (DHW) represents more than 61% of its annual energy requirement. In addition, over 50% of carbon emissions of the house arise from space heating and 20% from domestic hot water heating (Energy Saving Trust, 2010). The recent proposals by the UK government which require new housing to become progressively more energy efficient, leading to net zero-carbon dioxide emissions from 2016 (Communities and Local Government, 2008) and the UK's 2008 Climate Change Act which requires an 80% reduction in CO<sub>2</sub> emissions by 2050 from 1990 level (Miliband, 2008); both have stimulated research for more energy efficient technologies including building envelopes and building services. These requirements also imply that these zero-carbon homes will involve a range of low or zero-carbon on-site power generation technologies, low or zero-carbon space and water heating technologies (Energy Saving Trust, 2010). Therefore, achieving zero-carbon space and water heating presents a distinct set of infrastructural challenges to the industry and this is a demanding objective, which requires innovation.

### **1.1 Statement of the problems**

William Thomas, the first Lord Kelvin, described the theoretical basis for a heat pump in 1892, as a device that collects low-grade heat from water (such as a lake or river), ground, or atmosphere (air) and delivers it at higher temperature. At high

performances, heat pump systems have the potential to improve thermal comfort, at lower energy costs and reduce CO<sub>2</sub> emissions for low carbon homes. Heat pumps are available in different shapes and sizes and there are two types, absorption types (absorption cycle) and vapour compression types (compression cycle); but those operating on the vapour compression cycle are the most popular and are used for space and domestic hot water heating in buildings. Most vapor-compression heat pumps utilise electrically powered motors for their work input.

The ground/air sources heat pump technologies are well established, with over 400,000 units (80% are domestic) installed worldwide and about 45,000 installed annually (BRE, 2005). Traditionally, the overall Coefficient of Performance (COP) for ground source heat pumps is higher than for air source heat pumps due to the stable temperature of the ground in the winter as shown in the Figure 1.1; In winter, when heating is needed for space and Domestic Hot Water Heating (DHW), the ground temperatures are higher than the average air temperatures, and in summer, when cooling is needed the ground temperature is also lower than the ambient air. When used for heating a building, a typical air-source heat pump has a COP of 2.0 to 3.0 at the beginning of the heating season and then decrease gradually as the ambient air becomes cooler, whereas a typical ground source heat pump is in the range of 3.5 –4.0, also at the beginning of the heating season and then decrease gradually as heat is drawn from the ground. The COP of a heat pump depends on many factors such as installation, temperature differences, site

elevation, and maintenance. However, the COP is largely determined by the heat source which supplies the low-temperature heat for “pumping up”. In addition, the theoretical and practical coefficient of performance is dependent on the temperature difference, “lift”, between heat in (at the heat pump’s evaporator) and heat out (at the heat pump’s condenser); therefore, the COP increases as the temperature difference, or "lift", decreases between heat source and destination.

The space and domestic hot water heat demand rises as external temperature falls, and the lift increased, consequently reduces the heat pump’s COP. The situation is aggravated by the pattern of natural heat sources, i.e., air, soil, ground and surface water and solar radiation, to follow variations in external temperature through the seasons (see Figure 1.1). e.g., when an air-source heat pump is used to heat a house on a very cold winter day, it takes more work to move the same amount of heat indoors; this typically occurs around  $-5\text{ }^{\circ}\text{C}$  outdoor temperature for air source heat pumps. In addition, as the heat pump takes heat out of the air, some moisture in the outdoor air may condense and possibly freeze on the outdoor heat exchanger (evaporator) of the air source heat pump. In addition, In the UK, the “**heating only**” heat pumps, with carbon-dioxide emissions being 50 to 60% lower than even a gas-fired condensing boiler are the most promising renewable heat systems to compete with conventional fossil fuel heating devices, in addition they have a role to play in achieving zero-carbon homes in the UK (WYATT, 2004).

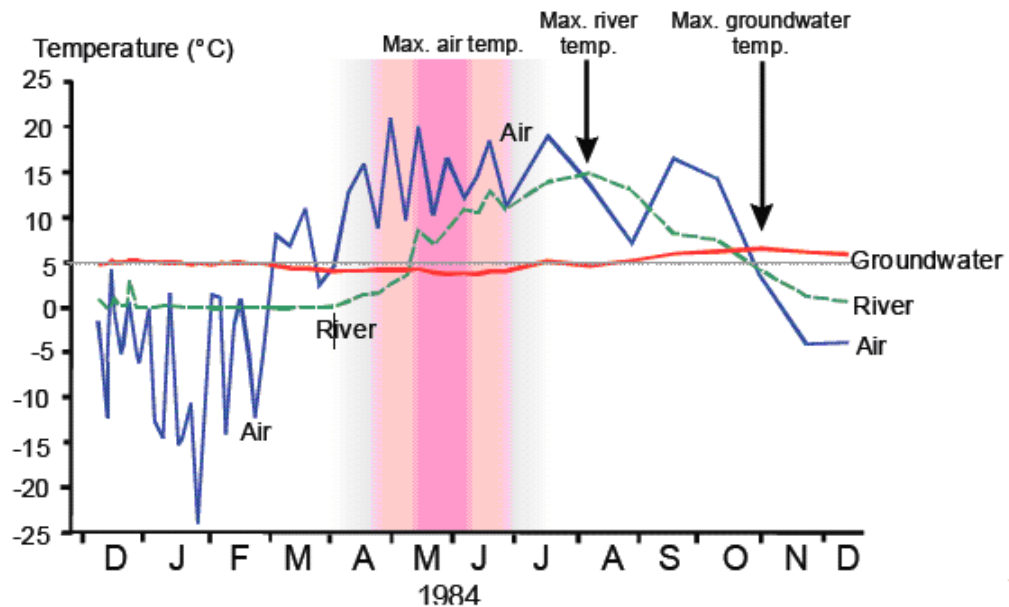


**Figure 1.1:** Variations in temperature of air, the River Glomma and shallow groundwater at a site in Norway, throughout one year (BRE, 2005)

Therefore the development of measures to improve the COP of Air Source Heat Pump (ASHP) and the length of the ground heat exchanger of the Ground Source Heat Pump (GSHP) are vital to widening their employment from 2016 on the net zero-carbon dioxide emissions' houses, in the UK and low carbon homes in Europe.

Historically, soil has been considered to be the most effective heat source for heat pumps operating on the vapour compression cycle, as it offers the highest COP. But soil presents certain difficulties, due to the high cost of drilling to position coils in the ground; Air has found renewed favour as an effective heat source, although frost formation on the evaporator in winter limits its use.

The aims of this project, therefore, were firstly to reduce the drilling length of the ground heat exchanger of the ground source heat pumps and to maintain high COPs of the air and ground source heat pumps from beginning to the end of the heating season; and secondly to develop a viable alternative evaporator for air source heat pumps to reduce frost formation during winter. These were achieved; the first aim through the combination of ground loops with solar-air panels or solar roof/collectors roof to ground heat exchangers loops to reduce the length of the boreholes, and to reduce the freezing effects around the boreholes, hence increase or maintain a constant temperature during heating season. The second aim was also achieved through development and validation of novel air source heat pump evaporator, using Direct Expansion (DX) black flat plate absorber or/and vacuum tubes for frost reduction.

## **1.2 Objective and scope of the project**

In order to achieve the above aims the following have been independently investigate, the novel evaporators for air source heat pump and the new concepts of combining solar-air collectors or solar roof/collectors roof with heat exchangers.

Therefore, the overall objectives of this research were :

- i) To enhance the Coefficient of Performance of air and ground source heat pumps;
- ii) To reduce the frosting issues on the external evaporator of ASHP system;

- iii) To reduce the drilling length of the boreholes and the lengths of the ground heat exchangers of the GSHP system; and
- iv) To reduce the long term freezing effects around the boreholes after 5 to 10 years heating cycles.

The targeted novel outcomes of the project were:

- The use of the heat pump systems to provide space and DHW heating for the zero-carbon homes in the UK;
- The use of the PV/heat pipe as evaporator for air source heat pump to efficiently collect heat from the sun or the air at a low temperature (atmosphere in winter,  $-5^{\circ}\text{C}$ ) with high COP in winter the UK;
- For the systems to use fewer parts, be inexpensive to install in a single house, and required minimal maintenance;
- For the systems to have high COP ( $>$  than 3 for ASHP) or ( $>$  than 4 for GSHP) than conventional heat pumps in the market and be economically feasible

### 1.2.1 Scopes

In order to successfully meet the above targets, the scopes of the project were divided into six separate areas:

- To review the background and literature review of past work on residential air and ground heat pumps' performances improvement.

- To carry out mathematical and experimental performances studies on Direct Expansion Solar-Thermal Heat Pump (DX-STHP) system and on Direct Expansion Photovoltaic/heat pipe-Heat Pump system (DX-PV/hp-HP).
- To construct and test small-scale field testing to validate the concept of charging the ground during summer months, in this case using solar roof/collectors combined with energy piles.
- To validate theoretical results findings with experimental results.
- To carry out a field trial on a full size occupied detached two-storey house in the city of Nottingham using GSHP combined with solar-air thermal collectors acting as a supplementary heat source for heap pump during winter or to charge the ground during summer.
- To discuss the technical, economical and environmental benefit of the new systems.

### **1.3 Novelty and timeliness of the project**

This project has the following novelty aspects:

- i) The use of evaporators which can effectively collect heat at a low temperature (when the atmosphere in winter is about  $-5^{\circ}\text{C}$ ) with no frost and to provide an air source heat pump for satisfying the heating requirements of a residential building without resort to additional heating system during the coldest weather are novel.

- ii) The use of solar roof/collector combined with short energy piles (10m deep) to harvest free heat from the sun during summer to assist the quick heat recovery of ground surrounding the piles after the heating season.
- iii) The use of solar-air panels combined with short boreholes (48m, deep) for residential GSHP as a supplementary heat source, or to collect solar heat on sunny days, bright-sky, and air warmth even during summer nights to warm the glycol/water to inject heat to ground for immediate needs (real-time), and surplus heat to be retained to use the same day (diurnally, heat storage) or during next winter (interseasonal heat storage).

These types of configurations ii) and iii) have not been reported, therefore, the use of such supplementary heats is original.

The project is timely in view of the UK government's commitment to reduce CO<sub>2</sub> emissions from new built homes by 100% from year 2016 (Communities and Local Government, 2008). The UK industry for domestic-size heat pump system is currently very small. These novel heat pump systems present an excellent opportunity to expand the market for space and water heating systems using heat pumps. These novel systems are also expected to contribute at low cost and low carbon emission towards zero-carbon space and DHW heating for the high level of sustainability requirements standard of the Code for Sustainable Homes in the UK.

## **1.4 Methodology approach:**

The project work involved the following stages:

### **Stage 1: Back ground and Literature Review**

A literature review was carried out to collect relevant information on the use of solar collectors as evaporators for heat pump systems and summarises previously published theory that is crucial to understanding this project and on residential air and ground heat pumps' performances improvement.

### **Stage 2: Mathematical modelling/thermodynamic Analysis**

Mathematical modelling has been used to evaluate the performance of the systems in various ways and under different operating conditions including different radiations; the sensitivity analysis of the effects of the physical characteristic of the collector/evaporator on the COP of the DX-air heat pump has also been investigated.

### **Stage 3: Testing Using Small-Scale Rig in the laboratory**

A small-scale test rigs have been designed and constructed to test the performance of the novels systems. Results were comparing with those obtained by mathematical modelling. Systems under various solar radiations were tested in a rig to determine the optimum performances.

#### **Stage 4: Small Scale field testing and Field trial**

A small scale field test study was undertaken to validate the concept of ground charging. The work was carried out on the solar roof/collector combined with energy-piles heat pump system to act as heat generation during summer period to charge the ground. A monitoring system was set up to measure during charging the energy injected in the ground. Metal roof and concrete tiles were also investigated. Then the field trial test was carry out on the solar-air panels acting as a supplementary source to a Ground Source Heat Pump (GSHP) with; an experimental system was installed on a full size occupied detached two-storey house in the city of Nottingham, UK. The energy output from ground heat exchangers was evaluated. The efficiency of the heat pump system, the energy delivered to the space and domestic hot water systems and the total energy consumed by the compressor of the heat pump for space and water heating were also investigated.

#### **1.5 Structure of the thesis:**

This report is made of eight chapters and the chart below (see Figure 1.2) illustrates the link between chapters and the plan of the thesis.

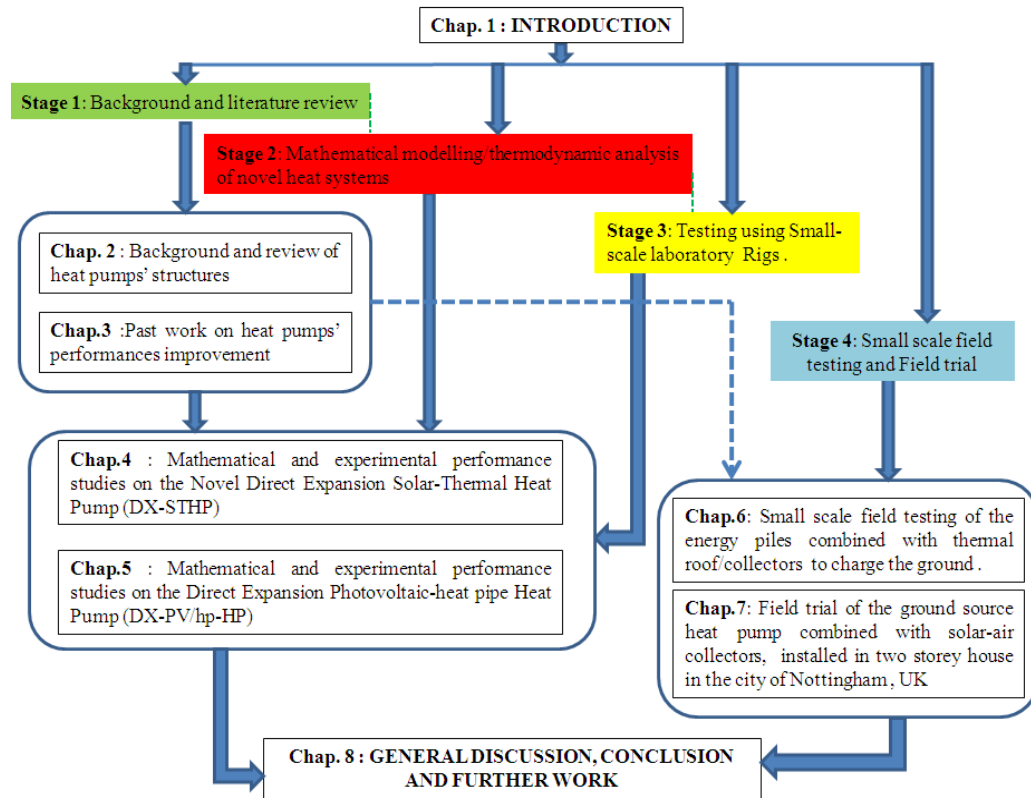


Figure 1.2: The chart illustrates the link between chapters of thesis

The eight chapters involve the following:

**The first chapter** covers the introduction to the project driving forces. The project objectives, scopes are detailed. The methods of approach to meet various objectives are also given in this chapter.

**The second chapter** covers the background of the research and summarises previously published concept and theory that is crucial to understanding this

project. It also provides a brief review of the various studies and the state of art heat pump technologies relevant to this work.

**Third chapter** reviews different technical arrangements and past work to improve heat pumps' performances such as the combination of heat pump and solar thermal energy to improve heat pump performance; many designs for heat pumps and supplementary systems have been suggested. This chapter also describes the designs, technologies and systems, which allow the unit to operate efficiently and minimise the effect of seasonal changes on heat pump performance.

**The fourth chapter** describes the experimental set-up of a direct expansion solar thermal heat pump (DX-STHP) and analyses design specifications of the main four components (collector/evaporator, compressor, condenser and expansion valve) which made the loop of refrigerant circuit of the experimental rig; and other components (receiver, filter, and sight glass) beyond these basic 4 are also explained. It also describes the mathematical model and experimental analysis of the DX-STHP system; evaluates the performance of the system in various ways and under different operating conditions; the sensitivity analysis of the effects of the physical characteristic of the collector/evaporator on the COP of the heat pump is also given.

**The fifth chapter** describes mathematical models and experimental performance analysis of the Direct Expansion Photovoltaic – heat pipe Heat Pump (DX-PV/hp-HP), the mathematical model of each component of the DX-PV/hp-HP system is presented; it also presents the performance evaluation of novel heat pump system in various ways and under different operating conditions, of Nottingham climates, and their effects on the COP of the heat pump is given.

**The sixth chapter** presents the small scale field trial of the solar roof/collector combined with energy piles, with the roof thermal acting as a supplementary heat source for quick recovery of the ground after heating season, the method of ground heat transfer have been presented, amount of heat injected in the ground was detailed in this chapter, Additionally the parameters known as the Pile-Water-Equilibrium Temperature (PWET) and Soil Charging Performance Factor (SCPF) were introduced and analysed respectively as a keys indicators of the ground changing temperature and the charging performances of the solar roof/collectors.

**The seventh chapter** describes the field trial on the solar-air panels acting as a supplementary source to a Ground Source Heat Pump (GSHP) installed on a full size occupied detached two-storey house in Nottingham. It also summarises the benefits of the novel systems.

**The eighth chapter** gives the general discussion, including environmental, social, and economical benefits of the novel heat pumps, it concludes, based on the theoretical and experimental investigation. It also suggests further works.

## **CHAPTER 2 - BACKGROUND AND OVERVIEW OF HEAT PUMP AND PERFORMANCES**

---

## **2. Background of the research**

This section summarises the driving force behind this project and in addition looks briefly into the basic hypothetical concepts that are crucial to understanding this project. This section also aims to review some of the more recent legislation drivers in new build in the UK.

### **2.1 Climate Change, Global Warming and Domestic Energy Consumption**

There is now a clear convergence of scientific and political accord in the World that global warming is happening, and climate change has been recognised as one of the greatest threats and challenge of the twenty first century. It is the key driver of a raft of international, European and national policy aimed at reducing carbon emissions and improving energy efficiency in new and existing buildings (Government memorandum, 2008). Climate change is an important challenge for present society; since it is affecting all areas of the society including homes (DCLG, 2008).

From the total UK primary energy consumption, there are three main sectors which are consumer of energy, Industry, transport, and buildings, A study by Perez-Lombard, Ortiz, and Pout (2007) compared final energy used in buildings in EU countries and UK; the study found that, building energy consumption in the EU was 37% of final energy, bigger than industry (28%) and transport (32%), and in the UK, the proportion of energy use in buildings (residential and non-

residential) was 45% slightly above the European figure, and Industry accounted for 21%, and transport 33% (Figure 2.3) (Bureau of Energy Efficiency, 2006).

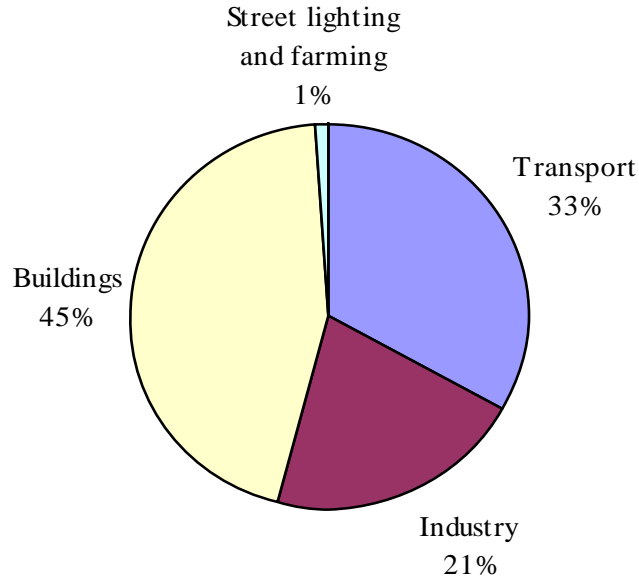


**Figure 2.3: Breakdown of UK energy consumption per sector (Bureau of Energy Efficiency, 2006)**

According to scientists, climate change will affect the world in extreme and unpredictable ways, bringing with it huge cost to the economy, environment and society. The sustainability has now become an issue and how buildings can become part of it and still keep a comfortable, safe healthy and productive environment. To achieve this, the following systems are used: Space heating devices, Domestic hot water heating systems, Lighting, Mechanical ventilation systems, Air conditioning and general electrical services such lifts; and every one of the system requires electricity or gas to operate. In the UK the majority electricity or gas is produced in power stations by the combustion of fossil fuels,

which release a huge amount of (CO<sub>2</sub>) and damage the environment. Therefore energy conservation in the building should be important to reduce cost and environment consequences of unsustainable energy consumption.

## **2.2 Carbon Footprint**

There is no universal definition of a carbon footprint and in addition, the term “Carbon footprint” has been used on scientific literature, publications as well as general media without being clearly defined in scientific community (WRI, 2005). The carbon footprint definitions vary in terms of the level and scope of a carbon footprint being assessed (Wiedmann & Minx, 2007). Recent research by Wiedman and Minx shown that some carbon footprint definitions by the World Resources Institute, (2005); Wiedmann & Minx (2007); and Trust (2004) mention carbon dioxide and others such as BP (2007); Patel(2006); Energetics (2007); POST (2006); ETAP (2007); Grubb & Ellis (2007); and The Carbon Trust (2006) include all Kyoto greenhouse gases (see Table 2.1) and measure emissions in terms of ‘Carbon dioxide equivalents’. And the approach of assessing, the carbon footprint range varies from simple online calculation to complex life-cycle analysis (BP, 2007).

The Edinburg Centre for Carbon Management (2008) defined a Carbon Footprint as a measure of the greenhouse gas (GHG) emissions related with individuals, a company activities or products. The Carbon Trust (2007) described the term “Carbon Footprint” as the total amount of CO<sub>2</sub> and other greenhouse gas (GHG) emissions for which an organisation or an individual is accountable. The World

Resources Institute (2005) describes the carbon footprint as follows: “a representation of the effect you, your buildings, or your organisation, have on the climate in terms of the total amount of greenhouse gases produced (measured in units of carbon dioxide)”. Parliamentary Office of Science and Technology (POST , 2006) also defined “A ‘Carbon footprint’ as the total amount of CO<sub>2</sub> and other greenhouse gases, emitted over the full life cycle of a process or product. It is expressed as grams of CO<sub>2</sub> equivalent per kilowatt hour of generation (gCO<sub>2eq</sub>/kWh), which accounts for the different global warming effects of other greenhouse gases.”

**Table 2.1 : The Kyoto protocol’s Greenhouse gases (IPCC, 2007)**

Kyoto gas	(GWP)*	Example source
Carbon dioxide (CO <sub>2</sub> )	1	Burning fossil fuels
Methane (CH <sub>4</sub> )	23	Cattle, landfill sites, leaks from disused mines, burning fossil fuels.
Nitrous oxide (N <sub>2</sub> O)	296	Emissions from fertilized soils, burning fossil fuels.
Perfluorocarbons (PFCs)	4,800 – 9,200	Electronics industries, fire extinguishers
Hydrofluorocarbons (HFCs)	12- 12,000	Leaks from air conditioning and refrigeration systems. LPG storage

\*GWP: **The Global Warming Potential** of a gas is its relative potential contribution to climate change over a 100 year period, where CO<sub>2</sub>=1

Nearly everything that we do produces Greenhouse Gas (GHG) emission (see Figure 2.3) either directly or indirectly (The Edinburg Centre for Carbon Management, 2008) and (Carbon Trust , 2007), however the most important greenhouse gas which concerned human activities is carbon dioxide (IPCC, 2007) and the direct GHG emissions source are usually easy to identify-for instance those from burning fossil fuels for electricity generation or space and water

heating. For an organisation or individual a carbon footprint can be broken down by activity as shown in the Figure 2.4. This project is focus to develop a heating device that can contribute to achieving zero-carbon buildings, thus 100% Carbon footprint reduction against a baseline of current building regulation Part L1a from energy usage and fabric of typical residential buildings in the UK.

Considering the definition of the Carbon Trust and the World Resource Institute, the Carbon footprint of a building can be defined as the amount of CO<sub>2</sub> for which the house is responsible. Most commonly described as direct emissions which result from combustion of fuels which produce CO<sub>2</sub> emissions (Patel, 2006), such as the gas used to provide hot water or space heating, and electricity used for equipments and lighting.

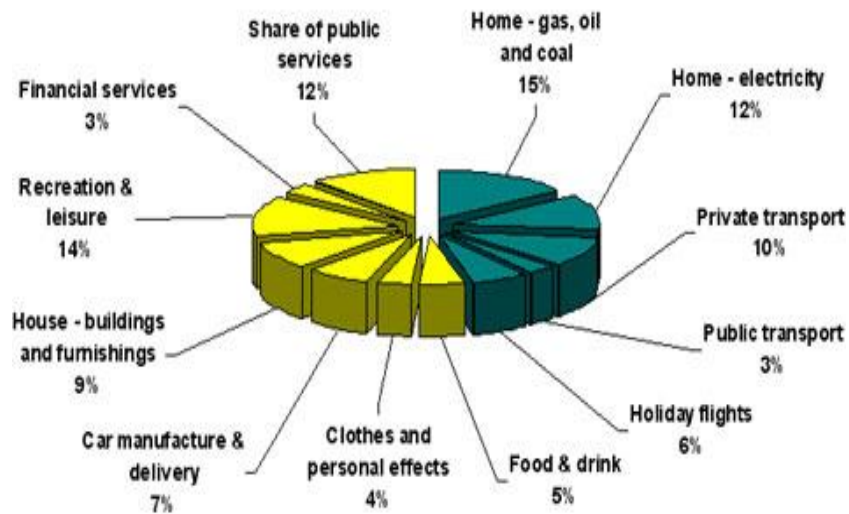


**Figure 2. 4:** This pie chart above shows the main elements which make up the total of a typical person's carbon footprint in the developed world (**Home of Carbon Management, 2011**).

In addition the building should also be responsible of the amount of CO<sub>2</sub> emitted into environment through its fabrics (walls, windows, doors or floor). However the basic steps needed to work out a carbon footprint whether it is a house, an organization, or production line, are as follow:

- 1- Establishment of assessment boundaries (see Figure 2.5).
- 2- Gathering data.
- 3- Calculation of carbon footprint emission.

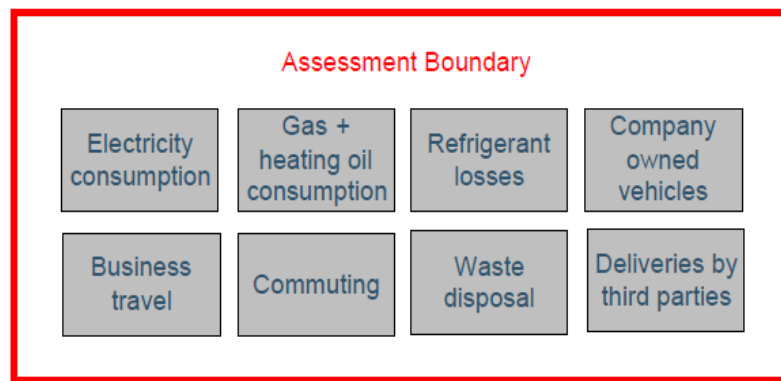


*Figure 2.5: Carbon footprint evaluation boundary (BP, 2007)*

### 2.3 Patterns of energy consumption in building

Pattern of energy used in the building is depending on the human activities for instance there are places of education, work, entertainment and living, and each individual building for example, residential building, hotels will have a different pattern of energy consumption throughout each day of the year. *Figure 2.4* shows the breakdown of the total energy consumption of a typical UK domestic property (Energy Use in Office, 1998). The pie chart in *Figure 2.6* has been drawn to

illustrate where the energy goes in buildings. It also shows that space heating energy is the largest, about 84% of all energy consumption.

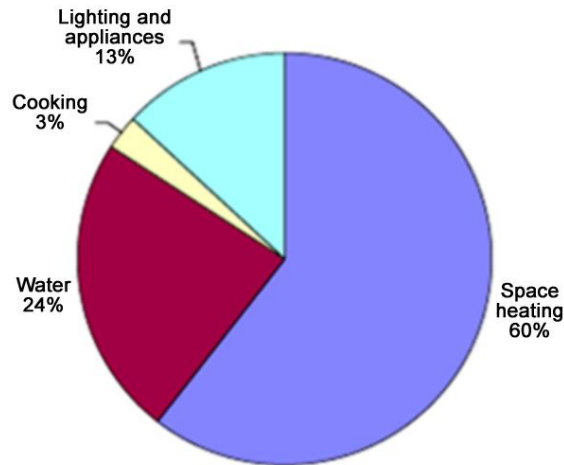


**Figure 2.6:** Breakdown of buildings energy consumption (Grubb & Ellis, 2007)

In addition to normalise energy consumption for the purpose of allowing a comparison, the total energy consumption in any building depends on climate, installed services, the building fabric and the floor area treated by the services (Nicholls, 2006). The energy consumption of a building is usually divided by the total annual energy used by its treated floor area. This gives energy consumption in kilowatt hours per square metre per year (kWh/m<sup>2</sup>/y).

### 2.4 Energy Performance Certificates

Under the Energy Performance of Building Directive, in the UK on the 1<sup>st</sup> August 2007, the UK Government introduced Energy Performance Certificates. These certificates indicate the environmental impact of a home and how energy efficient it is on a scale of ‘A’ to ‘G’. An ‘A’ rated home is the most energy efficient and

has lowest carbon dioxide emissions. From 2009, Energy Performance Certificates has been mandatory for all new and existing homes when sold or leased. It has also been required to be providing these certificates at the point of purchase or sale.

### **2.5 The Code for Sustainable Homes**

To fully implement EPBD; on 13<sup>th</sup> December 2006, the Department for Communities and Local Government has announced a strategic decision and published the Code for Sustainable Homes referred to in this project as “the Code”, “*A Step Change in the Sustainable Home Building Practice; 2006*” (Communities and Local Government, 2008). the UK Government believes that over the next 10 years, about 3 million of more homes will needs to be added to the UK housing stock (Wiedmann & Minx, 2007) and this could cause Carbon Dioxide (CO<sub>2</sub>) increases in the environment, since the average newly built home in the UK releases 0.86 tonnes of carbon a year, which come from lighting, appliances, space heating and Domestic Hot Water (DHW) heating (EPBD, 2003).

The Code measures the sustainability of a new home against categories of sustainable design, rating the ‘whole home’ as a complete package and uses a scale of 1 to 6 star rating system to communicate the overall sustainability performance of a new home (see Table 2.2 below), with 6 being the highest

sustainability standard, 100% of CO<sub>2</sub> reduction from the 2006 Building Regulations 'Part L1A level.

The Code level points are awarded across 9 key design categories:

- Energy efficiency/CO<sub>2</sub> (minimum mandatory standard at all levels)
- Water efficiency (minimum mandatory standard at all levels)
- Surface water management
- Site Waste Management
- Household Waste Management
- Use of Materials (minimum standard at Code entry level, 1)
- Health and wellbeing
- Ecology
- Lifetime homes (applies to Code Level 6 only)

And each category has specific assessment criteria, which must be met for credit to be awarded. In addition for five of these assessment issues, such as Energy, CO<sub>2</sub>, and Water, minimum standards are set which must be achieved before the lowest level of the Code can be awarded. However for Energy/CO<sub>2</sub> and Water minimum standards are mandatory at each level of the Code (see Table 2.2).

**Table 2.2: Levels in the Code of sustainable Homes (Communities and Local Government, 2008)**

Level and star	Levels in the Code of sustainable Homes					
	1 <sup>*</sup>	2 <sup>**</sup>	3 <sup>***</sup>	4 <sup>****</sup>	5 <sup>*****</sup>	6 <sup>*****</sup>
Energy/CO <sub>2</sub> (% required reduction CO <sub>2</sub> emission )	10%	18%	25%	44%	100%	<b>'Zero Carbon Home'</b>
Points for minimum performance for energy and water (Mpts)	2.7	5.0	10.3	13.9	23.9	25.1
Additional points required (Apts)	33.3	43.3	46.7	54.1	60.1	64.9
<b>Total points required for code level (Mpts + Apts)</b>	<b>36</b>	<b>48</b>	<b>57</b>	<b>68</b>	<b>84</b>	<b>90</b>

In table 2.2, Energy and Carbon Dioxide are based on the Target Emission Rate (TER) as used in the Part L1A of the 2006 Building Regulations. This means for Level 1 the home will have to be 10% more energy efficient than one built to the 2006 Building Regulations standards (Communities and Local Government, 2008).

From 2016, it will be mandatory for new homes to be “zero carbon”. Low carbon distributed energy technologies will be a key for developers to meet this requirement. Two ways of reducing the carbon dioxide emitted from buildings have been suggested. The first one it is to cut down on the amount of fossil fuel used, the second one it is to replace fossil fuel or partly based energy with renewable forms of energy that do not emit carbon dioxide when used; that is the reason why low-energy solutions for house heating and domestic hot water (DHW) generation are more and more investigated. In this regard, in the past decade, many researchers are given more attention to improve the efficiency of the heat pump system. Since energy efficiency/CO<sub>2</sub> is one the greatest requirement to achieve the highest Code Level standard, Therefore the ambitious

UK government target can only be achieved with high efficient space and water heating technology.

## 2.6 Technology/fuels to provide space and/or water heating for residential buildings

There are primarily nine varieties of heating system for buildings that are being used and it is not straight forward to formulate which system is best in terms of environment, economy and comfort, since each system has its own advantages and limitations (Wachter, 2009). This section reviews heating technologies applicable to residential buildings.

*Table 2. 3: Nine varieties of heating system for residential buildings*

<b>Technologies /fuels</b>	<b>Advantages</b>	<b>Limitations</b>
<b>Natural gas</b>	<i>Most environmental fossil fuel, especially when burned in a high efficiency boiler with heat recovery</i>	<i>-requires a gas network -Produces CO<sub>2</sub> when burning</i>
<b>The oil boiler</b>	<i>-Can use a similar system to the gas boiler -Does not require a network</i>	<i>-Expensive compare to others -Require a storage tank -Produces CO<sub>2</sub> when burning</i>
<b>Electrical heating</b>	<i>-efficient heating system -environmental friendly when electricity is generated from low carbon sources - works efficiently if the house or building is well insulate</i>	<i>- when electricity is generate from fossil fuel Produces CO<sub>2</sub> when burning -electricity is more expensive compare to gas -renewable energy power technologies are also due to the initial cost of installation</i>
<b>The heat pump</b>	<i>-very high efficiency -a best practice solution for relatively large buildings in temperate to cold climates (Energetics , 2007) -cost-effective if there is a</i>	<i>-requires low temperature heating system, such as underfloor heating to perform efficiently -requires large space -high initial cost</i>

	<p><i>sufficient heating demand</i>  <i>-could be use for both heating and cooling</i>  <i>-not generates CO<sub>2</sub> if renewable energy is use to supply the compressor and circulating pump</i></p>	
<p><b>Micro CHP</b>          (Combined Heat and Power)</p>	<p><i>-produces electricity and heat from one fuel</i></p>	<p><i>- use natural gas, or biomass</i>  <i>-requires matching heat and electricity demand</i>  <i>-produce too much heat for well insulated building</i>  <i>- Produces CO<sub>2</sub> when burning</i></p>
<p><b>District heating</b></p>	<p><i>-very good for cold climates</i>  <i>- the investment is justify if the buildings are well insulated</i></p>	<p><i>- Produces CO<sub>2</sub> when burning</i>  <i>- with a central CHP plant is only efficient in (compact) cities where buildings have a sufficient heat demand (Yumus, Cengel, &amp; Michael, 1998)</i></p>
<p><b>Coal stoves</b></p>	<p><i>-Produces comfortable heat atmosphere</i>  <i>-Fairly good efficiency</i></p>	<p><i>-CO<sub>2</sub> emission are high</i>  <i>-old technology</i></p>
<p><b>Biomass</b> (wood or wood pellets)</p>	<p><i>-may be consider as renewable</i></p>	<p><i>- CO<sub>2</sub> emission when burning</i>  <i>-lack of wood pellets distribution points</i></p>
<p><b>Solar thermal energy</b></p>	<p><i>-solar water boiler can be combined with low temperature heating for good efficiency</i>  <i>-not produces CO<sub>2</sub> emission</i></p>	<p><i>-low efficiency</i>  <i>-requires good sun</i></p>

The technologies recognised by the UK's Department of Business Enterprise and Regulatory Reform (BERR) (Communities and Local Government, 2008) and Low Carbon Building Programme (LCBP) are listed below, they may be considered under the Code as part of a low or zero carbon emission solution are :

- Solar (Solar Hot water , Photovoltaic)
- Biomass (single heaters/stoves, boilers, or community heating schemes)
- Combined Heat and Power (CHP) and micro CHP for use with the following fuels, natural gas, biomass, or sewerage gas and other biogases
- Community heating, including utilising waste heat from process such as large scale power generation where the majority of heating comes from waste heat
- Heat pumps (Air source heat pumps, Ground source heat pumps, or geothermal heating system) and to comply with the Code the heat source must be from a renewable source, for example soil, ground water and water source.

The overall efficiency of a domestic heating system usually depends on different factors including the type of fuel and heat distribution system installed in the house. Heat can be generated by a variety of fuel and is usually distributed to individual rooms by either forced-air ductwork, or hydronic (water filled) pipes. However, some well insulated low energy houses may not need any heating distribution system at all, they usually relying on centrally located woodstove or on individual point source space heaters.

Heat distribution system operates at different temperature, therefore it is important that a distribution system is properly designed, installed and operated to ensure maximum energy efficiency and comfort levels. Table 2.4 shows the

different operational temperatures range required for each building’s heating distribution system to operate at an adequate performance in the UK homes and Europe.

**Table 2. 4:** Typical delivery temperatures for various building heating distribution systems (Energetics , 2007)

Indoor heat distribution system	Heat carrier temperature °C
underfloor heating	30-45
low temperature radiator	45-55
(hydronic ) conventional radiators	60-90
forced-air ductwork (Air system )	30-50

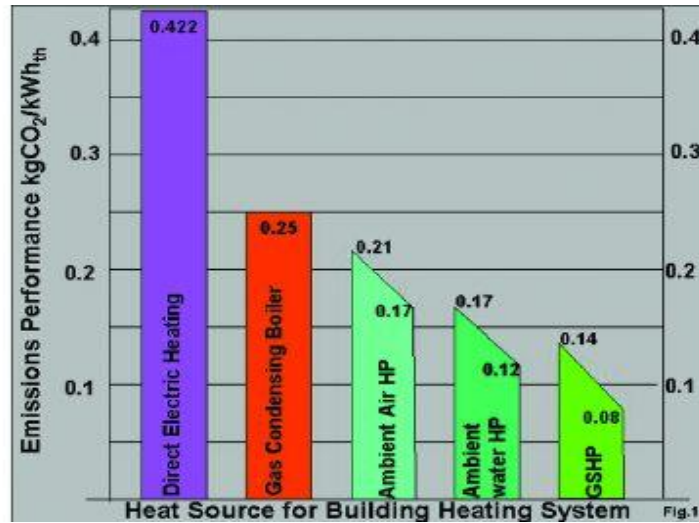


**Figure 2. 7 :** Heat pumps achieve lower carbon-dioxide emissions than other forms of heating with ground-source heat pumps performing best of all (WYATT, 2004).

Heat pumps, with carbon-dioxide emissions being 50 to 60% lower than even a gas-fired condensing boiler (see Figure 2.7), they have a key role to play in a low-carbon future in the UK and have the capability to achieve low or zero-carbon

heating system for the Code houses. Compare to other domestic heating system (Table 2.3 and Figure 2.5) Heat pumps systems have the potential to improve thermal comfort, at lower energy costs and also to reduce CO<sub>2</sub> emissions up to 100% if the fuel source is from renewable. Analysis by the Environmental Protection Agency determined that GSHP had the highest source heating season performance factor (SPF).

## **2.7 Overview of the Heat Pump and Performances**

### **2.7.1 Heat pump**

A heat pump is a mechanical device that uses external power such as electricity to transfer heat from a lower temperature heat source to higher temperature. The heat pump for heating in the residential sectors can supply 3 times or more energy for space and water heating than high—grade energy it consumes thereby making it attractive technology for future zero-carbon homes in the UK. The heat pump is relatively complicated technical device which consists of four main components (evaporator, compressor, condenser and expansion valve) in a refrigerant circuit loop (see Figure 2.8); and any others components (receiver, filter, and sight glass) beyond these basic 4 are identified as accessories.

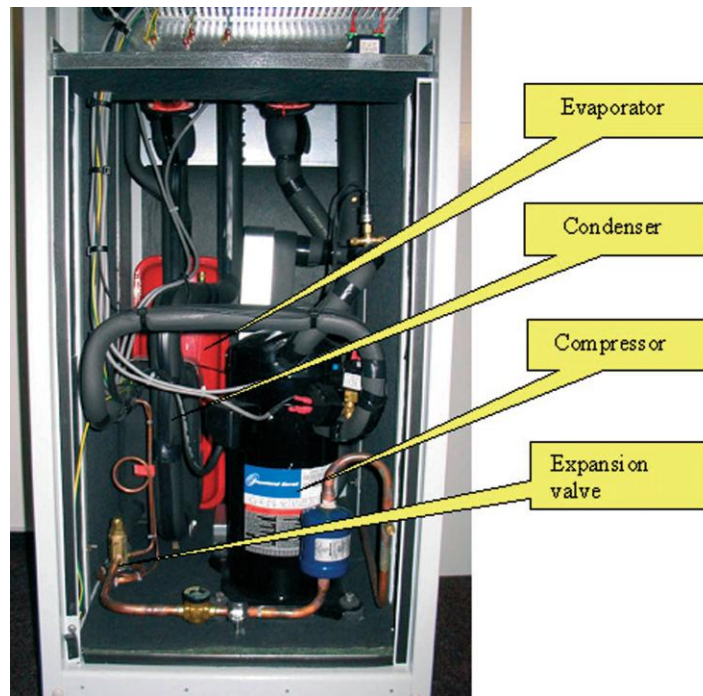


*Figure 2. 8: Four main components of the Refrigerant Loop of a Heat Pump*

### 2.7.2 Classification of heat pump technology

There are a wide range of heat pumps, which may be classified according to the purpose of application; they are available in many types, shapes and sizes and those operating on the vapour compression cycle are the most popular and are used for space and water heating in buildings. Classification of heat pumps for heating in buildings was first adopted in the United State (US) standards (2009), which categorises heat pumps by heat source and heat distribution or heat carrier, working fluid in the building. Table 2.5 shows the classification of common types of heat pump.

Table 2. 5: Classification of heat pumps for heating of buildings

Heat source	Heat carrier	Term used to classify the heat pump	Description used by heat pump suppliers
<b>Water</b> ( <i>lake, river, or sea</i> )	Warm water	Water to water heat pump	Ground soil or Underground water–GSHP
<b>Water</b> ( <i>lake, river, or sea</i> )	Warm air	Water to air heat pump	
<b>Air</b> ( <i>ambient or exhaust air</i> )	Warm water	Air to water heat pump	Air source heat pump (ASHP)
<b>Air</b> ( <i>ambient or exhaust</i> )	Warm air	Air to air heat pump	
<b>earth</b> ( <i>ground or rock</i> )	Warm water	Soil to water heat pump	Ground source heat pump –GSHP
<b>earth</b> ( <i>ground or rock</i> )	Warm air	Soil to air heat pump	
Solar radiation	Warm water	Solar radiation to water heat pump	Solar heat pump (or solar assisted heat pump-SAHP)
Solar radiation	Warm air	Solar radiation to air heat pump	

This work focused on the ASHP and the GSHP for space and domestic hot water heating in terms of improvement their coefficient of performances (COPs) and the factor affecting them. In addition, some new technologies, which have been suggested to improve their COP when heat demand is at the peak, have also been examined.

### 2.7.3 Heat source for heat pump

In most countries in the Europe and mainly in the UK, full air conditioning (heating and cooling) is not necessary or cost effective for domestic application. The “**heating only**” heat pump is the most promising system to compete with conventional fossil fuel devices. The operating characteristics and the

performance of a heat pump are largely determined by the characteristic of the heat source and the lift (see Chapter 1). The main heat source for heat pumps providing space heating and hot water is likely to be air, water or ground. However Table 2.6 shows summary of commonly used heat sources for domestic heat pump system and also details their advantages and limitations.

It is important that future research addresses the following aspects, if widespread economic operation of heat pumps is to be achieved for Code Levels houses:

- a) Reduction of the temperature difference between the delivered heat and the heat source.
- b) Analysis of different types of heat resource, which should ideally be available at any time at the highest possible temperature.
- c) Analysis of different types of heat pump technologies so that there is little energy consumption by the compressor, in order to minimise operating cost and improve overall COP.
- d) Identify heat sources for mass-produced, domestic heat pumps with little or no dependence on geographical situation, climate and soil conditions.

The remaining part of this chapter focused on the review of ASHP and the GSHP for space and domestic hot water heating in terms of their coefficient of performances (COPs) and some factors affecting them, moreover some important theories necessities to understand this work;. In addition, limits of new

technologies, which have been suggested to improve their COP when heat demand is at the peak, have also been examined.

**Table 2.6: Characteristics of heat sources for heat pump (CUBE & Fritz, 1981)**

<i>Heat source/properties</i>	<i>Air</i>	<i>Earth</i>	<i>Solar radiation</i>	<i>Ground water</i>	<i>Sea water</i>	<i>River water</i>
<i>Availability (locality)</i>	Everywhere	Only for buildings with open space around	Everywhere	Not ensured	Only exceptionally	In large towns
<i>Availability (Time)</i>	Always	Always	Very changeable unpredictable	Always, unless water shortage	Always, unless water shortage	Always, unless restricted
<i>Investment costs</i>	Comparatively small	High	High	Depends on cost of drilling well, usually high	Comparatively low	Lowest
<i>Operating costs</i>	Medium	Low	Very low, depending on design of solar collector	Low if drained into second well	Comparatively low	Lowest
<i>Temperature and temperature fluctuations (approximate values)</i>	-15 to +15° C, for 90% of the heating season above 0°C. Running counter to heat demand of the building	-5 to 15°C. Becoming cooler only towards end of heating season.	Above 0°C. running counter to heat demand	+10 to +15°C, constant	0 to 15°C, no longer usable below +2°C	+5 to +15°C
<i>Space requirements</i>	Large	Equipment occupies minimum space	Large construction	Small for equipment, space required for well(s)	Small	Small
<i>Suitability for mass production</i>	Good	Medium	Medium	Good	Good	Good

<p><b>Special characteristics and issues</b></p>	<p>In winter when heat demand is highest, lowest output available. Icing-over of outside coil necessitates automatic defrosting, large output for balancing, second heat source or additional heating. Control difficult because of large temperature fluctuations. Noise problem with external evaporator.</p>	<p>Limited by geological conditions (no rock). Installation costs difficult to estimate. Repairs to pipe coils almost impossible. Approximately 30 m<sup>2</sup> surface required per 1.16kW output. Danger of freezing when one farms on around the ground</p>	<p>Special constructional measures on south side of building or on roof. Free space facing east, south and west. Heat store or second heat source required. Approximately 2 m<sup>2</sup> solar collector surface required per 1.16kW.</p>	<p>Danger of corrosion or deposits in evaporator. Draining into public drains or second well required. Water temperature, composition and quantity mostly unknown before drilling. Water Board restrictions</p>	<p>Possibility of corrosion, deposits and algae growth. Provisions required in case temperature too low (additional heating). Water Board restrictions</p>	<p>Corrosion and deposits possible. Water Board restrictions</p>
--	---	---	--	---	--	--

#### 2.7.4 Heat pump theory

The intention of this section of the report was to look at some necessary theoretical background of the heat pump. Since the good understanding of the theory will help one to appreciate the limitation of the ground or air source heat pump. These limitations are imposed not only by mechanical and engineering problems but also by the laws of nature. As mentioned in the previous paragraphs, the most common type of heat pump cycle for building application is the mechanical vapour compression heat pump cycle (see Figure 2.7).

As illustrated in the *Figure 2.7*, the configuration of a domestic heat pump system, which consists of three main loops all linked by heat exchangers (evaporator and condenser), *loads side loop*, *refrigerant loop*, and *heat source loop*, but in the case of Direct Expansion (DX) heat pump system, the loops are reduced to two, refrigerant loop and loads loop; and linked by one heat exchanger (condenser).

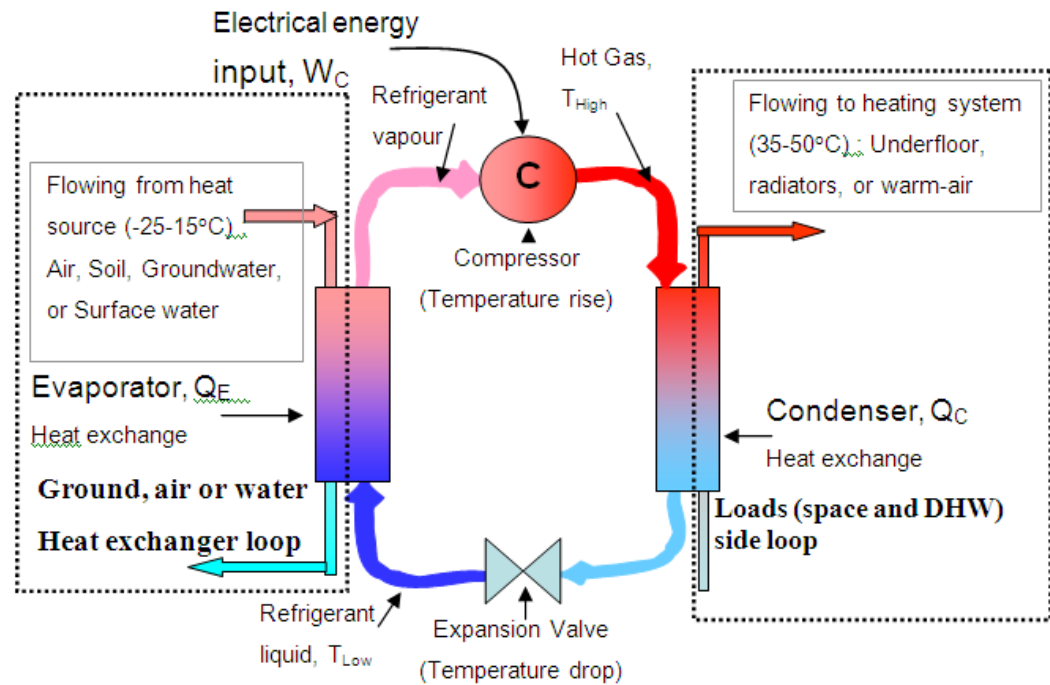


**Figure 2. 9:** Thermodynamic model of heat pump vapour compression cycle

In the refrigerant cycle as shown in the Figure 2.9, the heat pump requires a work input ( $W_C$ ) to remove heat from the low temperature ( $Q_E$ ) side (evaporator) and to deliver it to high temperature ( $Q_H$ ) (condenser); in the ideal case, heat is delivered isothermally at  $T_{High}$  and collected isothermally at  $T_{Low}$ .

### 2.7.5 Ideal Vapor-Compression Cycle

Pressure-enthalpy diagram defines the thermodynamic properties for the refrigerant in use and the performance of equipment. In the ideal cycle (see Figure 2.10), the refrigerant leaves the evaporator and enters the compressor as saturated

vapour. However, in practice, it might not be possible to control the state of the refrigerant so precisely. Therefore is worth to overdesign for slightly superheated (+ 2 °C) at the compressor inlet.

For heat pumps Process: the working fluid (refrigerant) undergoes four main thermodynamic states, from evaporation, compression, condensing and expansion.

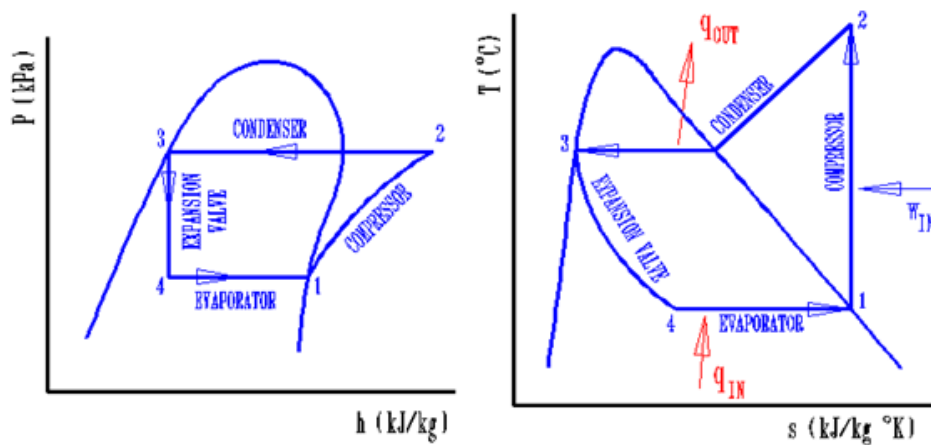


Figure 2.10: Thermodynamic model of heat pump vapour compression cycle

Pressure-Enthalpy (P-h) and Temperature-Entropy (T-S) diagrams shown in the Figure 2.10, illustrate the four mains processes of the refrigerant as follow:

*1-2 isentropic compression:* In an ideal vapour-compression refrigerant cycle, the working fluid enter the compressor at the state 1, as saturated vapour and is then compressed isentropically in the compressor at the condenser pressure; the temperature of the refrigerant increases during this isentropic compression

process to well above the temperature of water medium. The refrigerant then enters the condenser as super-heated vapour at state 2;

*2-3 Constant pressure heat rejection:* the super-heated gas at state 2 and leaves as saturated liquid at state 3 as result of heat rejection to the condenser or to the water medium;

*3-4 throttling, isenthalpic:* at the expansion valve, the temperature of the refrigerant at state 3 still above the temperature of the heat source, the saturated liquid refrigerant is then expanded to the evaporator pressure by passing through an expansion valve or capillary tube, and during this process the temperature of the refrigerant drops below the heat source temperature, the refrigerant enters the evaporator at state 4, as a low-quality saturated mixture (liquid and vapour);

*4-1 constant pressure and temperature heat addition:* in the evaporator, at state 4, the refrigerant completely evaporates by absorbing heat from the heat source, then leaves the evaporator at state 1, as saturated vapour and reenters the compressor at state 1, then ready to continue the cycle.

### **2.7.6 Heat pumps' working fluids**

A refrigerant is a fluid used for heat transfer in a heat pump system. Most refrigerants absorb heat during evaporation at low temperature and low pressure and reject heat during condensation at a higher temperature and higher pressure. The two sides of the condenser have different working fluid, on the first side is refrigerant and the second side could be water only in the hot climate with no winter period such as Africa or water/antifreeze mixture in the climate with winter period and according to the type of heat pumps.

#### **2.7.6.1 The impact of the working fluids**

The ability of a substance such as refrigerant to damage the ozone layer is known as the Ozone Depletion Potential (ODP), with 1 been the highest value. In addition the contribution of any chemical substance including refrigerant in the atmosphere to prevent the long wave radiation of the sun to reach the earth, which results in global warming and climate change. This contribution to global warming is known as the Global Warming Potential (GWP); it represents how much a given mass of substance contributes to the global warming, over given period of time, compare to same mass of Carbon Dioxide (CO<sub>2</sub>), which was given the value of 1.

Historically, refrigerant such as, R-717 ammonia, R40 methyl chloride (CH<sub>3</sub>Cl) and R764 sulphur dioxide (SO<sub>2</sub>) used in vapour compression systems were toxic, explosive and/or flammable, in 1920s, because of the methyl chloride leakage

from most domestic refrigeration systems using these refrigerants, serious health problems and several fatal deaths around the world were reported (Markowitz, Rosner, Deceit, & Denial, 2002). In 1930, General Motors (Markowitz, Rosner, Deceit, & Denial, 2002) charged Thomas Midgley, with the developing a non-toxic and safe refrigerant for household appliances. He discovered dichlorodifluoromethane, a chlorofluorocarbon (CFC) which he called Freon; it is colourless, nearly odourless liquid, with boils point at room temperature. This then replaced the various toxic and explosive refrigerant previously used as the working fluid in heat pumps and refrigerators. There are different variant of the Freon, some are made with organic compounds containing, hydrogen, carbon and fluorine, and some halogens such as chlorine. The first refrigerant from R22 was Freon, hydro chlorofluorocarbon (HCFC), made in 1936. However some variant of the Freon such as the CFC-11, trichlorofluoromethane or R-11 and CFC-12, dichlorodifluoromethane or R-12 have serious negative impact on the environment, CFC-11 has the greatest ODP of 1, and others substance are quoted relative to it. CFC-11 and CFC-12 also have a greater GWP which are respectively 4000 and 8500 (World Resources Institute, 2005). In order to reduce the environmental damage due to refrigerants, alternative refrigerants have been introduced, using a so called method of blends, the mixture of existing refrigerants. The promising alternative for eventually replacing R-22 in heat pumps is R410A (blend of R32 and R125), another blend is R407C (R32, R125

and R134a) which is more environmentally friendly refrigerant, with relatively low GWP and nearly zero ODP. It already used as the substitution of R22 in the heat pump applications.

#### **2.7.6.2 Side 1: Primary Refrigerant**

If high environmental benefits have to be achieved with heat pump system, a careful selection of the refrigerant is important. Ideal refrigerants should have good thermodynamic properties. The desired properties of a refrigerant is summarised in the *Table 2.7* below.

Water, ammonia, carbon dioxide and hydrocarbons (HC) are natural and environmentally friendly refrigerant; they have zero ODP and very low GWP and they also are cheap. Water is an excellent refrigerant with good thermodynamic properties, since it is neither toxic nor flammable.

*Table 2 7: The desired properties of refrigerants' heat pump*

<b>Property</b>	<b>Desired</b>	<b>Explanation</b>
Critical temperature	>condenser Temp.	To approach the Carnot cycle and hence achieve high COP
Freezing temperature	Low	Liquid only in evaporator. No freezing
Saturation pressure	>atmospheric	Avoid air leaks into the system.
Evaporation enthalpy	High	Reduces mass flow rates and high COP
Condensation pressure	Low	To reduce the strength requirements of the condenser and seals
Viscosity	Low	To reduce pumping power and frictional pipe loses
Specific volume	Low	Reduces compressor work and system size
Thermal conductivity	High	Good heat transfer rates
Toxicity/irritancy	Low	Avoid poisoning. Convenient handling
Ozone depletion	None	Prevent ozone layer depletion
GWP	None/very low	<1
Cost	Low	

However it is not suitable for domestic heat pump system because of its high range of temperatures from 80°C – 300°C of operation to be evaporated. CO<sub>2</sub> is a good refrigerant for vapour compression cycles as it is non-toxic, non-flammable has high volumetric refrigeration capacity and it is compatible with normal lubricants. However, it is non condensable at typical condenser pressure and temperatures and the theoretical COP is low. Regarding ammonia is also a very good refrigerant but it is toxic, flammable and highly corrosive to copper alloys and also it not accepted by the regulation on the domestic heat pump system.

### **2.7.6.3 Side 2: secondary refrigerants, water or water/antifreeze**

The secondary refrigerant in the heat pump system is generally water or a mixture of water/antifreeze. The secondary refrigerants have the functions of transferring from the ground to the heat pump in the case of GSHP and from the air to the heat pump in the case of ASHP, or working as a heat transfer medium between the heat pump condenser unit and the underfloor heating.

The secondary refrigerants should have an adequate protection against freezing since it operates in the low temperature as extracted heat from the ground or the ambient temperature at about  $-5^{\circ}\text{C}$ . Water as single refrigerant is corrosive and has a freezing point of  $0^{\circ}\text{C}$ , so water to be use in the lower temperature like  $-5^{\circ}\text{C}$ , so to reduce its freezing point solutions such as antifreeze solutions such as glycols is added.

## **2.8 Coefficient Of Performance (COP)**

The coefficient of performance of any heat pump cycle is defined as the ratio of the heating effect ( $Q_H$ ), to the net work required to achieve ( $W_C$ ) that effect.

### **2.8.1 Carnot heat pump COP:**

The Carnot cycle is a totally reversible cycle that consists of two reversible isothermal and two isentropic processes. This cycle has the maximum thermal efficiency for given temperature limits between the evaporator and the condenser

and it also serves as a standard which actual vapour compression cycles can be compared to. For the Carnot heat pump cycle:

$$COP_{\max} = \frac{T_{High}}{T_{High} - T_{Low}} \quad (2.1)$$

$$COP_{\max} = \frac{1}{1 - \frac{T_{Low}}{T_{High}}} \quad (2.2)$$

Equation (2.1) represents the *maximum* theoretical coefficient of performance for heat pump cycle operating between two regions at temperatures (in Kelvin)  $T_{Low}$  and  $T_{High}$ , for evaporator and condenser respectively. In addition a study of equation (2.1) and (2.2) has shown that as the temperature,  $T_{Low}$  of the evaporator increases the coefficient of performance of the Carnot heat pump increases. This quality is also exhibited by actual heat pump systems.

The COP of the heat pumps depends on many factors such as actual temperature lifts, distance between heat exchangers, the temperature of low-energy source, the temperature of delivered useful heat. Among those factors, the temperature of the heat source at the evaporator is the most important, therefore this work focuses on the evaporator design to enhance the COP of ASHP and GSHP for DHW and space heating, but this is not to suggest that other factors are of lesser importance. Therefore for successful application of heat pump is dependable of the cheap, reliable, and relatively high temperature heat source for the evaporator.

With the increase in mass-produced heat pumps, it is now clearly recognised that using external air was not the ultimate solution and therefore the search for a more suitable heat source is important. For instance, in winter, there are problems with the use of surface water or air because freezing limits their applications. Research concerning heat sources, and their most effective utilisation is as important to development of efficient heat pumps. The development of measures to improve the utilisation of heat sources is vital to increase the COP of heat pumps. A 'rule of thumb' is that the COP improves by 2% or 3% for each degree ( $^{\circ}\text{C}$ ) the evaporating temperature is raised, or the condensing temperature is lowered (Communities and Local Government, 2006). If it is possible to improve the efficiency of equipment by 10 to 15%, and to raise the average temperature of the cold side by 5 to 10 K by improving the utilisation of heat sources and the necessary heat exchangers, then the overall economics of heat pump for home heating becomes increasingly attractive (Bureau of Energy Efficiency, 2006).

Therefore in the real world for domestic heat pump, in the source side, for evaporator to have a high temperatures, the heat source suppose to be high temperatures, reliable and available all the year around. And in the building side, in order to reduce the condenser temperature the buildings 'envelops have to be energy efficient with low u-values.

### **2.8.2 The effectiveness of a heat pump :**

The effectiveness of a heat system is defined as the ratio of the actual COP of the heat pump of to the reverse Carnot cycle COP. The typical heat pump system effectiveness is in the range of twenty to twenty five per cent. However by increasing the COP of the actual heat pump, the effectiveness of a heat pump system can be increased and energy consumption at the compressor reduced. In order to evaluate the effectiveness of the actual heat pump system; for the Carnot cycle operation temperatures, the low temperature of the evaporator is the maximum temperature of the actual cycle, and the high temperature minimum temperature of the actual heat pump cycle.

### **2.8.3 Primary energy ratio (PER)**

The COP of a heat pump gives measure to the effectiveness of the system in converting small amount of work into useful one for space and water heating. But it does take into account how the work was produced in the first place. In the case of performance, work is generally more valuable than heat energy. This influences the COP.

The focus of this project is to increasing the yearly performance of heat pump system defined in a Seasonal Performance Factor (SPF). This SPF of the heat pump can be translated into the PER as the amount of useful heating energy delivery divided by the used (fossil) primary energy, it is also defined by the COP multiplied by the efficiency of the generation of the driving energy. In the case of

electric motor, which is common for domestic heat pump system, the average efficiency for power generation in the UK of 43.9% is used (Government memorandum, 2008). After subtraction of the distribution losses in the grid of 2%, 41.9% remains as net average efficiency of Power Generation for electric heat pump. PER can be summarised as:

$$PER = \frac{\text{Useful heat delivered by heat pump}}{\text{Primary energy consumed}} \quad (2.3)$$

$$PER = COP * \eta_{\text{Power Generation}} \quad (2.4)$$

In principal heat pumps can use renewable energy as driving force for electric heat pump systems; consequently the use of fossil fuel becomes zero and the PER becomes infinite.

#### **2.8.4 Seasonal performance factor (SPF)**

Seasonal Performance Factor (SPF) is used to assess the Heat pumps during a season. SPF is also called the seasonal COP of a heat pump. This is a representation of the total energy output (kWh) of a heat pump during a season divided by the total electrical energy used (kWh), to generate heat during the same period, the energy consumption takes into account the energy consumed by the circulating pumps and fans over the season. SPF can be summarised as follow:

$$SPF = \frac{\text{heat gain at the condenser} \left( \frac{kWh}{\text{season}} \right)}{\text{total energy consumption} \left( \frac{kWh}{\text{season}} \right)} \quad (2.5)$$

In case of electrically driven heat pumps, for ASHP, SPF is typically between 1.8 to 2.8; and the SPF for GSHP is typically between 3.0 – 3.8. However for high insulated buildings the optimum value of 4.0 and more can be achieved for GSHP.

## 2.9 Factors affecting heat pumps' performances

### 2.9.1 Factors Affecting the COP of Air Source Heat Pumps

Any air source heat pump will suffer from icing (frosting) of the evaporator with a consequent reduction in COP. It is therefore important that measures are taken to raise the temperature of the evaporator (defrosting) in most applications.

#### 2.9.1.1 Effect of defrost cycle

One of the disadvantages of defrosting method (b) is that the system cannot resume the heating mode smoothly after the defrosting process; the system may also break down due to triggering of the low-pressure switch. In addition, during the reverse-cycle technique, the compressor continues to use energy without heating the building. The monitoring programme of the Edison Electric Institute (Energetics , 2007) concluded that compressor power during defrost accounted for 0.5% of the total heating power; in the UK, trials performed by the Electricity Council (Austin & W.A.I, 1995) indicated the figure to be 1-2%.

The defrosting process could be improved by the addition of a solenoid valve in the defrosting mode; the solenoid would be energised during the defrosting process (Trilliant-Berdal, Souyri, & Fraise, 2006). This would allow the system to resume the heating mode smoothly after defrosting and would improve the overall performance of the air-source heat pump.

#### **2.9.1.2 Losses due to starting and stopping**

Non-continuous operation of the air source heat pump creates losses and poor heating due to starting and stopping. This reduces the COP. The COP could be improved by using a novel salt tower (see section 3.1.4).

#### **2.9.1.3 Losses at part load**

A loss at part load is one of main problems of the air source heat pump. The problem could be improved by one of two methods (1) using a variable speed compressor or (2) using energy storage. The first method is usually less effective and expensive, while the second method (see section 3.4.3) creates a temperature difference in the heat transfer and its application is complex.

#### **2.9.1.4 Heat exchanger between condenser and evaporator**

This is a good option to improve the COP of an air source heat pump, but it makes system complex.

### **2.9.1.5 Vapour density / volumetric capacity**

This factor is related to the size of the machine, but does not have a large effect on the COP.

### **2.9.1.6 Seasonal temperatures - variability with external temperature**

When the external temperature is in the range  $-20^{\circ}\text{C}$  to  $-5^{\circ}\text{C}$ , conventional air source heat pumps have difficulty satisfying the indoor load and COP is reduced. This can be improved by the use of multiple compressors. If however, the external temperature is in the range  $-5^{\circ}\text{C}$  and  $15^{\circ}\text{C}$ , the use of multiple compressors is not essential on either technical or economic grounds.

### **2.9.1.7 Mixture of refrigerant fluids**

Use of a mixture of refrigerant fluids has been proposed as a method to improve COP; however this can complicate system design, particularly if the refrigerants have different boiling points.

### **2.9.1.8 Effect of maximum temperature (tests with different temperatures)**

Heat demand rises as external temperature falls, and the increased temperature difference between ‘heat out’ and ‘heat in’ reduces the heat pump’s COP and cost effectiveness. The situation is exacerbated by the pattern of natural heat sources, i.e., air, soil, ground and surface water and solar radiation, to follow variations in

external temperature through the seasons (see Figure 2.9). Frost formation during winter may lower the practical COP still further.

### **2.9.1.9 Effect of vapour at the entrance to the evaporator**

A saturated vapour contains minimum thermal energy without condensing. The design of the evaporator is therefore crucial to achieving maximum COP.

### **2.9.1.10 Motor efficiency of the heat pump**

The compressor and drive motor, often mounted together as a motor compressor is the most important component of the heat pump system, and is crucial to the COP. If external air is used as the heat source, the compressor must operate over an evaporating temperature range of  $-35^{\circ}\text{C}$  to  $+15^{\circ}\text{C}$  and up to a condensing temperature of  $+65^{\circ}\text{C}$ . Compressor and drive motors must have the highest possible efficiency. Motor compressors for heat pumps, as opposed to refrigeration compressors, must be designed so that as little heat as possible is transferred to the environment, as these losses decrease the usable heat output.

## **2.9.2 Factors Affecting the COP of Ground Source Heat Pumps**

Thanks to a fairly constant ground temperature throughout the year, the *GSHP* can be used to heat and/or cool the building in the long term, if there is no unbalance of the ground at a high efficiency. Throughout the year, the ground has a constant temperature in depth ranging between 6 to 46 m; and they correspond

at the average temperature of the site; at the depth up to 6m, the ground temperature is directly related to climatic conditions; and below the depth of 46m, the ground temperature starts to increase of about 2°C -3°C per 100 m.

The GSHP can supply in the long term at high efficiency, space and domestic hot water heating for buildings. While ground is a convenient heat source for heat pump, it also suffers from a number of disadvantages which call for careful optimisation of heat pump design. Rybach (2000) and Trillat-Berdal & Souyri, (2007) state that the use of a geothermal heat pump with vertical borehole heat exchanger to heat buildings can create annual imbalance in the ground loads; as shown in the *Figure 2.11*; and then the coefficient of performance of the heat pump decreases and consequently the installation gradually becomes less efficient.

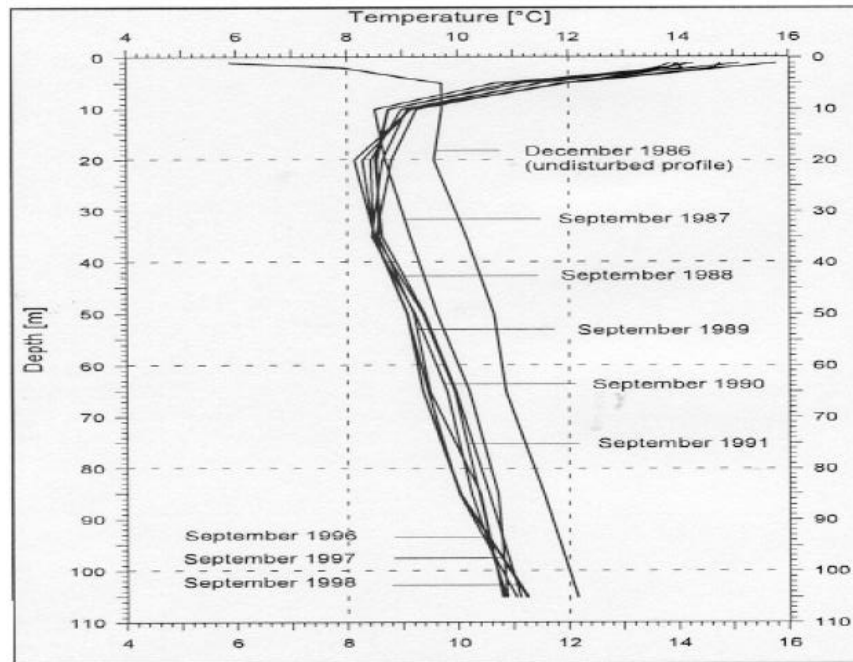


**Figure 2.11:** The annual variation of the ground temperature at a site in Newcastle, UK, throughout years (Kuang, Sumathy, & Wang, 2003)

In the recent work of Wood, Liu, & Riffat (2008) on heat pump performance and ground temperature of a piled foundation heat exchanger, Wood has done tests of the performance of the energy piles with sensors at different depths of the borehole. Results have shown that the ground immediately around the piles/borehole get cooler month by month (see *Figure 2.12*), and consequently could significantly affect the COP after 5-10 years cycle. In addition, at 1m distance the

change in temperature becomes much greater and results in a reduction of 2.5 °C in excess of seasonal change (Wood C. J., 2008).

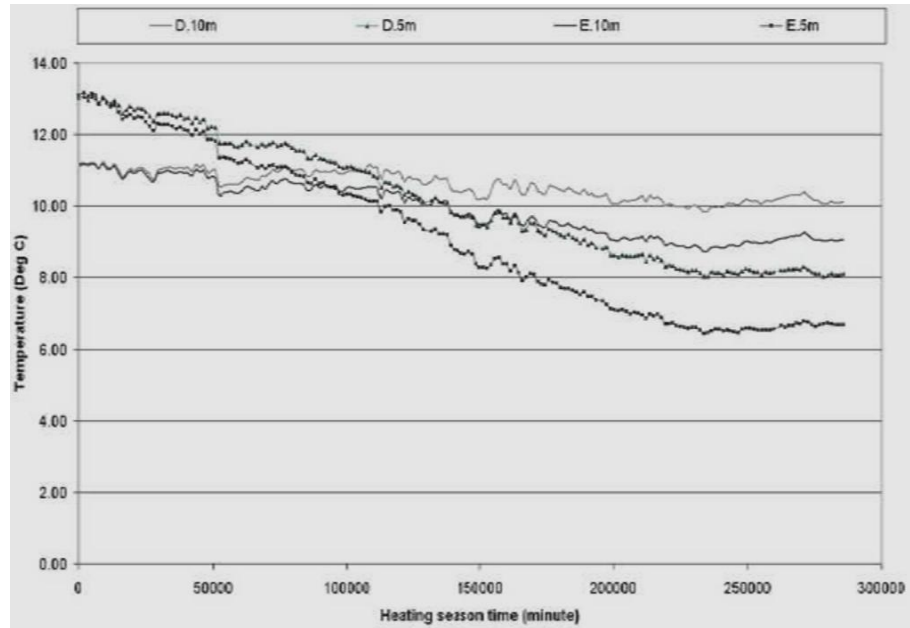


**Figure 2.12:** Ground temperature at 5m and 10m depth at a site in Burton-on-Trent, UK, throughout two years (Wood C. J., 2009)

In the previous work on energy piles heat pump by Wood, Liu, & Riffat (2008), it has been shown that the heat extraction of the energy pile have a long term changes in temperature across the depth of the piles. Figure 2.14 shows the comparison of the absolute temperature at various depths of the pile 11 and the undisturbed far field ground temperatures at location C. From the Figure 2.14, the comparison shows that the ground around the pile experience long term thermal cycle across its entire depth due to the heat extraction for the two heating seasons. Ordinarily the ground experience seasonal thermal fluctuation as seen at the

undisturbed far field location C (see Figure 2.13); which exhibits significant variation in temperature at 2.5 m depth with a 4 °C amplitude from 10 °C mean, but no apparent variation at 10 m depth. It can be seen that the heat extraction during the first heating season induces a seasonal temperature cycling across the full depth of the pile, with reducing amplitude with depth.

A point of interest is the ground recovery across the two heating seasons, for a year to year comparison, the absolute changes in temperature of the ground during summer recovery is observed to be about 2 °C at any point of the pile. It should be noted that this test has been performed in the absence of building upon the energy piles plot. In the real situation the ground would be sheltered by the building structure, which would reduce ground solar gain in summer months, therefore this could have affected the permanent changes in the ground temperature for than 2 °C.

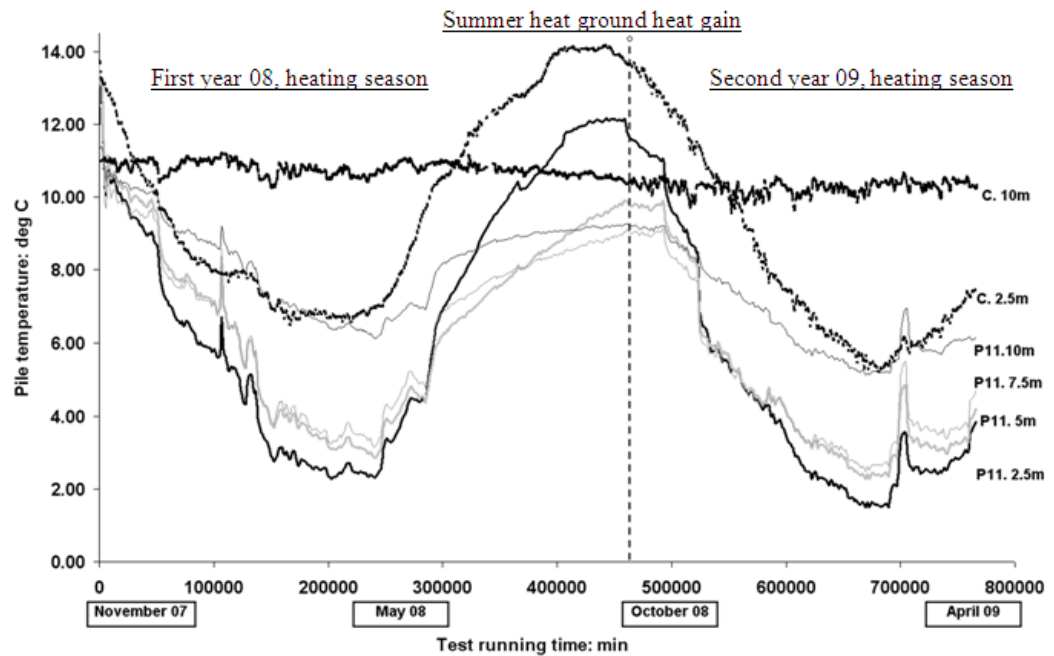


**Figure 2.13:** Long term thermal cycle across its entire pile depth due to the heat extraction for two heating seasons at a site in Burton-on-Trent, UK (Wood C. J., 2009)

It is understood from Wood et al (2008) findings that the ground temperature beyond the first year is reducing, though it is considered that year on year the rate of change of the temperature will fall before reaching a quasi-steady state level. In light of these findings it is considered that, the ground gets colder year by year and that it can schematically be represented by a declining SIN wave as shown in the *Figure 2.14*, after each year, the highest temperature recovered by the ground around the piles/borehole is never as high as in the previous year. After several cycles, say 5-10 years, depending on the conductivity of the soil and draw of the heat pump, the ground temperature around the piles/borehole will reach a new

stability at a lower temperature, causing a permanent reduction in COP of the heat pump.

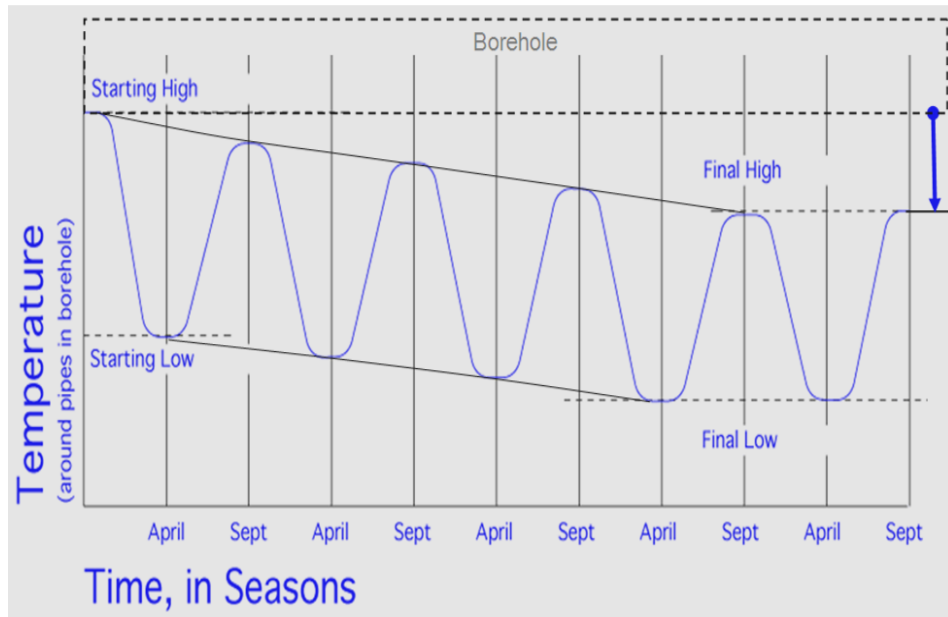


**Figure 2.14:** Schematic graph of annual decline in ground temperature in Burton-on-Trent, UK, throughout 5 years of heating seasons

In order to avoid the ground load imbalances during a year; two solutions have been proposed: i) Increase the total length of the boreholes, or ii) Hybridize the system with a supplementary heat source linked to the vertical ground heat source.

Since the major drawback of the vertical borehole heat exchanger is the drilling cost, the first solution is not most economical. Second solution, also identified as hybrid systems used supplementary component such as solar collectors or Roof

Thermal in the case of heating dominated buildings combine with the GSHP to reduce the drilling length of the borehole or to assist the quick recovery of the ground after the heating season. In the UK, this types of configuration have received little and no attentions to the best of the author' knowledge, therefore, the use of Solar-Air thermal panels acting as a supplementary source to a GSHP or Roof Thermal as supplementary heat source for ground recovery are novel.

### **Conclusion - Chapter 2**

This chapter covers the background of the research and summarises previously published concept and theories that is crucial to understanding this work. It provides a brief review of the various studies relevant to this work. In addition, factors affecting the ASHP and GSHP performance when heat demand is at the peak have also been examined.

In the UK, the 2008 Climate Change Act required an 80% reduction in CO<sub>2</sub> emissions by 2050 from 1990 level. To mitigate CO<sub>2</sub> emissions from buildings fabric, the Department for Communities and Local Government has announced a strategic decision and published the Code for Sustainable Homes, "*A Step Change in the Sustainable Home Building Practice, 2006*" (DCLG, 2008) referred to in this paper as "the Code". About 84% of energy use in residential building is for space and water heating, in addition residential buildings are responsible of about

27% CO<sub>2</sub> emission in the UK. The Carbon footprint of a building can be defined as the amount of CO<sub>2</sub> for which the house is responsible. Most commonly described as direct emissions which result from combustion of fuels which produce CO<sub>2</sub> emissions, such as the gas used to provide hot water or space heating, and electricity used for equipments and lighting. This project is focus to develop a heating device that can contribute to achieving zero-carbon buildings, thus 100% Carbon footprint reduction against a baseline of current building regulation Part L1a from energy usage for heating system.

Heat pumps systems have the potential to improve thermal comfort, at lower energy costs and also to reduce CO<sub>2</sub> emissions up to 100% if the fuel source is from renewable. In most countries in the Europe and mainly in the UK, full air conditioning (heating and cooling) is not necessary or cost effective for domestic application. The “**heating only**” heat pump is the most promising system to compete with conventional fossil fuel devices. The focus of this project is to increasing the yearly performance of heat pump system defined in a Seasonal Performance Factor (SPF).

The COP of the heat pumps depends on many factors such as actual temperature lifts, distance between heat exchangers, the temperature of low-energy source, the temperature of delivered useful heat. Among those factors, the temperature of the heat source at the evaporator is the most important, therefore this work focuses on

the evaporator design to enhance the COP of ASHP and GSHP for DHW and space heating, but this is not to suggest that other factors are of lesser importance.

Historically, soil has been considered to be the most effective heat source for heat pumps, as it offers the highest COP at the beginning of the heating season, but decrease gradually as enough heat drawn from the ground in addition soil presents certain difficulties, due to the space and the high cost of drilling to position coils in the ground. Air has found renewed favour as an effective heat source, air source heat pumps are considerably cheaper to install than ground source units, although the efficiency of the system is slightly lower than ground source due to the constant fluctuation in air temperature. In addition frost formation in winter can limit the use of the air source heat pump.

Numerous research and development activities have taken place to improve the heat pump COP and to identify reliable, economically and environmentally feasible alternate heat sources for heat pump. In order to avoid the ground load imbalances during a year; two solutions have been proposed: i) Increase the total length of the boreholes, or ii) Hybridize the system with a supplementary heat source linked to the vertical ground heat source. Since the major drawback of the vertical borehole heat exchanger is the drilling cost, the first solution is not most economical. Second solution, also identified as hybrid systems used

supplementary component such as solar collectors or Roof Thermal in the case of heating dominated buildings combine with the GSHP to reduce the drilling length of the borehole or to assist the quick recovery of the ground after the heating season.

The next chapter reviews different technical arrangements and past work and the state of art heat pump technologies to improve COPs; many designs for heat pumps and supplementary systems have been reviewed. It also describes and reviews the designs, technologies and systems, which allow the unit to operate efficiently and minimise the effect of seasonal changes on heat pump's performance.

## CHAPTER 3 - LITERATURE REVIEW

### **3. Overview of past works to improve COP of Heat Pump Systems**

In the UK, the application and investigation into the efficiency of a heat pump for residential space heating started in 1940s by Sumner (1976). In 1948, Sumner installed about 12 prototypes ground source heat pump, each with a 9 kW output, with average COP of 3. In recent years, in order to improve the COP of the heat pump, many technical combinations are been possible and many designs for heat pumps and supplementary systems have been suggested and investigated. Technology that combine a low temperature side of the heat pump to solar source are becoming possible today, and seem to be reasonable to get high COP, great reliability, simpleness and reduce both cost and maintenance costs, as well as the energy consumption and CO<sub>2</sub> emissions. This chapter provides a details literature-based review of the technologies that combine a heat pump to solar source and discusses application of these technologies.

#### **3.1 Past work on Technologies to Improve the COP of ASHP**

In the aim of sustainability and to increase the COP of the conventional heat pump systems. Many designs for heat pumps and supplementary systems have been suggested and investigated. This section describes their designs, technologies and systems, which allow the unit to operate efficiently and minimise the effect of seasonal changes on performance. As shown in the Figures 3.15 to 3.18, the basic schematic diagrams of these combinations systems, which have been based on the following principals: a) Heat pump with solar-assisted evaporator (Figure 3.15); b) Classical heat pump coupled to standard thermal solar collectors (Figures 3.16, 3.17) ; c) Multifunction appliance combining an

air-source heat pump, a thermal-regenerative Controlled Mechanical Ventilation (CMV) and a thermal solar collector for house heating and Domestic Hot Water (DHW) generation (Figure 3.18); .

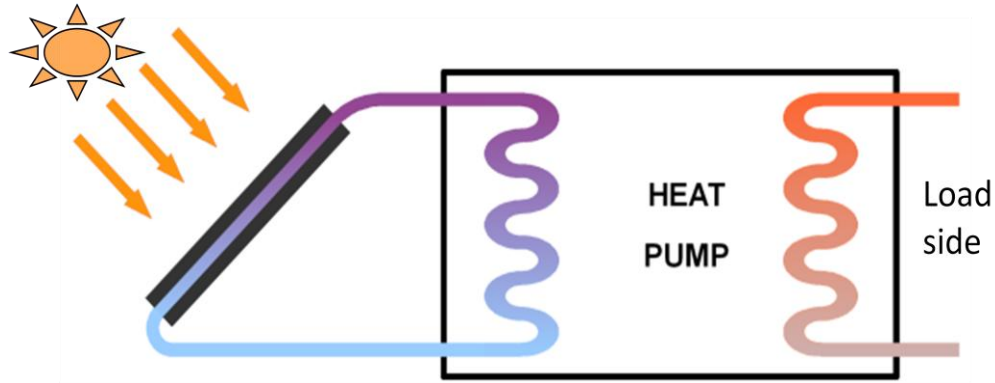


*Figure 3.15: Direct expansion solar collector/evaporator heat pump*

In the *Figure 3.15*, the configuration is a direct expansion heat pump system, which consists of a flat plate solar collector used as evaporator for the heat pump. During cold winter days or at night, the collector/ evaporator can extract heat from the ambient air by natural convection as a conventional air-source heat pump. And during sunning days, the collector uses hybrid heat sources, solar and air to provide heat sources for a working fluid flowing through the collector/evaporator. This system combination seems to be more attractive to increase the COP of the heat pump and in addition of its simplicity, it uses less space and could provide space and domestic hot water heating through the year at high energy efficiency. Additional benefits of such system are:

- i) The plant doesn't need hard work such as drilling or excavation to install heat exchanger coils in the ground; it can easily substitute a conventional air-source heat pump system or an existing domestic hot water system;

ii) The use of flat plate solar collector as evaporator allows avoiding the freezing problems. With the use of a lower boiling working fluid, the collector/evaporator could also extract heat from the snow and then be able to provide peak space and water heating demand when the ambient temperature falls significantly.

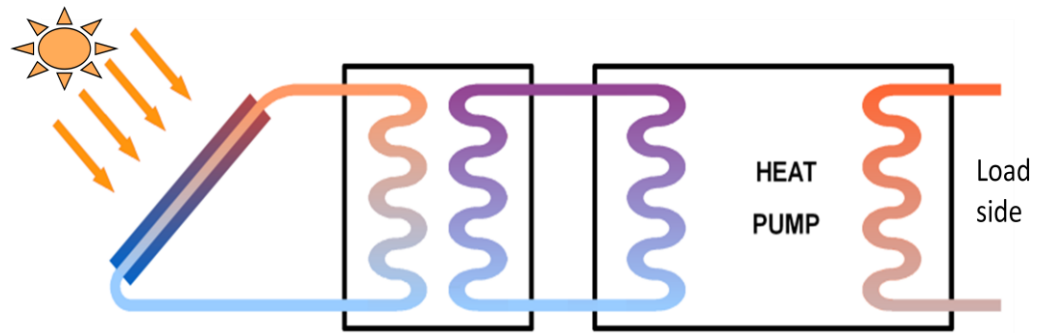


**Figure 3.16:** Conventional heat pump with solar-preheated water cylinder

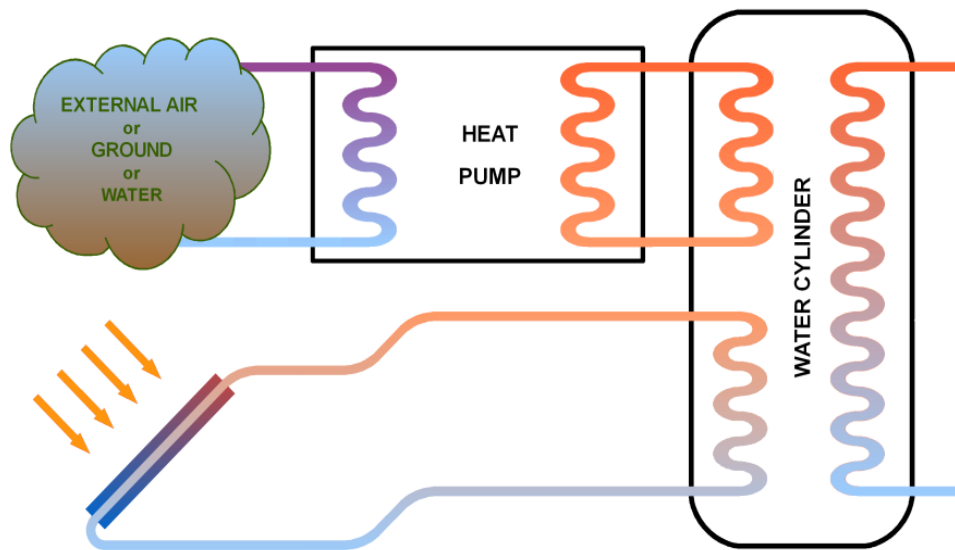


**Figure 3. 17:** Conventional heat pump with solar-preheated water cylinder

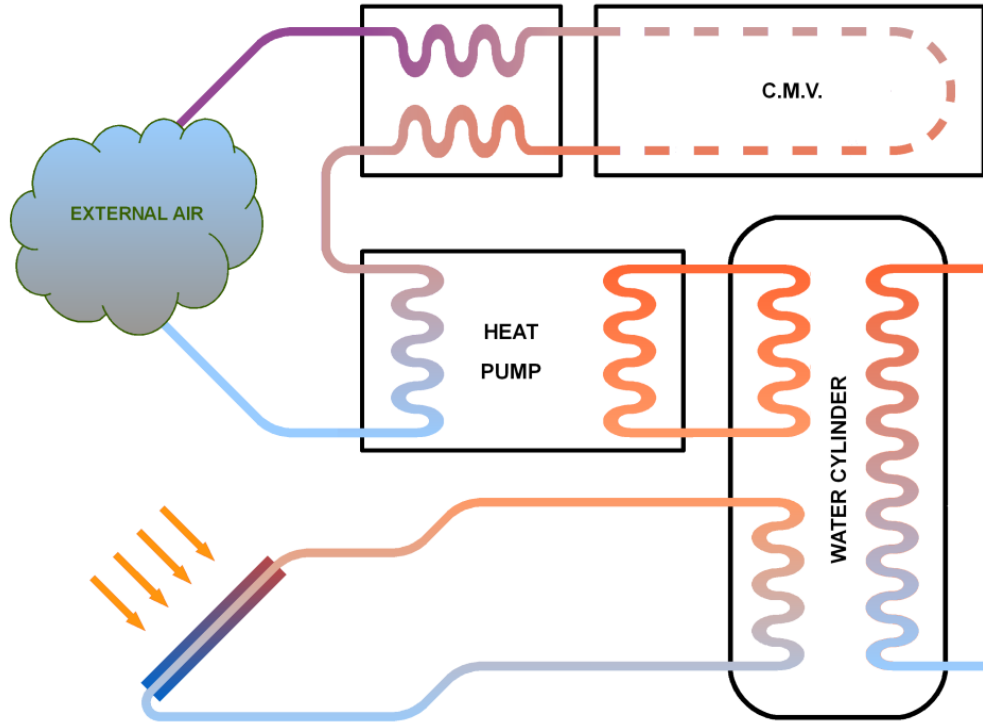


**Figure 3.18:** Multifunction heat pump

The refrigerant in the evaporator (solar collector) is directly heated in the solar collector to expand. The heated refrigerant vapour then enters the compressor, as shown in *Figure 3.19*. Kuang, Sumathy, & Wang, (2003) have carried out some tests on a DX-ASHPS, as shown in *Figure 3.20*. A 2m<sup>2</sup> bare flat plate solar collector without any glazing or back insulation was used as a heat source, as well as an evaporator for the refrigerant, Freon-22. It consisted of two aluminium absorber plates in parallel, and is made by a special process. This involved the piping network design being laid between two sheets of aluminium and retained after the sheets are bonded by rolling them together. The tubes are formed by over-pressurizing the network so that the serpentine fluid circuit is within the fin. As a result, the collector/evaporator is light weight and very thin. This allows it to





**Figure 3.20:** A prototype DX-SAHP water heater: (a) outdoor; (b) indoor. (Kuang, Sumathy, & Wang, 2003)

Ito & Miura, (2000) experimentally and theoretically investigated a dual heat sources heat pump system (Figure 3.21) for space and domestic hot water heating; the ambient air and water were used as low temperature sources to supply the evaporator. When the temperature of the water heat source was decreased, the heat from the water as well as the heat from the air was used for the heat pump performance until its temperature became approximately that of the evaporation temperature of the heat pump using the ambient air alone as heat source. When the water temperature dropped further, the evaporator absorbed heat only from the air like a traditional ASHP. In the case of dual heat sources, the heat could be absorbed from both heat sources at the same, this resulted in a higher evaporation temperature and COP than in the case of single heat source for ASHP and was 3.68 for theoretical analyse and 3.61 in the experiment and the temperature of the

air and water were respectively 10°C and 15°C. However, when only one heat source did not satisfy the evaporation conditions, in this case, the COP was a little greater compare to a conventional single source heat pump, when only the water source was used , the COP was 3.05 and the water was at 7.5°C. There were not significant advantages using both heat sources.

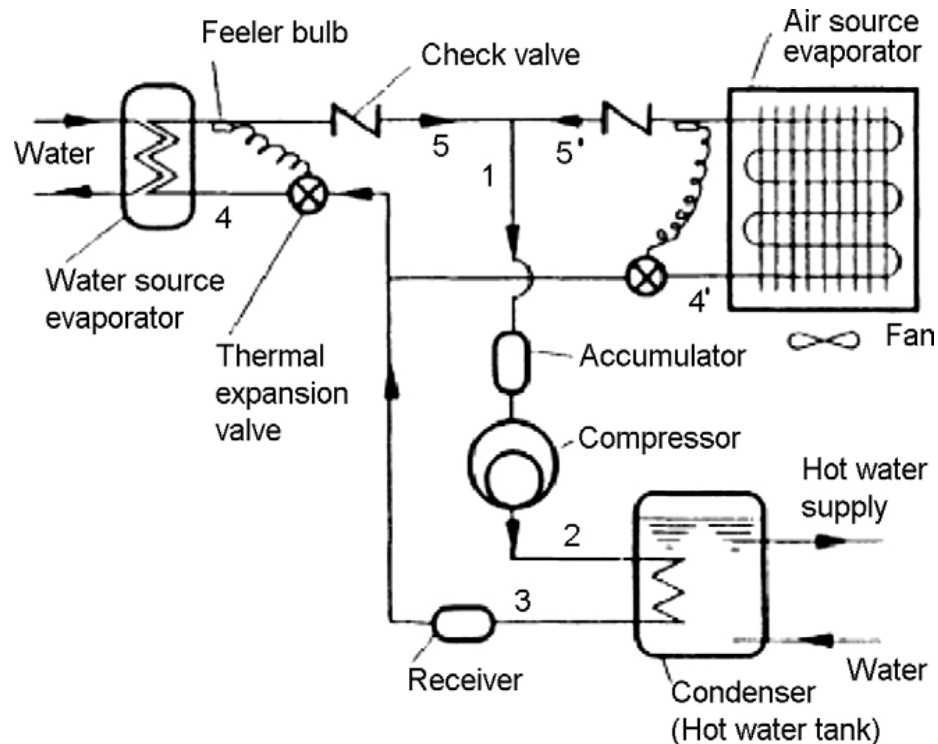


**Figure 3. 21:** Heat pump using dual heat sources in parallel arrangement for evaporation (Ito & Miura, 2000).

The proposed theoretical and experimental analysis on direct expansion heat pump system employed a bare collector which acted as the evaporator (see Figure 3.22) has been investigated by (Chaturvedi, Chen, & Kheireddne, 1996). The work focused on the effects of the compressor speed on the variation of the thermal performance of the Direct Expansion Solar-Assisted Heat Pump (DX-Blaise Mempoou, PhD thesis, 2011

SAHP). The results indicate that a significant improvement in system COP can be achieved by modeling the compressor capacity seasonal changes in ambient temperature occur. For the compressor frequency range of 30-70Hz, the COP is rating from 2.5 to 4.0. This work did not look at the benefits of collectors/evaporator on the COP, which is the focus of this work.

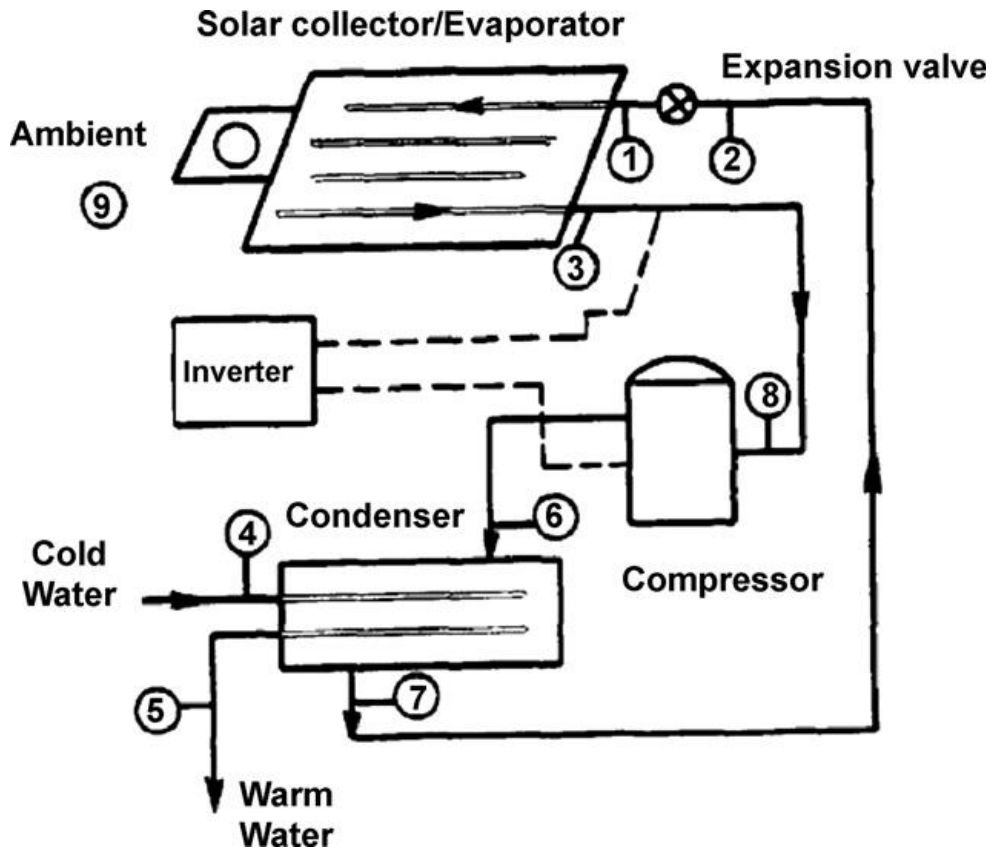
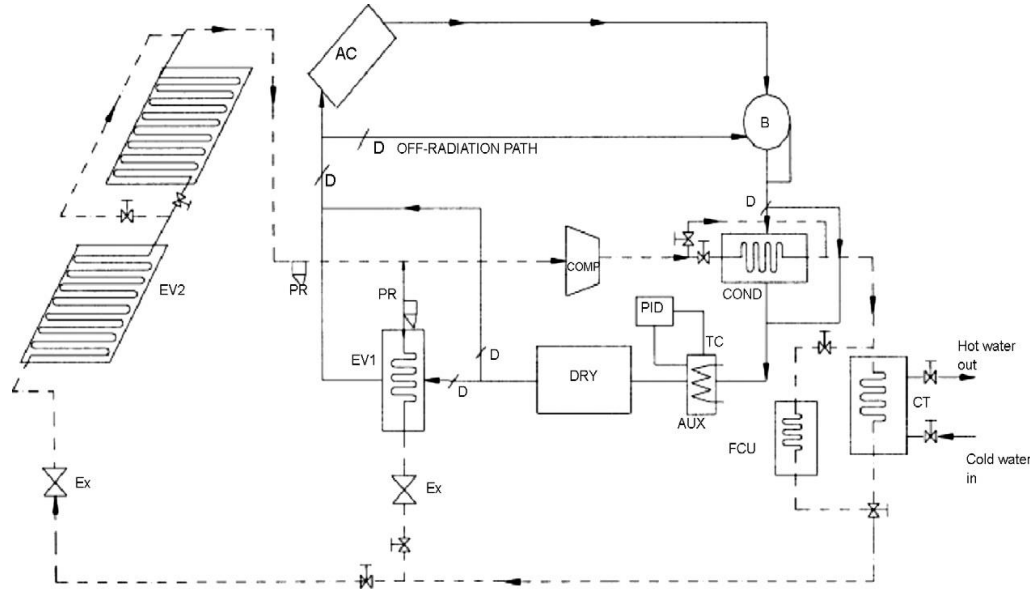


Figure 3.22: Schematic of DX-SAHP system (Chaturvedi, Chen, & Kheireddne, 1996)

Under the meteorological conditions of Singapore, A solar-assisted heat-pump dryer and water heater (see Figure 3.23) has been designed, fabricated and tested by Hawlader, Chou, Jahangeer, Rahman, & Eugene Lau (2003). A series of experiments were performed to validate the simulation. A simulation program was developed using FORTRAN language to evaluate the performance of the

system and the influence of different variables. The values of the COP, obtained from the simulation and experimental were respectively 7.0 and 5.0.



**Figure 3.23:** Schematic diagram of heat-pump assisted solar-dryer and water heater (Hawladar, Chou, Jahangeer, Rahman, & Eugene Lau, 2003)

(AUX) auxiliary heater; (AC) air collector; (B) blower; (COMP) compressor; (COND) condenser; (CT) condenser tank; (D) damper; (DRY) dryer; (EV1) evaporator 1; (EV2) evaporator 2; (EX) expansion valve; (TC) thermocouple; (PID) temperature controller; (-) air path; (- -) refrigerant path; (PR) pressure regulator; (FCU) fan-coil unit.

Under an environmental condition of Nanjing, China, a simulation study on the operating performance of a solar-air source heat pump water heater (SAS-HPWH), see *Figure 3.24* has been investigated by Guoying and al. (2006). The SAS-HPWH shown in the *Figure 3.24* used a specially designed flat-plate heat collector/evaporator with spiral-finned tubes to collect energy from both solar radiation and ambient air for hot water heating. The simulation based on 150L water heating capacity showed that such the system can efficiently heat water at up to 55°C under various weather conditions all year around. The influences of

solar radiation, ambient temperature and compressor capacity on the COP were analysed. The monthly averaged COP was 3.8 to 4.32. This system combination is more attractive to increase the COP of an ASHP and in addition of its simplicity, it uses less space and could provide space and domestic hot water heating through the year at high energy efficiency.

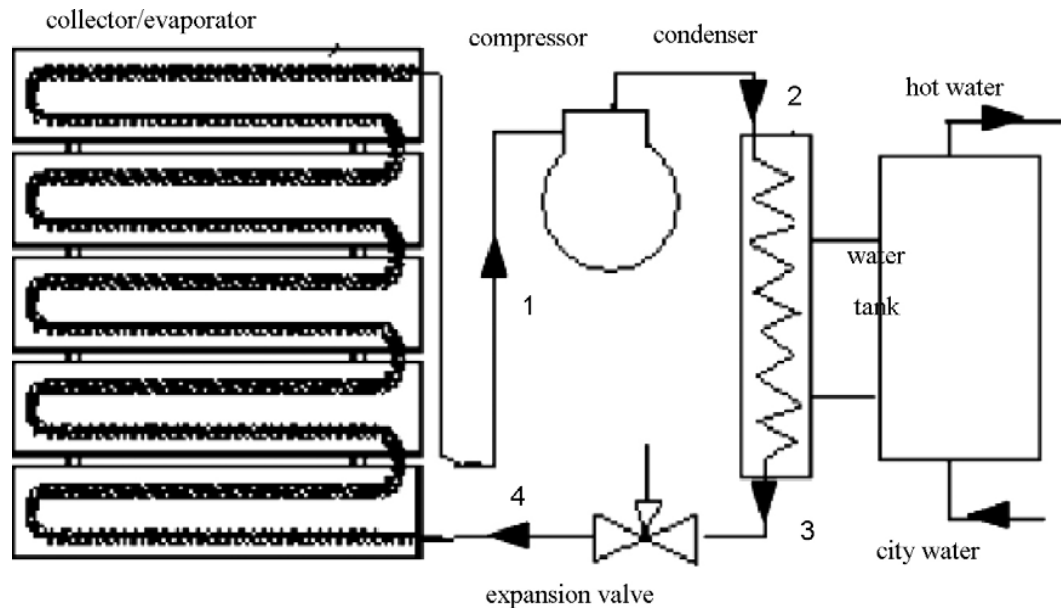


**Figure 3. 24:** The schematic diagram of the simulated SAS-HPWH (Guoying, Xiaosong, & Shiming, 2006).

Li, Wang, Wu, & Xu (2007), under typical spring climate in Shanghai, conducted an experimental study on a direct expansion solar heat pumps water heater. The system was consist of 4.2 m<sup>2</sup> direct expansion type collector/evaporator, R-22 rotary-type hermetic compressor with rated input power 0.75kW, 150l water heating capacity, with immersed 60m serpentine copper coil and external balance type thermostatic expansion valve (see Figure 3.25). The results shown that the COP of the system reached 6.61 at the average of 150l water varying from 13.4 to

50.5°C in 94 minutes. And the seasonal average values of the COP and collector/evaporator efficiency were measured to be 5.25 and 1.08 respectively. Under the climate of Shanghai, this direct expansion heat pump proven to be high efficient compare to conventional heat pump system, however since one of the killer of the COP is the temperature lift between the evaporator and the condenser of the heat pump, this heat pump might not perform well in the European climates, mostly during winter because on low ambient temperature which increase the lift.

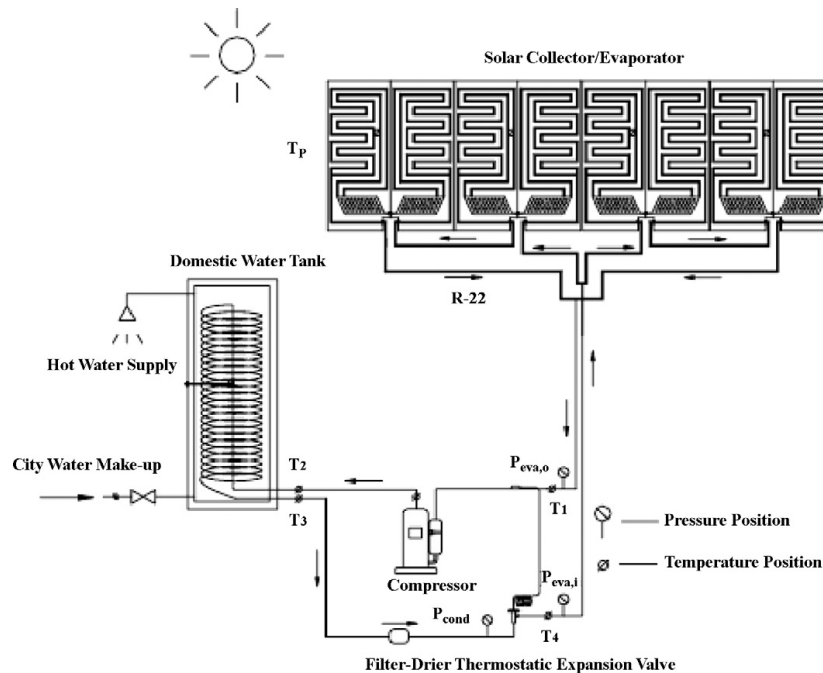


Figure 3. 25: Schematic of system circuit (Li, Wang, Wu, & Xu, 2007).

### 3.2 Past work on technologies to improve the COP of GSHP

In order to avoid the ground load imbalances during a year; two solutions have been proposed, one is to increase the total length of the boreholes, and the second one is to combine GSHP system with a supplementary heat. Since the major

drawback of the vertical borehole heat exchanger is the drilling cost, the first solution is not economical.

Trillat-Berdal & Souyri, (2007) presented the experimental study of Geo-solar GSHP system (see Figure 3.26), based on the combination of a GCHP and thermal collectors in a 180m<sup>2</sup> single-family house constructed in 2004 in France, and after eleven months in operation, the results show that combining solar collectors with GCHP in single system should make it possible to meet a residence's heating and hot water loads, and also provide a good comfort level. The power extracted and injected into the ground had average values of 40.3W/m and 39.5 W/m, respectively. During generation, the amount of heat injected in the ground increased but was not sufficient to improve the heat pump coefficient of performance (COP).

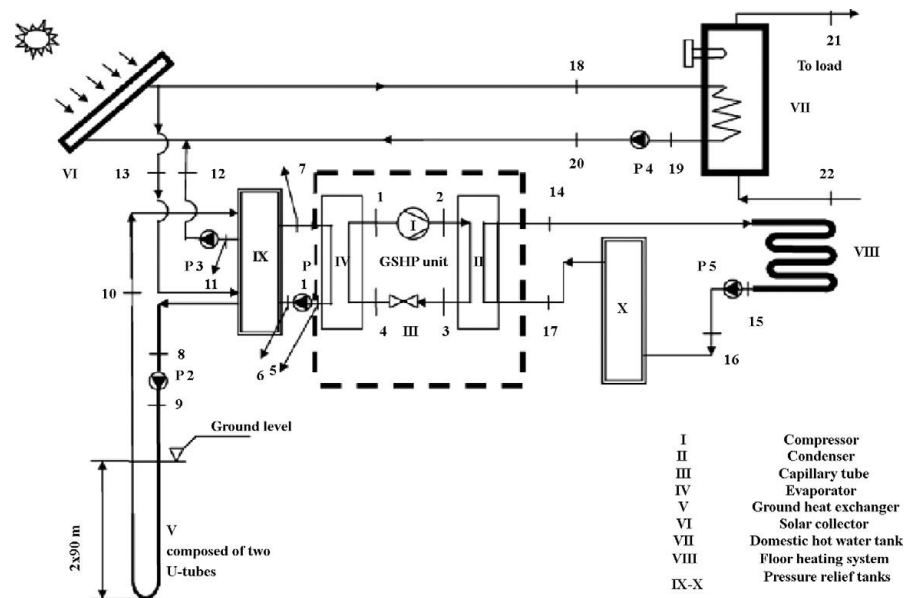


**Figure 3.26:** Schematic view of a solar-assisted domestic hot water tank integrated GCHP system (Trilliant-Berdal, Souyri, & Fraise, 2006)

Chiasson, (2003) has conducted a theoretical approach of the solar collectors coupled with ground source heat pump in single system, using typical meteorological year weathers data for six different U.S. cities. His results show that combining solar collectors with ground source heat pump can help at the design stage, to reduce the borehole length and also a reduction of the solar collector area for about 4.5 to 7.7m/m<sup>2</sup> according to weather conditions.

E. Kjellson (2004) investigated using the computer simulation a combined solar collector and ground source heat pump in a dwelling in Sweden. The results show that, there are advantages with recharging the borehole; firstly this may increase seasonal performance of the heat pump, and in addition give a possibility to use shorter boreholes and higher heat extraction from the borehole. Her results also show that it is particularly useful to recharge the ground if the boreholes are so close to each other, so the recharge could compensate the influence of the neighbouring boreholes with heat extraction.

### **3.2.1.1 Ground heat exchangers**

GSHP is an electrically powered system that takes advantage of the earth's relatively constant ground temperature to provide heating for domestic hot water and space. The water to water system heat pump is especially designed for supplying the hot water for underfloor heating. GSHP usually collects heat from the ground via Ground Coupled Heat Exchangers (GCHE) also called ground loops. There are usually two types of loops; open loops and closed, however

closed loops are the most acceptable GCHE for domestic heat pumps application. They are made of continuous high-density polyethylene (HDPE) pipes. And they can be installed in three ways (see Figure 3.27): horizontally, vertically, or in pond/lake a typical arrangements of Ground Coupled Heat Exchangers (GCHE) are summarised in the Tables 3.8.

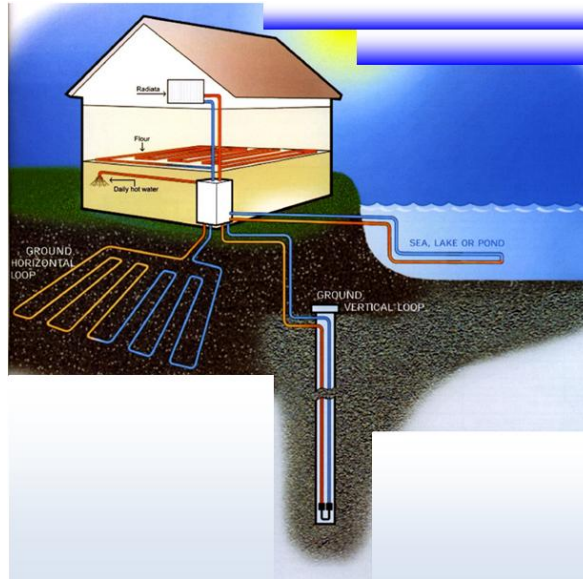
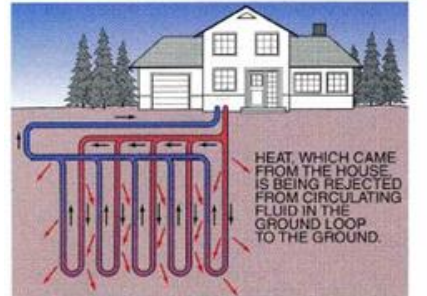
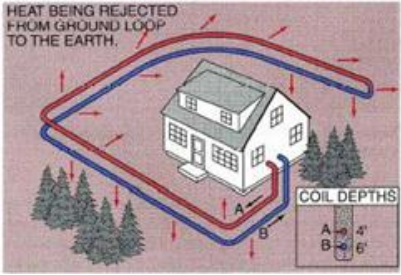
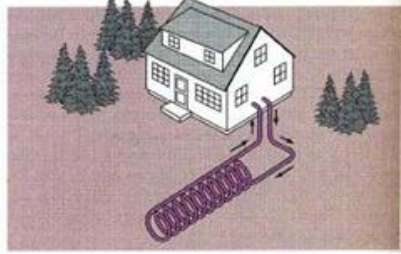
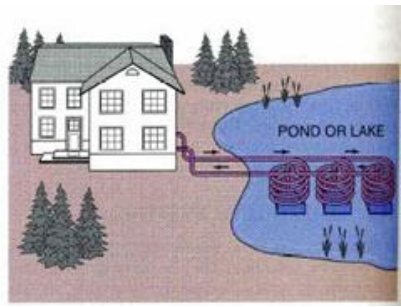


Figure 3. 27: Three ways of installation GCHE

Table 3. 8: Typical arrangements of Ground Coupled heat pumps (ground heat exchanger)

Diagram	Comments
 <p data-bbox="397 1711 820 1774">Reverse heat pump for cooling and heating</p>	<p data-bbox="852 1396 1412 1848"><i>GCEH in the parallel-vertical configuration: used limited land area, good thermal performance, more expensive than horizontal loops as they require specialised drilling equipments, no geological constraints, suitable to install in almost any place with no maintenance. The temperature of the heat source is more stable at 7 meter under the ground. Energy from the ground vertical loop, The vertical loop collects energy stored deep underground. The vertical loop is placed in a borehole drilled to a depth of up to 200 meters and one or more loops are then connected to the heat pump evaporator.</i></p>

 <p>HEAT BEING REJECTED FROM GROUND LOOP TO THE EARTH.</p> <p>COIL DEPTHS A = 4' B = 6'</p>	<p><i>In the depth of 1 meter a polyethylene tube is placed. This plastic pipe is filled with antifreeze liquid and connected to the heat pump. Easier to install, but require large areas, but the temperature of the heat source at the depth of 1 meter underground fluctuated with the air temperature.</i></p>
	<p><i>Slinky ground loop, denser than horizontal and vertical loops; less thermal performance due to pipe overlapping, require large areas, require some maintenance in term of one should not cover the above installed area of the loop with hard material to allow rain to carry the solar radiated to the surface to the GCHE</i></p>
 <p>POND OR LAKE</p>	<p><i>Require a lake, sea or river close to the house, best thermal performance if right amount of water is available to be pumped, also most expensive to install and maintain. Since the horizontal loop is at 1 meter, its temperature fluctuating with the air.</i></p>

### **Conclusion - Chapter 3**

This chapter provides a details literature-based review of the technologies that combine a heat pump to solar source and discusses application of these technologies. It also describes and reviews of the four mains components of the ASHP and GSHP system.

In recent years, in order to improve the COP of the heat pump, many technical combinations are possible and many designs for heat pumps and supplementary systems have been suggested and investigated (see Table 3.9). Technology that combine a low temperature side of the heat pump to solar source are becoming possible today, and seem to be reasonable to get high COP, great reliability, simpleness and reduce both cost and maintenance costs, as well as the energy consumption and CO<sub>2</sub> emissions. These combinations systems have been based on the following principals: a) Heat pump with solar-assisted evaporator; b) Classical heat pump coupled to standard thermal solar collectors; c) Multifunction appliance combining an air-source heat pump, a thermal-regenerative Controlled Mechanical Ventilation (CMV) and a thermal solar collector for house heating and Domestic Hot Water (DHW) generation. Details literature-based review of these technologies and application could be summarise as shown the Table 3.9 below.

**Table 3. 9: Main relevant recent studies conducted on heating only heat-pump systems**

Year	Researcher (s) and location	Method (s)		Application	Results and comments
		Theoretical (simulation)	Experimental	Heating only	
<b>Solar-assisted Heat Pump (SAHP)</b>					
1996	Chaturvedi et al (1996)	x	x	x	$COP_h = 2.5 - 4.0$
2003	Hawladar et al. (2003) Singapore	x	x	x	Under the meteorological conditions of Singapore $COP_{system} = 6.0$ , $\eta_{evap-coll} = 0.080$ , $\eta_{air-coll} = 0.080$
2003	Kuang et al (2000)	x	x	x	$COP_{monthly-avg} = 4 - 6.0$ , $\eta_{evap-coll} = 40 - 60\%$
2006	Guoying et al (2006) Nanjing, China	x		x	Under an environmental condition of Nanjing, China  $COP_{monthly-avg} = 3.98 - 4.32$ , $T_{water} = 55^\circ C$  The system can efficiently heat water at up to $55^\circ C$ under various weather conditions all year around.
2007	Li et al (2007) Shanghai		x	x	under typical spring climate in Shanghai $COP_{seasonal-avg} = 5.25$ , $\eta_{evap-coll} = 1.08$ , $T_{water} = 50.5^\circ C$ Under Shanghai climates conditions, this direct expansion heat pump proven to be high efficient compare to conventional heat pump system
<b>Air-source heat pump (ASHP)</b>					
2000	Ito and Miura (2000)	x	x	x	A dual heat sources (water and air) heat pump system At air temperature of $20^\circ C$ ; $COP = 4.0$ , and when air temperature at $10^\circ C$ ; $COP = 3.68$ There were not significant advantages using both heat sources.
<b>Ground-source heat pump (GSHP)</b>					
2004	Trillat-Berdal et al. (2004) France		x	x	The power extracted and injected into the ground had average values of $40.3 W/m$ and $39.5 W/m$ , respectively. During generation, the amount of heat injected in the ground increased but was not sufficient to improve the heat pump coefficient of performance (COP).
2003	Chiasson	x		x	Using typically a meteorological

	(2003) U.S.				year's weather data for six different U.S. cities. Results show that combining solar collectors with ground source heat pump can help at the design stage to reduce the borehole length and also permit a reduction of the solar collector area from about 4.5 to 7.7 m/m <sup>2</sup> according to weather conditions.
2004	Kjellson (2004)  Sweden	x		x	The results show that there are advantages with recharging the borehole; firstly this may increase seasonal performance of the heat pump, and in addition it may give a possibility to use shorter boreholes and higher heat extraction from the borehole.

## **CHAPTER 4 - NUMERICAL AND EXPERIMENTAL ANALYSIS ON THE PERFORMANCES OF A NOVEL DIRECT EXPANSION SOLAR HEAT PUMP (DX-SHP)**

---

## 4 INTRODUCTION

The overall aims of this chapter is to undertake an indoor experimental of the Direct-Expansion Solar Thermal Source Heat Pump (DX-STSHHP) system; In order to predict, COP and the thermal performance of the DX-SHP system under different solar radiations. The compressor's energy consumption, the heat gain at the condenser, and the coefficient of performance (COP) of the heat pump has been evaluated. The physical sensitivity analyses of the collector/evaporator on the COP have also been studied.

### 4.1 DX-SHP System Description

The system under consideration (*Figure 4.28*) is consists of an unglazed metallic black flat-plate solar collector (evaporator) directly exposed to incident solar radiations, a small compressor (SC15GH), a thermostatic expansion valve (TXV) and a plate heat exchanger (condenser); the characteristic of each component were summarised in the *Table 4.10*.

To start with the working fluid from the thermostatic expansion valve exit passes through the finned tubes of the collector/evaporator, where is evaporated by incident solar radiation and the ambient air. The saturated vapour passes through the compressor, which compresses it to a high pressure and temperature and then delivers it to a condenser. Heat is then extracted from the condenser and used to heat water at 35°C for space heating mode. The cold mix refrigerant (liquid +

vapour) is then passes to the TXV, where pressure and temperature are decreased and ready to go into the collector/evaporator ready to continue the cycle.

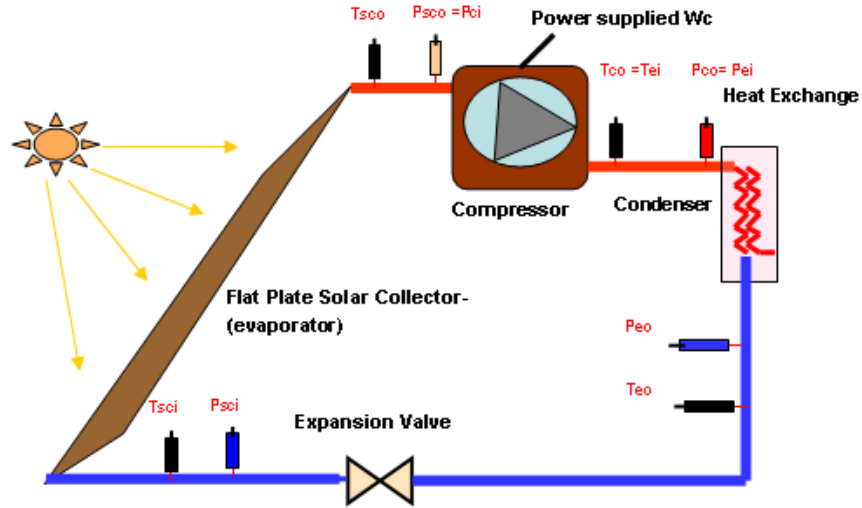


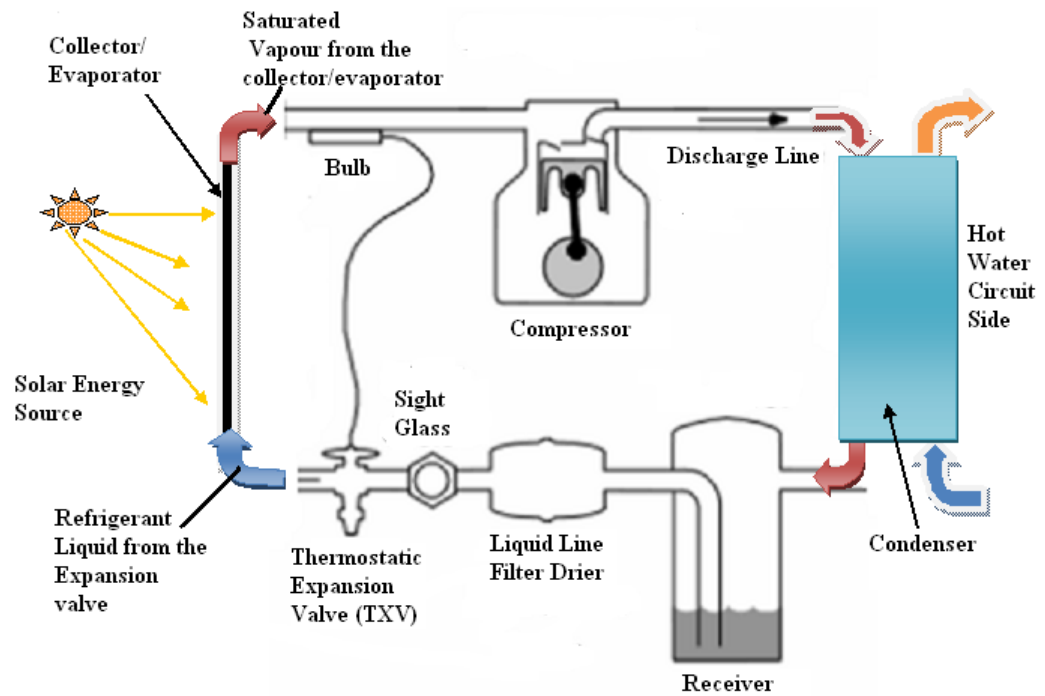
Figure 4. 28: Schematic Diagram of the DX-SHP System

Table 4. 10: Specification of main equipments in the DX-SHP system

Name	Type	Comments
<b>Collector/Evaporator</b>	Serpentine tubes in black unglazed flat-plate heat exchanger	Total area: 1.26 m <sup>2</sup> , Plate effective absorptivity:0.90; emissivity:0.90 , Tubes spacing 75mm, Tube diameter 6mm, Plate thickness 1.5mm, Plate thermal conductivity (Aluminium) 235W/mC tubes diameter (outer/inner) D=8.5/7mm, thermal conductivity (Aluminium) 235 W/m <sup>o</sup> C
<b>Compressor</b>	Hermetic constant speed compressor	SC15GH (Danfoss Compressor), for refrigerators R134a, displacement 15.28 cm <sup>3</sup> , rated input power: 360W
<b>Condenser</b>	Contraflow Flat plate L-line type heat exchanger	Made of stainless steel with a transfer area of about 172cm <sup>2</sup>
<b>Thermostatic Expansion Valve, Fixe orifice</b>	Thermostatic Expansion Valve (TXV)	Universal, TR6 Danfoss , Control device, it has a sensing bulb attached to the outlet of the collector/evaporator

## 4.2 Equipments and Instrumentation

There are four main components (collector/evaporator, compressor, condenser and expansion valve) in a refrigerant circuit loop (Figure 4.29) of the experimental rig; and any components (receiver, filter, and sight glass) beyond these basic 4 are identified as accessories. This section will take a closer look at the individual components of the refrigerant loop of the laboratory experimental rig system.



*Figure 4.29: Schematic Diagram of the Refrigerant Loop of the Experimental Test Rig*

#### 4.2.1 Experimentation heat source

In order to simulate the sun, a variable moveable lights (see Figures 4.30) simulator made up of twenty one 500W halogen lamps was used in the lab. This adjustable light simulated the solar radiations, and was placed tilted at 15 degrees in order to have horizontal radiations on the solar collector/evaporator, and a light regulator switch also shown in the Figures 4.30, allowed the variation of radiations to obtain a sun radiations range of 200 to 800W/m<sup>2</sup>.

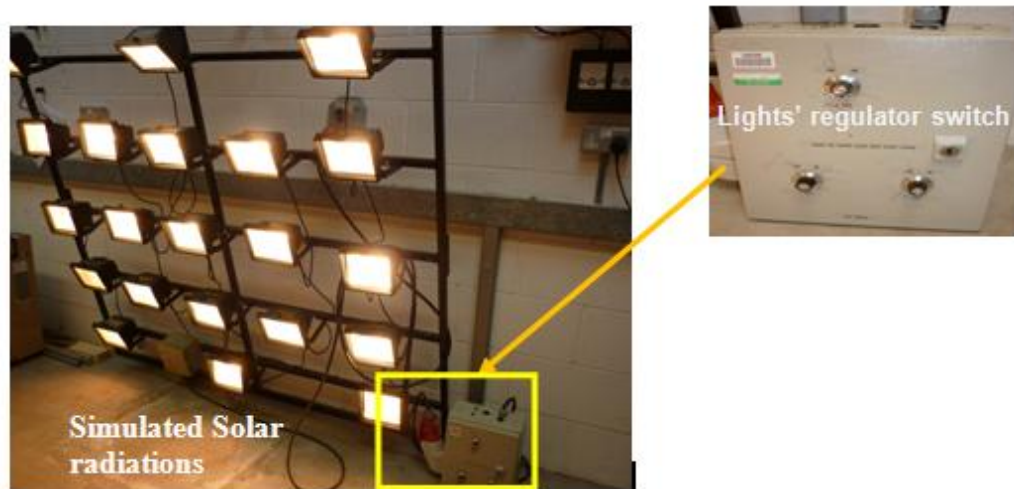


*Figure 4. 30: The twenty one 500W sun lights simulator and the regulator switch*

#### 4.2.2 Solar collector (evaporator)

One of the aims of this study was to optimise the rate of heat transfer between the heat source, solar radiation and the refrigerant. Copper and aluminium are proven to be very good thermal conductivity materials compare to other materials like iron. For this study, an aluminium unglazed flat plate collector/evaporator with

extruded built in finned tube of about 8.5 mm diameter for refrigeration has been used; the collector/evaporator has the refrigerant tubes centred in the plane of the plate forming an integral part of the flat plate collector/evaporator structure see *Figure 4.31* below. The total area of the collector was 1.225 m<sup>2</sup> and 1.50mm thick, with its surface painted in black to collector more radiations. There is no insulation at the back of the collector/evaporator, therefore it is exposed to the ambient air, and so could also collected heat from the air. Increasing surface area is another way to optimise the rate of heat transfer between the heat source, solar radiation and the refrigeration liquid in the collector. In this study to further enhance heat transfer the webs between refrigeration tubes were used as extended surfaces around the tubes to allow heat to easily travel in the flat plate's webs to the working fluid as presented in *Figure 4.31*, these also vastly increase the surface area that is exposed to the air. In addition, the collector/evaporator has no welded bond. Therefore the heat collected from the solar irradiation by the web between finned tube of the collector/evaporator flows directly to the working fluid without any resistance from the welded bond linking of the webs and the refrigerant tubes.

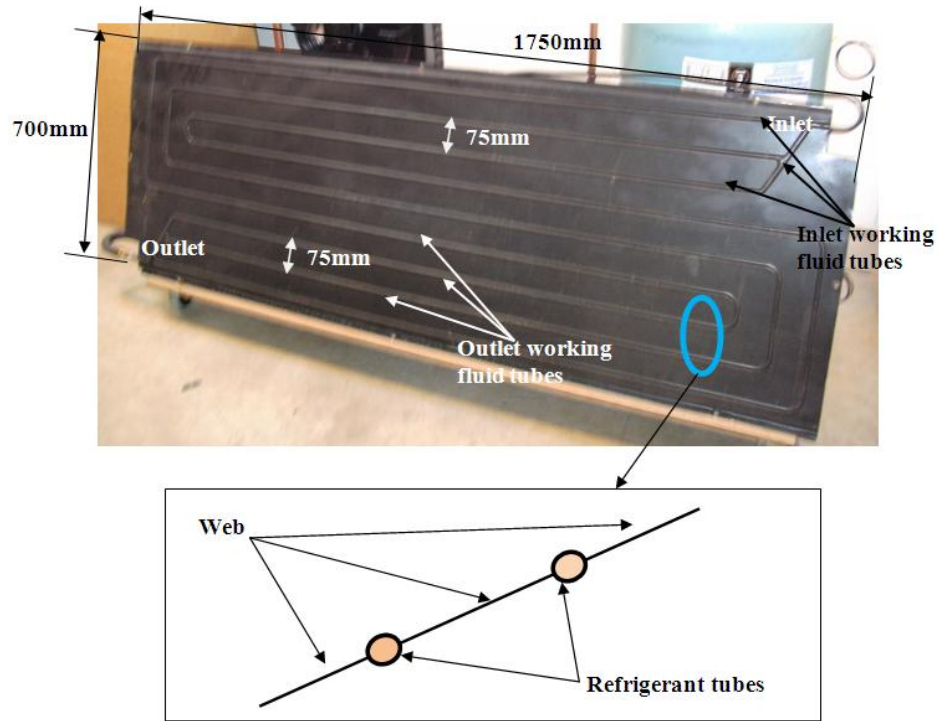


**Figure 4. 31:** The metal flat-plate collectors/evaporator and the schematic diagram of its structure

### 4.2.3 Compressor

In the refrigeration loop, the compressor performs 2 functions. The compressor receives refrigerant from the evaporator/collector in form of vapour, compresses it in form of the gas and moves the refrigerant around the loop. The compressor (SC15GH) used in this study is of the electrical rotary type (see Figure 4.32), which compresses the refrigerant gas and sends it on its way to the condenser. The compressor of this experimental has a rated capacity of about 360W, and uses R134A as refrigerant.

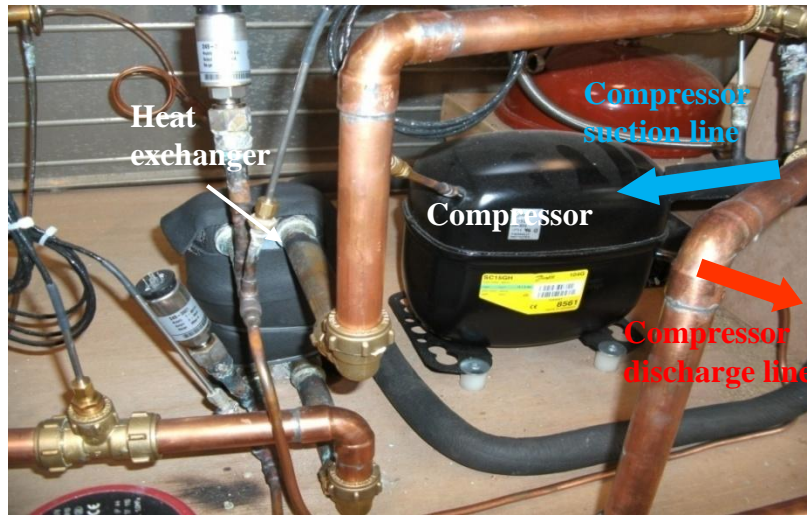


Figure 4.32: Compressor and Heat exchanger

#### 4.2.4 Condenser (*flat plate heat exchanger*)

The condenser receives refrigerant gas from the compressor, and then transfers heat to the water, so that the refrigerant gas can condense back into a liquid in preparation for a return trip to the collector/evaporator. The condenser used in this study is the flat plate L-line type heat exchanger (see Figure 4.33), made of stainless steel with a transfer area of about 172 cm<sup>2</sup>. As long as the compressor is running it will impose a force on the refrigerant to continue circulating around the loop and continue removing heat from solar radiation via the evaporator/collector and transfer it to the water via condenser (heat exchanger).

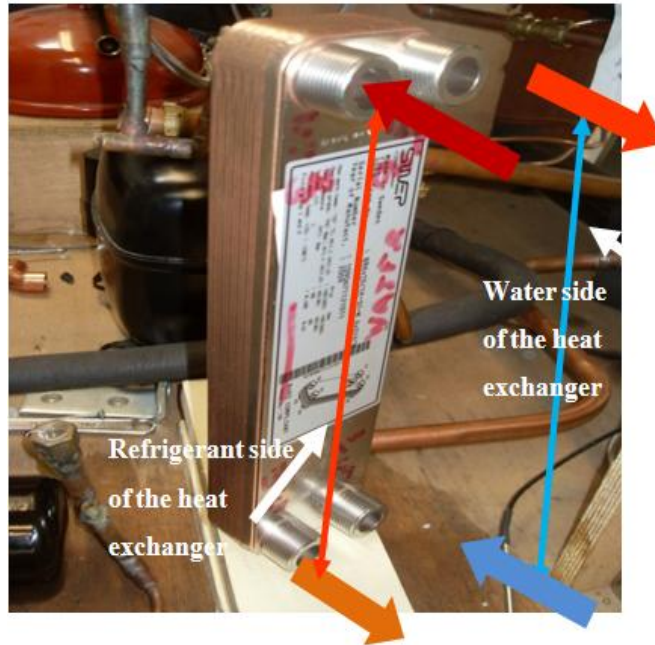
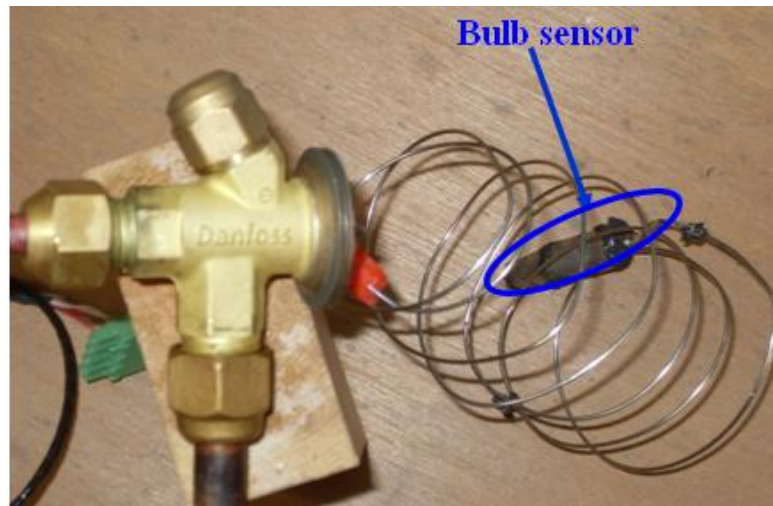


Figure 4. 33: Heat Exchanger (Condenser), SWEP: B8x10H/1P

#### 4.2.5 Thermostatic Expansion Valve (TXV)

The TXV (called a metering device) executes 2 functions; it causes the pressure of the refrigerant from the condenser to drop and adjusts the flow rate of the refrigeration. If the heat loads on the evaporator changes the valve can respond to change by modulating the refrigerant flow in the collector/evaporator, by increasing or decreasing the refrigerant flows accordingly. Figure 4.34 shows the expansion valve used for this study, Daffson type SC15GH the TXV has a sensing bulb attached to the outlet of the evaporator. This bulb senses the suction line temperature and sends a signal to the TXV allowing it to adjust the flow rate. The flow rate through a TXV is set so that not only is all the liquid hopefully changed to a vapour, but there is an additional 10°C, superheat, this is a safety margin to

insure that all the liquid is changed to a gas and that the gas returning to the compressor is several degrees away from the risk of having any liquid content.



**Figure 4. 34:** Thermostatic Expansion Valve (TXV)

Others components have been added along with TXV device in the condensate line. When the TXV reduces the flow of the refrigerant to the collector/evaporator there has to be somewhere for unneeded refrigerant to go and the receiver, see Figure 4.35. The type of receiver used in this experimental rig was, *AIRMENDER, CR-101*, with the capacity of 1.5 litres.

Additional components along with TXV are liquid line filter and a sight glass, shown in *Figure 4.36*. The filter catches unwanted particles such as welding slag, copper chips and other unwanted debris and keeps it from obstruction up important devices such as TX Valves. The filter also has another functions, since it contains a desiccant which can absorbs a minute quantity of water. And the

sight glass also shown in *Figure 4.36*, it is a viewing window which allows a technician to see if a full column of liquid refrigerant is present in the liquid line.



*Figure 4. 35: Refrigerant receiver, AIRMENDER, capacity of 1.5 litres*



*Figure 4. 36: Liquid Line Filter and a Sight Glass*

### 4.3 Mathematical Model and Simulation of the DX-SHP System

Governing equations describing the thermal performance of various components of the DX-SHP system have been formulated based on the following assumptions:

- The refrigerant at any tube cross-section in the collector/evaporator was in a single phase.
- The mathematical models are based on the single-stage R-134a vapour compression refrigeration cycle in quasi-steady state conditions within the investigating time interval.
- The refrigerant at the collector/evaporator and condenser exits is respectively saturated vapour and liquid.
- Expansion of the refrigerant is considered to be isenthalpic.
- Pressure drops in the collector/evaporator, piping and condenser are considered to be less than 15KPa and have negligible effect on thermal performance of the heat pump system.
- Thermal losses in the collector/evaporator, piping system and condenser are negligible.
- Compression of the refrigerant is considered to follow a polytropic process.
- The interaction between main components (Collector/evaporator, Compressor, and Condenser and Thermostatic expansion valve) of the DX-SHP is considered.
- The DX-SHP is supposed to operate with average collector/evaporator greater than ambient temperature.

#### 4.3.1 Assumptions

It was assumed that all components in the circuit (refrigerant loop) associated with vapour-compression refrigeration cycle were steady –flow devices and thus

could be analysed as steady-flow processes. In addition, the following assumptions were considered:

- The refrigerant in the collector exits as saturated vapour
- Steady state conditions apply to the heat pump system
- The thermal losses at the heat exchanger are neglected
- The thermal energy gain at the condenser ( $Q_C$ ) it can be consider to be sum of the energy consumed by compressor ( $W_c$ ) and the energy collected at the evaporator ( $Q_e$ ), therefore the following equation was applied  $Q_C = Q_e + W_c$ .

#### 4.3.2 EES Software

The Engineering Equation Solver (EES), which has built-in-functions for thermodynamic and transport properties of many substance, including R134a, water and others refrigerant, and the program allows user-written functions, procedures, modules and tabular data.

There are two major differences between EES and other equation-solving programs. First, EES allows equations to be entered in any order with unknown variables placed anywhere in the equations; EES automatically reorders the equations for efficient solution. Second, EES provides many built-in mathematical and thermo-physical property functions useful for engineering calculations. Transport properties are also provided for all substances. The library of mathematical and thermo-physical property functions in EES is extensive. EES

also allows the user to enter his or her own functional relationships in three ways. EES provides a facility for entering and interpolating tabular data, so that data can be directly used in the solution of the equation set.

In this study, the models were developed so that they can be integrated into EES. The EES was effectively used to perform a thermodynamic cycle of DX-SHP, also to investigate sensitivity analysis and COPs, and then use to verify the model against measured data collected during the experiment.

The enthalpy at each point was determined by interpolating through an R-134a fluid property table automatically using EES.

In order to determine how well the heat pump model in EES was predicting the actual heat pump performance, the COP, heat gain at condenser and compressor power consumptions were determinate at different radiations ( $200\text{W/m}^2$  -  $800\text{W/m}^2$ ); the output temperatures at the condenser,  $35^\circ\text{C}$  –  $45^\circ\text{C}$  for underfloor heating and  $55^\circ\text{C}$  –  $60^\circ\text{C}$  for Domestic Hot Water heating.

### **4.3.3 Unglazed Solar Collector/evaporator Model:**

The details configuration of the collector/evaporator under this investigation is shown in the *Figure 4.31* above. The evaporator temperature ( $T_{\text{evp}}$ ) for a given operating condition and ambient condition; the energy flow in the collector/evaporator was performed (see *Figure 4.37* and *Figure 4.38*).

As the collector absorbs was heated, its temperature was getting higher than that of the ambient temperature ( $T_a$ ) and heat is lost to the ambient of the room by convection and radiation (see Figure 4.37). The rate of heat loss ( $Q_l$ ) depends on the collector overall heat transfer coefficient  $U_l$  and the collector temperature,  $T_p$ .

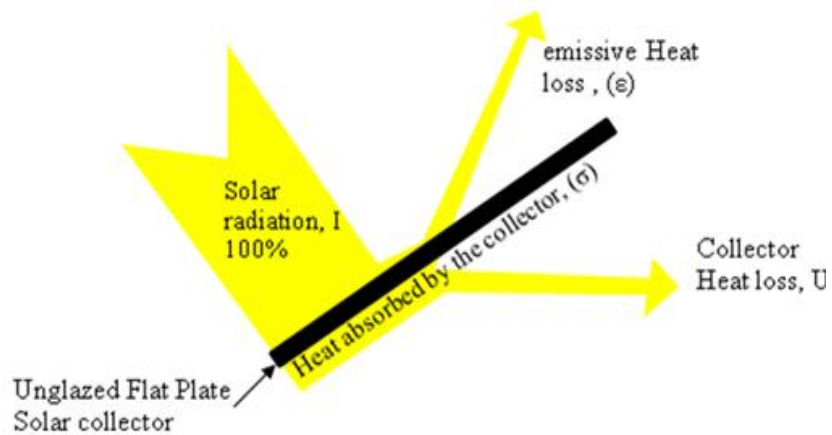


**Figure 4. 37:** Schematic Diagram of the Heat Flow in the flat plate solar collector/evaporator.

The thermal network for the evaporator ambient system is shown below, where  $S$  is equal to the incident solar absorbed by the plate,  $Q_l$  the energy loss,  $Q_{evp}$  the heat gain,  $T_a$  ambient temperature,  $T_{evp}$  collector/evaporator temperature and the  $U_l$  the collector loss coefficient. With  $A_c$  the area of the collector,  $T_p$  the temperature of the flat plate collector; the energy loss  $Q_l$  is defined as follow:

$$Q_l = U_l * A * (T_p - T_a) \tag{4.1}$$

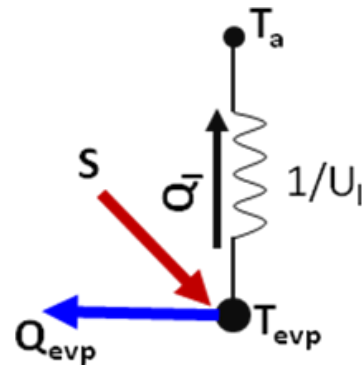


**Figure 4. 38:** The thermal network of the metal flat-plate collectors/evaporator.

In order to predict the thermal performance of the unglazed solar collector/evaporator; two methods have been suggested for formulating the governing equation of the collector/evaporator model (Kuang, Sumathy, & Wang, 2003). In the first method, in the saturated region, a couple of first order differential equations for temperature (or pressure) and quality are formulating then solved by an iterative method by Chaturvedi (2003); (Hawladar et al (2003); 2003); and Chaturvedi et al (1982), the pressure drop in the collector/evaporator' serpentine tubes was considered as a two-phase flow with assumption of equilibrium homogeneous flow. In second approach, so called simplified version of the collector/evaporator model, where the pressure drop throughout the collector/evaporator was neglected and a set of algebraic governing equations were developed. However, in the recent experimental work done by Kuang et al (2003) and Chaturverdi et al (1982) results from both methods shown good agreements when the pressure drop in the collector/evaporator is less than 20kPa.

For this investigation, the pressure drop in collector/evaporator is assumed to be less than 15kPa, therefore the simplified model to predict the collector performance seems to be necessary. The collector/evaporator temperature ( $T_{evp}$ ) and heat gain ( $Q_{evp}$ ) are predicted for the condensing temperatures (35 °C and 55 °C) and solar isolation and ambient temperature.

The rate of useful energy extracted by the collector ( $Q_{evp}$ ) expressed as the a rate of extraction under steady state condition is proportional to the rate of useful energy absorbed by the collector , less the amount lost by the collector to its surrounding. This is expressed as follows:

$$Q_{evp} = A_C [\alpha I - U_L (T_p - T_a)] \quad (4.2)$$

$$= F' A_C [\alpha I - U_L (\bar{T} - T_a)] \quad (4.3)$$

Where  $F'$  is the collector efficiency factor, which is depended on tube-and-sheet relationships, (See Figure 4.31 for details),  $\bar{T}$  the mean refrigerant temperature in the collector/evaporator,  $I$  the intensity of the solar radiation in  $W/m^2$ , and  $\alpha$  the collector absorption rate.

For this work, it is not necessary to develop a completely new analysis for the tube-sheet-sheet relation situation, Hottel-Whilliar-Blis have developed the collector efficiency factor  $F'$  (Duffi & Beckman, 2006), for the tube-sheet relation in the Figure 4.31 as following:

$$F' = \frac{1}{W \left[ \frac{1}{[D+(W-D)F]} + \frac{WU_L}{\pi D_i h_{fi}} \right]} \quad (4.4)$$

Where F is the fin efficiency factor of the collector plate, W pitch between the serpentine tubes of the collector, D refrigerant tube diameter;

$$F = \frac{\tanh[m(W-D)/2]}{m(W-D)/2} \text{ and } m = \sqrt{U_L/k_m \delta_m}$$

And  $\delta_m=1.5\text{mm}$  and  $k_m=235\text{W/m}^\circ\text{K}$  are the thickness and the thermal conductivity of the collector/evaporator flat plate respectively. Fin tubes internal heat transfer coefficient ( $h_{fi}$ ) of two-phase flow in horizontal tubes has been evaluated by Chaturvedi et al. (1996) using the following equation:

$$h_{fi} = \frac{0.0082k_l}{D_i} \left( \frac{Re_{D_i}^2 J \Delta x h_{fg}}{L} \right)^{0.40} \quad (4.5)$$

Where, J is a dimensional constant with a value 7785, and  $\Delta x$ , the change in quality of the refrigerant from collector/evaporator inlet to exit, assuming that any quality change in the collector/evaporator is largely due to enthalpy change and neglecting the quality difference due to pressure drop.

With  $\bar{T}$  been the mean refrigerant temperature in the collector/evaporator, which can be assumed to be same as the evaporating temperature ( $T_{evp}$ ) of the refrigerant in the collector/evaporator, and from equation (4.1) and (4.2),  $T_{evp}$  can be expressed as

$$T_{evp} = \frac{1}{F'} \left[ T_p - (1 - F') \left( \frac{\alpha l}{U_L} + T_a \right) \right] \quad (4.6)$$

The collector overall loss coefficient  $U_L$  is the sum of the top ( $U_t$ ) and bottom ( $U_b$ ) loss coefficients, mainly due to the convection and radiation heat-transfer from the top and bottom of the collector to ambient and can be summarised as follow:

$$\begin{aligned} U_L &= U_t + U_b \\ &= h_c + h_r \end{aligned} \quad (4.7)$$

Where  $h_c$  is the convection coefficient due to wind and  $h_r$  is the heat transfer coefficient by radiation. Since, for this study, the wind speed is very low, it can be assume that the free convection condition may dominate and will be determined using the dimensional equation from Watmuff et al (1985) work  $h_c = 2.8 + 3.0V$ , where  $V$  is the wind speed in m/s.

Following analysis given by Duffie & Beckman (1991), the heat transfer coefficient by radiation ( $h_r$ ) between the solar collector/evaporator and the sky is given by:

$$h_r = \varepsilon \sigma (T_p^2 + T_{sky}^2) (T_p - T_{sky}) \quad (4.8)$$

Where  $\varepsilon = 0.9$ , the emissivity of the collector, and  $\sigma = 5.7 \times 10^{-8} \text{ Wm}^{-2}\text{K}^{-4}$ , the Stefan –Boltzmann constant. Assuming that the sky temperature ( $T_{sky}$ ) is the same as the ambient temperature ( $T_a$ ), the radiation heat loss coefficient ( $h_r$ ) can be

$$\text{defined as: } h_r = \varepsilon \sigma (T_p^2 + T_a^2) (T_p - T_a) \quad (4.9)$$

$Q_{evp}$ , from the collector/evaporator may also be measured by means of the amount of heat carried away by the refrigerant fluid passed through it ( $\dot{m}_r$ ). And that can

be expressed in terms of the enthalpy change of the refrigerant from inlet ( $h_4$ ) to exit ( $h_1$ ) of the collector/evaporator and defined as follows:

$$Q_{evp} = \dot{m}_r (h_1 - h_4) \quad (4.10)$$

#### 4.3.4 Compressor Model:

The compressor under consideration is a hermetic constant speed compressor, and the mass of refrigerant pumped and circulated by the compressor is given as:

$$\dot{m}_r = \frac{V_d \eta_v}{v_1} \quad (4.11)$$

The pumped mass of the refrigerant by the compressor can also be expressed in terms of the rotary speed ( $N$ ) of the compressor as follows:

$$\dot{m}_r = \frac{NV_d \eta_v}{60v_1} \quad (4.12)$$

Where,  $V_d$ , is the displacement volume rate, and  $\eta_v$ , the volumetric efficiency of the compressor.  $v_1$ , The specific volume at the inlet of the compressor, the displacement volume ( $V_d$ ) for a reciprocating-type compressor can be expressed

$$\text{as: } V_d = \frac{S_c N \pi D_b^2}{4 * 60} \quad (4.13)$$

The volumetric efficiency ( $\eta_v$ ) can be estimated using the method suggested by Chow T. , He, Ji, & Chan (2007) as follows:

$$\eta_V = 1 + C - C \left( \frac{P_2}{P_1} \right)^{1/n} \quad (4.14)$$

In practice the compression process in the compressor is polytropic process, therefore the compressor work can be calculated as given below:

$$W_{oi} = \dot{m}_r \frac{P_1 v_1 n}{\eta_V (n-1)} \left[ \left( \frac{P_2}{P_1} \right)^{(n-1)/n} - 1 \right] \quad (4.15)$$

The indicated power for compression can also be calculated in term of the change of the enthalpy of the refrigerant from the inlet ( $h_1$ ) to outlet ( $h_2$ ) of the compressor as follows:  $W_{comp} = W_{oi} * \eta_{comp} = \dot{m}_r (h_2 - h_1)$  (4.16)

Where,  $W_{oi}$  is the total ideal input electric power to the compressor, and  $\eta_{comp}$  is the general efficiency of the compressor.

#### 4.3.5 Condenser Model:

The maximum temperature raise of the cold water at the heat exchanger would be from the inlet refrigerant temperature ( $T_{rcond i}$ ) to the cold water temperature ( $T_{wcond i}$ ) at the heat exchanger (Figure 4.39).

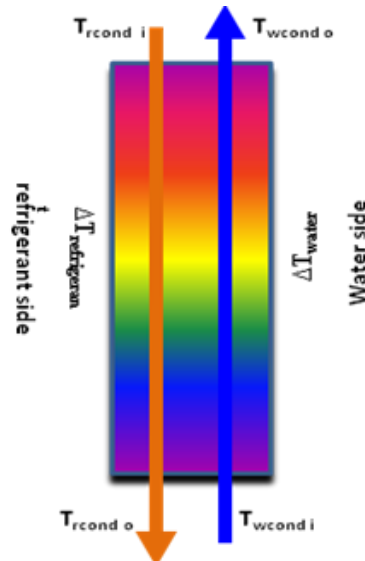


**Figure 4. 39:** Schematic diagram of the Contraflow Flat plate L-line type heat exchanger

In the refrigerant side of the heat exchanger the heat gain from the refrigerant can be estimated as:  $Q_{rcond} = \dot{m}_r C_{pr} (T_{rcond o} - T_{rcond i})$  (4.17)

Where,  $C_{pr}$  is the specific heat coefficient of the refrigerant; the heat gain from the refrigerant at the collector can also be calculated in term of the change of the enthalpy of the refrigerant from the inlet ( $h_2$ ) to outlet ( $h_3$ ) of the heat exchanger as follows:  $Q_{rcond} = \dot{m}_r (h_2 - h_3)$  (4.18)

In the water side of the heat exchanger the heat gain from the refrigerant can be estimated as:  $Q_{wcond} = \dot{m}_w C_p (T_{wcond o} - T_{wcond i})$  (4.19)

Where  $\dot{m}_w$  is the mass flow rate of the water,  $C_p$  the specific heat coefficient of the water, and  $T_{wcond o}$  and  $T_{wcond i}$  are respectively the temperatures of the water at the exit and the inlet of the condenser.

The coefficient of performance (COP) of heat pump system at any time instant (t) was calculated as:

$$COP_{hp} = \frac{Q_{wcond}(t)}{W_{comp}(t)} \quad (4.20)$$

Where  $Q_{wcond}(t)$  was the heat exchanger rate at condenser, and  $W_{comp}(t)$  was the power input (heat pump compressor and circulating pumps) to the system at any time instant (t). Within an operating test period of the duration  $\tau$ , the average  $COP_{heat\ pump}$  was defined as:

$$COP_{hp,avr} = \frac{\int_0^{\tau} Q_{wcond}(t)dt}{\int_0^{\tau} W_{comp}(t)dt} \quad (4.21)$$

#### 4.4 Analytical Results of the DX-SHP:

At the following radiations, 200W/m<sup>2</sup>, 400 W/m<sup>2</sup>, 600 W/m<sup>2</sup>, and 800 W/m<sup>2</sup>, a series of simulation was carried out using EES software and then used excel to plots the results. For each radiation, the COP of the heat pump, the heat rate gain at the condenser and the compressor energy consumption were evaluated, recorded and then plotted against evaporated temperatures; in addition the effects of the geometric design of the evaporator/collectors on the evaluated parameters were also investigated.

#### 4.4.1 The effect of the collector/evaporator and condenser temperatures on the Heat pump COP

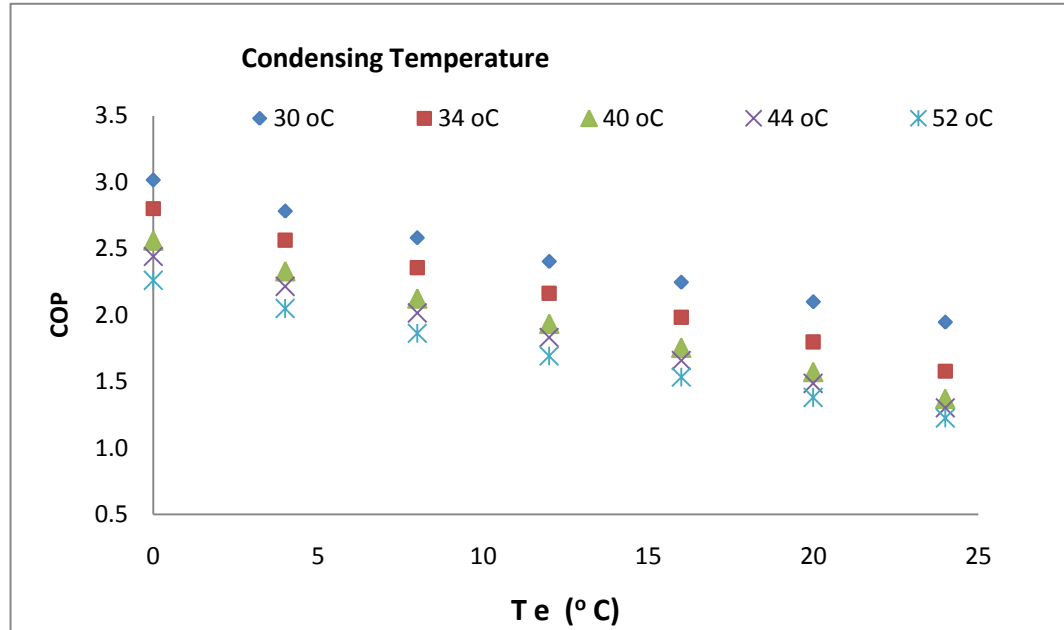


Figure 4.40: Condensing and Evaporating Temperatures Vs Heat Pump COP

Figure 4.40 shows how the COP of the heat pump changes with the temperatures at the condenser and the evaporator/collector. From the graphs, when the condensing temperatures increase the COP decrease as expected, because this increase the lift between the evaporator temperature and the condensing temperature. For the condensing temperature between 35°C and 55°C, the simulated COP was between 1.8 and 3.5 and was agreeing with the conventional ASHP COP for winter period. As the condenser temperatures increase, the COP decreases. But at the evaporator, when the inlet evaporation temperatures increase, the COP decreases due to the high heat loss to the ambient.

4.4.2 The effect of the collector/evaporator and condenser temperatures on the compressor power consumption

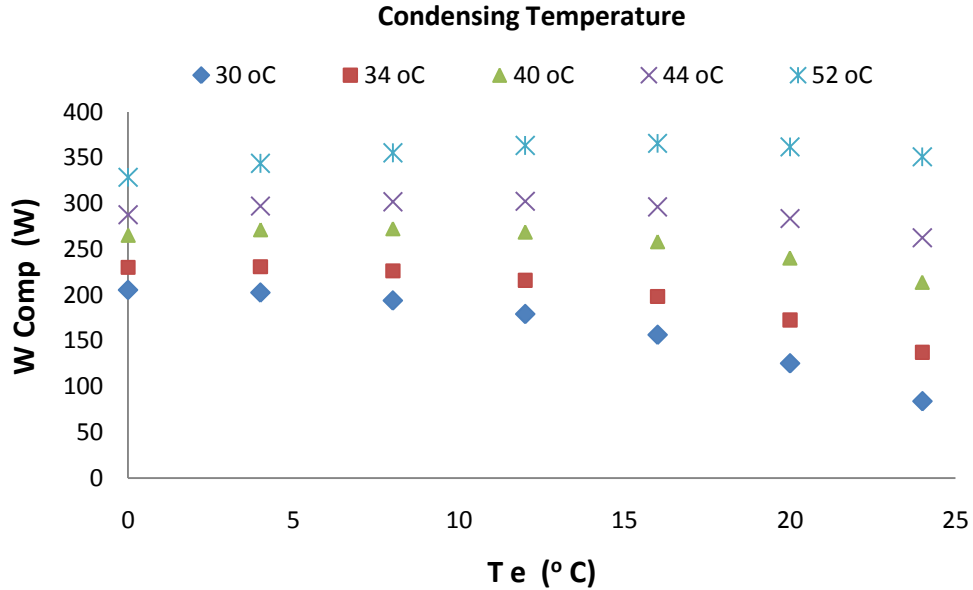
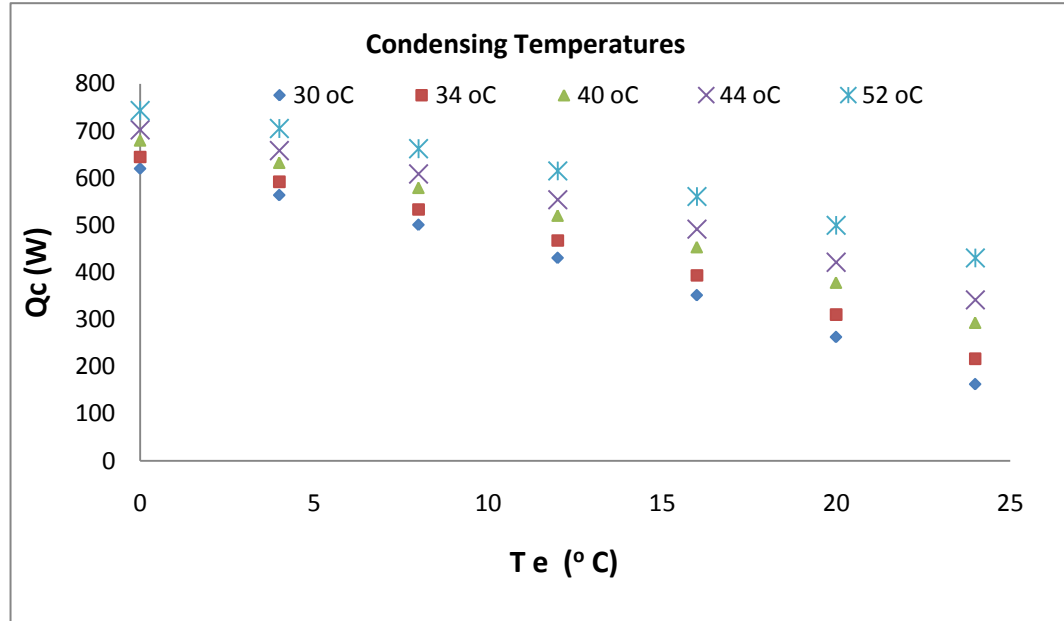


Figure 4.41: Condensing and Evaporating Temperatures Vs Compressor power consumption

Figure 4.41 shows how the power consumption of the heat pump compressor changes with the temperatures at the condenser and the evaporator/collector. From the graphs, when the condensing temperatures increased, the compressor power consumption was increased as expected, because of the lift between the evaporator temperature and the condensing temperature; so the compressor were supposed to work higher to achieve the condensing temperature. In addition, Figure 4.41 shows how the power consumption changes with the evaporator, from 0°C to 10°C, the power consumption of the compressor were constant, so this were useful information, because, this was a indication that the heat pump could still performing better during coldest day in winter.

**4.4.3 The effect of the collector/evaporator and condenser temperatures on the heat gain at the condenser**



*Figure 4.42: Condensing and Evaporating Temperatures Vs Heat gain at the Condenser*

Figure 4.42 shows how the heat gain at condenser changes with the temperatures at the condenser and the evaporator/collector. From the graphs, when the condensing and the evaporator temperatures increased, the heat gain at the condenser was decreased as expected, because of the increased lifted temperature between the evaporator temperature and the condensing temperature; and also because of the increased heat lost at the unglazed collector/evaporator when the radiation was high. From 0°C to 10°C at the evaporator, the heat gain at condenser was still practical, so this were useful information, because, this was a indication that the heat pump could still performing better during coldest day in winter.

#### 4.4.4 The effect of the collector/evaporator Area on the COP of the heat pump

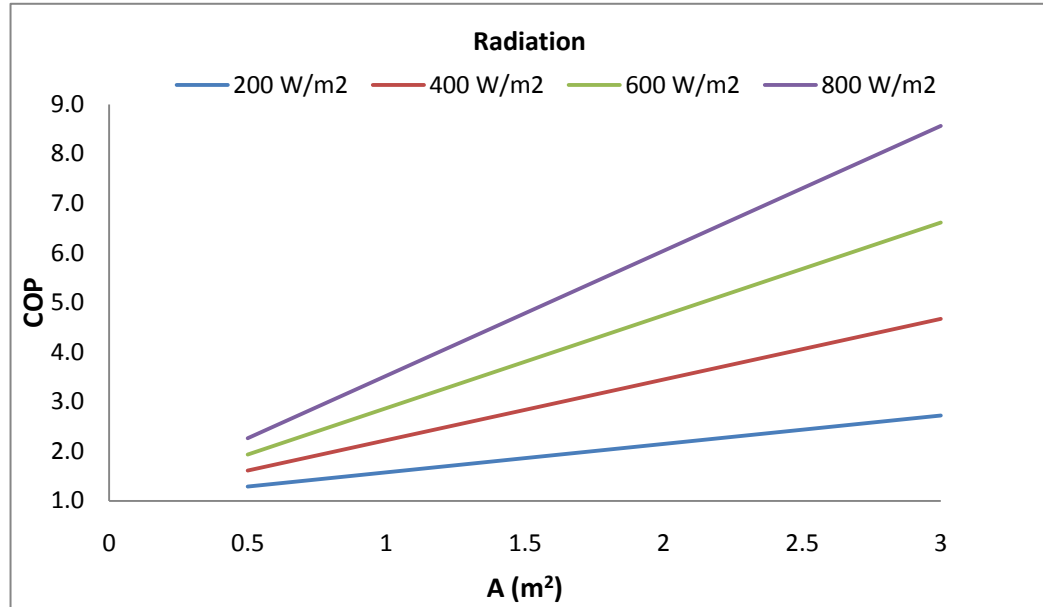
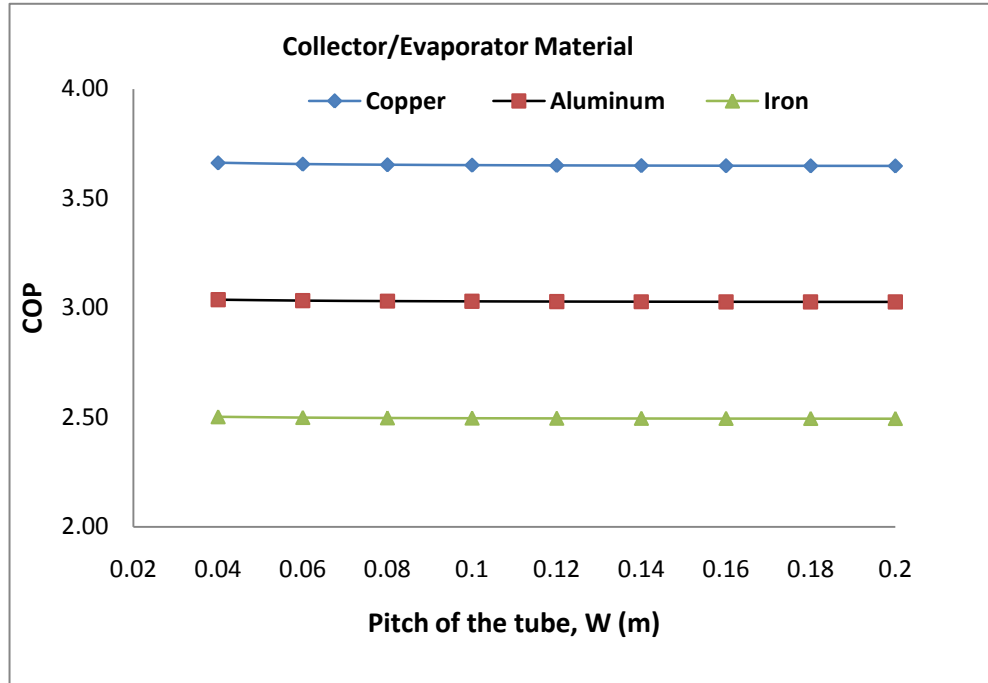


Figure 4. 43: Evaporator Area Vs Heat Pump COP

Figure 4.43 shows how the COP changes with the area of the collector/evaporator and also the solar radiations. From the graphs, it is clear that COP was depended to the areas of the evaporator. As the area of the evaporator increases, the COP also increases as expected; because the heat collected area was greater, given the possibility for the refrigerant flowing through collected as much heat energy as possible.

**4.4.5 The effect of the pitch between refrigerant’s serpentine tubes of the collector/evaporator on the COP of the heat pump**



*Figure 4.44: Pitch of the refrigerant /evaporator tubes Vs COP*

Figure 4.44 shows how the COPs change with the pitch of the refrigerant serpentine tubes at the evaporator; it also shows how the type materials influence the COP of the heap pump. From the graphs, it is clear that COP was independent to the pitch between the refrigerant tubes. However, the COP was dependent relative to the type of the material, from the results, the copper plate has a high COP compare to the iron and aluminium, this was because the cooper have a very good heat transfer properties.

#### 4.4.6 The effect of the diameter of the refrigerant's tubes of the collector/evaporator on the COP of the heat pump

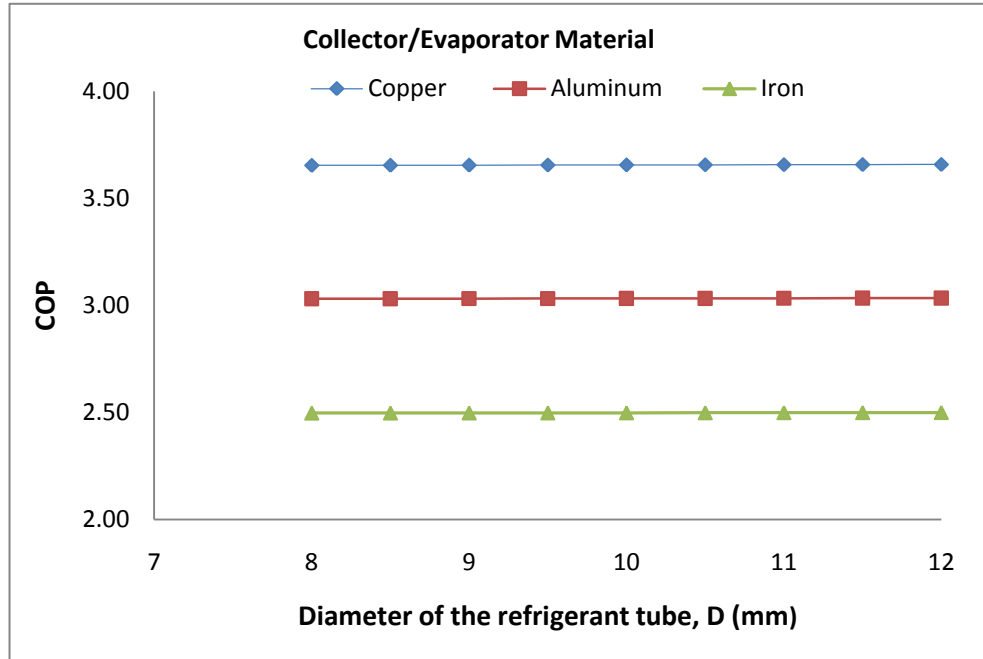


Figure 4. 45: Diameter of the Collector/Evaporator' tubes Vs COP

Figure 4.45 shows how the COP changes with the diameter of the refrigerant tubes at the evaporator; from the results the COP was not dependent to the diameter the refrigerant tubes as expedited; but, it was sensitive to the type of the material and radiation, because in the refrigerant loop; the expansion valve controlled the amount of refrigerant entering the evaporator, so when the refrigerant in the collector/evaporator was saturated vapour to interred the compressor, so the expansion valve closed, so it was dependent on the size of the refrigerant tubes as shown on the above Figure 4.45.

## 4.5 Experimental Study of the DX-SHP System

### 4.5.1 Methodology

In order to evaluate the heat pump efficiency (COP) and the heat gain at the condenser, a Data-taker was used to record temperatures and pressures at the key points in the circuit (see Figure 4.49); in addition the water mass flow rate ( $\dot{m}_w$ ) and compressor power consumption ( $W_C$ ) were also recorded. Then these data were then analysing using Microsoft Excel. The rate of heat gain out the heat exchanger may be measured by means of the amount of heat carried away in the fluid passed through it, and that was  $Q_c = \dot{m}_w C_p (T_{co} - T_{ci})$ , where,  $\dot{m}_w$  was the mass flow rate of the water,  $C_p$ , the specific heat coefficient of the water, and  $T_{co}$  and  $T_{ci}$  were the temperatures of the water at the exit and the inlet of the heat exchanger, respectively. The experiment performances obtained were also compared with simulation results and the Carnot's efficiency (COP).

### 4.5.2 Experimental Procedure

The DX-SHP system offered two fundamental operation modes i.e. space heating only mode (water at 35°C), and Domestic Hot Water (DHW) only mode (water at 55°C). In order to evaluate the thermal performance of the DX-SHP a series of experiments were conducted at the laboratory of the school of the Built Environment, Nottingham University. The procedures followed to conduct the

experiment are described below. The basic equipments involved at this stage and the way they were set up is illustrated diagrammatically in Figure 4.49.

The experimental procedure was as follows:

1. Make a note of the starting time;
2. Measure the ambient temperature and relative humidity;
3. Make a note of the water temperature of the water at the inlet of the heat exchanger, because the average performance of the heat pump system should be evaluated base on the time the water temperature goes from initial temperature up to useful temperature 35°C for space heating and 50°C for DHW;
4. Read the power of the compressor on the power meter
5. Make sure that all connection are tight and secure , and that there is not obstruction in front of simulate light,
6. Turn on the computer, check that all sensors and transducers are properly connected
7. Check that logging equipment is ready for test and will log data every five minutes;
8. Turn on the simulated light, and then set the experimental solar irradiation levels at 200W/m<sup>2</sup>, 400 W/m<sup>2</sup>, 600 W/m<sup>2</sup>, or 800 W/m<sup>2</sup> ;
9. Run the circulating pump of the water circuit, then take note of the water mass flow rate on the flow meter (l/min);

10. Run the refrigerant compressor and control the sight glass to ensure that there is enough refrigerant in the circuit and that the system is functioning properly;
11. Let the experiment warm up for approximately for 10 minutes; this brings the compressor up to its operating temperature and pressure, then check the temperature and pressure gauges on the low pressure and high pressure of the compressor for correct refrigerant charge and confirm the values with the vapour compression properties of the R134a;
12. After the warm up term control again the water temperature at the heat exchanger inlet and make a note and also check the temperature sensor on the computer and the fan controller display for repeatability and accuracy of the data recorded
13. Let the system run until the water temperature raise to the useful temperature of 35°C for space heating and 50°C for DHW;
14. When the system reaches the useful temperature, the fan automatically switches on and reject the heat in the room to keep the water temperature constant
15. Note the time again and the read the power of the compressor on the power meter
16. The test rig should be ready to repeat the experimental procedure
17. Shut down the compressor, but leave the water circulating pump running, so the water can cool down and be ready for the next experiment.

### 4.5.3 Experimental set-up

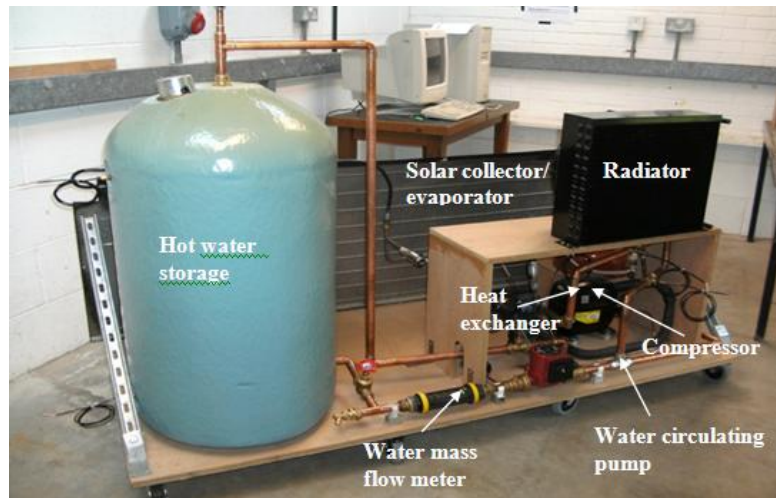


Figure 4.46: Picture of the DX-SHP under experimental Set-up



Figure 4.47: Simulated solar radiations on the experimental rig

#### 4.5.4 Data acquisition and Processing System

The following parameters were measured: electric power consumed by the compressor; temperatures of both water and refrigerant circuits recorded at different locations of the two loops; pressures of refrigerant at inlet outlet of the compressor, evaporator/collector and condenser were also measured. In addition, the ambient temperature, relative humidity, the incident solar simulation, and indoor air temperature were also measured.

Pressures were measured with GP pressure transmitter, which is a multipurpose, high performance stainless steel 0-100Mv output transducer transmitting at 4-20mA output range; temperatures were measured with K-type, thermocouples and platinum resistance thermometers (RTDs). A solar Pyranometer was placed at the middle of the collector/evaporator plate to measure the instantaneous simulated solar radiations (see Figure 4.48). Mass flow rate of the water was measured using flow meter. A digital power meter was used (Figure 4.54) to measure the power consumption of the compressor every five minutes. All data were measured, monitored and controlled by a personal computer via data logger software (Figure 4.48).



*Figure 4.48: Data Taker DT500 series 3 and expansion channel connected in the Experimental Rig*

#### 4.5.5 Experimental uncertainty

Any experiment incurs measurement errors and when these are extrapolated the uncertainty is increased. The error can however be minimised by careful calibration of equipment. Because of the errors and inaccuracies in equipment, measurement uncertainties must be computed and maintained as low as possible to provide accurate value of the experimental conditions and parameters after careful calibration of sensors and the basic equipment shown in Figure 4.51 & Figure 4.56. The following uncertainties were summarised in the *Table 4.16* below:

**Table 4. 11: Sensor uncertainty**

Sensor	Percentage error
Thermocouple	$\pm 1.85$
RTD	$\pm 1.25$
Pressure transducer	$\pm 0.25$
Pyranometer	$\pm 1.0$

For purpose of analysing experimental data, the Data-Taker (See Figure 4.48) in the *Figure 4.49*, was connected to the computer to store data in the computer for future reference and then transfer to spreadsheet for examination using appropriate software.

**Figure 4.49: Data logger wiring on the Experimental Test Rig**

## 4.5.6 Measuring Equipments

### 4.5.6.1 Measuring the Temperatures, solar radiation and relative humidity

There is a variety of temperature sensors used in research and the three sensors most commonly used are thermocouple; the platinum resistance thermometer (PRT); and the thermostat. *Table 4.12* compares and contrasts the three sensors. From the *Table 4.12*, thermocouples are not precision sensors; errors of 2°C are typical and were confirmed through calibration. However thermocouples have a wide temperature range of about -200°C to 2000°C, in addition they are relatively low cost and flexible. And after calibration of the temperature sensor, RTD, it has shown to have high accuracy compared to thermocouple and has been used to record temperatures at various points of the refrigerant loop, see Figure 4.50.

**Table 4. 12: The most commonly used temperature sensors and their properties (Technology Pico, 2001)**

	Thermocouple	RTD (Pt100)	Thermistor
<b>Operating Range</b>	-200 °C to 2000 °C	-250 to 850 °C	-100 to 300 °C
<b>Accuracy</b>	Low 1 °C common	Very High 0.03 °C common	High 0.1 °C common
<b>Linearity*</b>	Medium	High	Low
<b>Thermal Response**</b>	Fast	Slow	Medium
<b>Cost</b>	Low	High	Low to moderate
<b>Noise Problems</b>	High	Medium	Low
<b>Long term stability</b>	Low	High	Medium
<b>Cost of measuring instrument</b>	Medium	High	Low

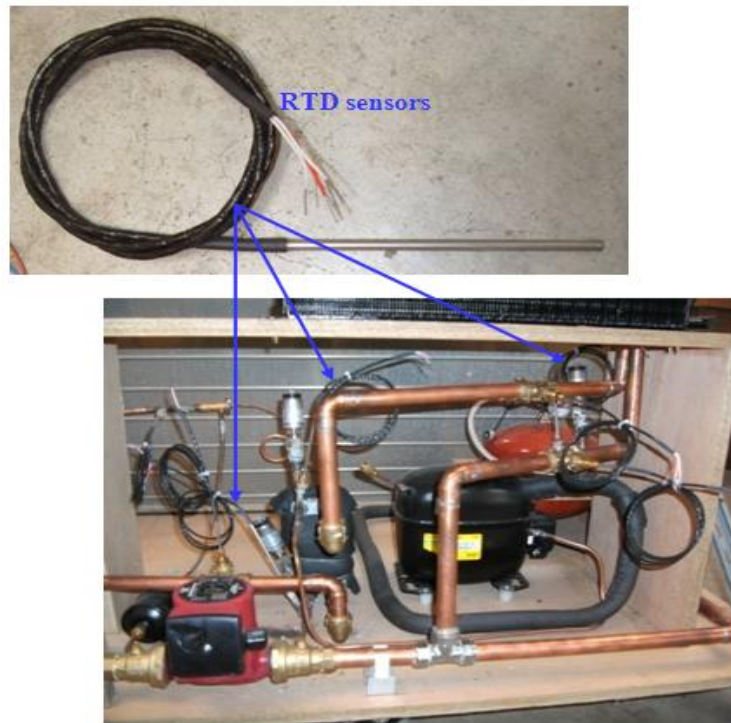


**Figure 4.50:** Illustration of the temperature sensors of the test rig

The tests were conducted at the Laboratory of the Department of Built Environment, University of Nottingham, UK. The room temperatures were measured using the high performance Humidity & Temperature Probe Meter shown in the *Figure 4.52* and specification summarised in the Table 4.14. For accuracy purpose a second measurement on the temperature was done at different points of the water and refrigerant loop using K-type Digitron Thermometer (specification in the Table 4.15) shown in the *Figure 4.55* was used to measure the temperatures at different points of the rig to double check the values logged by the Data taker. In addition, a low dome thermal offset error, Kipp & Zonen CM11 Pyranometer was used to measure the simulated solar radiation (see *Figure 4.56*) with its specification summarised in the Table 4.16. In order to evaluate the performance of the heat pump loop, the following data were also measured and recorded,

mass flow rate of the water across the heat exchanger using mass flow meter shown in the Figure 4.53 and the power consumption by the compressor using single phase power meter shown in the Figure 4.54 .

#### 4.5.6.2 Measuring the Pressures

The GP pressure transmitter is a multipurpose, high performance stainless steel 0-100Mv output transducer transmitting at 4-20mA output range (see Table 4.13). The pressure range is 0 - 10bar. It is a temperature compensated strain gauge technology with a +/- 0.25% accuracy full scale. *Figure 4.51* shows both GP pressure transducer and the mode of installation on the test rig with the extension output cable to the data logger.



**Figure4. 51:** GP Pressure transducer

**Table 4.13: Specification of the pressure transducer**

Category	Pressure Sensors
Proof Pressure	2 x Range (x5 Burst Pressure)
Analogue Output	4 to 20mA
Supply Voltage	12 to 36Vdc 0-5V output(Transducers) -40 to +100/125oC transmitter/transducer range 2x rated overpressure up to 250mb

**4.5.6.3 Measuring ambient temperature and relative humidity**

**Table 4.14: Specifications of Digital temperature**

Range	Humidity : 0-100%RH Temp. -20 – 60°C
Accuracy	Humidity : ±3.5%RH Temp. ±2°C
Resolution	0.1%RH, 0.1°C
Operation Temperature	0°C -40°C (<80% R.H.)



**Figure 4.52: Digital temperature and humidity meter**

**4.5.6.4 Measuring water mass flow rate**



**Figure 4.53: Water flow meter**

#### 4.5.6.5 Measuring the compressor power consumption



Figure 4. 54: The single phase watt hour meter

#### 4.5.6.6 Second temperatures control

Table 4. 15: Specifications of the digital thermometer

Range	From -199 °C to +199.9°C
Accuracy	0.01%rdg. ±0.2°C
Resolution	0.1°C



Figure 4. 55: A digital thermometer, Digitron T208

#### 4.5.6.7 Measuring the simulated solar radiation

*Table 4. 16: Specifications of the CM11 Pyranometer*

<b>Specifications of the CM11 Pyranometer</b>	
Spectral range	305 – 2800 nm (50% points)
Sensitivity	$4.56 \times 10^{-6}$ V/Wm <sup>2</sup>
Accuracy	Humidity : $\pm 3.5\%$ RH Temp. $\pm 2^\circ\text{C}$
Response time (95%)	15 sec
Temp. dependence of sensitivity	$< \pm 1$ W/m <sup>2</sup> % (beam 1000 Wm <sup>2</sup> )
Directional error	$< \pm 1\%$ (-10 to +40°C)
Impedance (nominal)	700 – 1500 $\Omega$
Operation Temperature	-40°C to +80°C



*Figure 4. 56: Kipp & Zonen, CM11 Pyranometer*

#### 4.6 Analysis

The coefficient of performance (COP) of heat pump system at any time instant (t) was calculated as:

$$COP_{hp} = \frac{Q_{wcond}(t)}{W_{comp}(t)} \quad (4.22)$$

Where  $Q_{wcond}(t)$  was the heat exchanger rate at condenser, and  $W_{comp}(t)$  was the power input (heat pump compressor and circulating pumps) to the system at any

time instant ( $t$ ). Within an operating test period of the duration  $\tau$ , the average  $COP_{\text{heat pump}}$  was defined as:

$$COP_{hp,avr} = \frac{\sum_0^{\tau} Q_{wcond}(t)dt}{\sum_0^{\tau} W_{comp}(t)dt} \quad (4.23)$$

The effectiveness of the DX-SHP system ( $eff_{DX-STSHP}$ ) was defined as the ratio of the actual COP of the heat pump of the reverse Carnot cycle COP expressed as follow:

$$eff_{DX-STSHP} = \frac{COP_{avr,exp}}{COP_{avr,Carnot}} \times 100 \quad (4.24)$$

#### 4.7 Experimental results and discussion

A series of tests were undertaken at the follow simulated radiations  $200\text{W/m}^2$ ,  $400\text{W/m}^2$ ,  $600\text{ W/m}^2$ , and  $800\text{ W/m}^2$ ; and when the room temperature was in the range between  $18^\circ\text{C}$  to  $22^\circ\text{C}$ . The relation between COP, heat gain at condenser, electrical power consumption of the compressor, condensing temperatures and the inlet temperature of the refrigerant in the collector/evaporator were investigated and the results for each radiation were summarised below as following:

### 4.7.1 Performance investigation of DX-SHP at solar radiation of 200W/m<sup>2</sup>

All experiment data plotted in the *Figure 4.57*, *Figure 4.58*, and *Figure 4.59* were changing with time expect the solar irradiance and condensing temperature, which were simulated constant at 200W/m<sup>2</sup> and the water temperature at the condenser kept constant at 35°C for space heating purpose through underfloor heating or 55°C for DHW.

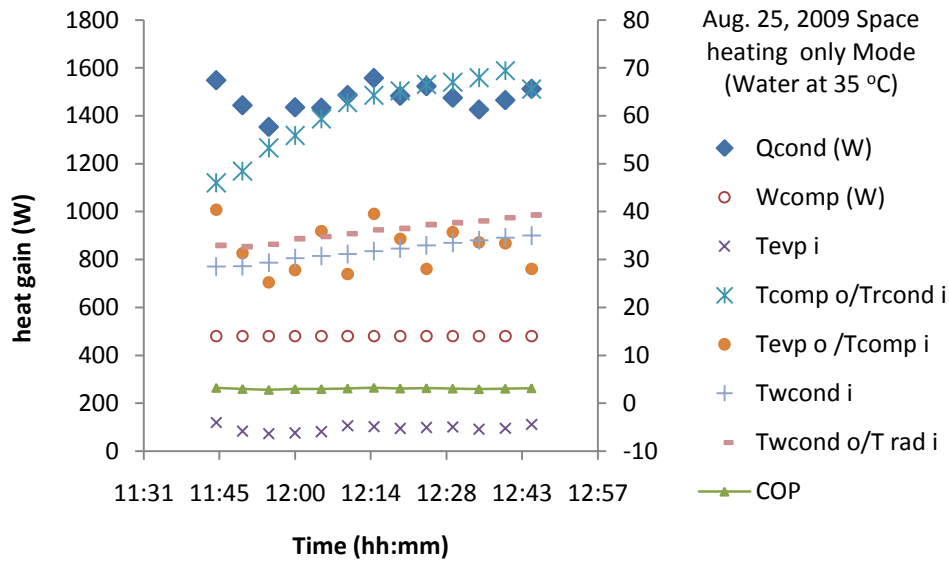


**Figure 4. 57:** Test results obtained on August, 25, space heating mode, with 35oC water temperature at the condenser at 200W/m<sup>2</sup>

*Figure 4.57* shows the experimental results obtained during August 25<sup>TH</sup>, 2009, when the room temperature was in the range between 18°C to 22°C. The data were recorded automatically by a data logger, every 5 minutes. From the graph at constant radiation of 200W/m<sup>2</sup>, the COP, evaporator inlet temperature and compressor power consumption were not dependent to the time. The degree of

superheat at the exit of the collector/evaporator was less than 10°C. The temperature difference across the condenser water side was 5°C. The heat gain at the condenser was sensitive to the time variation.

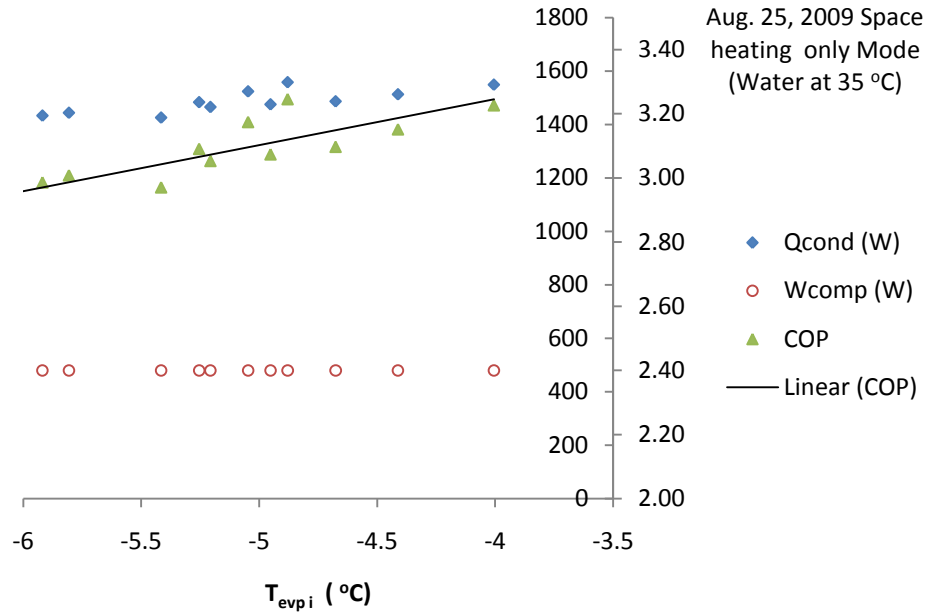


**Figure 4. 58:** The effects the collector/evaporator inlet temperature ( $T_{evp i}$ ) on the COP of the heat pump, the heat rate gain at the condenser, and the compressor energy consumption at  $200W/m^2$

Figure 4.58 shows, the relation of the COP, heat gain at condenser, and electrical power consumption of the compressor with inlet refrigerant temperatures at the evaporator. From the results, when the water temperature at the condenser was set constant at 35°C, with the simulated radiation at  $200W/m^2$ , which closed the one in winter months, the inlet temperature at evaporator were between -6 to -3.5, and the energy gain at the condenser was fluctuated between 1500W to 1580W, after

one hour, and the COP was between 3.20 and 3.30, and was within the range of the air source heat pump performance standard at the beginning of winter. These results were informative, because they shown that the system could perform better in coolest day during winter.

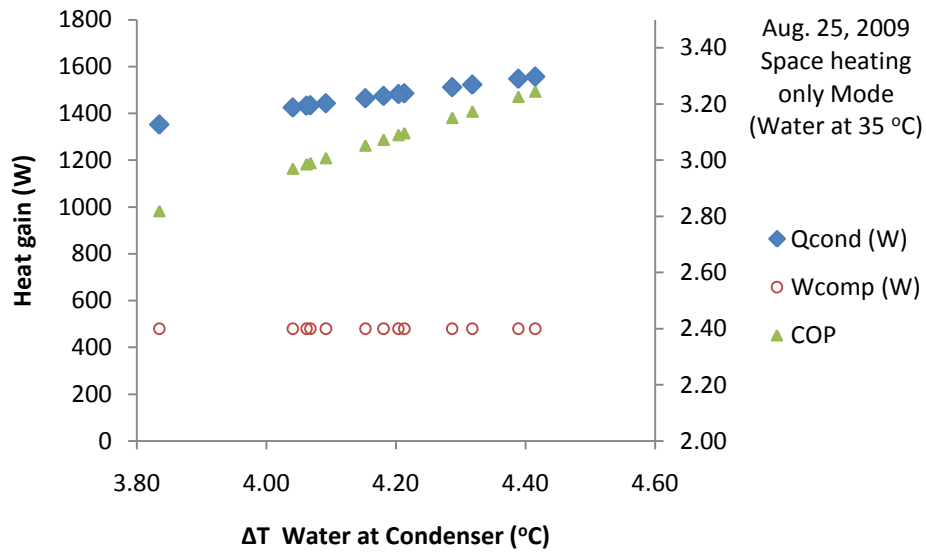


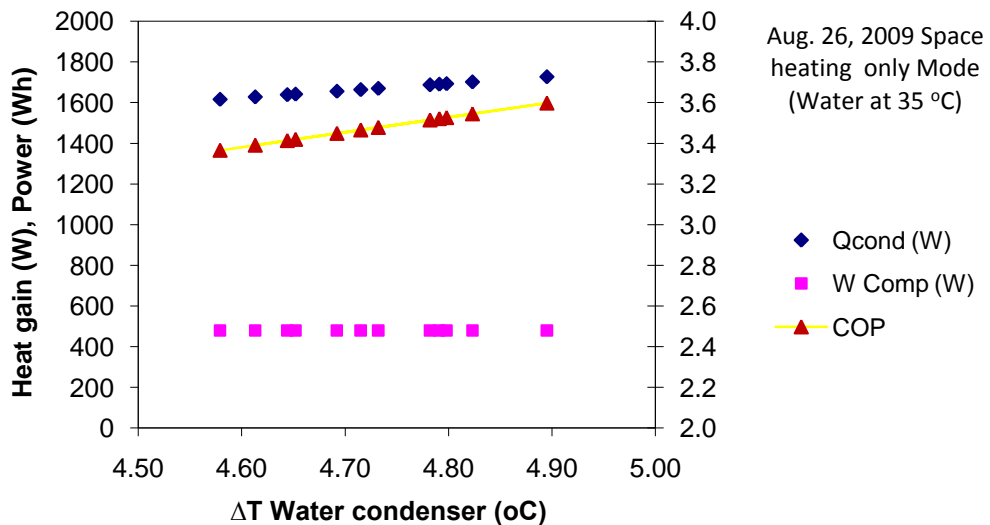
Figure 4. 59: Test results obtained on August, 25, space heating mode, with 35oC water temperature at the condenser at 200W/m<sup>2</sup>

Figure 4.59 shows, the relation of the COP, heat gain at condenser, and electrical power consumption of the compressor with the change water temperature across the condenser. From the results, when the water temperature at the condenser was set constant at 35oC, with the simulated radiation at 200W/m<sup>2</sup>, which closed the one in winter months, the inlet temperature at evaporator were between -6 to -3.5, and the temperature gain at the condenser were between 4°C to 5°C, and was

enough to provide useful water temperature to achieve DHW at 55°C, after one hour under the simulated radiation at 200W/m<sup>2</sup>.

#### 4.7.2 Performance investigation of DX-SHP at solar radiation of 400W/m<sup>2</sup>

All experiment data plotted in the *Figure 4.60*, *Figure 4.61*, and *Figure 4.62* were changing with time expect the solar irradiance and condensing temperature, which were simulated constant at 400W/m<sup>2</sup> and the water temperature at the condenser kept constant at 35°C for space heating purpose through underfloor heating or 55°C for DHW.



**Figure 4. 60:** Heat gain at condenser, the COP Vs temperature change across the condenser at 400W/m<sup>2</sup>

Figure 4.60 shows the experimental results obtained during August 26<sup>TH</sup>, 2009. The data were recorded automatically by a data logger, every 5 minutes. From the graph at constant simulated radiation of 400W/m<sup>2</sup>; the heat gains at the condenser have the same trend with the temperature change of the water at the condenser. The COP was between 3.40 and 3.80, and was within the range of the air source heat pump performance standard. The temperature difference across the condenser water side was 5°C and was enough to achieve useful temperature at least than 25 minutes under 400W/m<sup>2</sup>.

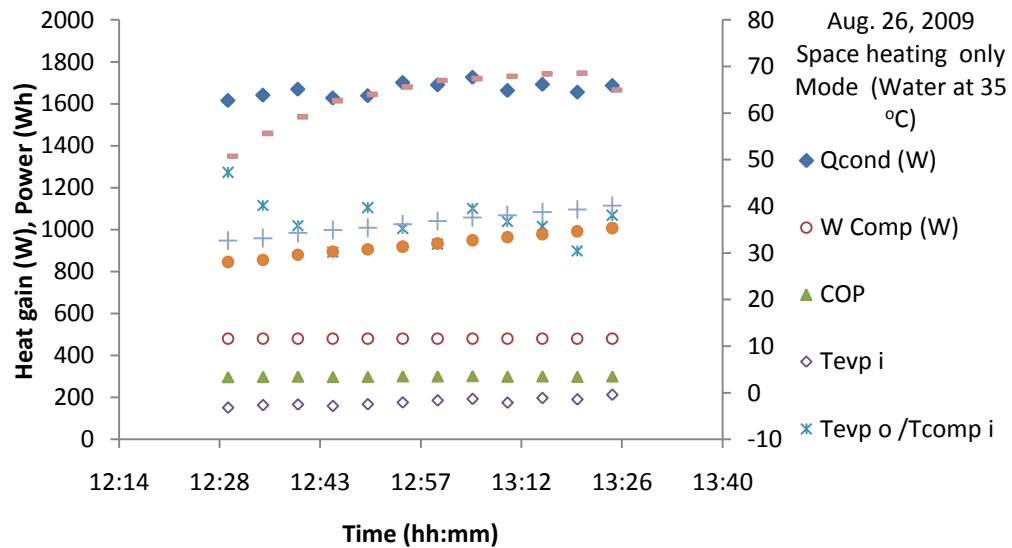


Figure 4. 61: Test results obtained on August, 25, space heating mode, with 35oC water temperature at the condenser at 400W/m<sup>2</sup>

Figure 4.61 shows the experimental results obtained during August 26<sup>TH</sup>, 2009, when the room temperature was in the range between 18°C to 22°C. The data were recorded automatically by a data logger, every 5 minutes. From the graph at

constant radiation of  $400\text{W/m}^2$ , the COP, evaporator inlet temperature and compressor power consumption were not dependent to the time. The degree of superheat at the exit of the collector/evaporator was less than  $10^\circ\text{C}$ . The temperature difference across the condenser water side was  $5^\circ\text{C}$ . The heat gain at the condenser was dependent to the time variation.

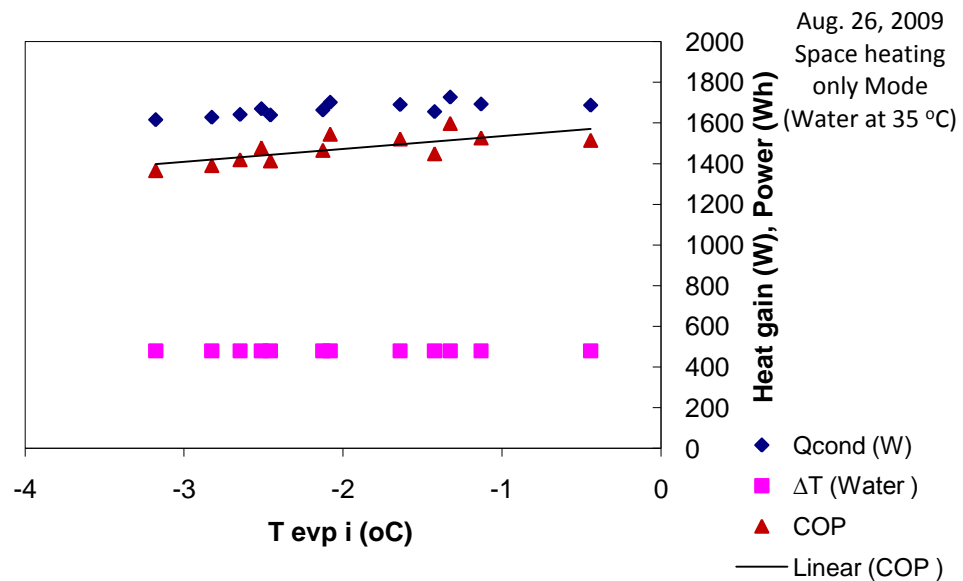


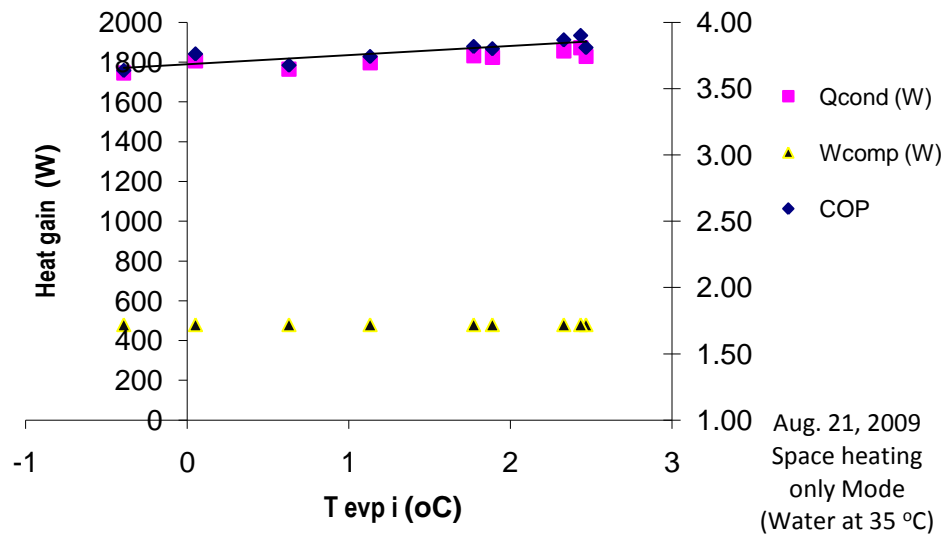
Figure 4. 62: Test results obtained on August, 26, space heating mode, with 35oC water temperature at the condenser at  $400\text{W/m}^2$

Figure 4.62 shows, the relation of the COP, heat gain at condenser, and electrical power consumption of the compressor with inlet refrigerant temperatures at the evaporator. From the results, when the water temperature at the condenser was set constant at  $35^\circ\text{C}$ , with the simulated radiation at  $400\text{W/m}^2$ , which closed the one in winter months, the inlet temperature at evaporator were between  $-4$  to  $0$ , and the energy gain at the condenser was fluctuated between  $1500\text{W}$  to  $1580\text{W}$ , after

47 minutes and the COP was between 3.80 and 3.80, and was within the range of the air source heat pump performance standard at the beginning of winter. These results were informative, because they shown that the system could perform better in coolest day during winter.

#### 4.7.3 Performance investigation of DX-SHP at solar radiation of 600W/m<sup>2</sup>

All experiment data plotted in the *Figure 4.63*, *Figure 4.64*, and *Figure 4.65* were changing with time expect the solar irradiance and condensing temperature, which were simulated constant at 600W/m<sup>2</sup> and the water temperature at the condenser kept constant at 35°C for space heating purpose through underfloor heating or 55°C for DHW.



**Figure 4. 63:** The effects the collector/evaporator inlet temperature ( $T_{evp i}$ ) on the COP of the heat pump, the heat rate gain at the condenser, and the compressor energy consumption at 600W/m<sup>2</sup>

Figure 4.63 shows, the relation of the COP, heat gain at condenser, and electrical power consumption of the compressor with inlet refrigerant temperatures at the evaporator. From the results, when the water temperature at the condenser was set constant at 35°C, with the simulated radiation at 600W/m<sup>2</sup>, which closed to the summer radiation months, the inlet temperature at evaporator were between 0 to 3degC, and the energy gain at the condenser was fluctuated between 1600W to 1800W, after one hour and the COP was between 3.70 and 4.01, and was within the range of the air source heat pump performance standard in summer. These results were informative, because they shown that the system could perform better event during hot days in summer, with not excessive heat gain at the evaporator or with a danger for the compressor.

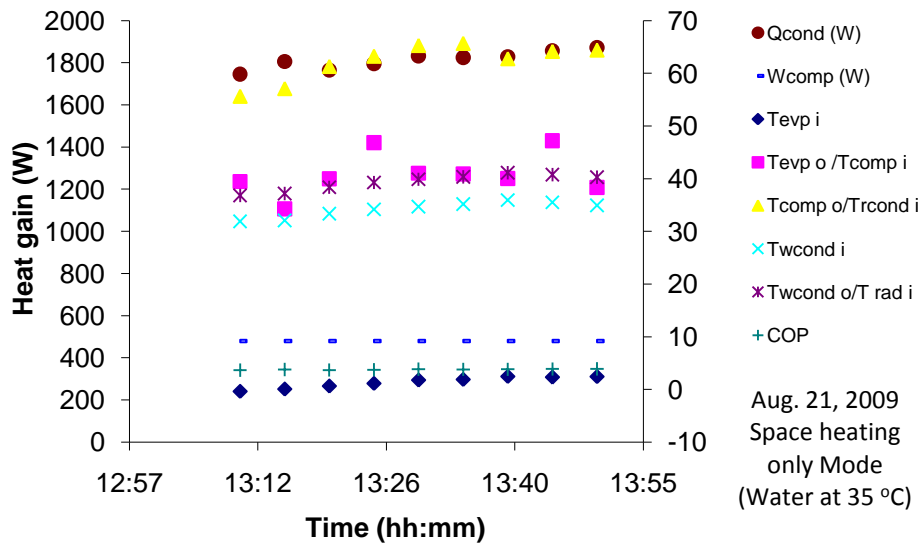


Figure 4. 64: Test results obtained on August, 21, space heating mode, with 35oC water temperature at the condenser at 600W/m<sup>2</sup>

The relation of the COP, heat gain at condenser, and electrical power consumption of the compressor with the time were summarised in the Figure 4.64. The data were recorded automatically by a data logger, every 5 minutes. From the graph at constant radiation of  $600\text{W/m}^2$ , the COP, evaporator inlet temperature and compressor power consumption were not dependent to the time. The degree of superheat at the exit of the collector/evaporator was less than  $10^\circ\text{C}$ . The temperature difference across the condenser water side was  $5^\circ\text{C}$ . The heat gain at the condenser was link to the time variation; due to the fact that as the time passed, the evaporator was heat up, and the temperature of the collector also increased therefore was enough to influence the heat gain at the condenser.

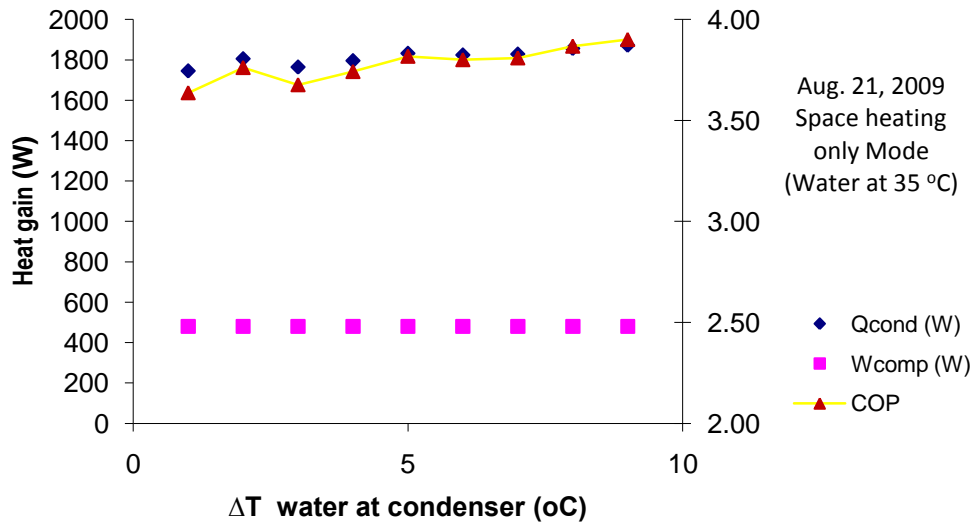
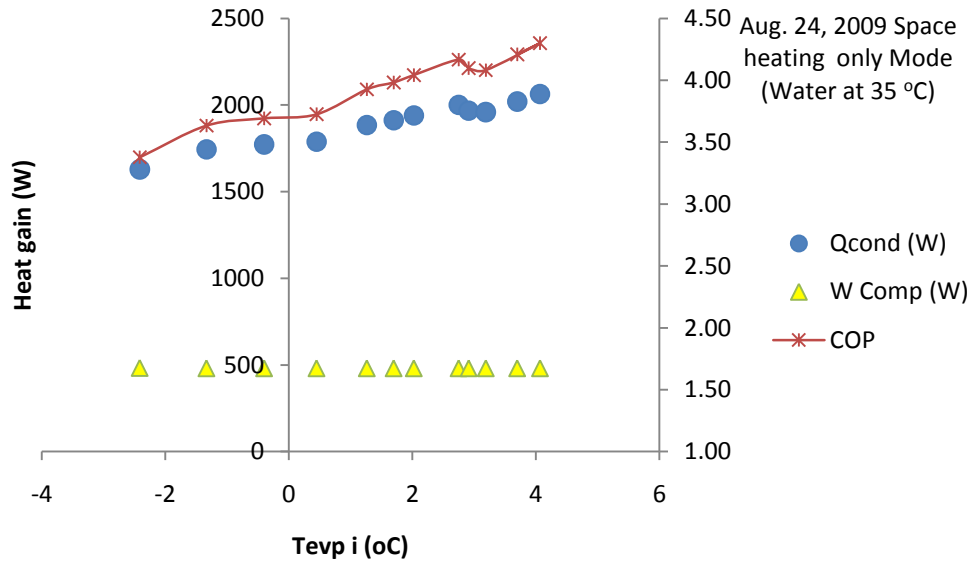


Figure 4. 65: Test results obtained on August, 21, space heating mode, with  $35^\circ\text{C}$  water temperature at the condenser at  $600\text{W/m}^2$

*Figure 4.63* shows the experimental results obtained during August 21<sup>st</sup>, 2009. The data were recorded automatically by a data logger, every 5 minutes. From the graph at constant simulated radiation of  $600\text{W/m}^2$ ; the heat gains at the condenser have the same trend with the temperature change of the water at the condenser. The COP was between 3.40 and 3.80, and was within the range of the air source heat pump performance standard. The temperature difference across the condenser water side was  $5^\circ\text{C}$  and was enough to achieve useful temperature at least than 25 minutes under  $600\text{W/m}^2$ .

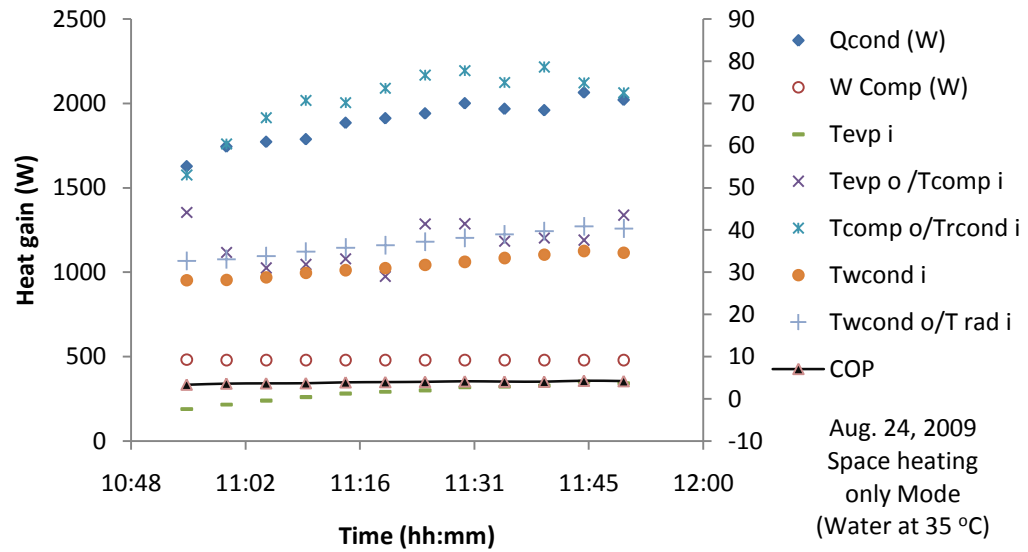
#### **4.7.4 Performance investigation of DX-SHP at solar radiation of $800\text{W/m}^2$**

All experiment data plotted in the *Figure 4.66*, *Figure 4.67*, and *Figure 4.68* were changing with time expect the solar irradiance and condensing temperature, which were simulated constant at  $800\text{W/m}^2$  and the water temperature at the condenser kept constant at  $35^\circ\text{C}$  for space heating purpose through underfloor heating or  $55^\circ\text{C}$  for DHW.



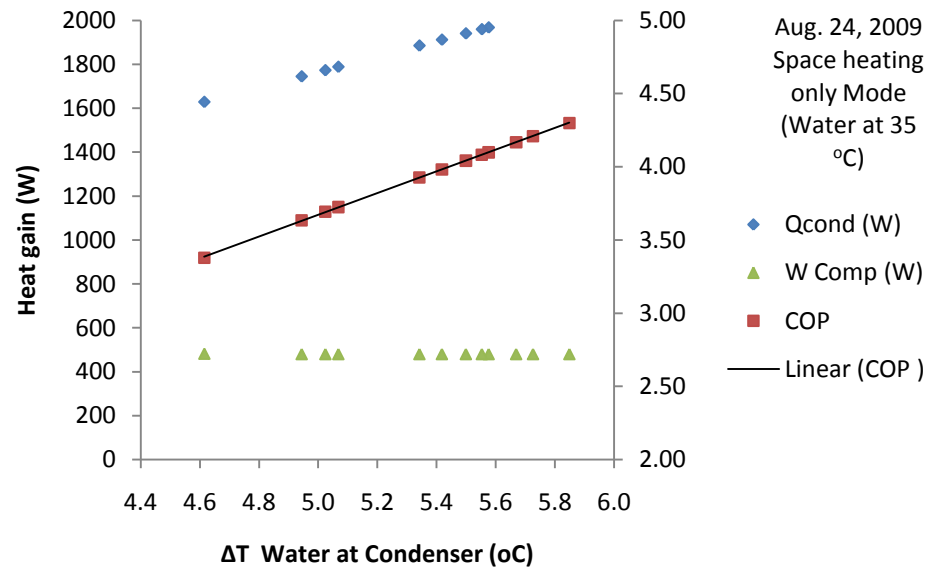
**Figure 4. 66:** The effects the collector/evaporator inlet temperature ( $T_{evp i}$ ) on the COP of the heat pump, the heat rate gain at the condenser, and the compressor energy consumption at simulated radiation  $800W/m^2$

Figure 4.66 shows, the results, when the water temperature at the condenser was set constant at  $35^{\circ}C$ , with the simulated radiation of  $800W/m^2$ , which closed to highest radiation in summer months in the UK, the inlet temperature at evaporator were between  $-2$  to  $4^{deg}$  C, the energy gain at the condenser was fluctuated between  $1700W$  to  $2400W$ . The COP was between  $3.70$  and  $4.40$ , and was within the range of the air source heat pump performance standard in summer. These results were informative, because they confirmed that the system could perform better event during hottest days in summer, with not excessive heat gain at the evaporator or with a danger for the compressor receiving highest saturated refrigerant for the evaporator.



**Figure 4. 67:** The effects the COP of the heat pump, the heat rate gain at the condenser and the compressor energy consumption with time at 800W/m<sup>2</sup>

The relation of the COP, heat gain at condenser, and electrical power consumption of the compressor with the time were summarised in the Figure 4.67. The COP, evaporator inlet temperature and compressor power consumption were not dependent to the time. The degree of superheat at the exit of the collector/evaporator was less than 10°C. The temperature difference across the condenser water side was 5°C. The heat gain at the condenser was affected by the time variation; due to the fact that as the time passed, the evaporator was heat up, and the temperature of the collector also increased therefore was enough to influence the heat gain at the condenser.



**Figure 4. 68:** Test results obtained on August, 24<sup>th</sup> space heating mode, with 35°C water temperature at the condenser at 800W/m<sup>2</sup>

Figure 4.68 shows the experimental results obtained during August 24<sup>th</sup>, 2009. From the graph at constant simulated radiation of 800W/m<sup>2</sup>; the heat gains at the condenser have the same trend with the temperature changes of the water at the condenser. The COP was between 3.40 and 4.40, and was within the range of the air source heat pump performance standard. The average temperature difference across the condenser water side was 5°C and was enough to achieve useful temperature at least than 20 minutes under 800W/m<sup>2</sup>.

#### 4.8 Theoretical results Vs Experimental results:

Using equation 4.23, the average experimental COP of the DX-SHP system were calculated then compared with the Carnot vapour compression cycle and the theoretical analysis results; then plotted in the Figure 4.69. From the graphs, it is clear that average COP was 30- 40% of the Carnot cycle, and was in good agreement with the mathematical modelling of the heat pump system. And the system had shown to perform well even at lower radiation and evaporation temperature. This characteristic is helpful for the implementation of the DX-SHP for domestic space heating and DHW, this mean that, during the winter, when the ambient temperature will be lower the system will still operate at high COP.

In the *Table 4.17* and *Figure 4.69*, for each simulated radiation, the COP of the heat pump, the heat rate gain at the condenser and the compressor energy consumption were recorded and then plotted against evaporated temperatures.

The results indicated that for solar radiation range from 200-800W/m<sup>2</sup>, it was taken between 50 to 60 minutes for heating 117 litres of water from 28°C to 35°C and the evaporating temperatures vary from -5.24 to 1.49°C, the total electric consumption for the compressor was between, 479 – 480Wh. The average COP of the heat pump for space heating mode was between 3.07 – 3.94.

As shown in the *Table 4.17*, the heat capacity of the DX-SHP was between 1473Wh-1890Wh and was sensitive to the solar radiations, which is also linked to the evaporation temperatures. And the COP was also sensitive to the evaporation temperatures as predicted. When the evaporator temperature was in the range of minus -5 and 0 °C, and with the condensing temperature at 35°C, the heating COP of the DX-SHP was about 3.07-3.49. Based on this, the DX-SHP provides a greater heating capacity compare to a conventional air source heat pump, and well perform with frost formation. *The Table 4.17* also indicates that the magnitude of the heat gain at the condenser increased about 300Wh, for every 2°C at the evaporator/collector. The DX-SHP has the capability to also provide in about 30 minutes, 117L of energy storage, to be used at night when the outside temperature is low. However the DX-SHP also has the capacity to extract heat from the ambient air, but not thoroughly investigated in this study. This might avoid high drop in the evaporation temperature at the collector/evaporator.

In the *Figure 4.49*, when the solar radiation was 200W/m<sup>2</sup>, the experimental results shown the evaporator temperatures lower of about 2° than the theoretical ones. At 400W/m<sup>2</sup>, the experimental results shown the evaporator temperatures lower of about 1° than the theoretical ones. And at 600W/m<sup>2</sup>, there was a good agreement between the theoretical and experimental COPs. There was slight difference between the experimental and analytical COP results at 800W/m<sup>2</sup>; experimental COP was greater that the analytical one, this is probably due to the

some experimental errors. However because the results summarised in the Figure 4.69, the COP of the DX-SHP would not be influence by the suddenly change of the solar radiations.

Table 4. 17: Summary results of the performance testing of DX-SHP

Date of the Test	$I_{avr}$ ( $W/m^2$ )	Start water Temp. ( $^{\circ}C$ )	$\tau$ (Minutes) Time to go from start T to $35^{\circ}C$	$T_{evp, i, avr}$ ( $^{\circ}C$ )	$T_{fplate, avr}$ ( $^{\circ}C$ )	$T_{wcond, i, avr}$ ( $^{\circ}C$ )	$T_{wcond, o, avr}$ ( $^{\circ}C$ )	$Q_{h, avr}$ (W)	$W_{comp, avr}$ (W)	$COP_{avr}$	$T_{room, avr}$ ( $^{\circ}C$ )
25/08/2009	200	28	60	-5.24	23	31.75	35.93	1473	480	3.07	$20 \pm 2$
26/08/2009	400	28	55	-0.14	28	31.73	36.46	1667	480	3.49	$20 \pm 2$
21/08/2009	600	28	52	-1.98	30	34.19	39.33	1814	480	3.78	$20 \pm 2$
24/08/2009	800	28	50	1.49	32	31.48	36.83	1890	479	3.95	$20 \pm 2$

Theoretical Performance Vs Experimental Performance

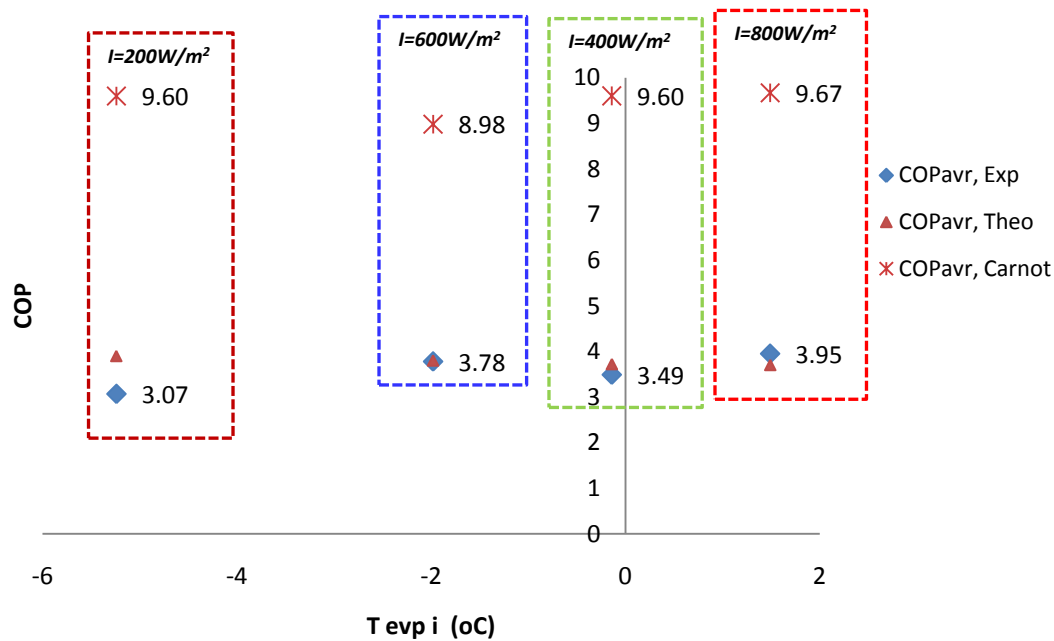


Figure 4. 69: Summary of Theoretical Performance Vs Experimental Performance

### 4.8.1 The effectiveness of the DX-STSHP:

The effectiveness of the DX-SHP system ( $eff_{DX-STSHP}$ ) was defined as the ratio of the actual COP of the heat pump of to the Reverse Carnot cycle COP.

$$eff_{DX-STSHP} = \frac{COP_{avr,exp}}{COP_{avr,Carnot}} \times 100$$

Table 4. 18: Effectiveness of the DX-SHP

$I_{avr}$ (W/m <sup>2</sup> )	$COP_{avr, exp.}$	$COP_{avr, Carnot}$	$eff_{DX-STSHP}$
200	3.07	9.60	32 %
400	3.49	9.60	36 %
600	3.78	8.98	42 %
800	3.95	9.67	41 %

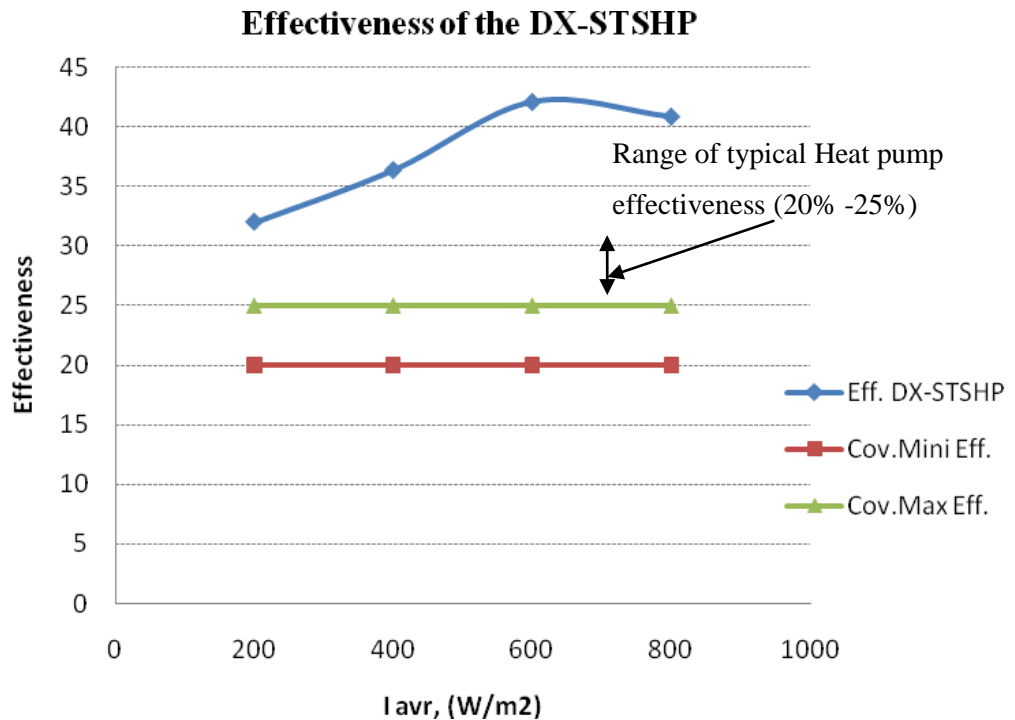


Figure 4. 70: Effectiveness of DX-SHP compare to conventional one

From the *Figure 4.70*, the Conventional heat pump system effectiveness is in the range of 20 to 25%. However by increasing the COP of the actual heat pump, the effectiveness of a heat pump system can be increased as shown in the *Figure 4.70* and *Table 4.18* the effectiveness of the DX-SHP system under consideration was between 32% to 41%, therefore the novel DX-SHP has a comparatively high COP and with the benefice on low energy consumption at the compressor.

#### **4.9 Conclusion - Chapter 4**

This chapter presented indoor thermal performances analysis of the potential for a DX-SHP system to provide space and water heating for low carbon homes in the UK and Europe. The investigation was based on the steady-state modelling of the thermodynamic vapour compression cycle. The tests were operated at solar collector/evaporator temperatures greater than room temperature. The system consists of a single unglazed solar collector with built in serpentine tubes to contain refrigerant (R134a), a positive displacement compressor, a flat plate heat exchanger (condenser) and a thermostatic expansion valve (TXV). The collector/evaporator, where the evaporation directly took place was exposed to simulated solar radiation from 200 to 800 W/m<sup>2</sup>. The compressor received the working fluid from the serpentine tubes of the collector as saturated vapour, compressed it to a high pressure and temperature, and then delivered it to the condenser. The heat was extracted from the condenser and used to heat water to 35°C or 55°C, according to the demand. In order to evaluate the thermal performance of the DX-SHP a series of indoor tests were performed at the laboratory of the school of the Built Environment, University of Nottingham. and

the results shown that, the average rate of heat gain at the condenser for space heating operation mode (*water temperature 35°C*) was about 1700 Wh per day after one hour, and the average COP varied from 3.07 to 3.94. For water heating mode (*water temperature at 55 °C*) the DX-SHP has the capability of supplying about 117 litres of hot water a day with a final temperature of about 55 °C under various solar radiation conditions. Despite the few parts and low investment cost of the DX-SHP is simple, easy to install and could perform well at high COP and at different weather conditions in the UK.

The experimental results were compared with the theoretical model predictions and they showed distinct differences between the ideal and real situations. These provide an opportunity for further investigations to improve and optimise the performance of DX-SHP.

#### **4.10 Further Works**

##### **4.10.1 DX-Solar roof Heat Pump**

The DX –SHP preliminary results have shown that the system could well operate in different conditions, including when the ambient temperature was supposed to be lower, about -5 °C, the COP was about 3.07. Future works are needed to develop integrate the prototype as part of the roof for residential building (see Figure 4.71); by scaling up or developing a prototype system to match the heating loads of a domestic home of two storey detached family home in the UK, then carry out much more experimental and theoretical studies on the performance of the system and its capacity to provide water and space heating.

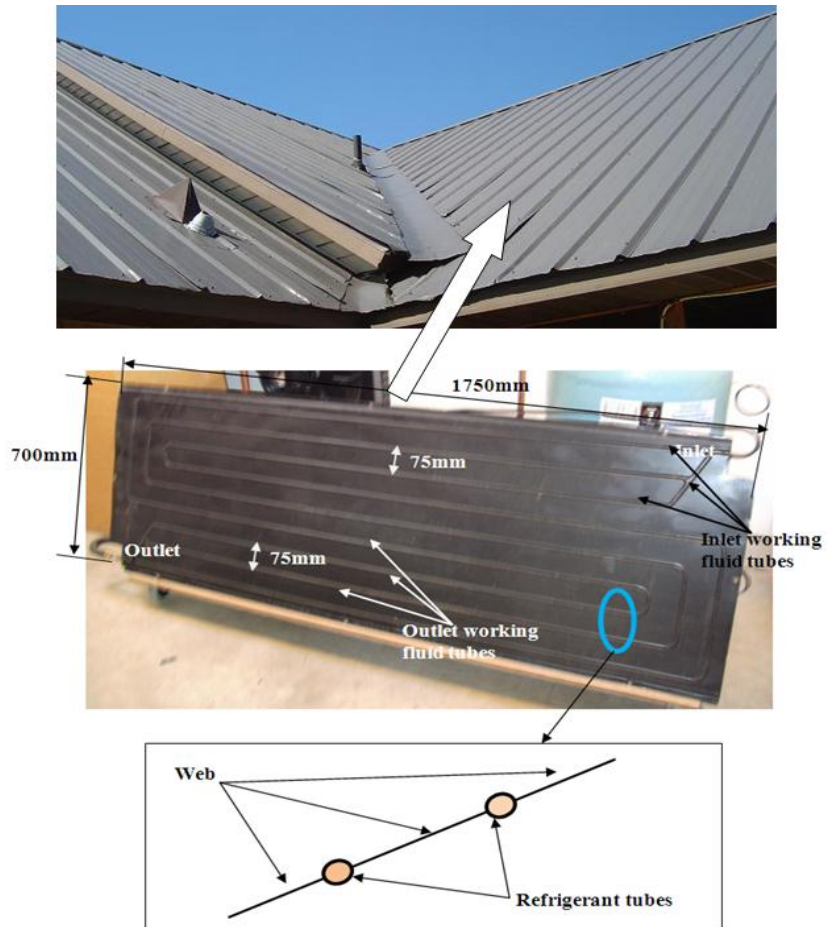


**Figure 4. 71:** Illustration of the development of the evaporator as a roof module

If the evaporator/collector has a transparent cover to increase the evaporative temperature instead of a bare solar collector, two fans could be required to circulate the air between the cover and solar absorber, as shown in *Figure 4.72* and *Figure 8.73*. When the solar radiation is low, the fan starts to work to introduce air from outside the collector so maximise evaporator heat input. The refrigerant can be chosen to have a freezing point well below the local air temperature to avoid it freezing in operation. Future works are needed to develop such evaporator, as DX- heap pump system.

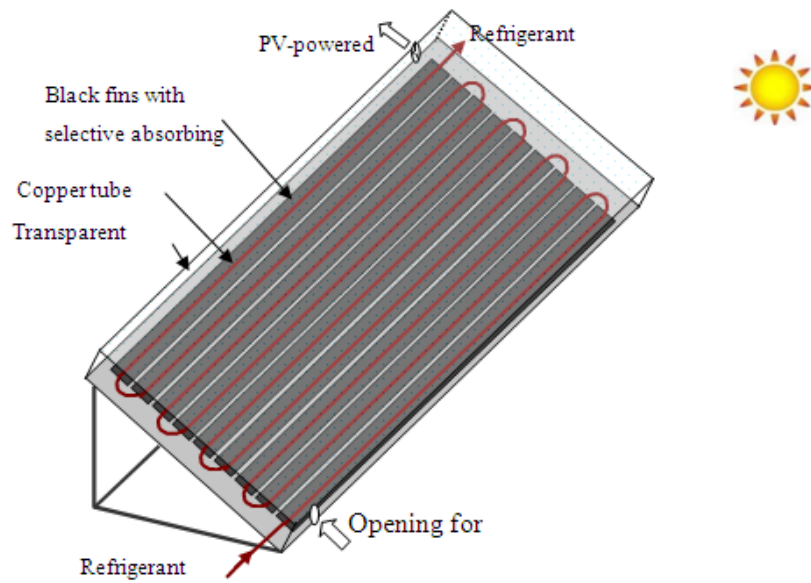


**Figure 4. 72:** A solar collector with a transparent cover as an evaporator of a DX-ASHPS

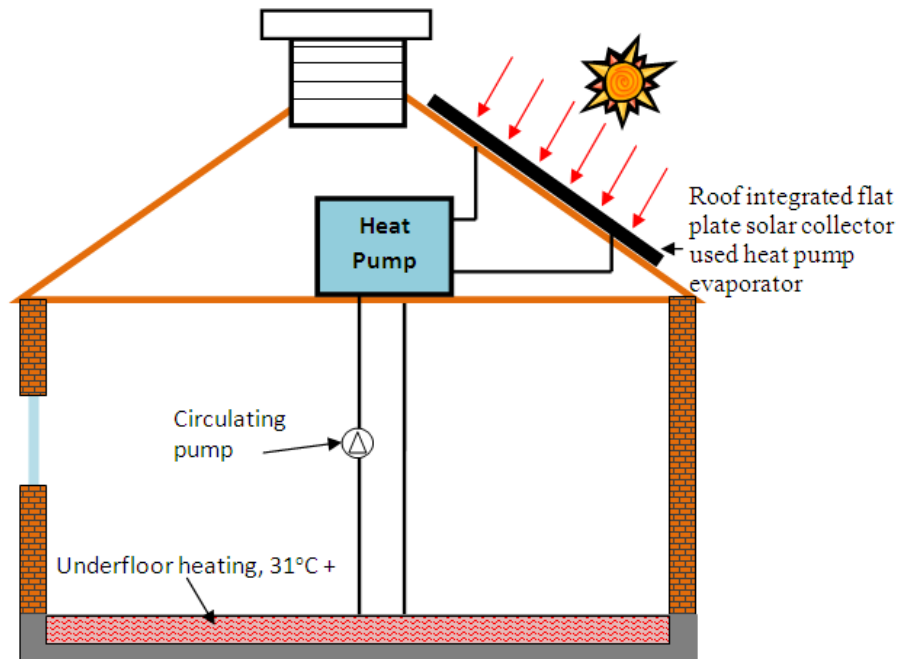


**Figure 4. 73:** illustration of the solar collector/evaporator integrated in the roof as an evaporator of the DX-ASHPS



## **CHAPTER 5 - NUMERICAL AND EXPERIMENTAL ANALYSIS ON PERFORMANCE OF A NOVEL DIRECT- EXPANSION PHOTOVOLTAIC/HEAT-PIPE - HEAT PUMP SYSTEM**

---

## 5. INTRODUCTION

The aim of this chapter is to carry out a preliminary investigation on a novel Photovoltaic/heat-pipe (PV/hp) collector able to work with an air source heat pump as direct expansion cycle to provide electricity and heat for buildings with enhanced efficiency for both, the air source heat pump and PV panels. The system comprises prefabricated PV/hp collector that are inter-connected and put into vacuum tubes to form a panel to act as an electricity generator and the solar collector/evaporator for the heat pump. The system also incorporates a compressor, a condenser, an expansion valve and a heat storage device. Integration of PV and heat pipes in a prefabricated collector will provide high efficiency in terms of solar energy conversion, space and domestic hot water requirements, and in so doing, offer the potential to create a low cost solution for electricity and heat production for low carbon homes in the UK and Europe.

### 5.1 Brief background of this work

In terms of solar electricity, PV modules are the main products available for generating solar electricity and they can be integrated within building facades. However, the drawbacks of their wide deployment in the building sectors are their cost and inefficiency in terms of solar-to-electricity conversion, largely because of the PVs' high cell operation temperature (Messenger Roger & Ventre, 2004). Numerous research and development activities have been taken place to improve the PV cells' efficiencies, Niccolo, Giancarlo, & Francesco (2008), Hegazy, (2000), Tonui & Tripanagnostopoulos (2007), Muharomad, Baharudin, Sopian,

& Muharomad (2007), Dubey & Tiwari (2006), Chow T. , He, Ji, & Chan (2007), and Tripanagnostopoulos (2007). Air and water have been suggested as cooling fluids to pass across the PVs to reduce the cells' operation temperatures and thus increase the solar electrical efficiency. The heat extracted by the air or water from the PVs can also be used to supply space and/or domestic hot water heating of buildings, while improve the total performance of the PVs.

Niccolo et al (2008) carried out a research on a hybrid PV/T air collector with the upper cover of glass-PV sandwich. The thermal efficiency was found to vary in average from 20% to 40% and the average electrical efficiency was around 9-10%. Hegazy (2000) presented a computational investigation of four common designs of PV/T air collector with the air flowing either over the absorber or under it and on both sides of the absorber in a single pass or in a double pass fashion. Tonui et al. (2007) employed a suspended thin flat metallic sheet (TMS) at the middle or fins at the back wall of an air duct as heat transfer augmentations in an air-cooled photovoltaic/thermal (PV/T) solar collector to improve its overall performance. A finned double-pass photovoltaic-thermal (PV/T) solar collector was developed by Muharomad et al. (2007). This hybrid system consisted of monocrystalline silicon cells pasted to an absorber plate with fins attached at the other side of the absorber surface. Air as heat removing fluid was made to flow through an upper channel and then under the absorber plate or lower channel of the collector.

Dubey et al. (2008) and Chow et al. (2006) studied the effect of PV covering ratio on energy performance of solar water heater. A Hybrid Photovoltaic–Thermal

collector system manufactured in a copolymer material (polycarbonate) for the ‘absorber–exchanger’ has been employed for thermal behaviour investigation by Christian et al. (2009) in France. It was found that the annual average efficiencies equalled to 55.5% for thermal one, 12.7% for PV one. Chow et al. (2007) proposed a new design of thermal absorber with flat-box structure. They found that the new type collector had an annual average thermal efficiency of 38.1% and a payback period of 12 years.

A new type of PV/T collector with dual heat extraction operation, either with water or with air circulation was developed by Tripanagnostopoulos (2007). He also made further modifications on the air channel of the PV/T dual solar collectors with TMS, FIN and TMS/RIB type modifications. It was found that the sum of thermal and electrical outputs from the PV/T dual systems were about 70% and 55% for the water and the air heat extraction modes respectively and for operation at about 20 °C in both heat extraction modes. The above studies used air or water as cooling fluids for the PV cells, and then concluded that water is better than air.

The aims of this study was to use refrigerant (R134a) as the cooling fluid, with its lowest cooling temperatures compare to water and the air, refrigerant has the capability to achieve better cooling effects on the PV modules. Since the refrigerant was passed through the u-shape tube of the vacuum-tube-PV collector/evaporator of the heat pump system. In addition, the PV cells’ temperature was

reduced to a relatively low temperature due to the lowest boiling point temperature of refrigerant, about  $-21\text{ }^{\circ}\text{C}$ .

## 5.2 PV/hp-HP system description

The PV/hp heat pump system shown in *the Figure 5.74* was a direct expansion (DX) heat pump system. The system comprises four main components, compressor, expansion valve and water-cooled condenser as well as PV/hp evaporator; the principals' characteristics of each component of the system are summarised in *Table 5.19*. The PV/hp evaporator is the key part of the system shown in the *Figure 5.75*. It consists of 12 vacuum glass tubes divided into two parallel-connected groups with 6 tubes in series for each group, to avoid overheating. *Figure 5.76* shows a cross-sectional view of the vacuum glass tube, and the characteristic dimensions of parts compile the PV-Aluminium sheet-cooper tubes sandwich are shown in the *Table 5.20*. The sandwich is made of aluminium sheet which adhered on the back of the PV with the aid of heat transfer pasta for heat extraction; the sandwich was placed at the centre of the vacuum glass tube. Three quarters of the u-shape copper tubes' diameter was tightly rolled with the aluminium sheet at the side-ends along the cooper tube providing a good contact between aluminium sheet and copper tube. This enables a good heat transfer from aluminium sheet to refrigerant.

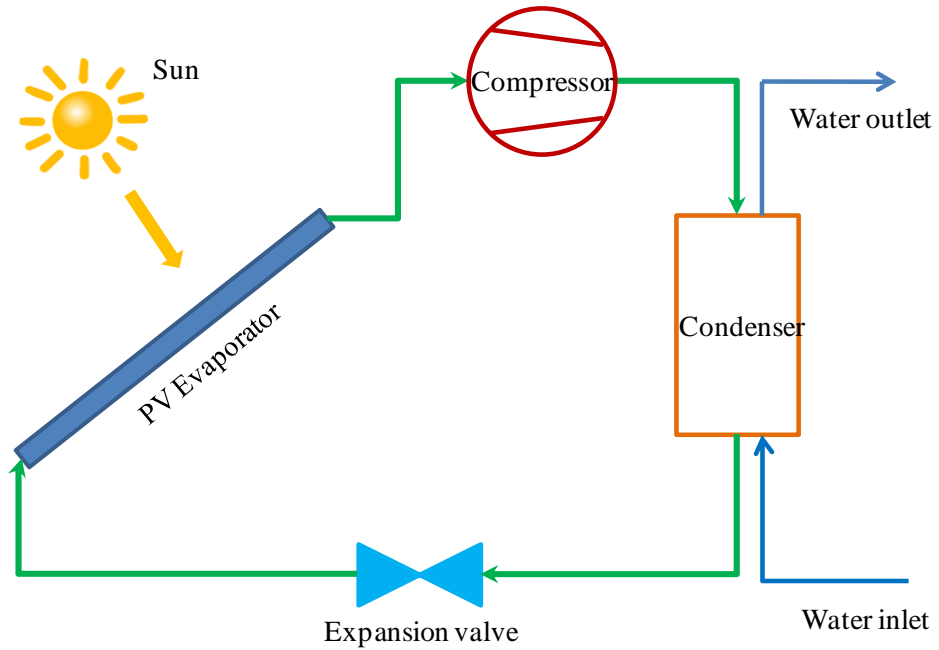


Figure 5.74: Schematic diagram of the DX-PV/hpS-Heat pump system

Table 5. 19: Specification of main equipments in the DX-STSHP system

Name	Type	Comments
<b>Collector/Evaporator</b>	Serpentine tubes in black unglazed flat-plate heat exchanger	Aluminium sheet effective absorptivity: 0.90; emissivity:0.90 , Tubes spacing 40mm, thermal conductivity (Aluminium) 235 w/m°C
<b>Compressor</b>	Hermetic constant speed compressor, TL 3F	TL 3F (Danfoss Compressor), for refrigerators R134a, displacement 15.28 cm <sup>3</sup> , rated input power: 107W
<b>Condenser</b>	Contraflow Flat plate L-line type heat exchanger	<i>SWEP: B8x10H/1P</i> , Made of stainless steel with a transfer area of about 172cm <sup>2</sup>
<b>Thermostatic Expansion Valve, Fixe orifice</b>	Thermostatic Expansion Valve (TXV), type TEN 2, variable orifice with external equalizer.	Angle way valve body, inlet size 3/8 inch, outlet size 1/2 inch, capillary tube length 1.5 m, max. Working pressure 34.0 bar.  TE 2, flare/flare, versions with external equalization: equalization connection size 1/4 in. / 6 mm.

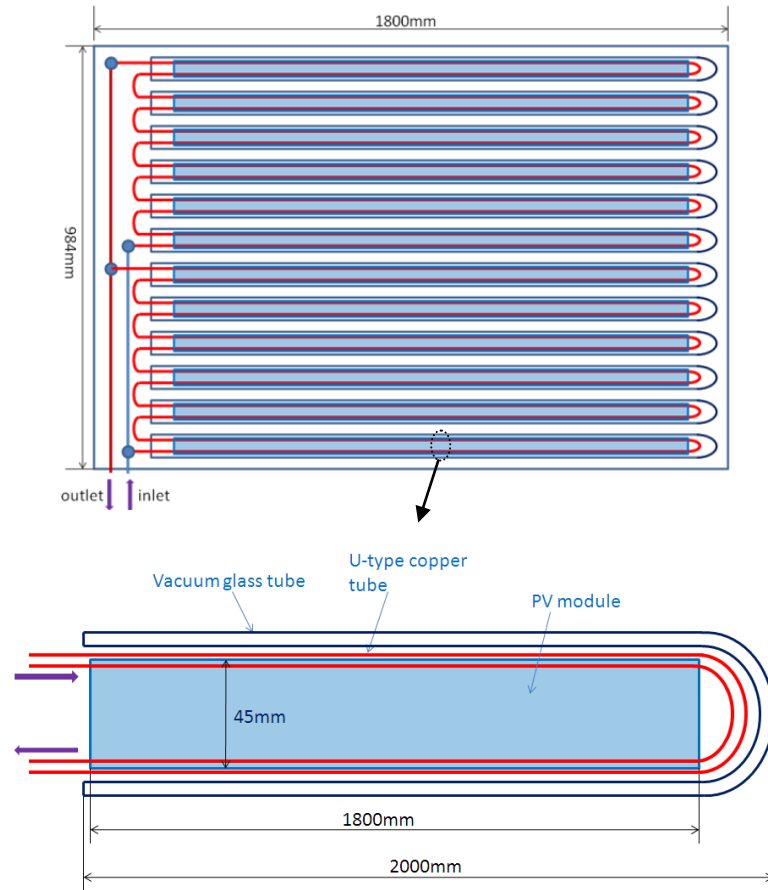


Figure 5.75: PV/heat pipe Evaporator panel

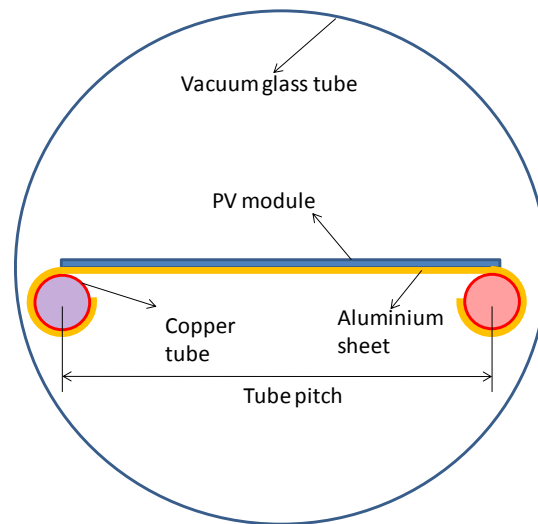


Figure 5.76: A cross-sectional view of vacuum glass tube

**Table 5.20:** Characteristic dimensions of PV evaporator panel (mm)

Component	Parameter	
Evaporator panel	Length	1,800
	Width	984
Vacuum glass tube	Diameter	56
	Length	1,500
PV module	Width	40
	Thickness	2
	Length	1,500
Aluminium sheet	Width	55
	Thickness	1
	Length	1,500
Copper tube	External diameter	10
	Internal diameter	8
	Length	3,200*12
	Tube pitch	40

### 5.1 Mathematical model and simulation of the DX-PV/hp-HP system

Zondag et al. (2003) built four numerical models for the simulation of PV/hp collector: a 3D dynamical model and three steady state models that are 3D, 2D and 1D. The study showed that the 1D steady state model performs almost as good as the others. Ji et al. (2009) presented a dynamic model of the PV evaporator in a PV/T solar-assisted heat pump. The simulation results indicated that there were very small temperature differences distributed at PV module, aluminium plate and refrigerant respectively. Therefore, for this work, the simplify 1D steady state model simulation is used and based on the following assumptions:

- The system is in quasi-steady state.
- The panel with vacuum tubes were treated as flat plate solar panel
- The heat capacity of the PV/hp system has been neglected.

- The heat capacities of PV module, aluminium sheet and copper tube have been neglected.
- A mean temperature is assumed the same across each layer.
- The pressure drop of the PV/T system has been neglected.
- For the purpose of the preliminary results, the view factor of the vacuum tube was neglected

### 5.1.1 EES Software

In this study, the models were developed so that they can be integrated into EES. The advantages of EES over others engineering equation-solving programs, the inputs and outputs to EES have been summarised in Chapter 4, section 4.3.1.

### 5.1.2 PV/hp evaporator Models

#### 5.1.2.1 Vacuum glass tube model

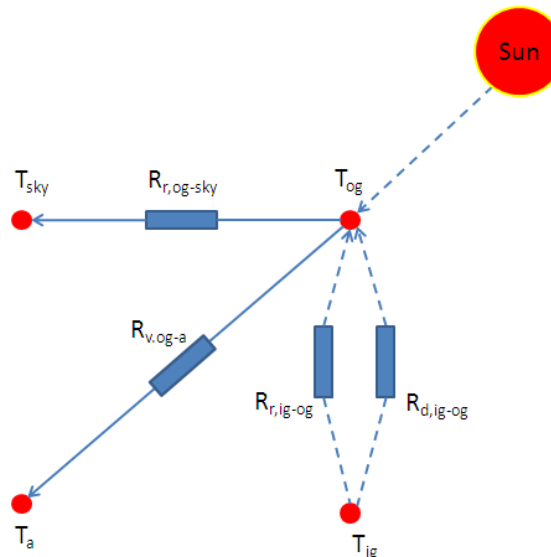


Figure 5.77: The thermal network of the Internal Vacuum glass tube

The heat balance equation at the vacuum glass tube (see Figure 5.77) is given by

$$0 = \beta_g G(A_g/2) + q_{r,p-g}A_p + q_{r,al-g}A_{al} - q_{r,g-sky}(A_g/2) - q_{v,g-a}A_g \quad (5.1)$$

where  $\beta_g$  and  $A_g$  are respectively the absorptance and outer surface area of the vacuum glass tube “g”;  $G$  is the solar radiation ( $\text{W/m}^2$ );  $A_p$  and  $A_{al}$  are respectively the area ( $\text{m}^2$ ) of the PV module “p” and the aluminium sheet “al”.

The heat radiation from the PV module “p” to “g” is given by:

$$q_{r,p-g} = \varepsilon_p \sigma (T_p^4 - T_g^4) \quad (5.2)$$

Where  $\varepsilon_p$  is the emittance of “p”;  $\sigma$  is the Stefan-Boltzmann constant;  $T_p$  and  $T_g$  are the temperature (K) of “p” and “g” respectively.

The heat radiation from the aluminium sheet “al” to “g” ( $\text{W/m}^2$ ) is given by

$$q_{r,al-g} = \varepsilon_{al} \sigma (T_{al}^4 - T_g^4) \quad (5.3)$$

Where  $\varepsilon_{al}$  and  $T_{al}$  are the emittance and temperature (K) of “al”.

The heat radiation from “g” to sky ( $\text{W/m}^2$ ) is given by

$$q_{r,g-sky} = \varepsilon_g \sigma (T_g^4 - T_{sky}^4) \quad (5.4)$$

Where  $T_{sky}$  is the background sky temperature (K) with a function of the ambient temperature  $T_a$  (K), i.e.

$$T_{sky} = 0.0552 \cdot T_a^{1.5} \quad (5.5)$$

The heat convection from “g” to ambient air “a” ( $\text{W/m}^2$ ) is given by

$$q_{v,g-a} = \alpha_{g-a} (T_g - T_a) \quad (5.6)$$

Where  $\alpha_{g-a}$  is the convectonal heat transfer coefficient between “g” and “a” ( $\text{W/m}^2\text{K}$ ), which is a function of wind velocity; according to Duffie and Beckman (2006),

$$\alpha_{g-a} = 2.8 + 3.0 \cdot u_{wind} \quad (5.7)$$

### 5.1.2.2 PV module model

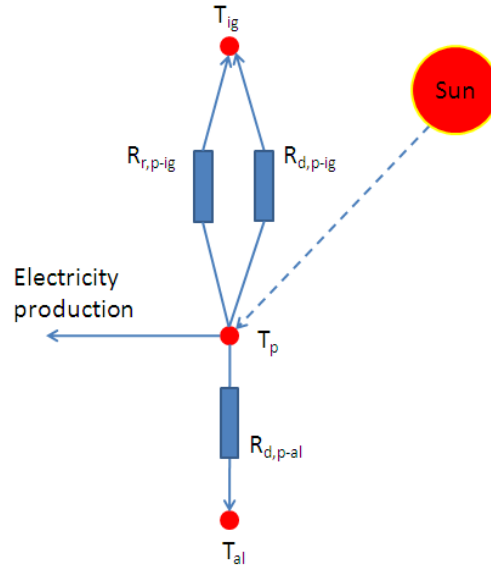


Figure 5.78: The thermal network of the PV module

The heat balance equation (see Figure 5.78) at PV module is given by

$$0 = G(\beta\tau)_c f_c + G(\beta\tau)_p (1 - f_c) - E - q_{d,p-al} - q_{r,p-g} \quad (5.8)$$

Where  $(\beta\tau)_c$  and  $(\beta\tau)_p$  are the effective absorptance of the solar cells and base plate respectively. According to Duffie and Beckman (2006),

$$(\beta\tau)_c = \frac{\tau_a \tau_\rho \beta_c}{1 - (1 - \beta_c) R_g} \quad (5.9)$$

and

$$(\beta\tau)_p = \frac{\tau_a \tau_\rho \beta_p}{1 - (1 - \beta_p) R_g} \quad (5.10)$$

Where  $\tau_a$  is the transmittance of “g” considering only absorptance loss and  $\tau_\rho$  is the transmittance of “p” considering only reflection loss;  $\beta_c$  and  $\beta_p$  are the absorptance of solar cells and base plate respectively;  $R_g$  is the diffuse reflectance of “g”. The electricity production (W) is given by

$$E = \eta_c f_c (\beta\tau)_p G \quad (5.11)$$

Where  $\eta_c$  is the temperature-dependent electrical efficiency of solar cell “c”;  $f_c$  is the ratio of cell area to PV module area.

$$\eta_c = \eta_{rc} [1 - \beta(T_p - T_{rc})] \quad (5.12)$$

Where  $\eta_{rc}$  is the reference electrical efficiency (0.15) at the reference operating temperature  $T_{rc}$  (298K) and  $\beta$  is the temperature coefficient (0.0045) (Ji, et al., 2009); the heat conduction from “p” to the aluminium sheet “al” (W/m<sup>2</sup>) is given by:

$$q_{d,p-al} = \frac{(T_p - T_{al})}{\frac{\delta_p}{2\lambda_p} + \frac{\delta_{al}}{2\lambda_{al}}} \quad (5.13)$$

Where  $\delta_p$  and  $\lambda_p$  are the thickness (m) and heat conductivity (W/mK) of “p” respectively and  $\delta_{al}$  and  $\lambda_{al}$  are the thickness (m) and heat conductivity (W/mK) of “al” respectively.

### 5.1.2.3 Aluminium sheet model

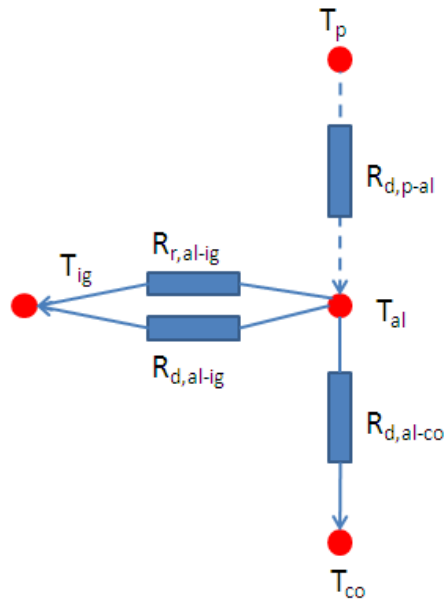


Figure 5.79: The thermal network of the Aluminium sheet

The heat balance equation at the aluminium sheet (see Figure 5.75) is given by

$$0 = A_p \cdot q_{d,p-al} - A_{al-co} \cdot q_{d,al-co} - A_{al} \cdot q_{r,al-g} \quad (5.14)$$

Where  $A_p$  and  $A_{al}$  are the areas ( $m^2$ ) of “p” and “al”.

The contact area between “al” and copper tube “co” ( $W/m^2$ ) is given by

$$A_{al-co} = 2\left(\frac{3}{4}\right) \cdot \pi d_{o,co} \cdot L_p \quad (5.15)$$

Where  $d_{o,co}$  is the external diameter of “co” (m);  $L_p$  is the length of “p” (m).

The heat conduction from “al” to the copper tube “co” ( $W/m^2$ ) is given by

$$q_{al-co} = \frac{(T_{al}-T_{co})}{\frac{\delta_{al}}{2\lambda_{al}} + \frac{\delta_{co}}{2\lambda_{co}}} \quad (5.16)$$

Where,  $T_{co}$ ,  $\delta_{co}$  and  $\lambda_{co}$  are the temperature (K), thickness (m) and thermal conductivity ( $W/mK$ ) of “co”.

#### 5.1.2.4 Refrigerant’s Copper tube model

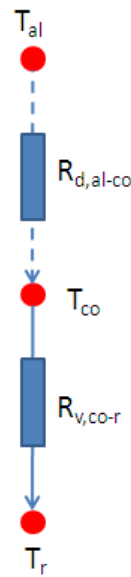


**Figure 5.80:** The thermal network of the Refrigerant’s copper tube

The heat balance equation at the copper tube (see Figure 5.80) is given by

$$0 = A_{al-co} \cdot q_{d,al-co} - A_{i,co} \cdot q_{v,co-r} \quad (5.17)$$

Where  $A_{i,co}$  is the internal surface area of “co” ( $m^2$ ), given by

$$A_{i,co} = \pi d_{i,co} L_{co} \quad (5.16)$$

Where,  $d_{i,co}$  and  $L_{co}$  are the internal diameter (m) and length (m) of “co”.

The heat convection from “co” to the refrigerant “r” ( $W/m^2$ ) is given by

$$q_{v,co-r} = \frac{(T_{co}-T_r)}{\frac{1}{\alpha_r} + \frac{\delta_{co}}{2\lambda_{co}}} \quad (5.17)$$

Where  $T_r$  is the refrigerant temperature (K);  $\alpha_r$  is the convective heat transfer coefficient ( $W/mK$ ) between “co” and “r”, given by

For single-phase flow:

$$\alpha_r = 0.023 \frac{Re^{0.8} Pr^a \lambda_r}{d_i} \quad (a=0.3 \text{ for liquid, } a=0.4 \text{ for vapour}) \quad (\text{Duffi \& Beckman, 2006}).$$

For two-phase flow:

$$\alpha_r = \alpha_l \left[ (1-x)^{0.8} + \frac{3.8x^{0.76}(1-x)^{0.04}}{Pr^{0.38}} \right] \quad (5.18)$$

Where  $x$  is the average dryness fraction of the refrigerant:

$$Pr = \frac{\mu_r C p_r}{\lambda_r}, \quad Re = \frac{\rho_r u_r d_{i,co}}{\mu_r}. \quad (5.19)$$

### 5.1.2.5 Refrigerant in the panel model

The heat balance equation at the refrigerant is give by

$$0 = 6 * A_{i,co} \cdot q_{v,co-r} - m_r \cdot \Delta h_r \quad (5.20)$$

where  $m_r$  is the mass flow rate of refrigerant (kg/s);  $\Delta h_r$  is the refrigerant enthalpy difference (J/kg).between copper tube inlet and out let

### 5.1.3 Compressor model

Neglecting the pressure drop in the discharge line, the relationship been the temperature and pressure at the discharge and suction sides of the compressor can be given by

$$T_{dis} = T_{suc} \left( \frac{P_{dis}}{P_{suc}} \right)^{\frac{1-\kappa}{\kappa}} \quad (5.21)$$

where  $T_{dis}$  and  $T_{suc}$  are the discharge temperature (K) and suction temperature (K) respectively;  $P_{evap}$  and  $P_{cond}$  are the discharge pressure (Pa) and suction pressure (Pa) respectively;  $\kappa$  is the polytropic exponent.

The refrigerant mass flow rate is given by

$$m_r = \eta_v \frac{nV_{th}}{60v_{suc}} \quad (5.22)$$

Where  $\eta_v$  is the volumetric efficiency;  $n$  is the rotation speed (rpm);  $V_{th}$  is the theoretical displacement volume ( $m^3$ );  $v_{suc}$  is the specific volume at suction side ( $m^3/kg$ ). The effective power (W) input to the compressor is given by

$$W_{eff} = \frac{m_r \Delta h_{is}}{\eta_{eff}} \quad (5.23)$$

Where  $\Delta h_{is}$  the enthalpy variation between the suction and the isentropic discharge is conditions (J/kg);  $\eta_{eff}$  is the effective efficiency.

#### 5.1.4 Expansion valve model

The throttling process is regarded as the isenthalpic one. The mass flow rate is given by

$$m_r = K_{ex} \sqrt{\rho_r (P_{cd} - P_{ev})} \quad (5.24)$$

Where,  $K_{ex}$  is a proportionality constant and is changed as required to maintain the superheat in the evaporator;  $P_{cd}$  and  $P_{ev}$  are the condensing and evaporating pressure (Pa) respectively.

#### 5.1.5 Condenser model

The condensing temperature was kept at 45°C. The heat balance equations at the refrigerant side of the condenser were similar to that when it flows through the

PV evaporator. But at the water side of the condenser, there is no phase change and the heat balance equation can be given by Duffi & Beckman (2006):

$$0 = m_w C p_w (T_{w,out} - T_{w,in}) - \alpha_w A_w (T_{w,out} - T_{w,in}) / \ln \frac{(T_{hx} - T_{w,in})}{(T_{hx} - T_{w,out})} \quad (5.25)$$

where  $m_w$  is the water flow rate (kg/s);  $C p_w$  is the specific heat of water (J/kg K);  $T_{w,out}$  and  $T_{w,in}$  are the water temperature (K) at the outlet and inlet respectively;  $\alpha_w$  is the convective heat transfer coefficient between water and the heat exchanger plate (W/m<sup>2</sup>K);  $A_w$  is the contact area between water and the heat exchanger plate (m<sup>2</sup>);  $T_{hx}$  is the temperature of the heat exchanger plate (K)

### 5.1.6 Coefficient of performance (COP)

The coefficient of performance (COP) of heat pump system at any time instant (t) was calculated as:

$$COP_{hp} = \frac{Q_{wcond}(t)}{W_{comp}(t)} \quad (5.26)$$

Where  $Q_{wcond}(t)$  was the heat exchanger rate at condenser, and  $W_{comp}(t)$  was the power input (heat pump compressor and circulating pumps) to the system at any time instant (t). Within an operating test period of the duration  $\tau$ , the average

$COP_{\text{heat pump}}$  was defined as:

$$COP_{hp,avr} = \frac{\sum_0^{\tau} Q_{wcond}(t) dt}{\sum_0^{\tau} W_{comp}(t) dt} \quad (5.27)$$

## 5.2 Numerical results and discussion

In order to predict the performance of the novel evaporator and his effect on the COP of the heat pump; the numerical simulation study of the DX-PV/hp-HP was carried out based on the climatic data of Nottingham, UK, located at 53°N and - 1.3°E. The PV/hp evaporator was assumed to be south-facing with a tilt angle of 30°. EES (Engineering Equation Solver) was used for the calculation. The simulated results were summarised below:

### 5.2.1 Solar radiation and ambient temperature

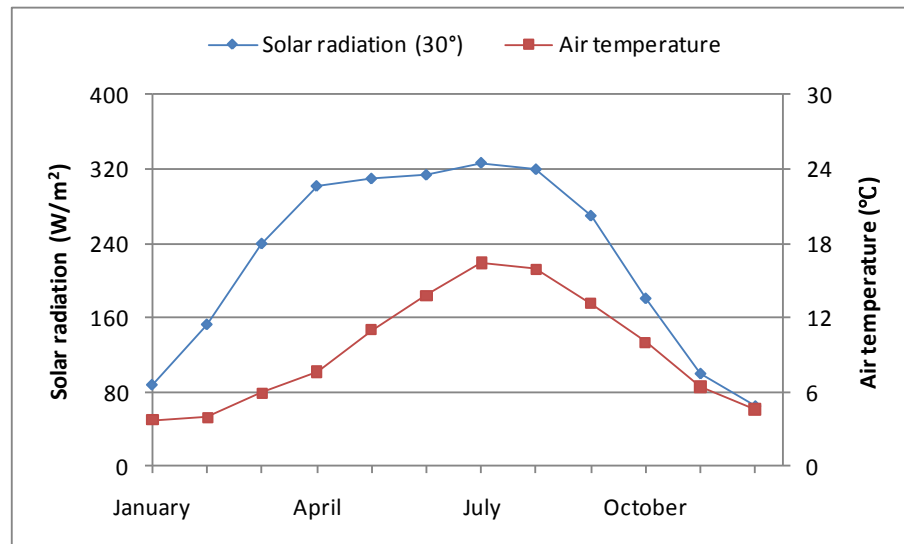


*Figure 5.81: The monthly average solar radiation (30°) and ambient temperatures*

The climatic data including monthly average horizontal solar radiation and air temperature were obtained from the British Atmospheric Data Centre, BADC (2011) and the horizontal solar radiation was converted to that on tilt surface for calculation and plotted in the Figure 5.81.

Figure 5.81 shows the monthly average solar radiation on tilt surface with an angle of 30° and ambient temperature. It can be seen that the monthly average solar radiation varies from 65 W/m<sup>2</sup> in December to 327 W/m<sup>2</sup> in July. It fluctuates slightly between 300 and 330 W/m<sup>2</sup> from April to August. The annual average solar radiation is 223 W/m<sup>2</sup> in the south facing. The ambient temperature varies from 3.7 °C in January to 16.4 °C in July with an annual average one of 9.4 °C.

### 5.2.2 Temperatures at different layers

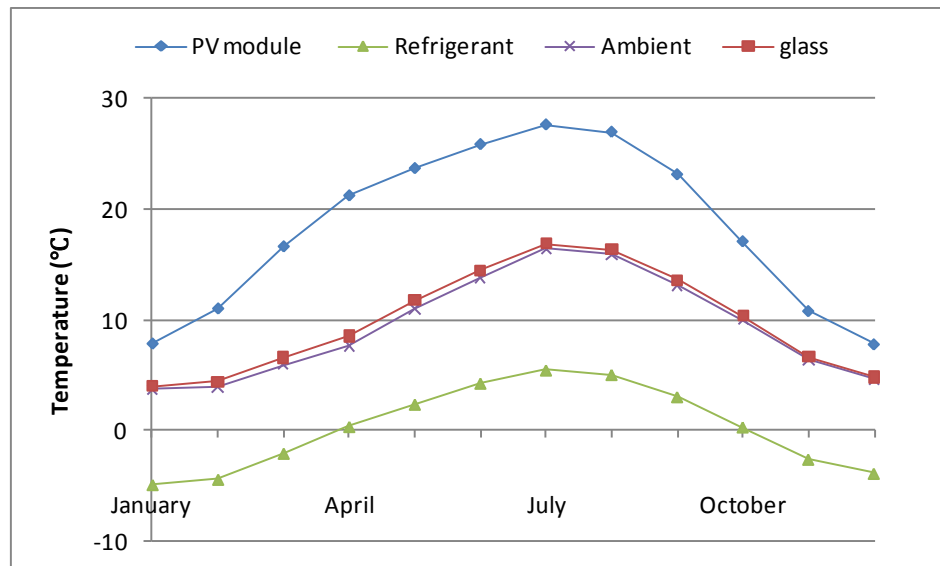
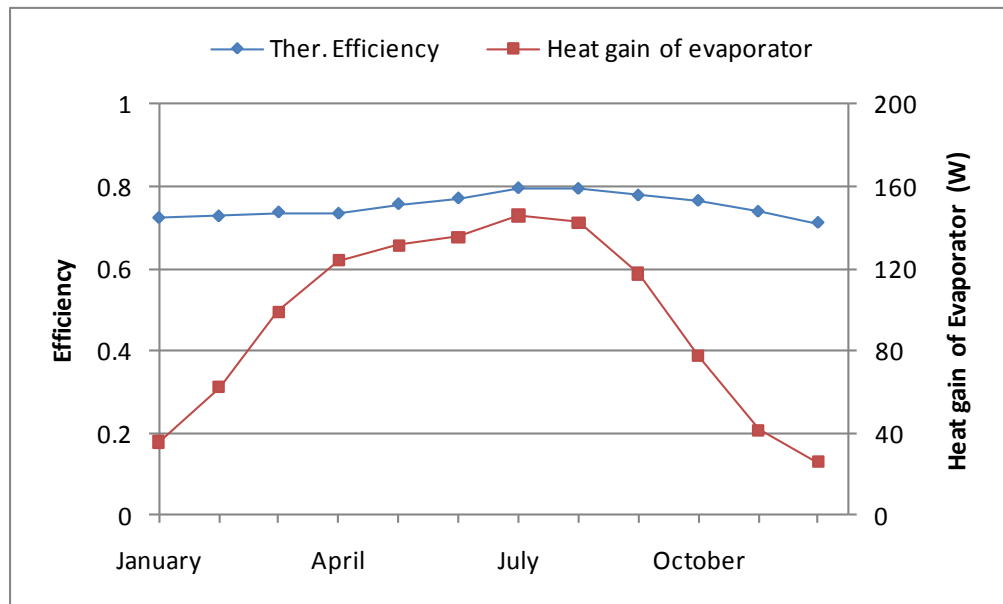


Figure 5.82: The temperatures at different layers

Figure 5.82 shows the temperatures at different layers. It can be seen that the temperature curves of PV module and refrigerant have the same trend as that of ambient temperature, rising up to the maximums in July and going down. The temperature of PV module varies from 7.7 to 27.6 °C, lower than that of typical water-cooled PV module, about 30~50°C. The temperature difference ranging

from 10 to 25 °C between PV module and refrigerant provides the motivation for heat extraction. The glass tube temperature is very close to the ambient due to the vacuum insulation and the heat loss from glass tube to the ambient.

### 5.2.3 Thermal performance of PV/hp evaporator



**Figure 5.83:** The monthly average thermal efficiency and heat gain of evaporator

Figure 5.83 shows the monthly average thermal efficiency and heat gain of PV/hp evaporator. The heat gain ranging from 26 to 146Wh changes with the solar radiation. The thermal efficiency varies from 0.711 to 0.796 with an average value of 0.752, which is much higher than the typical thermal efficiency of 0.4-0.5 for the conventional flat plate PV/hp panels, because the vacuum glass tube reduces the heat loss to the ambient.

### 5.2.4 Electrical performance of PV evaporator

Figure 5.84 shows the monthly average electrical efficiency and output of PV evaporator. The electrical efficiency has an opposite trend with the solar radiation and ambient temperature. Using equation 5.12, it was varying from 0.148 to 0.162 with an annual average value of 0.155. The power output and daily electricity output vary with the solar radiation. The annual average power output is 17 W and the annual average daily electricity output is 0.22 KWh, equal to 0.124KWh/m<sup>2</sup>. They should be much higher in some low latitude locations with better solar radiation.

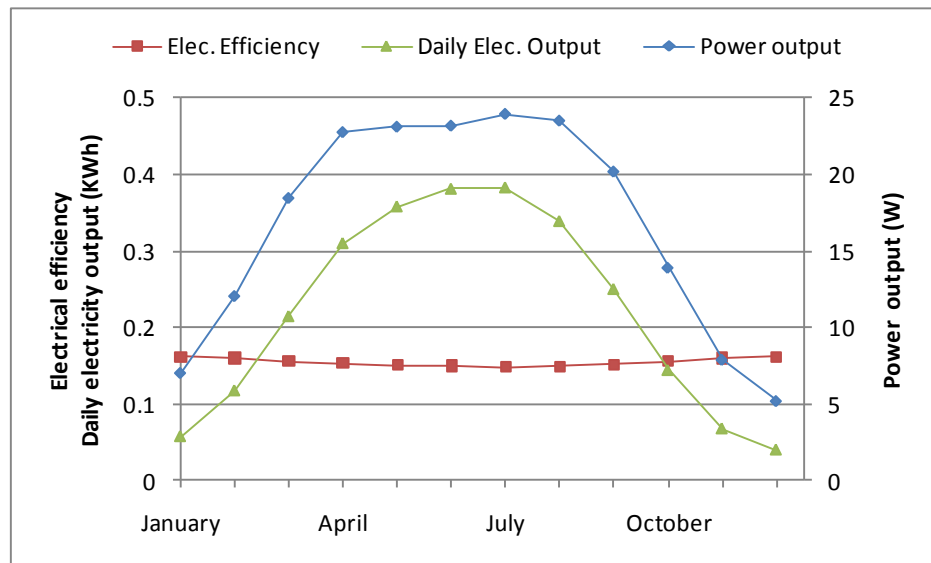
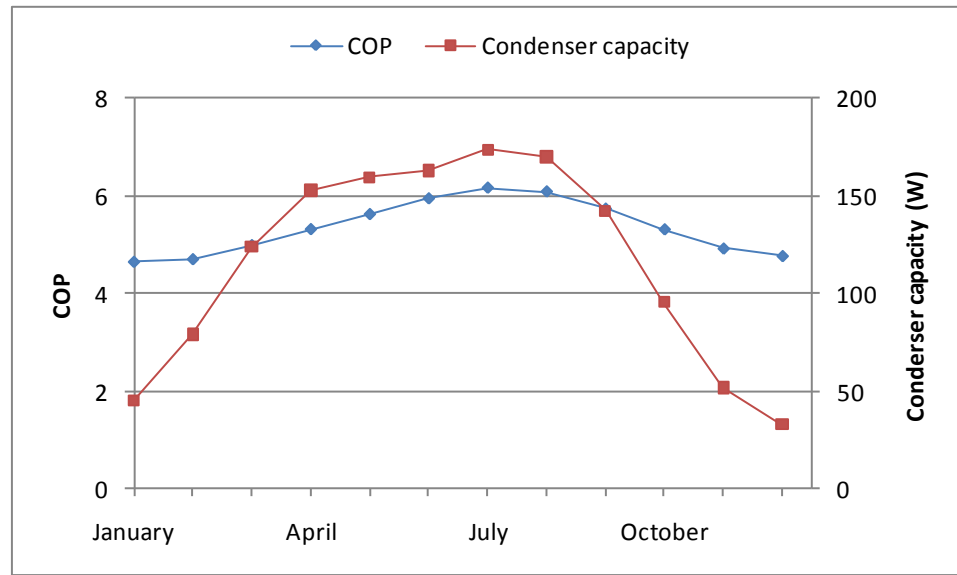


Figure 5. 84: The monthly average electrical efficiency and output of PV evaporator

### 5.2.5 COP and condenser capacity



**Figure 5.85:** The monthly average COP and condenser capacity of PV/hp heat pump system

Figure 5.85 shows the monthly average COP and condenser capacity of PV/T heat pump system. The COP varies from 4.65 to 6.16 with an annual average value of 5.35. It could be much higher under higher solar radiation. The condenser capacity ranging from 33 to 174 W would provide the heat source for space heating and domestic hot water.

### 5.3 Preliminary experimental study of the DX-STs/HP system

#### 5.3.1 Methodology

In order to evaluate the performance of the novel system; series of tests were undertaken at the following simulated radiations  $250\text{W/m}^2$ ,  $300\text{W/m}^2$ ,  $500\text{W/m}^2$ ,  $650\text{W/m}^2$  and  $850\text{W/m}^2$ ; and when the room temperature was in the range between  $18^\circ\text{C}$  to  $22^\circ\text{C}$ . Three stages of investigation were undertaken, to evaluate the effect of any added new features (Flat plate, Vacuum tube, and PV panel) on the collector/evaporator on the COP and the temperature of the PV panel.

The first stage was to evaluate the performance of the collector/evaporator without the PV panels and vacuum tubes using six heat absorber plates made of black coated aluminium sheet and u-shape copper tube for refrigerant oil r134a as presented in the *Figures 5.86* and *Figure 5.87*.

The method used in this experiment was the same utilised in the Chapter 4 and details in the section 4.4.1.

### 5.3.2 Layout of the testing rig set-up



Figure 5.86: The sep-up pictures of the preliminary test rig of DX-PV/hp -HP

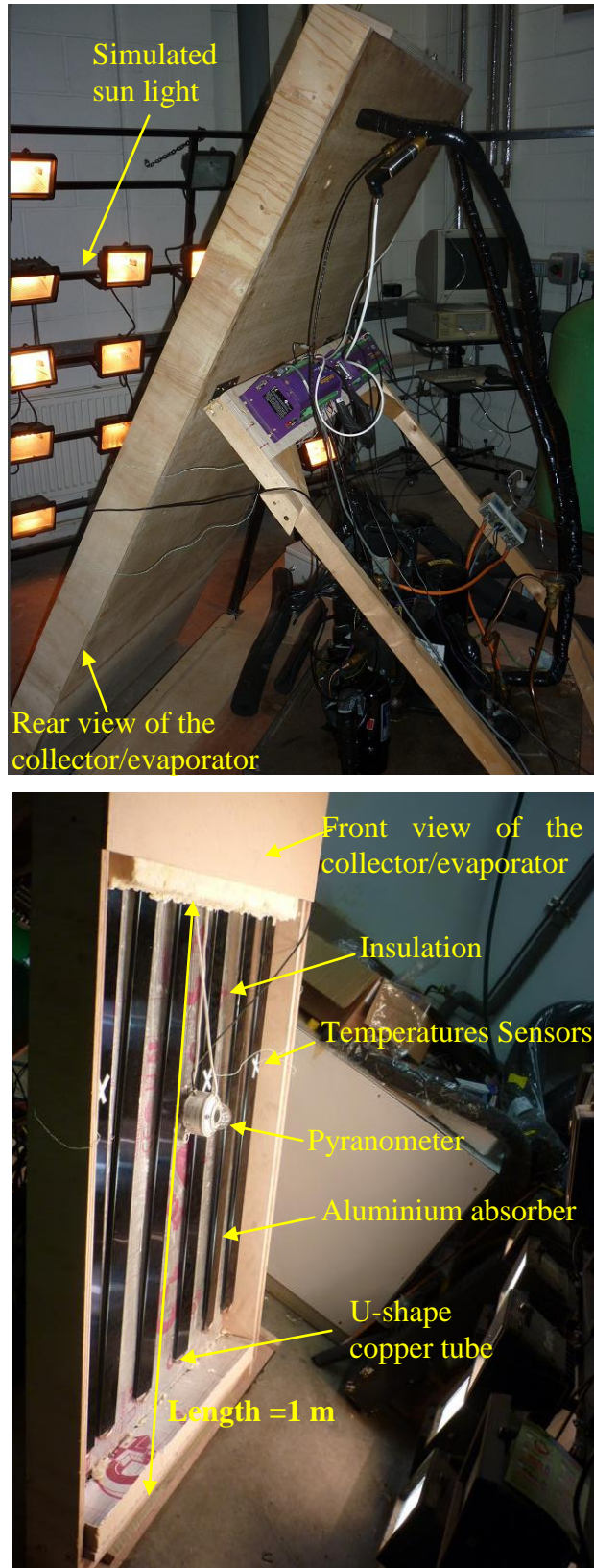


*Figure 5.87: Simulated solar radiations on the collector/evaporator without vacuum tubes*

### 5.3.3 Equipments and Instrumentation

There are four main components (collector/evaporator, compressor, condenser and expansion valve) in a refrigerant circuit loop (Figure 5.86) of the experimental rig; and any components (receiver, filter, and sight glass) beyond these basic 4 are identified as accessories. This section will take a closer look at the individual components of the refrigerant loop of the laboratory experimental rig system.

#### 5.3.3.1 Solar collector (evaporator)

One of the aims of this study was to optimise the rate of heat transfer between the heat source, solar radiation and the refrigerant and also to reduce the operation temperature of the PV panel. Copper and aluminium are proven to be very good thermal conductivity materials compare to other materials like iron. For this study, an aluminium sheet heat absorber (1.50mm thick) with copper tube for refrigeration has been used see Figure 5.87. The total area of the collector was  $1.2 \text{ m}^2$  and, with its surface painted in black to increase heat radiations. Insulation was used at the back of the aluminium sheet to reduce heat lost collector/evaporator; therefore it is exposed to the ambient air. In order to increase the heat between aluminium sheet surface and the heat source, solar radiation and the refrigeration liquid in the collector, three quarters of the u-shape copper tubes 'diameter was tightly rolled with the aluminium sheet from one side to the end of the sheet. In addition, the collector/evaporator has no welded bond. Therefore the heat collected from the solar irradiation by the web between finned tube of the collector/evaporator flows directly to the working fluid without any resistance from the welded bond linking of the webs and the refrigerant tubes.

### 5.3.3.2 Compressor

In the refrigeration loop, the compressor performs 2 functions. The compressor receives refrigerant from the evaporator/collector in form of vapour, compresses it in form of the gas and moves the refrigerant around the loop. The compressor (TL3F, Danfoss) used in this study it is of the electrical rotary type, which compresses the refrigerant gas and sends it on its way to the condenser. The compressor of this experimental has a rated capacity of about 107W, and uses R134A as refrigerant oil.

### 5.3.4 Condenser (flat plate heat exchanger)

The condenser receives refrigerant gas from the compressor, and then transfers heat to the water, so that the refrigerant gas can condense back into a liquid in preparation for a return trip to the collector/evaporator. The condenser used in this study is the flat plate L-line type heat exchanger (see Figure 5.88), made of stainless steel with a transfer area of about 172 cm<sup>2</sup>. As long as the compressor was running it was imposed a force on the refrigerant to continue circulating around the loop and continued removing heat from solar radiation via the evaporator/collector and transferred it to the water via condenser (heat exchanger below).

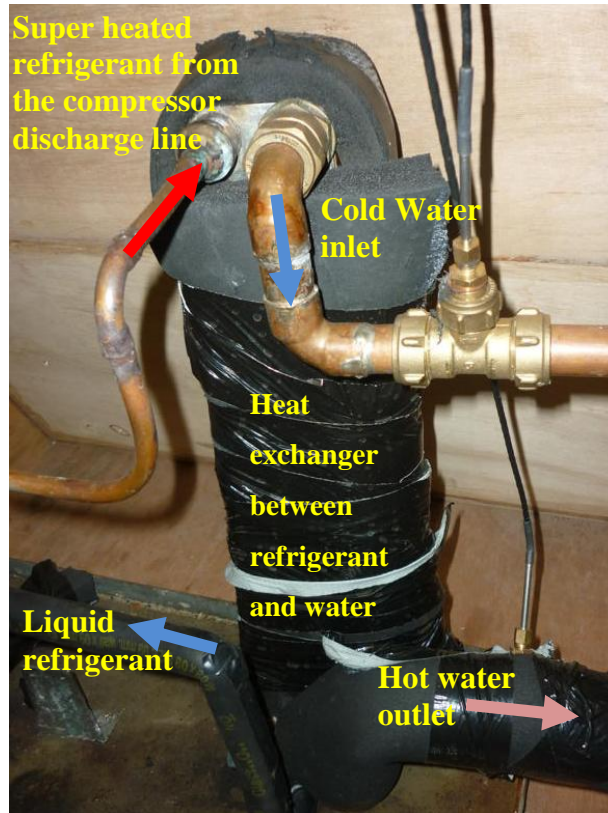
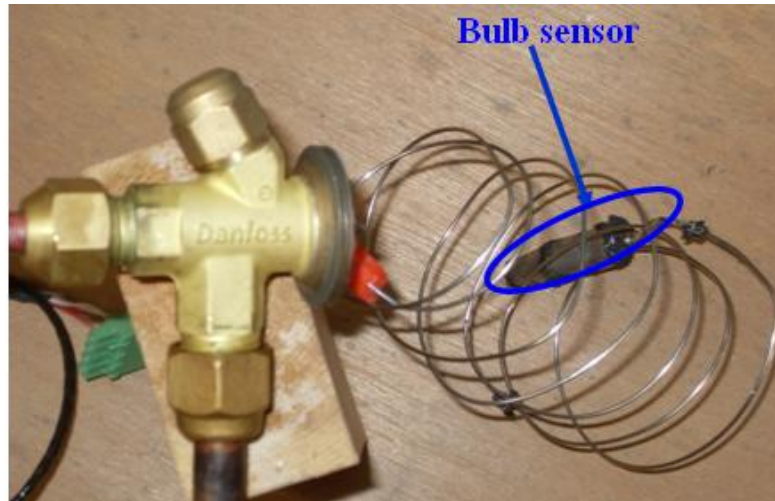


Figure 5. 88: Heat Exchanger (Condenser), SWEP: B8x10H/1P

### 5.3.5 Thermostatic Expansion Valve (TXV)

Figure 4.89 shows the expansion valve used for this study, *Danfoss* type with fixed orifice and external equaliser. The TXV had a sensing bulb attached to the outlet of the evaporator. This bulb sensed the suction line temperature and sends a signal to the TXV allowing it to adjust the flow rate. The flow rate through a TXV was settled so that not only that all the liquid hopefully changed to a vapour, but there was an additional 10°C, superheat, this was a safety margin to insure that all the liquid changed to a gas and that the gas returning to the compressor was several degrees away from the risk of having any liquid content.



*Figure 5. 89: Thermostatic Expansion Valve (TXV, Danfoss)*

Others components have been added along with TXV device in the liquid line. While the TXV reduces the flow of the refrigerant to the collector/evaporator the remaining one needed somewhere for unneeded refrigerant to go and the receiver in the *Figure 5.90* below. The type of receiver used in this experimental rig was, *AIRMENDER, CR-101*, with the capacity of 1.5 litres.

Additional component along with TXV was liquid line filter shown in *Figure 5.91*. The filter caught unwanted particles such as welding slag, copper chips and other unwanted debris and keeps it from obstruction up important devices such as TX Valves. The filter also has another functions, since it contains a desiccant which can absorbs a minute quantity of water in the refrigerant.



Figure 5. 90: Refrigerant receiver, AIRMENDER, capacity of 1.5 litres



Figure 5. 91: Liquid Line Filter

### 5.3.6 Experimental Procedure

In order to evaluate the preliminary thermal performance of the DX-PV/hp-HP a series of experiments was conducted at the laboratory of the school of the Built

Environment, Nottingham University. The procedures followed to conduct the experiment are described in Chapter 4, section 4.4.3.

### 5.3.7 Data acquisition and processing system

The following parameters were measured: electric power consumed by the compressor; temperatures of both water and refrigerant circuits recorded at different locations of the two loops; pressures of refrigerant at inlet outlet of the compressor, evaporator/collector and condenser were also been measured. In addition, the ambient temperature, relative humidity, the incident solar simulation, and indoor air temperature were also measured. The mass flow rate of the water was controlled using vane valve.

Pressures are measured with GP pressure transmitter, which is a multipurpose, high performance stainless steel 0-100Mv output transducer transmitting at 4-20mA output range; temperatures were measured with K type, thermocouples and platinum resistance thermometers (RTDs). A solar pyrometer was placed at the middle of the collector/evaporator plate was used to measure the instantaneous solar radiation. Mass flow rate of the water was measured using flow meter. A digital power meter was used to measure the power consumption of the compressor every five minutes. All data was measured, monitored and controlled by a personal computer via data logger software.

In order to record experimental data (solar radiation, compressor temperatures, condenser and evaporator temperatures), the Data-Taker in the *Figure 4.78* is

connected to the computer and, using appropriate software, one stores data in the computer for future reference and then transfer to spreadsheet for examination.

#### 5.4 Preliminary experimental results and discussion

A series of preliminary test have done, and the results for each radiation were summarised in the *Table 5.21* and plotted in the *Figure 5.92* and *Figure 5.93*, for each simulated radiation, the average COP of the heat pump and heat rate gain ( $Q_{h,avr}$ ) at the condenser were recorded and then plotted against time.

The results indicated that for solar radiation range from 250-850W/m<sup>2</sup>, the evaporating temperatures vary from -5.24 to 3.25°C; the total electric consumption for the compressor was between, 99 – 107W. The averages COP of the heat pump for space heating mode was between 3.40 – 4.17, and was in good agreement with conventional air source heat pump performance.

I, avr (W/m <sup>2</sup> )	Tevp, i,avr (°C)	T Alum, avr (°C)	Q <sub>h, avr</sub> (W)	COP <sub>avr</sub>	Troom, avr (°C)
250	-5.24	14.31	364.01	3.40	21±2
300	-0.14	16.61	365.47	3.42	21± 2
500	-1.98	18.62	396.84	3.72	21±2
650	1.49	18.73	398.24	3.71	21±2
850	3.25	21.56	445.70	4.17	21±2

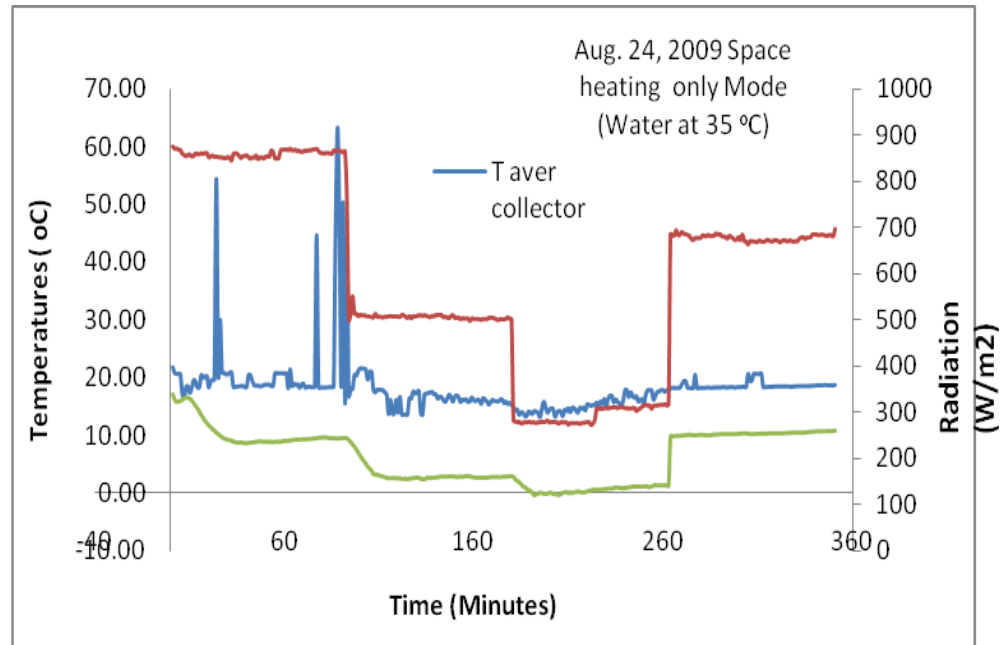


**Figure 5.92:** Preliminary results of PV/hp- heat pump testing

From *Figure 5.92*, the temperature of the aluminium sheet was about 20°C for all simulated radiation; however there were some short high temperature variation between 45°C and 60°C, due to high radiation about 850W/m<sup>2</sup>. The temperature of the refrigerant has the same trend with the radiations as expected. When the temperatures of the refrigerant inside the copper heat pipe enrolled underneath of the aluminium sheet were fluctuated between 15°C and 8°C when the radiation was between 700- 850 W/m<sup>2</sup>; and were between 8°C and 0°C when the radiation was between 250- 500 W/m<sup>2</sup>.

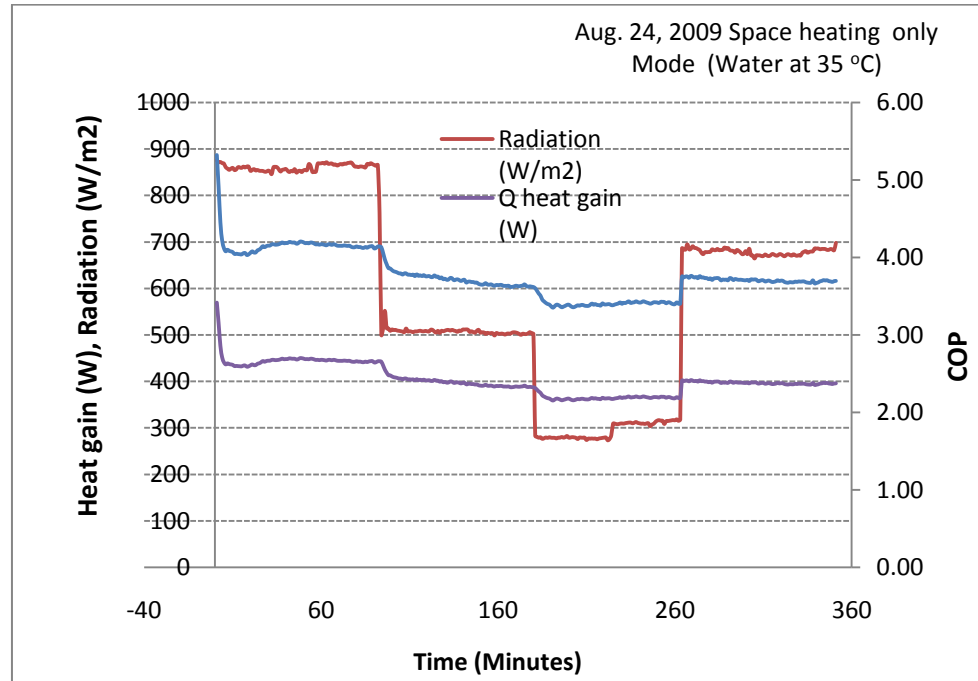


Figure 5.93: The testing average COP and condenser capacity of PV/hp- heat pump

In the Figure 5.93, the average COP of the PV/hp- HP was sensitive to the solar radiation as expected; when radiation increased, the COP also increased and was between 3.40 and 4.17.

### 5.5 Conclusion - Chapter 5

A novel DX-PV/hp-HP system has been introduced in this chapter. In order to predict the performance of the novel system; under the climatic conditions of Nottingham, UK, Numerical steady models have been performed for each component of the heat pump loop and for each part of the PV/hp-sandwich absorber. The models were developed so that they can be integrated into EES. The EES was effectively used to perform a thermodynamic cycle of DX-PV/hp-

heat pump cycle, also to investigate sensitivity analysis and COPs, and then use the results to compare other researchers work.

From the simulation results, the following can be concluded:

- (1) When the PV/hp evaporator absorbers are placed inside the vacuum and then cooled using refrigeration oil. The novel PV/hp-heat pump system has a better energy performance than the typical air-cooled or water-cooled flat plate PV collectors due to the vacuum insulation for the reduced heat loss and the lower boiling temperature of R134a, which increased heat extraction from PV modules.
- (2) The monthly average thermal efficiency varies from 0.711 to 0.794 with an average of 0.752 and the monthly average electrical efficiency varies from 0.148 to 0.162 with an average of 0.155. Both the thermal and electrical efficiencies are higher than that of conventional PV/T collectors.
- (3) The novel PV/hp-heat pump system has a COP ranging from 4.65 to 6.16 with an average of 5.35. The condenser capacity ranging from 33 to 174 W would provide the heat source for space heating and domestic hot water. The energy performance of the novel PV/hp-heat pump is not as good as expected due to the low solar radiation. It should be much better in some low latitude locations with better solar radiation.

The first stage of the preliminary test to evaluate the performance of PV/hp collector as evaporator has been done using 6 absorber plates, made of aluminium sheet and u-tube copper tubes for working fluid, R134a. To increase heat transfer between aluminium sheet and the u-shape copper, very good contact has been

done using three quarter of the copper tube diameter have been tightly rolled underneath of the aluminium sheet to form a so called web between the arms of the u-shape copper tubes.

A series of tests at the follow simulated radiations were undertaken  $250\text{W/m}^2$ ,  $300\text{W/m}^2$ ,  $500\text{W/m}^2$ ,  $650\text{W/m}^2$  and  $850\text{W/m}^2$ , and the results for each radiation were summarised in the *Table 5.21*. The results indicated that for solar radiation range from  $250\text{--}850\text{W/m}^2$ , the evaporating temperatures vary from  $-5.24$  to  $3.25^\circ\text{C}$ ; the total electric consumption for the compressor was between,  $99 - 107\text{W}$ . The averages COP of the heat pump for space heating mode was between  $3.40 - 4.17$ , and was in good agreement with conventional air source heat pump performance.

## 5.6 Further Works

### 5.6.1 Propose research on PV/hp roof modules

The overall aim of the proposed research is to investigate a novel PV/hp (photovoltaic/heat-pipe) roof module able to work with a heat pump cycle to provide electricity and heat for buildings with enhanced efficiency. The system comprises prefabricated PV/hp roof modules that are inter-connected and fitted into the roof truss to act as the roof finish, an electricity generator and the solar collector/evaporator for the heat pump. The system ( see *Figure 5.94*, and *Figure 5.95*) also incorporates a compressor, a condenser, an expansion valve and a heat storage device. Integration of PV and heat pipes in a prefabricated roof

module will provide high efficiency in terms of solar energy conversion and roof space requirement, and in so doing, offers the potential to create a low cost solution for electricity and heat production. The PV/hp modules would be architecturally pleasing and easy to install.

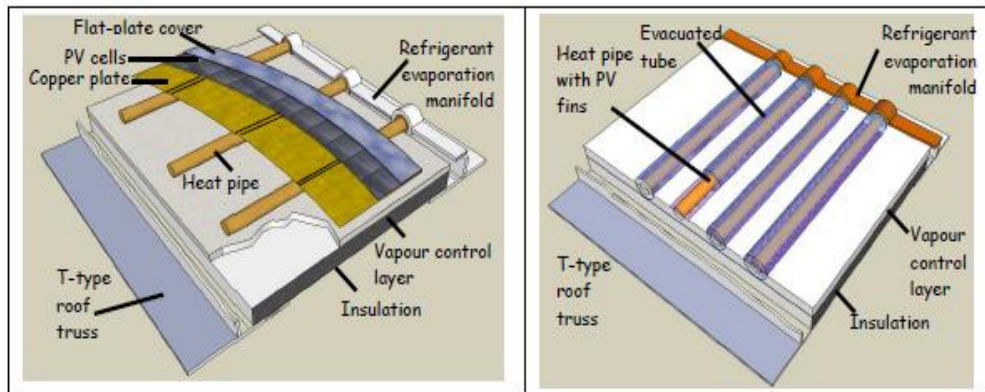


Figure 5.94 : Schematic of the PV/hp roof modules: Flat plate PV/hp structure, Evacuated tube (rectangle or circle) PV/hp structure

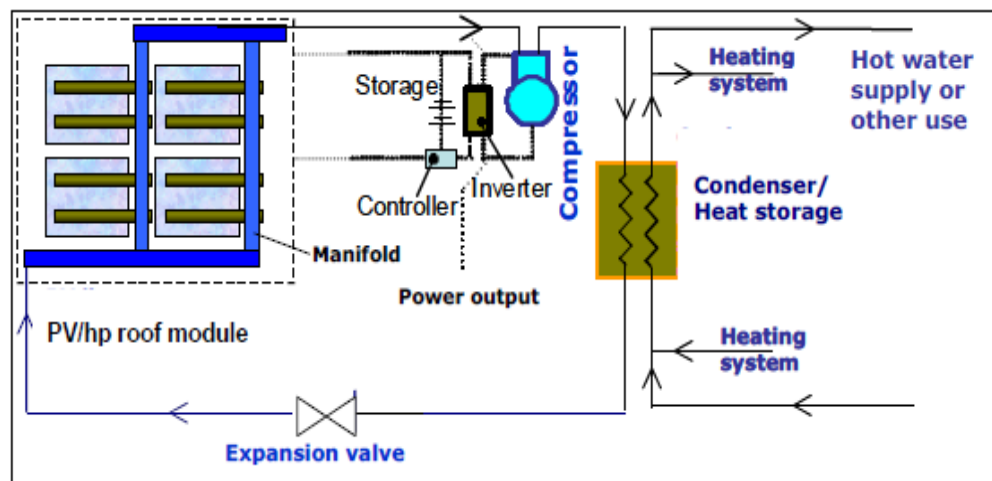


Figure 5.95: The PV/hp roof module based heat pump system

## **CHAPTER 6 - SMALL SCALE TESTING OF A NOVEL SOLAR ROOF/COLLECTORS ASSISTED QUICK RECOVERY OF THE GROUND SURROUNDING ENERGY PILES IN SUMMER**

---

## 6 INTRODUCTION

This Chapter presents initial findings from a recent monitoring of a novel solar roof/collector used to assist a quick heat recovery of the ground surrounding energy, the energy pile uses the concrete foundation piles as ground loop heat exchangers for ground source heat pump. In this novel system, solar roof/collector is designed and combined with the piles to harvest free energy from the sun and warm air during summer for ground heat recharging.

### 6.1 Brief background of this work

The conventional GSHP loops are installed in deep vertical boreholes of about 100m deep or laid horizontally in trenches at depth of about 1.5m. In addition the high cost of the vertical ground loop installation or the lack of surrounding land around houses tends to reduce the widespread take-up of the GSHP as a heating solution, particularly in the UK residential market.

In recent years piled foundations for residential dwellings have become technically and economically feasible alternative to traditional trench fill strip footings. In this regard, Roger Bullivant Ltd (2008) believed that the piled foundation combined with GSHP with short borehole, and could provide the structural heat source solution for residential dwelling. However due to the close spacing of residential piles, it is considered that the thermal interference between neighbouring piles had an effect of reducing the specific piles energy extraction. Therefore in the long term, say 5-10 years, the energy yield surrounding the piles decreased and the local

ground temperature fall; therefore affected the seasonal performance factor of the heat pump and also the COP.

In this regard over two heating seasons, full 2007/ 2008 heating season and 2008/2009 heating season, Wood et al (2009) have tested piled foundations by incorporating loops into their structure to produce so called ‘Energy piles’.

Results shown that the SPF has reduced over the testing period from 3.62 to 3.40, which could be indicative of a cooling of the surrounding ground around the piles and the far field; across both the heating seasons it was reasonable to conclude that temperature reduction in the ground (see Chapter 2, paragraph 2.9.2) was responsible for the fall of performance and thus a lowering of the SPF. Such a fall in SPF from one season to the next was typical for conventional borehole fields, particularly in the first five years until a quasi-steady state is reached with the surrounding ground. Across the season the COP was seen to fall from 4.2 at the beginning of the season to a minimum of 3.1 before rising towards the end of the season to 3.44. This recovery was partly due to the heat load reduction towards the end of the season and also the rise in the local ground temperature due to the greater solar influence upon the ground towards the spring.

It is understood that if the “soil battery” volume underneath a building (Figures 6.96) was to be the only heat source of the energy pile (neglecting heat movement from beyond the perimeter) supplying the heat pump to fulfil a dwellings heating requirement. In order to enable a system to have longevity of efficient operation; it was therefore understood that the heat supply of the

surrounding ground was imperative to the continued recharge of the ground heat store.

In order to prevent long term cooling of the ground surrounding of the piles; it has been suggested to take advantage of the free energy from the sun during the year, as consequence to maintain the ground temperature at 7 °C or greater. One of the approaches is using the roof as solar collector to charge the ground or conventional solar collectors. Some concepts have been proposed as shown in Figures 6.96, 6.97 and 6.98; in the these concepts, solar roof/collectors were used to assist the ground quick heat recovery, and they would had the priority of heating DHW first, and when this is satisfied any additional heat would be sent to space heating thermal store and then to the ground trough energy piles system for storage. So in the summer months, the heat pump could only provide additional backup for DHW requirements.

To enable high COP of the heat pump, the temperature lift between the heat source and the heat load have to be reduce. For these novel concepts of the solar roof/collectors systems, it was considered that building space heating load should be further reduced by means of Mechanical Ventilation with Heat Recovery (MVHR) and increased insulation on buildings' fabrics. Additionally solar roof/collector for ground heat recharge has also be suggested, it would be used to warm circulating water-glycol mixture in the summer months to assist the ground for quick heat recovery. In this respect these novel concepts system with

“supplemental” heat recharge have been suggested based upon the assumption that the solar roof/collectors could provide all necessary ground heat recovery.

The first concept (Figure 6.96) used the concrete roof tiles as solar collector to achieve a solar input heat in the ground; the system is combined with the structural element of the roof. From previous work by Bapshetty on concrete panels, he has shown that, with solar concrete an efficiency of 42% could be obtained under optimal conditions (Wood C. J., 2009).

The second concepts was to use the complete roof area as a solar collector to charge the ground, in this case, the roof was pitched in order to maximise the sun on the total area. This concept (Figure 6.97), used metal roof as solar collector, and from the research performed by Medved (2007) on metal roof panel construction, he has shown that simple steel roof panel construction modified with fluid circulating pipes can attain a thermal efficiency of approximately 25% in the summer months.

Evacuated tubes panels (Figure 6.98) are typically expensive and integrate them underneath of the roof would not but practicable solution, especially it will required special skills. In addition, particularly in summer months, vacuum tubes have low energy yield compare to conventional solar collectors, including solar metal and roof collectors. However evacuated tubes are suitable to provide a greater energy yield in the winter months when the solar radiations are lower.

***Figure 6. 96: Concept 1-Solar roof/collector using concrete tiles***

***Figure 6. 97: Concept 2-Solar roof/collector using Metal tiles***

**Figure 6. 98:** *Concept 3-Solar roof/collector integrated with evacuated tubes*

The main aim of this work is to demonstrate the feasibility of these concepts, using a small scale testing facility at Roger Bullivant Ltd side. This work also aims to decrease the risk of freezing the ground surrounding a conventional ground heat exchanger used for space and water heating after a long term cycles say 5 to 10 years. Additional; benefice of this invention is to reduce the power consumption and operating time of the heat pump and to significantly reduce the required depth and cost of boreholes and the CO<sub>2</sub> from heating system for residential buildings.

## 6.2 CASE STUDY

### 6.2.1 The Foundation piles and heat pump

The foundation piles considered in this case study was installed by Wood (2009) for his PhD experimental rig system. the system was a representative of a 72m<sup>2</sup> ground floor of a detached two-storey house with piled foundation on a plot of 21x10 m deep continuous flight augured piles, 300m diameter (See Figure 6.99) , each pile had a 32 mm OD U-tube absorber pipe inserted to a depth of approximately 10m. In addition the spacing between piles was consistent with the requirement of load bearing formation as typically installed by foundation company, Roger Bullivant Ltd (see Figure 6.99). Two temperatures sensors (thermocouples) were incorporated to each pile to monitor at a depth of 5 and 10m also the ground temperature surrounding the foundation was monitored as shown in Figure 6.100. As there was no house build upon the foundation piles, the space heating and DHW loads were simulated using the buffer tank combined with heat rejection system (see Figure 6.100); the heat load for the test was based upon a typical modern “low energy” dwelling, which according to the standard EN12831 stated that a low energy home requires 40W/m<sup>2</sup> and an energy efficient home would required 10W/m<sup>2</sup>, but for this test the loading of 27W/m<sup>2</sup> was used, since the one floor plan was 72 m<sup>2</sup> and over two floors equated to 144m<sup>2</sup>, so the total maximum heater load was 3888W for space heating. The hot water load was also considered and was in accordance with DIN4708 part 2, which required that one person in a detached home would use 50L of 45°C hot water per day and 4 adults were assume to be leaving the suppose house, consequently the maximum

domestic hot water heating load was considered to be 8kWh per day. A total of 210m of pile were used for the ground heat extraction. The heat pump used in this work has a heat output of 5.7kW nominal (EN255 [35° C flow temperature]). From Wood (2009) work, the total heating season heat production was 17.24MWh at an SPF of 3.26 , therefore the heat extraction from 160m of pile was 12.48MWh, so an average of 78kWh/m of pile.

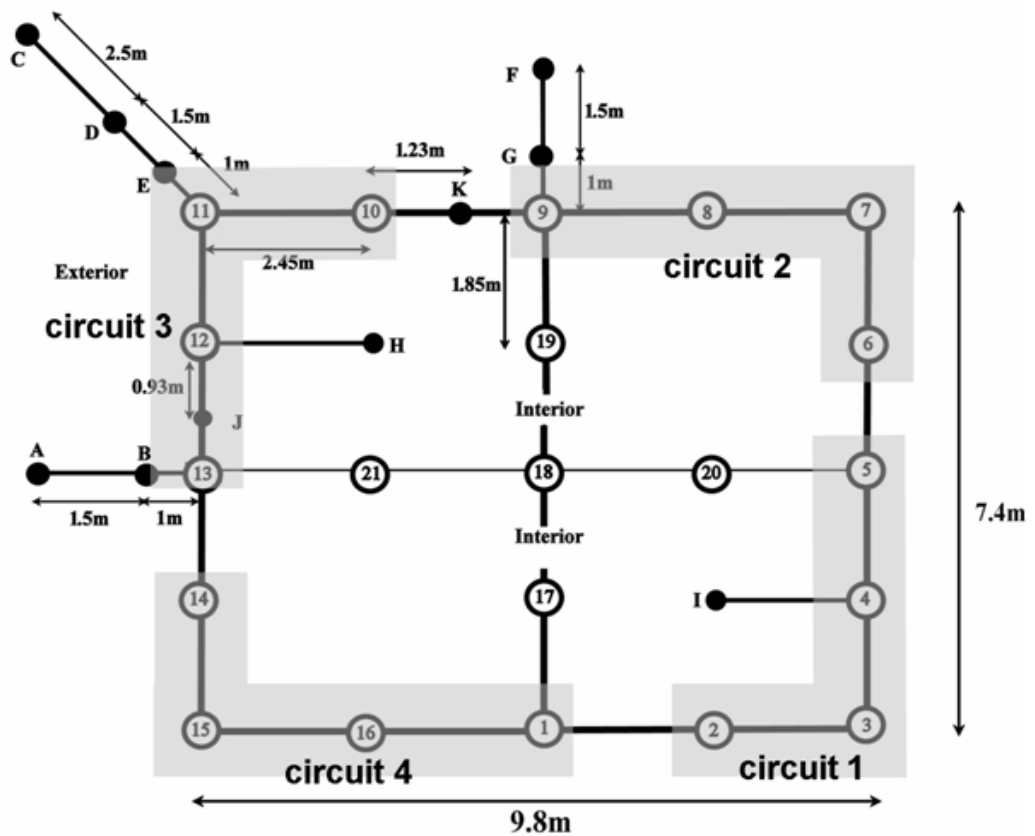


Figure 6. 99: Pile Foundation and thermocouple array layout (Wood C. J., 2009).

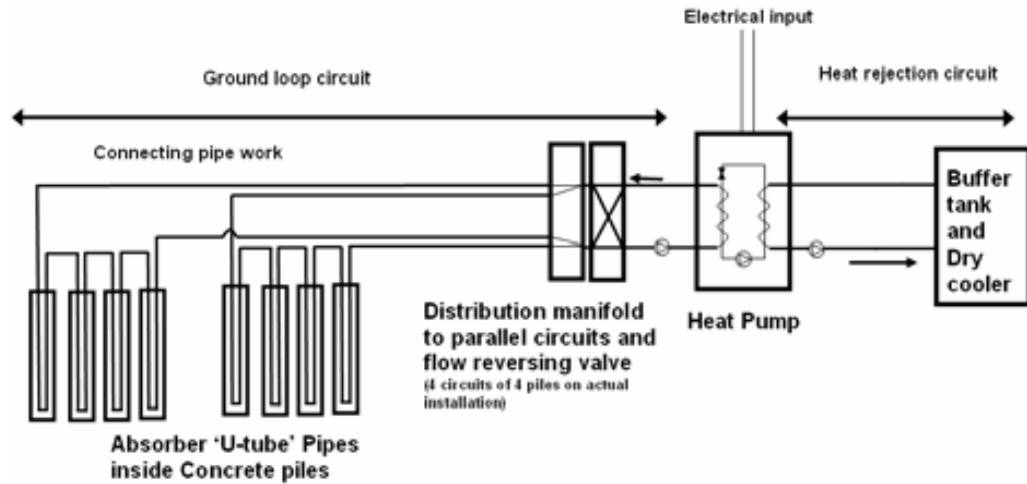


Figure 6.100: Schematic of a ground source heat pump with energy piles and simulated loads

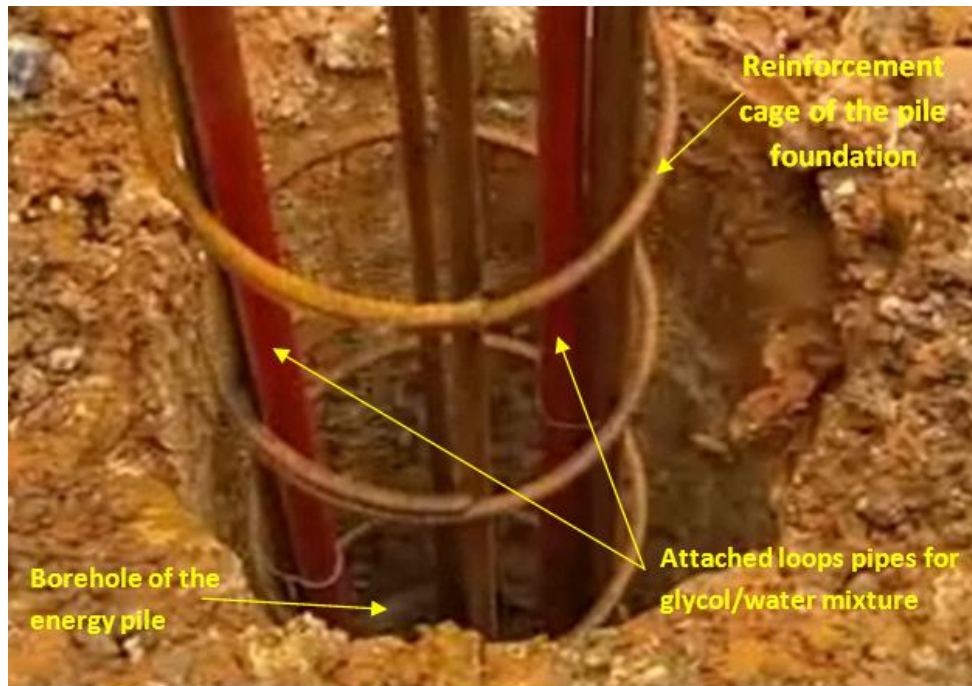


Figure 6.101: Set-up of the piled Foundation of a detached two storeys House



*Figure 6.102: Piled Foundation of a detached two storeys House*

### **6.2.2 The Solar roof collector**

The solar roof collector for ground heat recharging system is diagrammatically shown in *Figure 6.103*. The south facing solar roofs/collectors was split in two; one half ( $15.89 \text{ m}^2$ ) was covered with a traditional concrete tile and the other half also  $15.89 \text{ m}^2$  was covered with a metal tile. Underneath the tiles, there were aluminum-plates with pipes for working fluid (water/glycol mixture) (see Figures 6.103 and 6.105). Fluid was circulated through the pipes in the roof and to the energy-piles, by means of Grundfos circulatory pump. The flow rates were respectively  $0.0539 \text{ (l/s)}$  and  $0.0532 \text{ (l/s)}$  for metal solar roof/collectors loop and

for concrete solar roof/collector loop. The idea is to recharge the ground heat. The solar roofs/collectors collected heat on sunny days, bright-sky and from warm air under the roof tiles during summer to warm the glycol/water. The heated glycol/water was sent directly to the energy piles then to the soil.

For the experimental purpose, the concrete roof/collector had one circuit and this was connected to 4 piles in the ground (circuit 4 of the energy-piles used by Wood et al (2008). The metal tile circuit was also connected to the energy pile circuit 3 (see above paragraph 6.2.1). Whilst the solar roof was recharging the ground the heat pump was not running. ie. There was only a circulation between the solar roof/collector and the energy-pile circuits (see Figure 6.103).

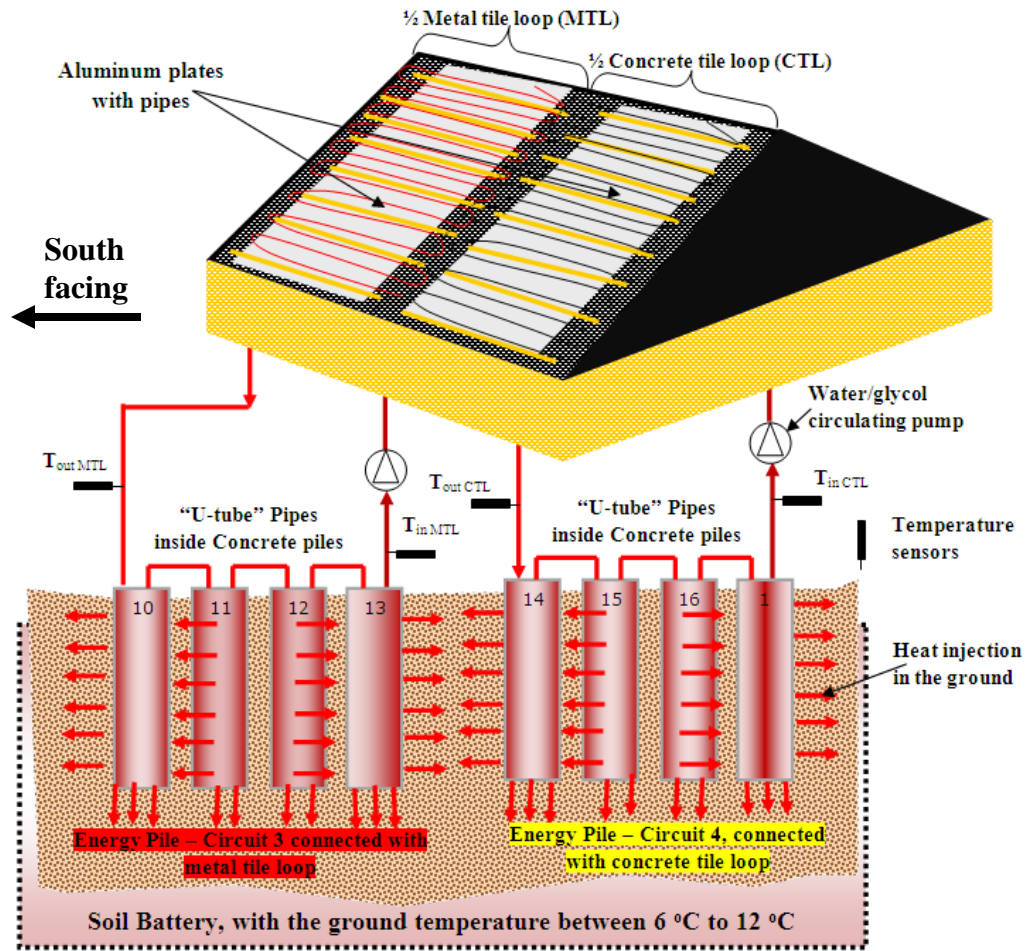


Figure 6. 103: The basic schematic diagram of the Case Study 2- Solar roof for ground heat recharging (Inter-seasonal heat storage)

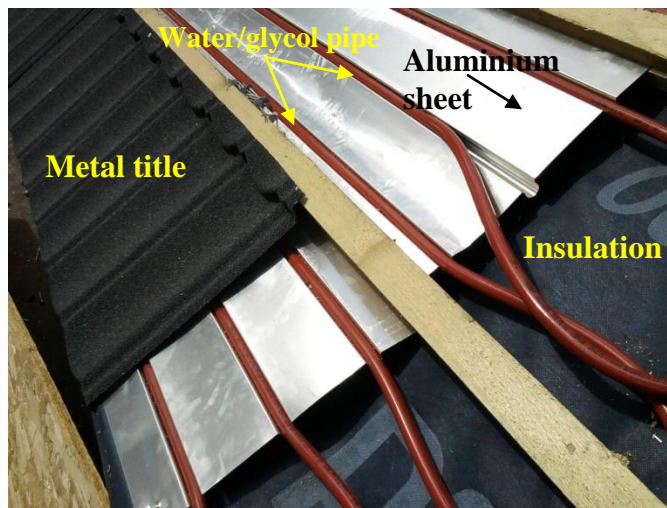


Figure 6. 104: Aluminium sheet and water/glycol pipe under the metal tiles

Some 130m of polyethylene red piping (see Figure 6.99) were fitted in the aluminium sheet, underneath of the metal roof.



Figure 6.105: Solar roof thermal collector under construction, at the experiment side

The relevant technical data for this experiment were summarised in the Table 6.22 below as follows:

Table 6.22: Summary of the technical data for this experiment

a	Solar roof/collector areas / roof type	Metal tile loop (MTL), Concrete tile loop (CTL)	16 m <sup>2</sup> 16 m <sup>2</sup>
b	Solar roof/collector inclination and orientation	$\theta=40^{\circ}C$ , and South facing	
c	Aluminium Sheet Area / roof type	12.5 m <sup>2</sup> (per roof type)	
d	Red HDPE absorber pipes	Outside diameter ( $d_o=25\text{mm}$ ), internal diameter ( $d_i=20\text{mm}$ )	
e	40m run of energy piles/circuits (3 and 4) and 300mm diameter/pile		
f	20m absorber pipes per pile		

g	Heat carrier fluid: 70% water and 30% antifreeze (glycol)		
h	Circulating pump, GRUNFOS Super Selectric UPS 15-60 of 55W		
i	Mass flow rates	Metal tile (MTL)	0.0539 (L/s)
		Concrete tile (CTL)	0.0532 (L/s)
j	Minimum inlet temperature water-glycol mixture	MTL Circuit 3	9.5° C
		CTL Circuit 4	10° C
k	Maximum outlet temperature water-glycol mixture	MTL Circuit 3	24° C
		CTL Circuit 4	25° C

### 6.3 Heat Transfer between Solar-roof/collector and Water/glycol mixture

Assuming that the walls of the absorber pipes of Solar roof/collectors have the same temperature as the surrounding aluminium plate or warm air between the tiles and pipe respectively reduces the complex thermal problem (Figure 6.106) to the heat transfer from pipe wall to absorber fluid (heat carried fluid). This is essentially influenced by the flow behaviour of the fluid in the pipe that is laminar or turbulent.

Laminar flow in a pipe is based on flow paths with different velocity  $u$  and interface friction  $\tau$ , which is proportional to the velocity gradient  $du/dx$  perpendicular to the flow direction. The coefficient of proportionality is the viscosity  $\eta$ , which increases with temperature. The mean velocity of laminar flow is  $u_{mean}=0.5u_{max}$ , and for turbulent flow  $u_{mean}= (0.80 - 0.85)u_{max}$ . The transition from laminar to turbulent flow condition is described by the Reynolds number, Re

$$Re = \frac{ud}{\nu} \text{ with } \nu = \frac{\eta}{\rho} \quad (6.1)$$

Where  $u$  is the mean velocity (m/s),  $d$  is the pipe diameter (m),  $\nu$  is the kinematic viscosity ( $m^2/s$ ),  $\eta$  is the dynamic viscosity (kg/ms), and  $\rho$  is the density of the water. Below the critical Reynolds number  $Re = 2300$  laminar flow occurs; above

$Re > 10^4$  full turbulence exists or if  $Re > 2300$  the flow is turbulent. Turbulence in the flow increases the diffusive transfer of the energy, impulse and mass. This effect increases with flow velocity.

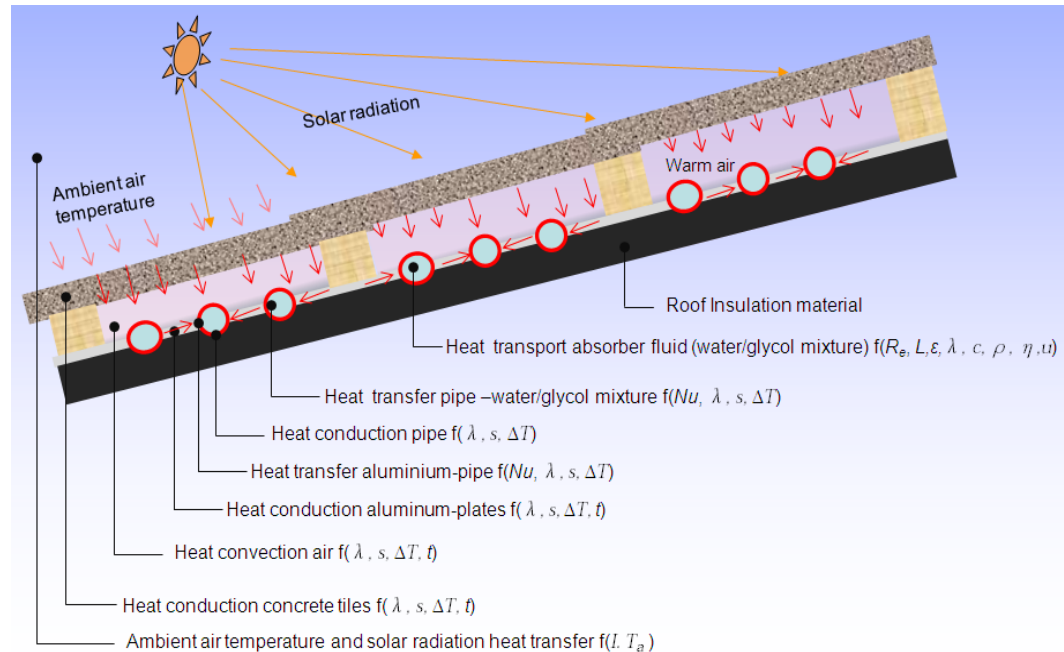


**Figure 6.106:** Heat transport from ambient air/solar radiation to heat carried fluid (water/glycol mixture) within the absorber pipe of the solar roof/collector

The circuit of the solar roof/collector – energy piles (Figure 6.103) was closed loop system. One of the main tasks of this work was to determine whether the water/glycol flow was turbulent or laminar. This was determined by calculating Reynold’s number for water/glycol flow in the cross section of the pipes of the experiment system.

$$Re = \frac{\rho u d}{\mu}, Q = \frac{\text{flowrate} (\frac{L}{s})}{1000}, (\text{volumetric flow rate, m}^3/\text{s}) \quad (6.2)$$

Where  $d$  is the internal diameter of the absorber pipe,  $\mu$  ( $0.801 \times 10^{-3} \text{ kg.m}^{-1}\text{s}^{-1}$ ) is the viscosity of water. The flow rates for the experiment were 0.0539 (L/s) for the metal roof tile and 0.0532 (L/s) for the concrete roof tile and the u-tube had a 25mm outside diameter (OD) and 21mm inside diameter (ID).

$$A = \frac{\pi d^2}{4} = \frac{\pi(0.021)^2}{4} = 0.34 \times 10^{-3} \text{ m}^2,$$

$$u = \frac{0.0539}{0.34} = 0.15853 \text{ m/s (Metal roof)}$$

Hence,  $Re = \frac{1000 \times 0.021 \times 0.15853}{0.8011 \times 10^{-6}} = 4156 \times 10^3 > 10^4$  for the metal roof loop, full turbulence exists.

$$u = \frac{0.0532}{0.34} = 0.156470 \text{ m/s (Concrete roof)}$$

Hence,  $Re = \frac{1000 \times 0.021 \times 0.156470}{0.8011 \times 10^{-6}} = 4101 \times 10^3 > 10^4$  for the concrete roof loop, full turbulence exists.

The calculated Reynold's number was then used to determine the pressure loss due to friction across the supply and return paths of the U-tube. The frictional pressure drop is given by:

$$h_f = \frac{4flu^2}{2dg}, \text{ where } g \text{ is the acceleration due to gravity.}$$

$$f = \frac{0.0539}{Re^{0.25}} = \frac{0.0539}{4156000^{0.25}} = 1.2 \times 10^{-3} \text{ (Metal roof)}$$

$$f = \frac{0.0532}{Re^{0.25}} = \frac{0.0532}{4156000^{0.25}} = 1.2 \times 10^{-3} \text{ (Concrete roof)}$$

Assuming the equivalent length of valves and T-connectors for the U-tube circuit is negligible relative to the total length:

$$l = (3 \times 2.45) + (2 \times 5) + (8 \times 10) = 97 \text{ m is the water travelling length.}$$

Hence,

$$h_f = \frac{4 \times 1.2 \times 10^{-3} \times 97 \times 0.15853^2}{2 \times 0.021 \times 9.81} = 0.41202 \text{ m of water, thus the equivalent frictional}$$

pressure drop is given by

$$\Delta P_{friction} = h_f \times \rho \times g = 0.41202 \times 1000 \times 9.8 = 4037.796 \text{ Nm}^{-2} \text{ (Pascal). This was}$$

use to select the circulating pump.

A pump capable of handling the head loss and differential pressure loss of the system was required. The GRUNFOS Super Selectric UPS 15-60 pump was selected and was capable of handling a maximum head of 5m with a corresponding differential pressure loss of 60kPa.

#### **6.4 Heat Transfer Budget and Geothermal Situation of the Soil Battery**

Soil has a complex heat transfer mechanism, which involves conduction, radiation, convection, vaporisation & condensation process and freezing thawing processes (Brandl, 2006). However in the case of GSHP system the heat transfer between the ground heat exchanger and the soil is highly dependent on the thermal properties of the ground. And the ground functions as thermal storage volume; the heat is extracted from the ground for heating requirements during winter, and the re-introduce during summer or during some sunny days in winter via solar roofs/collectors. Assuming that there is no geochemical component to the soil battery heat budget, as shown in the *Figure 6.107*, therefore it should be consider only the amount of heat extracting from the soil battery during winter time and

generating during summer time. In this case throughout a year, the soil battery may be discharged ( $Q_h$ ) in winter and recharged ( $Q_{SC}$ ) in summer.

- If  $Q_h > Q_{SC}$  over the course of a year, soil battery will be over discharged and in the long term there will be a tendency for the ground to cool down (Freeze)
- If  $Q_h < Q_{SC}$  over the course of a year, soil battery will be over recharged and in the long term there will be a tendency for the ground to heat up
- if  $Q_h = Q_{SC}$  over the course of a year, soil battery will be balance between discharged and recharged, this will result in minimal disturbance to the long-term soil battery heat budget and consequently to its temperature and heat pump performance.

However thermal properties of the ground are important design parameters, since it dictates the length of the ground heat exchanger for a giving heating load. The parameters that influence the heat conduction from the energy pile to the soil are the following : thermal conductivity,  $\lambda$ , which represents the ability of the heat to travel through the ground and expressed in W/mk, heat capacity of the ground,  $c_g$ , is the energy required to raise the temperature of unit mass of soil by one degree, it is expressed in J/kgk, density,  $\rho$  of the ground in  $\text{kg/m}^3$ , and the thermal diffusivity,  $\alpha$ , which is a measure of the ground ability to conduct heat relative to its ability to store heat ( $\text{Wm}^2/\text{J}$  or  $\text{m}^2/\text{day}$ ) (see Figure 6.107).

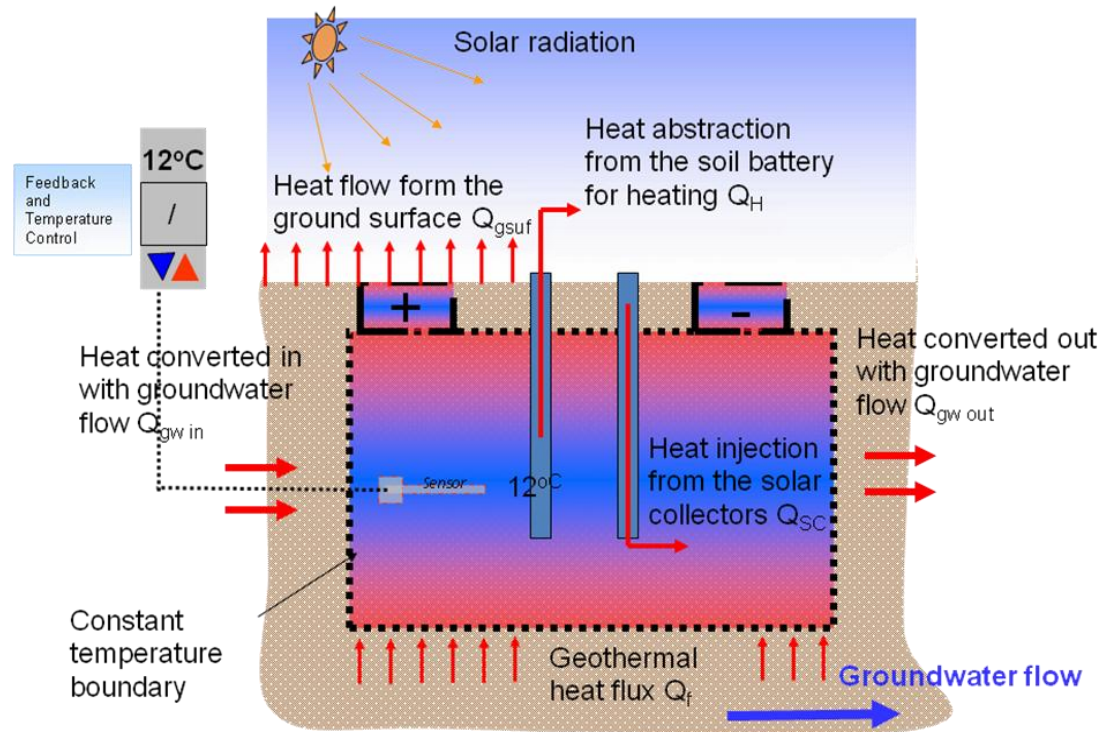
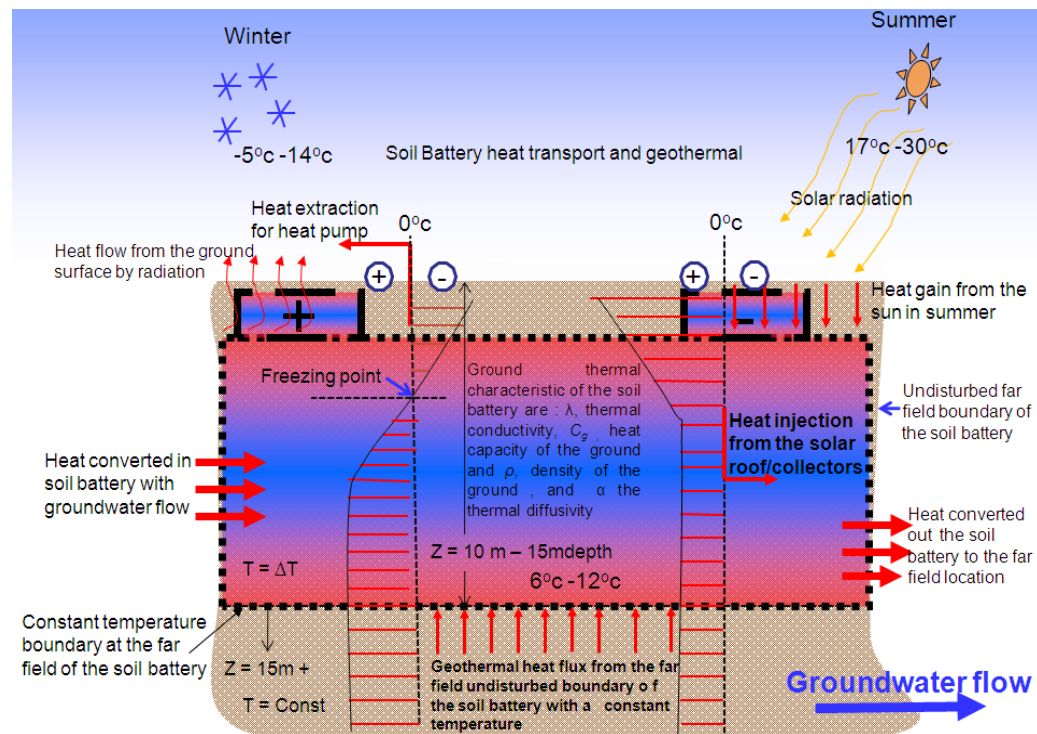


Figure 6.107: Heat Budget of the Soil Battery

The high moisture content in the soil resulting in an increase in the thermal conductivity of the soil around the ground heat exchanger piles and representing an additional heat transport medium; It is clear that as the moisture content increases for any particular soil type due to heavy rainfall or moisture migration (groundwater flow) as shown in the *Figure 6.109*, the resistivity decrease, hence this increasing the conductivity of the soil. In addition is also interesting to note that the lower the density of the soil, the higher the conductivity of the soil.

For a given soil type the thermal conductivity is relatively constant above a specific moisture content index, referred to as the *Critical Moisture Content*

(CMC). Below the CMC the thermal conductivity drops significantly. During summer, when recharging the soil, in this process the heat is injected in the ground through energy piles to the surrounding ground (see Figure 6.109). And this will drive away the moisture from the soil near the piles. In a situation when the soil is at or near its CMC, the reduction in the moisture could significantly reduce the soil's thermal conductivity. A soil of such characteristic is thermally unstable and can significantly degrade the ground heat exchanger performance.



**Figure 6. 108:** Heat transfer and geothermal situation of the Soil Battery during winter and summer

In most region of Europe including of the UK, the seasonal ground temperatures remain relatively constant beyond a depth of 10m. Values between 6°C and 12°C

predominate to a depth of about 15m, and then 12°C-15°C predominates to a depth of about 50m (Figure 6.108). Such temperatures represent ideal conditions to permit economical space and water heating by using energy piles structures and heat pumps. Substantial temperature fluctuations in summer and winter during the year would reduce the efficiency of heat pump systems. The soil battery know as thermal energy storage using energy piles in the residential sectors is an existing technology but not yet proven in the UK, one of the drawback could be because of the extremely variable characteristics of the UK ground that is use to balance winter cold and summer heat gain by storing heat. One of the purposes of the further work from this project could be to investigate the capability of UK soil to store heat.

### **6.5 Local geology of the ground at the experiment side**

The geology of the site where the experimental system was installed was a non-homogeneous, it was a typical of a “brown filed” site. The first 0 to 3m depth was consisted of the mixture of gravels, concretes, cobbles, fine to coarse sands, quartz; and between 3 to 10m depth, also a non-homogenous layer of very soft red-brow clay, with slight gravel content.

For this work before the energy piles was installed in the ground, the moisture content of the soil was investigated by means of slow baking a known mass method; the samples were bagged in a plastic bags and then sealed for two weeks. Observation of the bags showed an indication of the moisture content in clay layer,

which was the greater region of homogenous layer between 3.3m to 10m depths the results of the moisture content analysis were summarised in the *Table 6.23*.

**Table 6. 23:** Results of the moisture content analysis of the soil around the piles

Sample N <sup>o</sup> and extraction method	Depth and ground type (m)	Wet weight (g)	Dry weight (g)	Moisture weight (g)	Net wet (g)	Net dry (g)	Moisture (wet basis) %
1, Drill cutting	5.5m to 10 m, clay (bag1)	183.60	164.82	18.78	116.85	98.07	16.07
2, Drill cutting	5.5m to 10 m, clay (bag2)	190.75	168.92	21.83	127.68	105.85	17.10
3, Drill cutting	3.3m to 5.5 m, clay	159.91	141.93	17.98	75.03	57.05	23.97
4, Core sample	0.58 depth	245.66	230.15	15.51	178.76	163.25	8.68
5, Core sample	5.5m to 10 m, clay	251.37	239.86	11.51	172.45	160.94	6.67

From the *Table 6.23*, it can be conclude that, the moisture content in clay layer around the piles varied from about 23% water at 3.5 depth to 16% at 5.5m depth and plus. However the most important thermal soil parameter is the thermal conductivity  $\lambda$ . The moisture content of a ground has a direct relationship with the effective thermal conductivity of the soil and moist ground will have higher conductivity compare to dry grounds as explained in the previous paragraph of this chapter. Further from this high moisture, the soil become frozen faster around the piles, however such condition around an energy pile has to be avoided. Because freezing of the ground causes the volume occupied by the water to increase and such the grounds “heaves”; and cause upwards pressure. Even after recharging the ground through solar roof/collectors, where frozen ground has defrosted the

displaced soil may not fall back to its original compact state. In this case it is seen that tiny voids within the ground would have formed. These voids then reduce the overall thermal conductivity due to these “insulating” pockets.

In a situation where the heat is been injected in the ground, one have to consider avoiding high temperature between the ground and the pile to dry the moisture due to excessive heat injection to ground surrounding the pile and causing a migration of moisture away from the piles and therefore thermal conductivity of ground can reduce over time if there is no significant ground water movement.

From the above assumption, it is important to carefully evaluate the thermal conductivity  $\lambda$ , of the energy pile for future consideration, when designing or determine the size of the heat injection device such solar roof.

PhD work of Wood (2009) on energy pile at the same location of this work has used the thermal response testing method to determine the thermal conductivity value of the pile and further from this a borehole thermal resistance.

The thermal response test set-up (see Figure 6.109) used the energy pile with loop to circulate a warm fluid (water or water-glycol mixture); the fluid was heated by an immersion electric heater with constant power input, and then the system was run over a minimum of 50hours and the flow and return temperature to and from the pile were measured in addition to the power input. An un-vented domestic hot water tank with double skinned and internal insulation; the un-vented tank was used as the pile “heater”, by mean of immersion electric heater, which was rated at 3kW at 240V, then reduce to suitable level at 110V and since the experiment was

outside in the open air, tarpaulin insulation was used to protect the tank from the wind, sun and rain. Working fluid was circulated by mean of a Grundfos circulating pump also shown in the *Figure 6.109* and the flow rate was monitored and was 0.165L/s and the associates Reynolds number was calculated and was found to be  $10006 > 10^4$  (taken from water at 25 °C, with a dynamic viscosity of  $7.8 \times 10^{-4}$ ), and such conditions the flow in the pipe was full turbulent, which also a important requirement for this type of test.

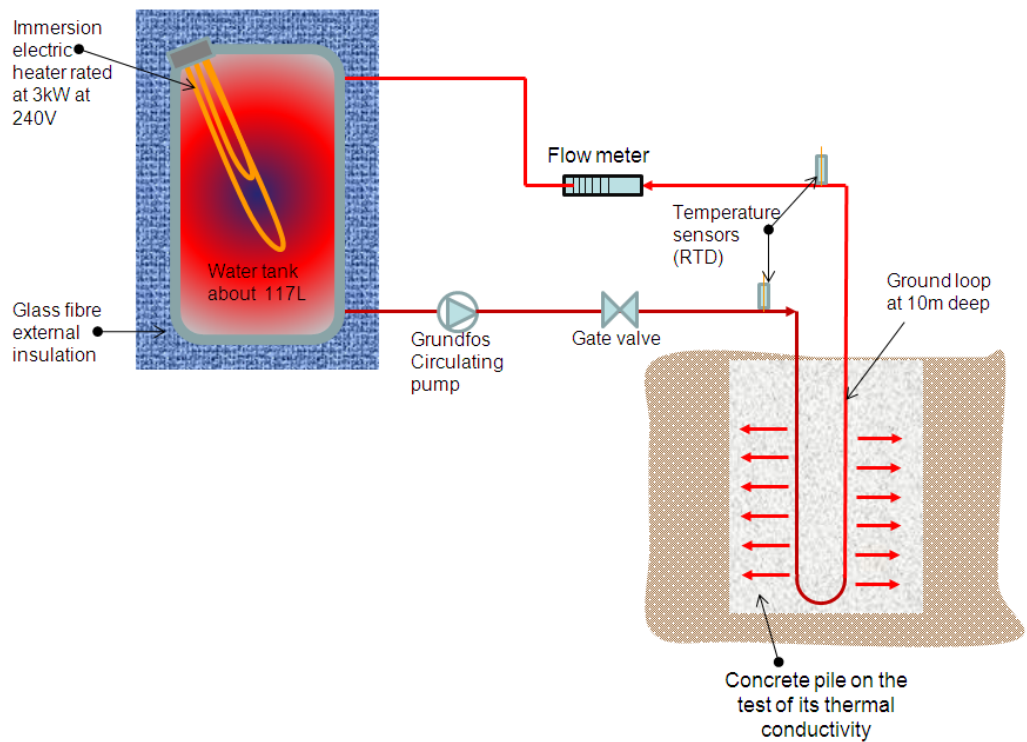


**Figure 6.109:** The set-up of the thermal response testing to determine thermal conductivity value of the concrete pile

In order to limit error on the thermal respond test by Austin (1995) recommended running, the test for more than 50 hours, this test was run for over 92 hours which was more above the 50 hours requirements. The average mean average power

across the whole running period was recorded and was found to be 625.5W. By mean of the following equations for direct current (DC), Power (P) = Current (I)\*Voltage (V) and Voltage (V) = Current (I)\*Resistance (R). With the temperature change across the pile and the flow rate, it was possible to determine the heat input, consequently the transient heat conduction regime equation was determine  $y=2.27x-2.5084$ , with  $R^2=0.984$ .

And the gradient of the slope was 2.27 and with high confidence value of 98%. From the above data, the thermal conductivity,  $\lambda$ , of the concrete pile was then determined, the value was provided to be 2.19W/m k, the calculation procedures are details in the Wood's PhD thesis.

Soil density was also determined by mean of testing, by taking a core slice of known volume and weighing of clay ground at the experimental location, the sample clay was first balance on an electronic balance, and then pressed into a container of known volume. From the test the following results were obtained (Table 6.24):

**Table 6. 24:** test results of the ground density of the energy pile location

Sample	Depth and type of the sample	Density (kg/m <sup>3</sup> )
1	5.5m to 10 m, clay (bag1)	2408
2	5.5m to 10 m, clay (bag2)	2392
3	3.3m to 5.5 m, clay	2233
4	0.58 depth, core sample	2277
5	2.41m depth, core sample	204
<b>Average weighted mean density (<math>\rho</math>)</b>		<b>2260</b>

The specific heat capacity,  $C_m$ , of the soil at side of the experimental was also determine by experiment, before the energy piles were installed. The details

procedures of the test was summarised in the PhD thesis by Wood (2009); the experiment results indicate that the mean value of the specific capacity of the soil surrounding the energy pile was about  $C_m=1.5\text{kJ/kg.k}$ .

From the above the specific heat capacity,  $C_m$ , the thermal diffusivity “ $a$ ” was calculated using the following equation  $a \text{ (m}^2\text{/s)} = \lambda/\rho C_m$ , where  $\rho \text{ (kg/m}^3\text{)}$  was the density of ground under consideration. The thermal diffusivity was found to be  $a=6.5 \times 10^{-7} \text{ m}^2\text{/s}$  and was within the range of the thermal diffusivity for heavy clay with 15% water suggested by ASHRAE (2003) to be between  $[4.86 - 7.06] \text{ m}^2\text{/s}$ .

### 6.6 Heat transfer between water/glycol and energy pile (concrete)/soil

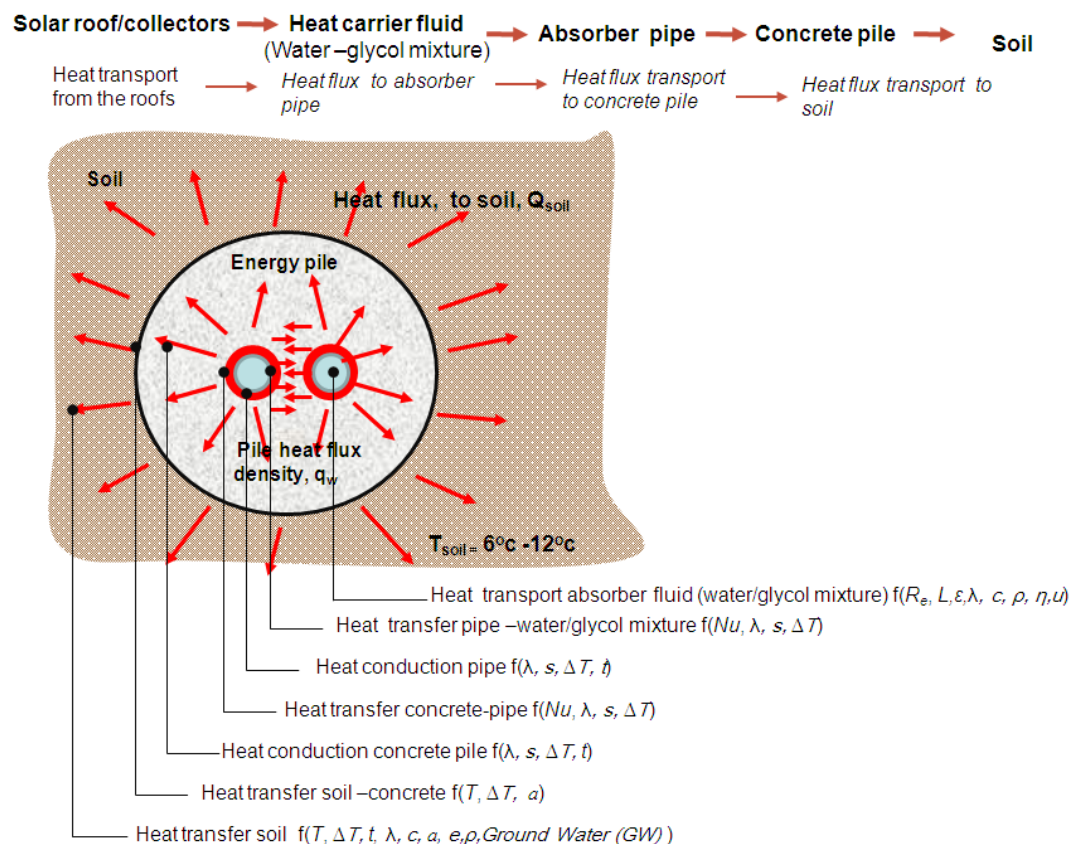


**Figure 6.110:** The set-up of the thermal response testing to determine thermal conductivity value of the concrete pile

Figure 6.110 gives a schematic overview of the heat transport from heat carrier fluid, within the pile to the soil under steady –state condition. Assuming that the internal wall of the absorber pipes of the ground heat exchanger have the same temperature as the surrounding concrete or soil respectively reduces the complex thermal problem (Figure 6.110) to the heat transfer from pipe wall to heat carried fluid (water/glycol mixture). This is essentially influenced by the flow behaviour of the fluid, that is, laminar or turbulent. Figure 6.110 illustrates that the heat flux,  $q_w$  transported by heat carried fluid in the circuit is given by the specific heat capacity  $C_m$ , the mass flow  $m_w$ , and the temperature difference  $\Delta T$  across the solar roof/collector.

Figure 6.110 shows the temperature distribution in the section of the absorber pipe and the concrete pile. Complex energy pile group and ground properties require numerical modelling of the geothermal recharging system.

$$\begin{aligned} \dot{Q}_s &= \int_0^{l_{pile}} \dot{q}_s C_{pile} dL_{pile} \xleftrightarrow{\text{heat flux from pipes}} \int_0^{l_{pile}} n_{pipes} \dot{q}_w C_{pipe} dL_{pipe} \\ &= \int_0^{l_{pile}} n_{pipes} \alpha (T_{outw} - T_{inw}) C_{pipe} dL_{pipe} \\ &= Q_{\text{heat gain at the roof}} = \dot{m}_{\text{water/glycol}} C_{\text{water/glycol}} \Delta T_{\text{across the solar roof}} \end{aligned}$$

Where

- $\dot{Q}_s$  = heat flux (W),
- $\dot{q}$  = heat flux ( $W/m^2$ )
- $C$  = circumference of the energy pile (m)
- $l_{pile}$  = energy pile length (m)
- $n_{pipes}$  = quantity of absorber pipe (unity)
- $\alpha$  = heat transfer coefficient ( $W/(m^2k)$ )
- $c$  = specific heat capacity ( $J/(kgk)$ )
- $\dot{m}$  = mass flow rate ( $kg/s$ )
- $T$  = Temperature ( $^{\circ}C$ )

## 6.7 Method

A short time monitoring method was applied to prove the novel concept of charging the ground through the piles structure. A small scale rig was built and the investigation was performed whereby the K-type thermocouples were inserted in water that was heated with the solar roof/collectors at the inlet and outlet. The thermocouples were connected to the data logger, DT500 (Figure 6.111), which in turn was connected to the PC to store data, which were then transferred to Excel spreadsheet for examination. Data were recorded every 1 minute, all the thermocouples were tested for calibration before the testing commenced and the maximum deviation was found to be  $\pm 0.3^{\circ}\text{C}$ . The system was run for one month from the 21<sup>st</sup> June to 21<sup>st</sup> July 2010. A monitoring system was set up to measure during charging the energy injected in the ground and energy collected by the solar roof/collectors from the warm ambient air, the total energy consumed by circulating pumps were also recorded. Since this experimental was to investigate the capability of the novel solar roof/collectors, because of time constraint, in this work, the soil temperatures were not monitored, this will be done during 2010 heating season and will then be compared with the performance obtained by Wood et al (2008) works on performance investigation of energy piles during 2008 and 2009 heating seasons.

Ground charging performance were observed by monitoring of the usual heat transfer parameters, the electrical energy input at the circulating pump, water-glycol mixture flow rates and temperatures changes across the solar roof

/collectors. Additionally the parameters known as the Pile-Water-Equilibrium Temperature (PWET) and Soil Charging Performance Factor (SCPF) were analysed respectively as a keys indicators of the ground changing temperature and the charging performances of the solar roof/collectors.

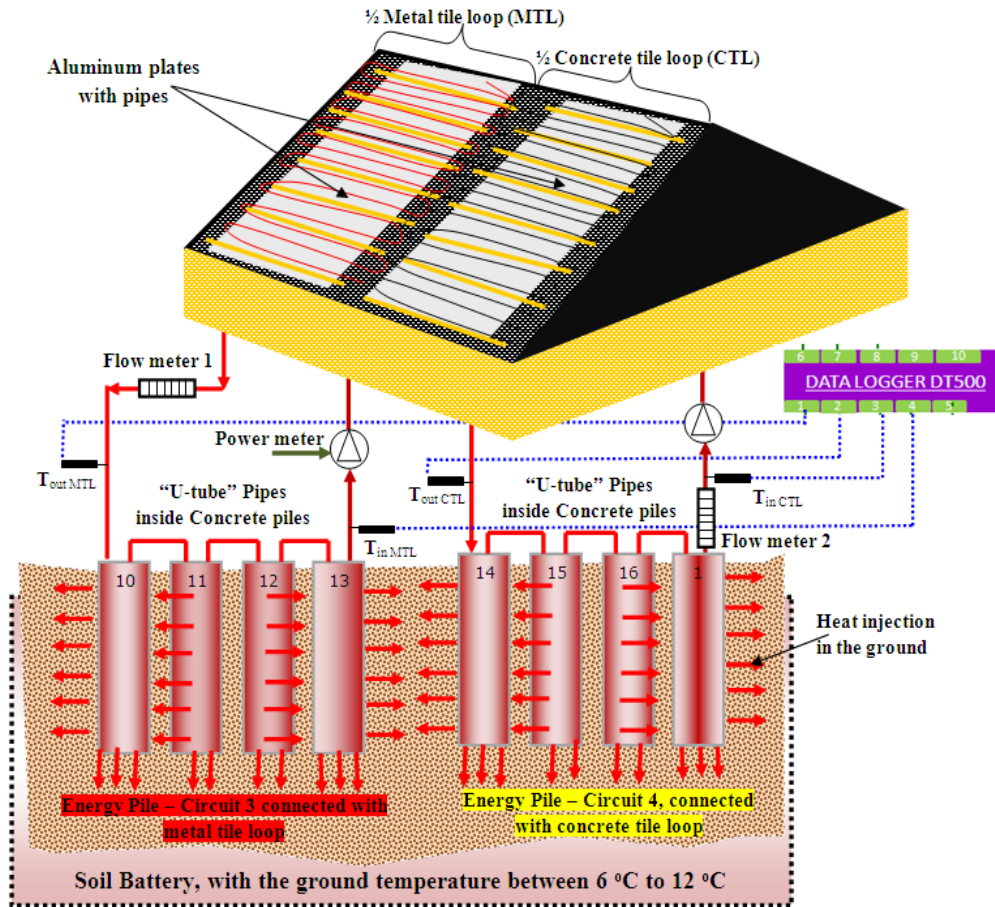


Figure 6.111: Schematic diagram of the Wiring of the Data Logger DT500

PWET was an instantaneous average of the flow and return water-glycol mixture temperatures to the energy piles from the solar roof/collectors; this average was calculated from recorded temperatures whilst the heat carrier fluid was circulating

by the pump within a single day. The PWET was a good indicator, since it provides a long term indication of the thermal changing of the ground surrounding the energy piles.

The PWET of the water from the piles at any time instant (t) was calculated as:

$$PWET = \text{average} (T_{\text{flowing in piles}} \text{ and } T_{\text{flowing out piles}}) \text{ at the time } (t)$$

SCPF was the instantaneous ratio of the heat injected in the ground through energy piles over the power consumption of the circulating pump at the same temps. Since the sun energy was free energy source and the only power consumption while generated heat to inject in the ground was the power of the circulating pump. The SCPF was the indicator used to control if the amount of power consumed by the circulating pump was greater that the power injected in the ground.

The SCPF of the solar roof/collector system at any time instant (t) was calculated

$$\text{as: } SCPF = \frac{\text{Heat injected in the soil at time } (t)}{\text{Power consumption by the pump at time } (t)} = \frac{Q_{\text{injected}}(t)}{W_{\text{pump}}(t)}$$

## 6.8 RESULTS AND DISCUSSION

The results of the short term monitoring to prove the concept of using the solar roof/collectors to charge the soil battery with the aim to maintain the ground temperature between 6°C -12°C and a constant COP of the heat pump system from the beginning and the end of the heating season. The figures below show the experimental results obtained during a testing period in July 2010, when the ambient temperatures were in the range between 13°C and 30°C. The daily charging cycle started at 7.00hrs and ended at 21.30 hrs, so the circulating pump ran for 14.30hrs per day. The system was tuned off during the nights for 10.30hrs.

### 6.8.1 Metal tiles roof/collector and energy piles, Circuit 3

*Figures 6.112 and 6.113* show the testing results obtained in 14 days on July 2010. *Figure 6.112* illustrates the heat gain from the metal roof/collector with time and its relation with the ambient air temperatures. The heat gained at the metal roof and injected to the ground was sensitive to the ambient air temperature. When the ambient temperature increased the heat gain at the metal also roofs/collectors increased, and were yielding between 0.3 kWh and 1.8kWh per day, when the ambient temperature fluctuated between 13°C and 31°C. On the *Figure 6.112*, there were short periods of negative heat flow at the start of a daily cycle, these must be because during the night, the roof and ground were cold and increase the thermal capacity of the ability of the roof to as heat sink to the environment, so in the morning, when the cycle started, most heat was dumped before the ambient and the roof temperatures increased. However those negatives heat flow were not serious to be investigated.

Figure 6.113 illustrates the Pile-Water-Equilibrium Temperature (PWET) for the metal tiles roof/collector, this was a good indicator of the pile temperature during the testing period and in the assumptions that the temperature of the soil was the same with that of the pile, PWET were between 10° C - 14° with corresponding The average Soil Charging Performance Factor (SCPF) of 11, so this was also very good indicator that since the energy collected from the sun was free, for 1 watt used by the circulating pump, an average of 11watts were injected to the ground.

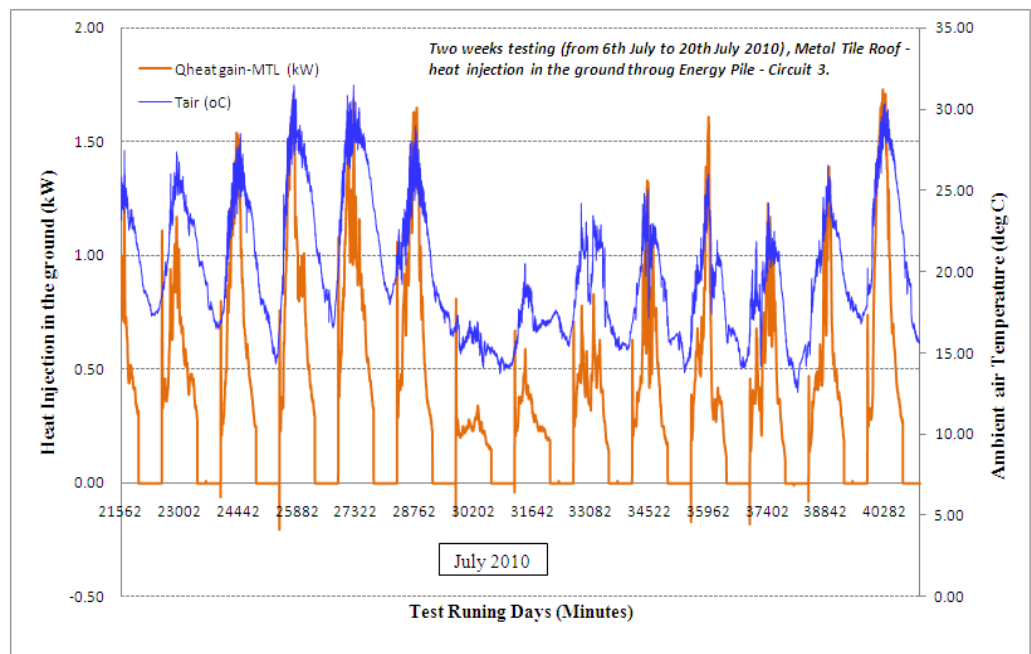
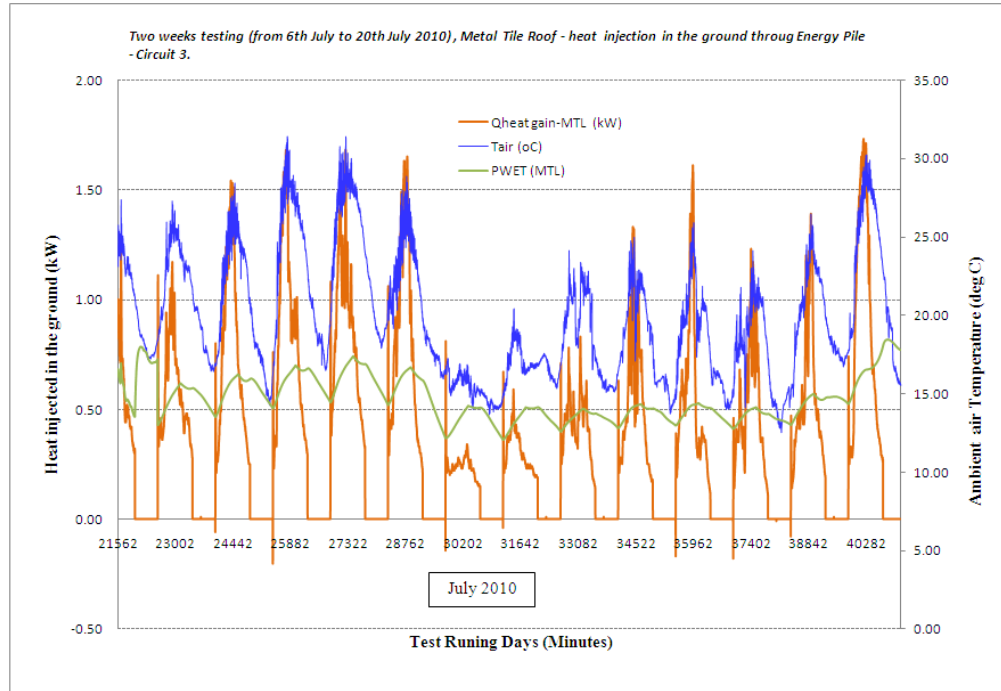


Figure 6. 112: The relation of energy injected in the ground, ambient air temperatures and the Time for the metal tile roof/collectors loop (Circuit 3)

It was instructive to look the thermal change of the pile and the surrounding ground around it, the PWET was a very good indicator for that observation, from the Figure 6.113, during the day when the circulating pump was on, the pile temperature increases and stabilises, at night when the circulating pump was off,

the heat dissipated in the soil, then the PWET dropped. The PWET was also sensitive to ambient temperatures; for the first 5 days around 28762 testing minutes, the ambient air temperature was greater than 25°C, from the Figure 6.113, it clear the starting point of the PWET of a daily cycle was different, and was gradually increased, so that was a good indication that the ground was getting warmer days by days, however when the ambient temperature dropped below 25°C, the yielding energy generate at the roof also dropped, and the previous heat stored rapidly dissipate in the soil and the PWET dropped. The PWET rapidly increased this was due to the ground sun gain, when the ambient temperature increased. The increased of the PWET was a very good indication of the heat increased of the surrounding ground around energy piles.



**Figure 6. 113:** The relation of energy injected in the ground and the PWET for metal tile roof/collectors loop (Circuit 3)

### 6.8.2 Concrete tiles roof/collector and energy piles, Circuit 4

Figures 6.114 and 6.115 show the experimental results of the circuit 4 obtained in 14 days on July 2010. It was informative to observe the concrete tile roof/collector heat gain profile for the testing period and the corresponding effect upon PWET and the SCPF.

For the concrete tiles roof/collectors, the heat gained and injected to the ground was sensitive to the ambient air temperature; as shown in the Figures 6.114; when the ambient air temperatures were fluctuated between 13°C and 31°C, the heat gains at the concrete roofs/collectors also changed and were yielding between 0.3 kWh and 1.8 kWh per day. The average SCPF was about 11.5, so this was also

very good indicator of the charging performance of the concrete solar roof/collectors.

It was expected the PWET to increase in the summer months due to solar radiation incident on the surrounding ground of the energy piles, would lead to a ground “heat recharge” in those months, these coupled with the solar roof/collectors heat injected to the ground. Spaced boreholes are inefficient because they have reduced surface area to the surroundings. But if the boreholes are charged with external supplied heat, the opposite is the case, as they ‘nurse’ their charge, reducing losses to the surroundings.

According to the results for concrete roofs/collectors, It is shown in the Figure 6.114 that when the average ambient air temperature was about 26°C, the PWET has increased over the testing time period between 21562 minutes (6<sup>th</sup> July 2010) and 28762 minutes (11<sup>th</sup> July 2010) and was about 13°C, which could be indicative of a heat gain of the surrounding ground, compared to the “undisturbed” far field which could be about 12°C, in summer at the same ambient temperature. Such increase in the PWET towards the end of the testing period of about 40282 minutes (on the 19<sup>th</sup> July 2010), from this short period of testing, it is reasonable to conclude that the solar concrete tiles collectors would be responsible for the temperature increase in the energy pile, particularly when the ambient temperature is greater than 25°C. Indeed in this short period of testing the PWET remained slightly above 9°C at all the time, even when the ambient temperature was dropping of about 12°C.

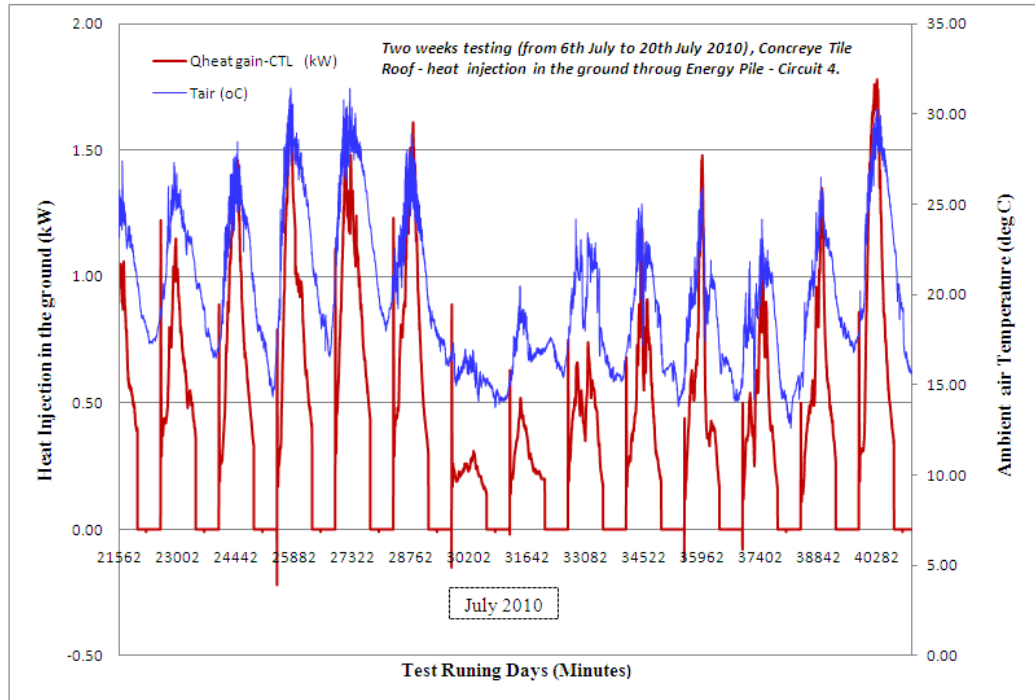


**Figure 6. 114:** The relation of energy injected in the ground, ambient air temperatures and the Time for the concrete tile roof/collectors loop (Circuit 4)

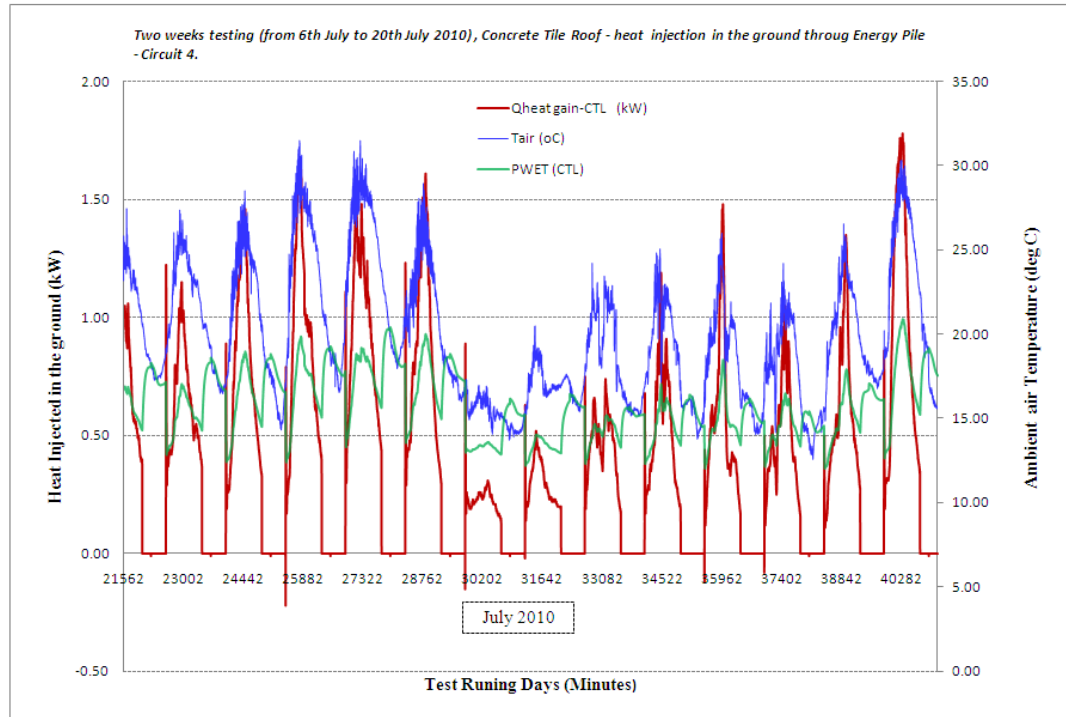


**Figure 6. 115:** The relation of energy injected in the ground and the PWET for concrete tile roof/collectors loop (Circuit 4)

Across the testing season around the time period of 29768 minutes (12<sup>th</sup> July 2010) and 29768 minutes (14<sup>th</sup> July 2010) the level of PWET significantly decreased but not less than 9°C before rises at the end of the testing period. This was results of the low ambient temperatures, and the increase of the PWET towards the end of the testing period was result of the warming of the surrounding ground due to high ambient temperatures.

### 6.8.3 Solar roofs/collectors temperature gain

Figure 6.116 illustrates how the temperature changes across each solar roof/collectors circuit and their corresponding PWET, and their relations with the

ambient temperature. An initial observation of the *Figure 6.116* reveals that heat gain at both roof types was not greater than 10°C, across the testing period. During the night, the heat dissipated in the ground, caused the temperature across the roofs to drop below 0°C. For comparison reason between the effect of concrete tile and metal tile on the PWET, both PWETs were plotted on the *Figure 6.116*, it is observed that the observation of these graphs shown that the concrete roof/collector perform better that the metal roof/collector. The metal roof has displays the greatest change in temperature across the testing period as would be expected, as this is highly influenced by the air temperature and solar radiation, in addition to the heat rejected in the environment during the night.

A point of interest in the observation was the profiles of the temperature difference for each type of solar roof/collectors; this comparison shows that the PWET was sensitive to the type of tiles. Concrete tile roof has a good thermal conductivity and thermal storage compare to the metal tile roof, which makes it an ideal medium as an energy absorber (heat exchanger), for the solar roof/collectors for ground heat recharging.

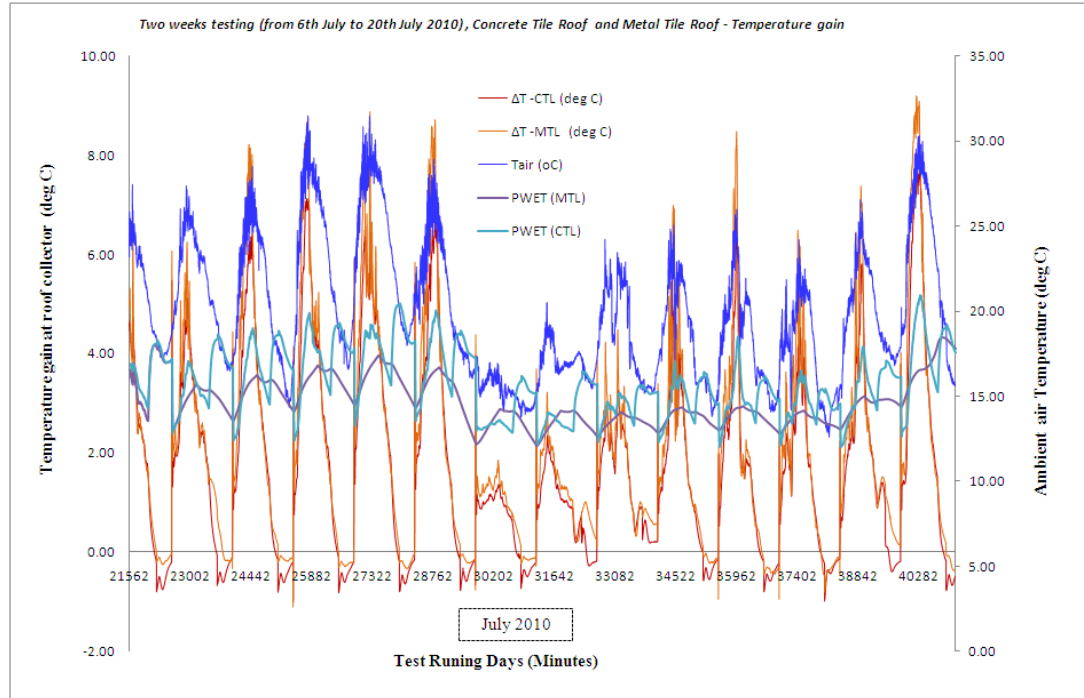


**Figure 6.116:** The relation of the temperature gain at the solar roofs/collectors with the ambient temperatures

#### 6.8.4 Solar roof/collectors Vs Reverse operation of a heat pump

Since one of the aims of this work was to investigate the practicability of charging the ground using a novel solar roof/collectors, also a reverse operation of a heat pump could provide both cooling and heat to recharge the ground during summer months, in the second case the ground acts as heat sink for the heat pump.

Therefore it is useful to compare the ground heat recharging by mean of the reverse heat pump and by mean of the novel solar roof/collectors during summer months. In the UK the reverse heat pump is not popular in the residential applications, also because of the UK climate, the cooling demand for residential are very little or close to zero. So it should not be possible to use a reverse heat

pump system to charge the ground; since the cooling requirement is not sufficient for providing the necessary ground heat recovery. This option could increase energy consumption and the CO<sup>2</sup> emission from heating system. However for the solar roof/collectors systems is also required electricity to power the circulating pump. But when compare both system the heat pump will consume more electricity, because of the high capacity of the compressor compare a circulating pump.

## **6.9 Conclusion Chapter 6**

This chapter has summarised the investigation on the practicability of charging the ground using a novel solar roof/collectors acting as a supplementary heat source to assist the quick heat recovery of the ground surrounding energy piles during summer months.

The solar roof/collectors for ground heat recharging under consideration was a installed on the south facing roof, which was split in two; one half (15.89 m<sup>2</sup>) was covered with a traditional concrete tile and other half also 15.89 m<sup>2</sup> was covered with a metal tile. Underneath the tiles, there were aluminum-plates with pipes for working fluid (water/glycol mixture). Working fluid was circulated through the pipes in the roof and to the energy-piles. The idea was to recharge the ground heat using the solar radiation and the warm air during hot days. For the experimental purpose, the concrete roof had one circuit and this was connected to 4 piles in the ground (circuit 4 of the energy-piles used by Wood et al (2008). The metal tile circuit was connected to the energy pile circuit 3 (see above paragraph 6.2.1).

Whilst the solar roof/collector was recharging the ground the heat pump was not running .i.e. there is only a circulation between the solar roof circuit and the energy-pile circuits.

For this experiment, the working fluid (water-glycol mixture) was circulating by means of Grundfos circulatory pump. The flow rates were respectively 0.0539 (l/s) and 0.0532 (l/s) for metal solar roof/collectors loop and for concrete solar roof/collector loop, and the associated Reynolds numbers of the pipes fluid flow were calculated to be respectively  $4156 \times 10^3 > 10^4$  and  $4101 \times 10^3 > 10^4$  for the metal roof loop and for the concrete roof loop as such the flows were considered to be full turbulent, which were the requirements for high heat transfer in the working fluid.

The preliminary findings, which illustrated the capabilities of the solar roofs/collectors system to assist a quick heat recovery of the ground during summer months have been summarised in the *Table 6.25* below:

**Table6. 25:** Summary results of two weeks testing from 6 July to 19 July 2010

Roof type and circuits	Average ambient air temperature during testing period (°C)	Average heat gain and injected a day (kWh)	Specific heat injection per linear meter of pile (W/m)	Wood (2009)	Percentage of ground heat recovery from the roof compare to the heat extracted in the heating season (%)	Average PWET (°C)	Average SCPF
				Specific heat extraction per linear meter of pile (W/m)			
<b>CTL</b>	21	0.64	15.94	26	61.31	12±3	11.5
<b>MTL</b>	21	0.60	15.10	26	58.10	12±2	11

It was informative to observe that, when the average ambient temperature was about 21°C, the specific heat injected per linear meter of piles by the two types of roofs were respectively representing 61.32% and 58.10% for concrete tiles roof/collector and metal tiles roof/collector of specific heat extracted per liner meter of pile during heating season. The average minimum and maximum Pile-Water-Equilibrium Temperature (PWET) were respectively 9.5° C - 15° C and 10° C - 14° for concrete tiles roof/collector and metal tiles roof/collector, these a good indicator of the pile temperature during the testing period. The average Soil Charging Performance Factor (SCPF) were respective 11.5 and 11 for concrete tiles roof/collector and metal tiles roof/collector, this was also very good indicator that since the energy collected from the sun was free, for 20 watt used by the circulating pump, an average of 220 watts were injected to the ground.

Concrete tile roof has a good thermal conductivity and thermal storage compare to the metal tile roof, which makes it an ideal medium as an energy absorber (heat exchanger), for the solar roof/collectors for ground heat recharging.

In the initial testing, the real time and diurnal benefits have been immediately realised. The results show that there are advantages with recharging the ground (soil battery); firstly this may increase seasonal performance of the heat pump if the lower soil temperature was maintained at 12°C; this also enables the heat pump to work closer to an expected constant coefficient of performance (COP) of 4.0 through the heating season.

In the UK, experimental and theoretical data using this type of configuration has not been reported. Using initial testing of data, the diurnal benefits have been immediately realised. The results show that there are advantages with recharging the ground (soil battery); firstly this may increase seasonal performance of the heat pump and allow maintaining the lower soil temperature between 7°C at 12°C. Therefore, there was no intention to raise the temperature of the soil – however the prevention of long term cooling around the energy piles should be expected. The benefits of the solar roofs/collectors – energy piles system will continue to be minatory during summer 2011 and summer 2012, and to investigate the inter-seasonal performances of the system, during winter the heat pump will also be investigated.

## **6.10 Further Works**

### **6.10.1 Renewable Heat for Ground Heat Recharge**

Further experimental work is required to investigate the effect of adding renewable heat system to an energy pile system. The idea is to produce heat with existing renewable energy technologies, such wind turbine; solar collector and PV (see *Figure 6.117*). Solar collectors absorb the solar energy, which heat the working fluid (Water and glycol) and that heat will then injected in ground via piles/heat rods to charge the soil battery. Wind turbine via electrical resistance using DC or AC current to generate heat and then store it in the soil battery through piles/Heat Rods, as shown in *Figures 6.116*, and *Figure 6.118*, and

Photovoltaic (PV) could also generate heat through resistance to charge a soil battery as presented in the *Figures 6.116*.

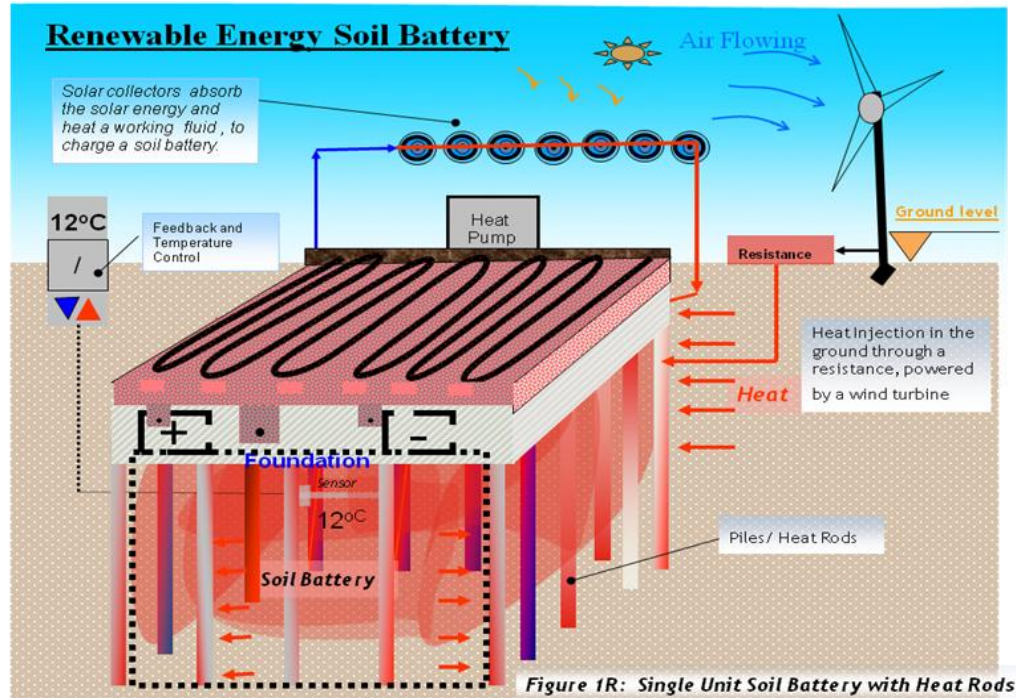


*Figure 6. 117: Renewable Heat Energy and Soil Battery Concept*

As far as the GSHP performance (COP) is concern, from the view of housing developers, a system with longevity in term of performance during heating season is required to be able to guarantee the heating system for year to come. In addition in order to guarantee the while deployment of ground source heat pump from 2016 to achieve higher standard of the Code for years to come; as the ground type varies greatly over short distances within the UK, any heat pump installation must have an ability to function in all grounds. It is therefore considered that renewable

heat will become an integral part of the residential ground source heat pump system including the residential energy pile ground source system.

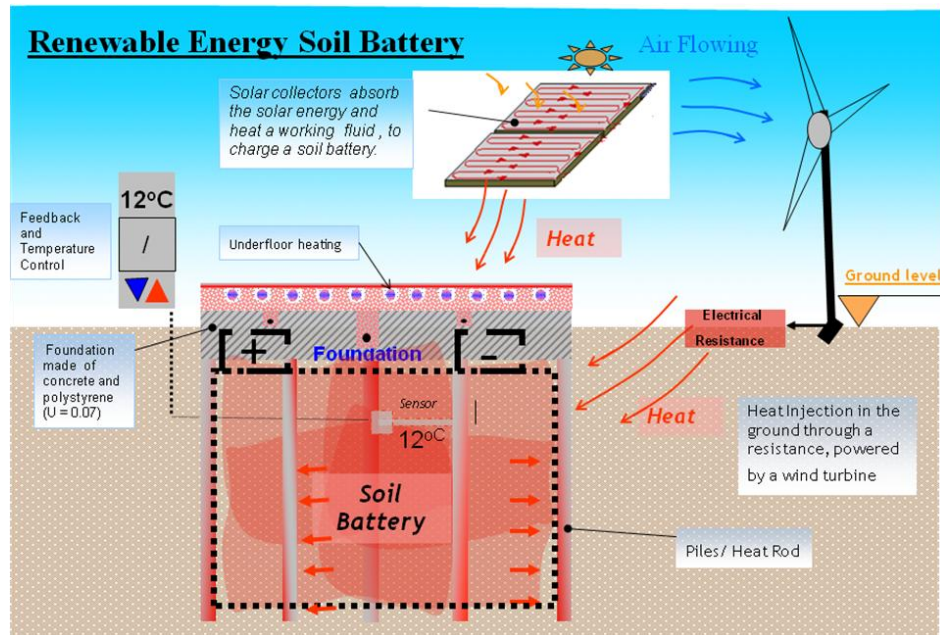


**Figure 6. 118:** Renewable Heat Energy and Soil Battery Concept in 2D

Further work is required to investigate each existing renewable energy technologies of their heat generation performance and construction techniques for their incorporation in existing building and new residential buildings. In addition renewable heat technologies need to be economically viable and also efficient enough to provide the necessary heat input.

In the case of urban areas where houses are crowded; further research is required to investigate the effect of multiple units of soil battery (see Figure 8.117). It is required that further modelling work could be performed to investigate the long term effect of the heat injected in the ground for multiple plots in one area. In this regard, the seasonal ground variation would need to be included as major variable

for the investigation. In addition it could also be informative to investigate the effect of heat generated from solar collectors, photovoltaic (PV) or wind turbine through resistance on multiple plot area, soil battery as shown in *Figures 8.117* below.

***Figure 6.119: Renewable Heat Energy and Soil Battery Concept in 2D for 10 Unit Developments***

Finally, further research is also needed for the urban application of solar roofs/collectors and sunboxes incorporation into urban architecture, to support the many heat pumps which will be installed in the future. Charging the ground for future low carbon homes have greatest potential, mostly when buildings are clustered and ground is shaded. It is considered that a mathematical model of the above systems are develop; with the use of this study's data for correlation and for providing confidence in the results of this work concerning solar roof/collector and solar-air panels combined with GSHP system or energy piles.

## **CHAPTER 7 - A FIELD TRIAL OF THE GROUND-SOURCE HEAT PUMP PERFORMANCE ENHANCED WITH THE EARTH CHARGING BY MEANS OF SOLAR -AIR COLLECTORS**

---

## 7. INTRODUCTION

The GSHP at high performance can supply in the long term space and domestic hot water heating for residential buildings. While ground is a convenient heat source for heat pump, it also suffers from a number of disadvantages which call for careful optimisation of heat pump design. (Rybach, 2000), and Trillat-Berdal, Souyri et al. (2006) state that the use of a geothermal heat pump with vertical borehole heat exchanger to heat buildings can create annual imbalance in the ground loads; and then the coefficient of performance of the heat pump decreases and consequently the installation gradually becomes less efficient.

The previous chapters (Chapter 2 and Chapter 6) explained that to avoid the ground load imbalances during a year or after long term heating cycle, 5 to 10 years; two solutions could be adopted; first by increasing the total length of the boreholes up to deep where the ground temperatures would undisturbed by the ambient air temperature and second by hybridizing the system or use a supplementary heat source linked to the vertical ground heat exchanger. Since the major drawback of the vertical borehole heat exchanger is the drilling cost, the first solution is not most economical, so the second solution have been consider and investigated in the Chapter 6 using small scale field testing on solar roof/collectors to charge the ground through energy piles.

This Chapter presents initial findings from a field trial of a hybridizing GSHP system that uses custom designed solar-air panels combined with the GSHP to

harvest free energy from the sun and warm air during summer months to charge the earth. This field trial aims to confirm the benefits of using supplementary heat to assist the ground heat recovery during summer months and its advantages on the COP during winter months. The system has been installed in a full size occupied detached two-storey house constructed in the city of Nottingham, UK.

## 7.1 THE FIELD TRIAL DESCRIPTION

### 7.1.1 The Building

The building used for this research was a full size occupied detached two-storey house, which was completed March 2007. The total floor area is 120 m<sup>2</sup>; the house is shown in *Figure 7.120*. The house was considered as a single zone building, with the room heating target of 21.5 °C and the DHW target of 52 °C. The solar-air-panels were installed in March 2010; the house was constructed using fully-filled cavity walls with 100mm insulation and thermal break double glazing windows. The roof is concrete tiled ridge-roofed with ample loft space for storage. The Levels of insulation are good by UK standards. The U-values of the main building elements are summarised in the *Table 7.26*. The internal block leaves and partitions are dense concrete block, and the upper floor has a sand layer, so these elements provide substantial thermal storage. The house does not require summer cooling. Heat is distributed by under-floor heating on the concrete ground floor and sand-filled timber first floor. The family occupying the house consists of two permanent adults, and two grown up children regularly visiting for short stays.

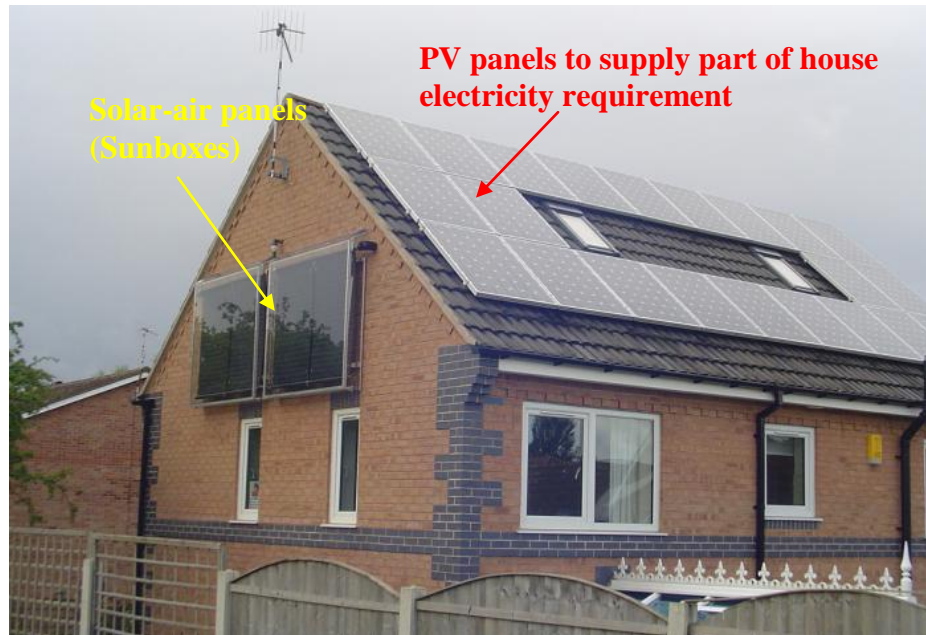


*Figure 7.120: Case Study House with the SUNBOXES-Ground Hybrid Source Heat Pump (13% DHW and 87 % space heating)*

The house has the largest rooftop photovoltaic array that a small house can have under the tariff, 4kW from 22 Sharp NU180 solar panels. These are separately metered. Being purely electrical, they have no heating function, and have zero interference in the thermal research with the GSHP and Solar-air collector (Sunboxes).

**Table 7. 26: Building construction materials**

Building Elements	Materials	U-value
External wall	Concrete block and brick	0.4W/m <sup>2</sup> C
Glazing	24 mm double glazing	1.7 W/m <sup>2</sup> C
Internal partition	Plasterboard and insulation	0.71W/m <sup>2</sup> C
Roof construction	Concrete tiles	4.298m <sup>2</sup> C

### 7.1.2 The heating system

The heating system consists of water -to- water heat pump with 165 litre internal DHW storage (See Figure 7.121). The heating system was sized with the expectation of room temperature to be 20°C when the outside temperature was -2°C. The pump and borehole sizing is in accordance with manufacturers' recommendations (Enerfina, 2008). The annual heating loads were estimated by the manufacturer to be 14,600kWh/annum, including DHW, of which 9,800 kWh was estimated to be drawn from the ground (Nicholson-Cole & Wood, 2009). The heat pump was expected to be able to provide the entire annual heating, with 74% for space-heating and 26% for Domestic Hot Water (DHW). The heat pump was designed / sized to deliver a flow temperature capable of heating the under-floor system as shown diagrammatically in the *Figure 7.122*.

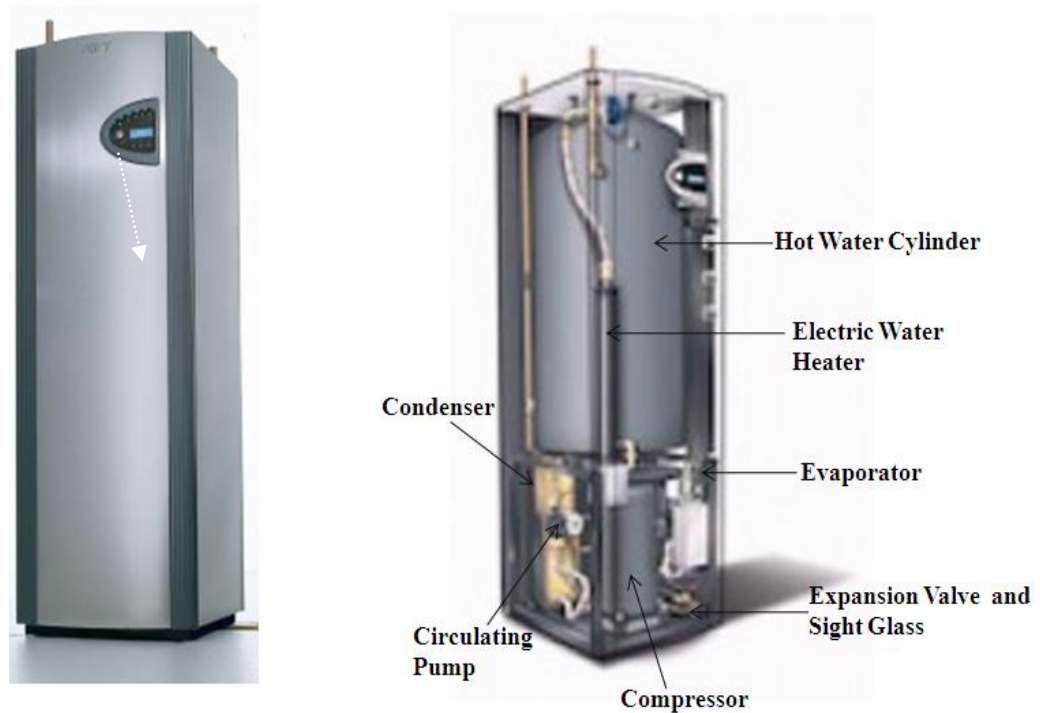


*Figure 7. 121: Hot Water Tank Integrated Heat Pump (Enerfina, 2008)*

The refrigerant used was R407C, which has a low global warming potential and no ozone depletion or chlorine. The solar-air sunboxes were positioned vertically on the South wall of the house (See Figure 7.120& 7.122). The ground heat exchanger was a vertical loop pipe (PE 40/36mm), about 200 m long, buried in twin boreholes (Figure 7.123) to a nominal depth of 48 metres below the ground level. The pipe loop contains antifreeze solution (glycol-water mixture), to prevent freezing; the glycol is an environmentally friendly mono-propylene glycol. The soil around the borehole is dense marl, a mixture of clay and limestone fragments all the way down. The heat injected in the ground through the boreholes disperses into the soil surrounding the boreholes as shown in the

Figure 7.121. Heat from the heat pump was delivered either to domestic hot water or to underfloor heating for space heating. The DHW was well insulated a jacket around a mains-pressured cylinder (capacity 185 litre) which has an electric heater as back-up.

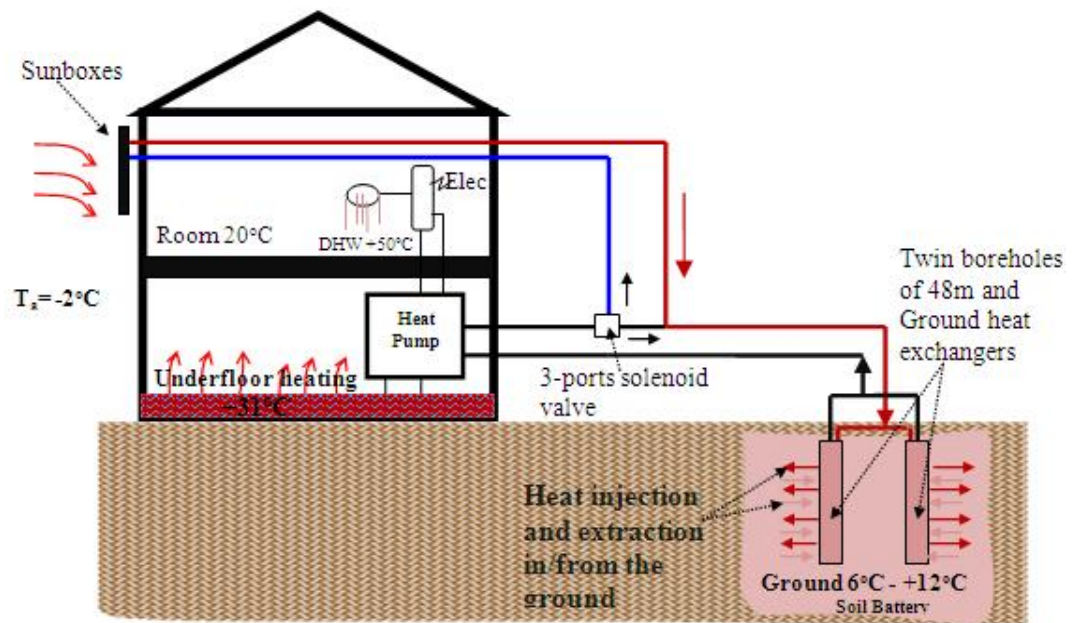


**Figure 7.122:** The basic schematic diagram of the field trial, the House with the Sunboxes-combined with the GSHP

When conditions were right, the water-glycol mixture from the heat pumps ground loop was pumped rapidly through the solar-air panel (sunboxes) on the south wall. Two controllers managed the process: the GSHP's management system balances air and liquid temperatures; a differential thermostat activates the sunboxes when air temperatures or delta-T are high, switching the liquid flow through a 3-port solenoid valve (see Figure 7.122). Thus, the sunboxes can support the heat pump directly, making it in effect, a 'Solar-Air-Ground Source' Heat Pump (SAGS-HP), tricking its controller into completing each heating cycle more quickly with a

reduced refrigeration workload. When the heat pump was satisfied and ‘sleeping’, the sunboxes continue to circulate liquid slowly, charging the ground with heat for later use. In this experiment, the soil battery was 48 metres deep, approx 22654 m<sup>3</sup> of marl.



*Figure 7. 123: Drilling of the boreholes to a nominal depth of 48 metres*

### **7.1.3 Solar –air Source Panels (Sunboxes) on the south wall of the house**

The practical purpose of having solar-air collectors, so called Sunboxes, on the south- facing wall was to capture heat to charge the ground using warm air and direct Sunlight.

The sunboxes were 1 cubic metre of air space in a pair of microclimatic glazed boxes containing 4 square meters (m<sup>2</sup>) of black thermal polypropylene collectors (Figure 7.124), enclosed in boxes of 6 mm polycarbonate with light aluminium framing. They work on the principle of a small Solarium, building up warmth

inside (from sun or a bright sky), and avoiding wind-chill. The black collectors were originally swimming pool panels. The front panels of the sunboxes were top-hung hinged for maintenance access only. The sunbox materials were corrosion free, so maintenance access was merely for adding thermal sensors or attending to leaks. Being vertical, they worked effectively even at low sun angles, in equinox and winter.

The polycarbonate boxes protected the black collector panels from formation of frost and also helped to keep the panels at a fair temperature at any ambient conditions, so after the ground heat exchanger provided heat to heat pump, the glycol temperature drops so the sunboxes assisted to warm the glycol before the next heat cycle. The Sunboxes do not require direct sunshine; a cloudy bright sky was sufficient to warm air in the sunboxes.

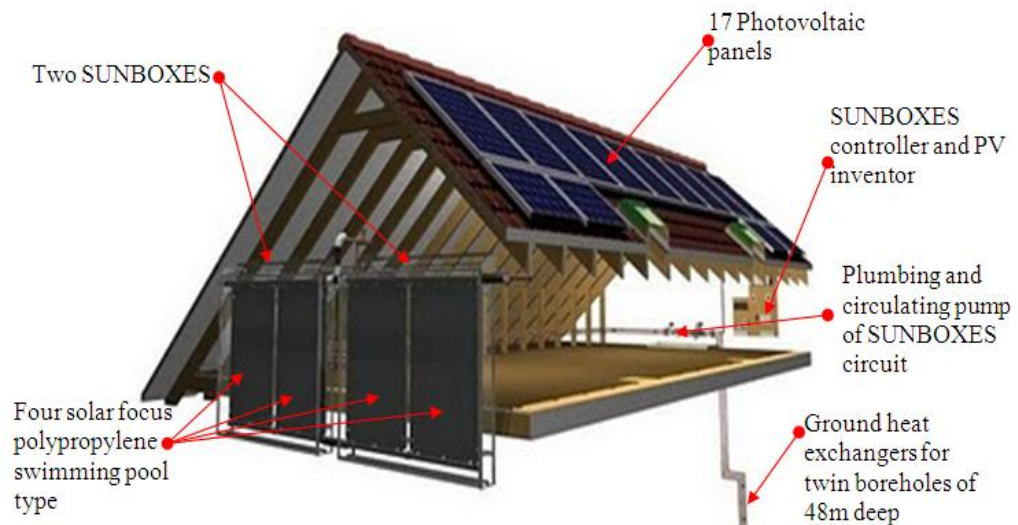


**Figure 7. 124:** Concept diagram of the sunboxes on the south wall

#### 7.1.4 SAGS-HP Operation Modes

The operating modes of the SAGS-HP change according to the temperature difference between the Sunboxes' air temperature ( $T_{sb\ air}$ ) and the ground heat exchanger inlet temperature ( $T_{g1}$ ). In fact, when the temperature difference between the Sunboxes' air and the inlet glycol of the ground heat exchanger is equal or greater than  $5\ ^{\text{deg}}\text{C}$  the Sunboxes' circuit goes on, and when the temperature difference is less than  $5\ ^{\text{deg}}\text{C}$ , it went off. The Hysteresis was  $1.0\ ^{\text{deg}}\text{C}$ , to avoid the system 'hunting'. In winter, equinox and summer times, depending on the sunbox air temperature, the following working modes of the SAGS-HP are possible:

**Mode 1: Ground source only:** When  $(T_{sb\ air} - T_{g1}) < 5\ ^{\text{deg}}\text{C}$  and Heat pump on - too cold for Sunboxes to work. The circulating pump Cp2 is active, ground heat exchangers only provided heat source to the condenser of the heat pump for space and domestic hot water heating. In this mode the pump Cp3 goes on for underfloor heating circulation, and mains pressure enables domestic hot water distribution (see Figure 7.125), and given that the temperatures of air is too cold for Sunboxes to work, then Cp1 goes off.

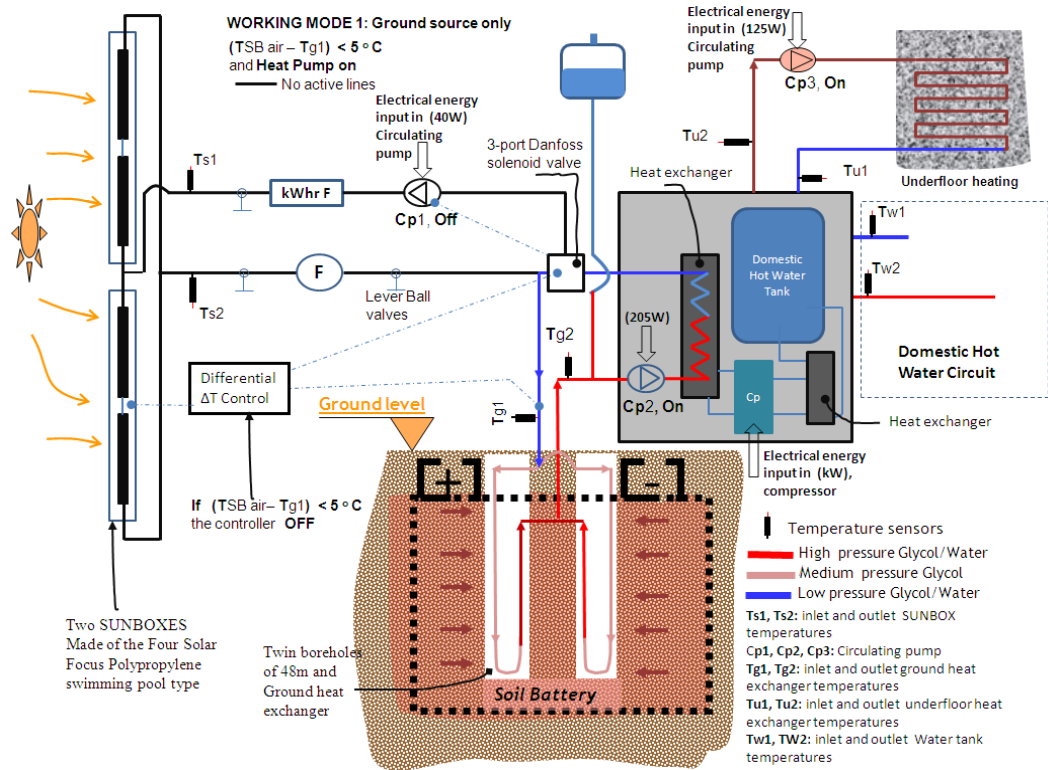
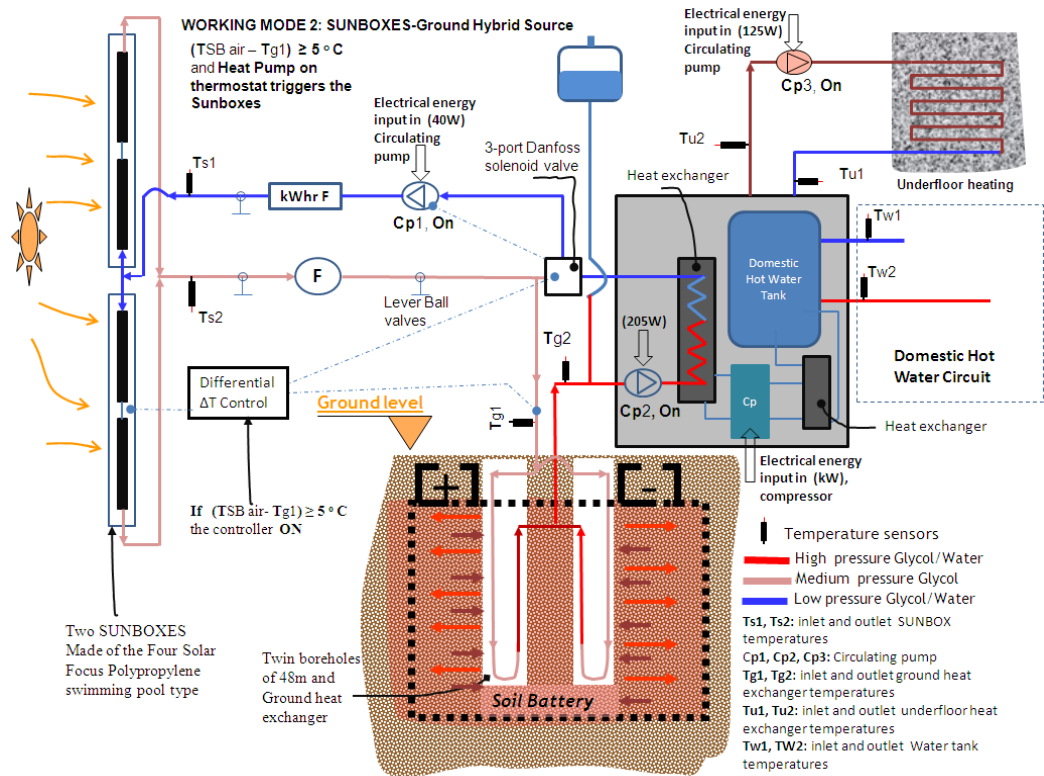


Figure 7. 125: Schematic diagram of the GSHP's performance testing with SUNBOXES in working Mode 1, Ground source only

**Mode 2: SUNBOXES-Ground Hybrid Source:** When  $(T_{sb\ air} - T_{g1}) \geq 5^{\text{deg}}\text{C}$  and Heat pump is on – thermostat triggers the sunboxes. The circulating pumps Cp1, Cp2 and Cp3 were all activated; the sunboxes inject heat first into the ground then to the heat pump – whose source thus become a hybrid of Sunboxes heat and Ground heat. In this mode Cp1 and Cp2 working together send ALL the liquid from the ground up to and through the sunboxes at approx 30 liters/min (see Figure 7.126). This flow rate was rapid, consequently preventing any chilling effect in the ground loop. Meanwhile Cp3 continued to pump the underfloor heating circuit.



**Figure 7. 126:** Schematic diagram of the GSHP's performance testing in working Mode 2, SUNBOXES-Ground Hybrid Source

**Mode 3: Charging, heat injection in the ground only:** When  $(T_{sb\ air} - T_{g1}) \geq 5^{\circ}C$  and Heat pump is off – warm air or sunny conditions. The circulating pumps Cp2 and Cp3 were off. Only circulating pump Cp1 was on for the Sunboxes, at slow mass flow rate of 0.1 kg/s (with photovoltaic power) (see Figure 7.127). In this mode, the heat injected into the ground restored heat used in the previous heating cycles (i.e. prevents chilling), and stores surplus for long term used.

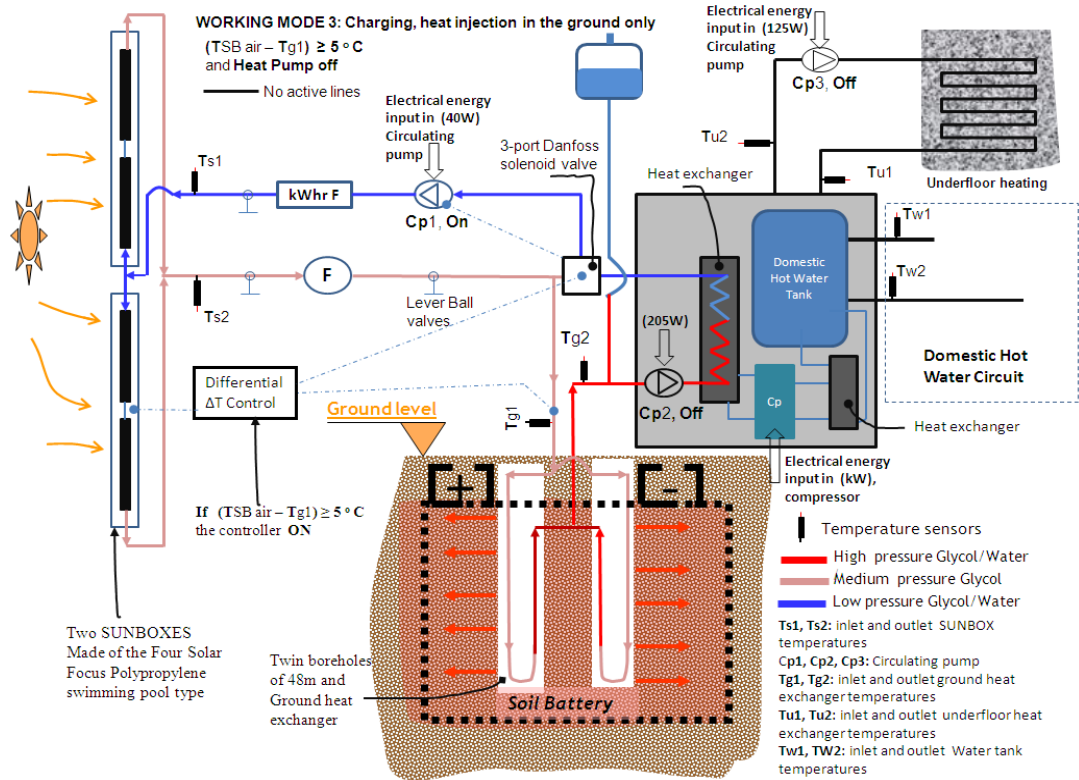


Figure 7.127: Schematic diagram of the GSHP's performance testing with SUNBOXES in working Mode 3, Charging

### 7.1.5 Modes and Status Control

In order to identify and control the different modes (1, 2 and 3) the AKO 14732 Differential 2-channel programmable thermostat was used. The thermostat controlled the 5<sup>deg</sup>C difference between the Sunbox air temperature and the ground loop temp. Omron relays indicated On/Off conditions of Cp1 and Cp3 to the data logger, and a digital clock display allowed recording how long the system was running for.

## 7.2 Method

During summer months, since space heating was not required, the heat pump was off most hours a day and was running for a very short time for domestic hot water heating only. In the month of May 2010, a short monitoring method was first applied to validate the concept as following: - the system was run for three days with the sunbox system loop ON, and then run other three days with the sunbox system circuit turned OFF. The performances were only compared for the periods where the average weather conditions were roughly equivalent. After the concept was validated, a long term (July 2010– October 2010) monitoring of the heat injection in ground was then undertaken. The monitoring system was set up to measure during charging the energy injected in the ground, the energy output from ground collector, the Ground-Water-Equilibrium Temperature (GWET) and Soil Charging Performance Factor (SCPF) were analysed respectively as a keys indicators of the ground changing temperature and the charging performances of the solar air collectors.

In November, when the ambient temperature drops and the space and water heating is needed, the heat pump is then run for more hours compared to summer months. The efficiency of the heat pump system, the energy delivered to the space and domestic hot water systems and the total energy consumed by the compressor of the heat pump for space and water heating is recorded. In addition, temperatures at various points of the heating system and the status of the heat pump and Sunbox loops are monitored to provide information on the details of operation of the

sunboxes and the heat pump. Also for assessment purpose the house is considered as a single zone with target room air temperature of 21.5°C, and the outside air temperature and the sun radiations are also recorded. The data-logger (DT500) is used to record and to store data, which is then transferred to Excel spreadsheet for examination.

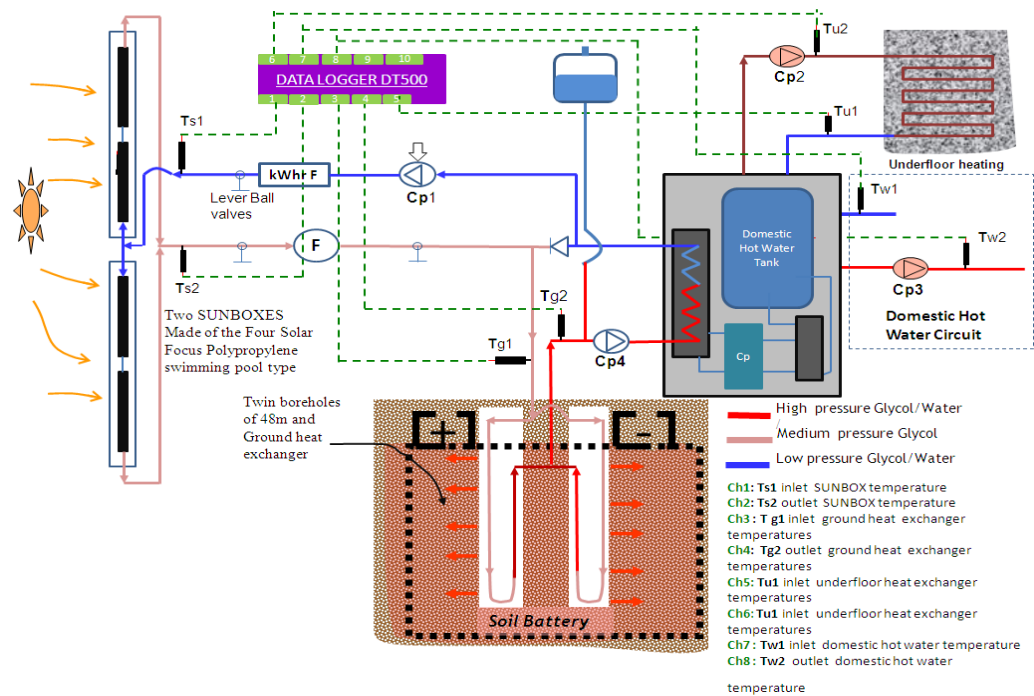


Figure 7.128: Schematic diagram of the Wiring of the Data Logger DT500

### 7.2.1 Measured Parameters

From the Figure 7.128, the data logger was used to measure the following data:

Temperatures: Channel (Ch) Ch1- Temperature of the refrigerant inlet solar collector ( $T_{sci}$ ), Ch2- Temperature of the refrigerant at the compressor inlet ( $T_{ci}$ ), Ch3- Temperature of the refrigerant at the compressor outlet ( $T_{co}$ ), Ch4-

Temperature of the refrigerant at heat exchanger outlet ( $T_{\text{exro}}$ ), Ch5- Supply water temperature to the radiator ( $T_{\text{ri}}$ ), Ch6-Temperature of the water at heat exchanger inlet ( $T_{\text{exwi}}$ ), Ch7- Return water temperature from the radiator ( $T_{\text{ro}}$ ), Ch8- Temperature of the water at the top part of the heat storage tank ( $T_{\text{hsup}}$ ), and Ch9- Temperature of the water at the bottom part of the heat storage tank ( $T_{\text{hsdown}}$ ). In addition power consumption was measured at the following points, at the compressor ( $W_c$ ), and at the water circulating pumps ( $W_{\text{cp}}$ ). The mass flow rates on the water/glycol circuit were recorded.

### 7.3 RESULTS AND DISCUSSION

The results of the short term monitoring to prove the concept of using the solar-air panels to charge the soil battery with the aim to increase the COP or maintain constant the COP of the heat pump throughout winter are summarised in this section. The figures below show the experimental results obtained during a spring season days when the ambient evening temperatures were in the range between 10°C and 12°C. The temperature of the Domestic Hot Water (DHW) was kept constant at 51°C.

#### 7.3.1 SHORT TERM MONITORING

The *Figures 7.129 and 7.130* show experimental data of Mode 3; the amount of heat injected in the ground was determined by the sunbox air temperatures. When the warm air temperature in the sunbox was greater temperature than the ambient

temperature say, at 31°C the amount of heat injected in the ground was about 142Wh. From *Figure 7.129* it was clear that the heat injected was greater than the consumption power of the circulating pump 30W, indeed in this short period of testing the GWET remained slightly above 9°C at all the time, even when the ambient temperature dropped of about 12°C. It was expected the GWET to increased in the summer months due to solar radiation incident on the surrounding house. The average Soil Charging Performance Factor (SCPF) was about 3.50, this was also a very good indicator that since the energy collected from the sun was free, for illustration purpose, 1 watt used by the circulating pump, an average of 3.5watts were injected to the ground, in addition the power to circulate the working fluid (water-glycol mixture) in the solar-air panel loop was from the photovoltaic on the roof. However the period was too short to notice significant change in the ground temperature. From *Figure 7.129*, the generated heat was lower than the injected heat because the power of the circulating pump contributed to the total amount of heat injected in the ground.

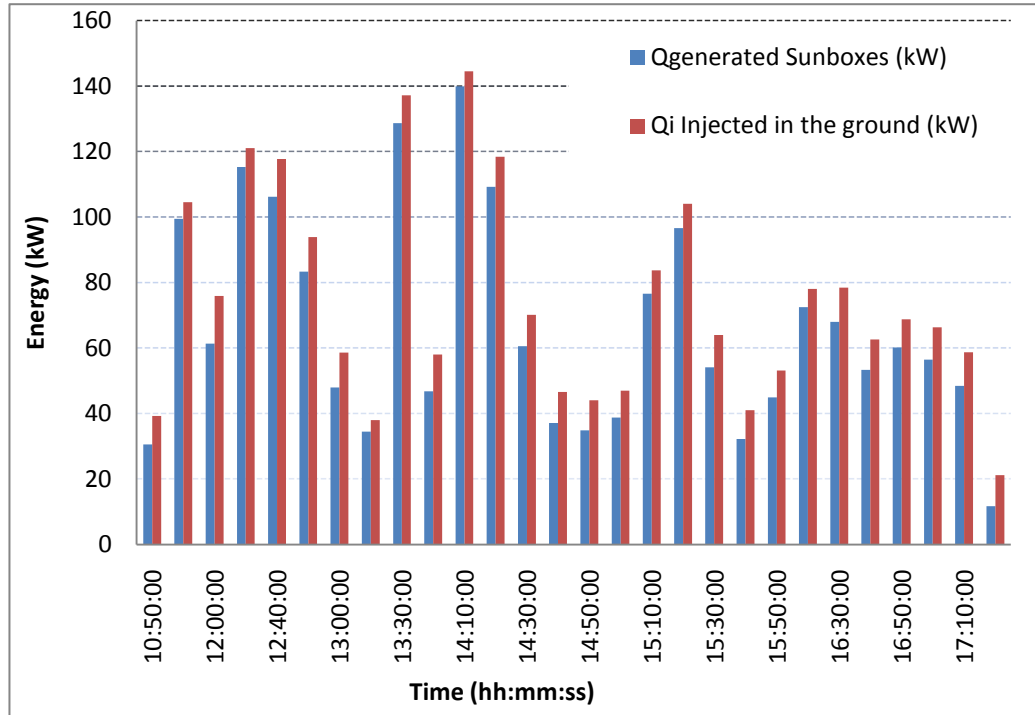


Figure 7.129: The relation of energy injected in the ground and the time

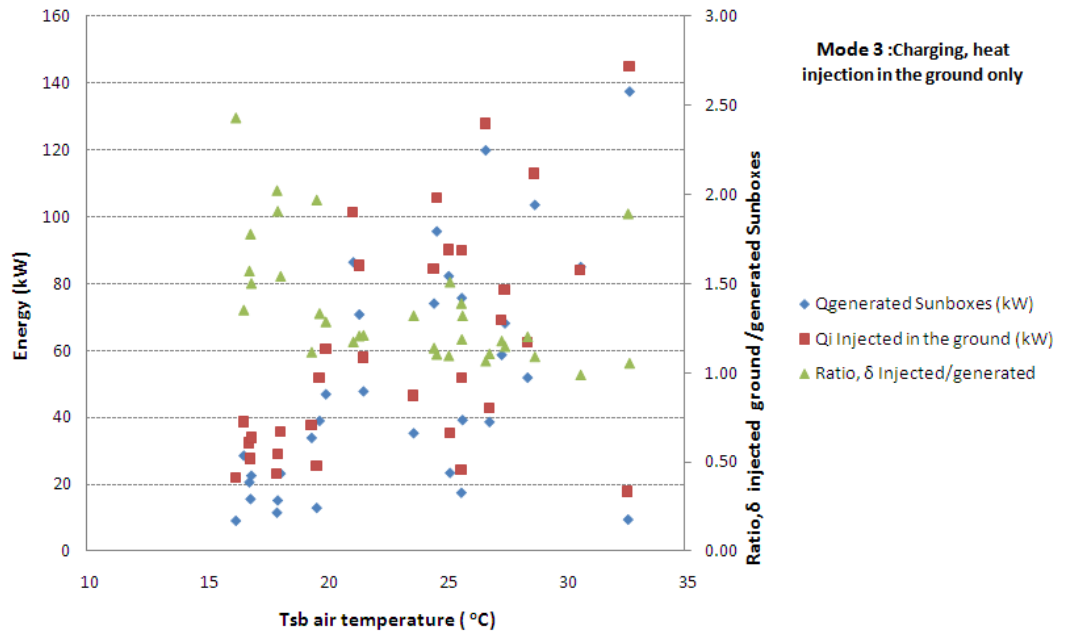


Figure 7.130: The relation of energy injected in the ground and Sunboxe air temperatures

### 7.3.2 LONG TERM MONITORING

The results of the long term monitoring to investigate the amount of heat injected to the ground during from July 2010 to October 2010 and their effect of the GWET and consequently to the ground temperature have been reported in this section (summarised in Table 7.27). The COP of the Ground source heat pump in month of November 2010 was also summarised in this section.

#### 7.3.2.1 Method used to measure the deep ground temperature

While the ground heat exchangers were putting in the ground, K-type thermocouples were provided to attach to water/glycol loops, so they could be used to monitor the deep ground temperature around the boreholes. However, with the work on the heat exchangers, the sensors might have been broken so during the experiment they were not working. So in order to assess the deep ground temperature during the testing period, the following method was applied: in the evening after the testing period (From 9 am to 10pm), so around 10pm each day after the last heating cycle of the heat pump. The heat pump was then stop for 4 hours; the time for the heat around the boreholes to dissipate in the ground then settle. The GSHP water/glycol circulating pump was then ran for about 20 minutes, the time necessary for the water/glycol of the ground heat exchanger loops to mixing and have a consistent temperature. The temperature at this stage was considering being a reasonable representation of the deep ground temperature around the borehole of that day. In this case after one year ground charging using

solar-air collector describe in the previous sections, the deep temperature was 11.3°C. (see Figure 7.131) and was far higher than expected because the last a small amount of sunshine during the year, followed by days of low fog and cloud with periods of drizzle; however the solar-collector was seem to get quite a lot of sun energy due to sunny days in February and March 2010. The usual springtime drop of ground temperature occur, as presented 7.12, the GWET drop, and when the sun came early enough, this prevent frosting to occur penetrate the ground (see Figure 7.132).

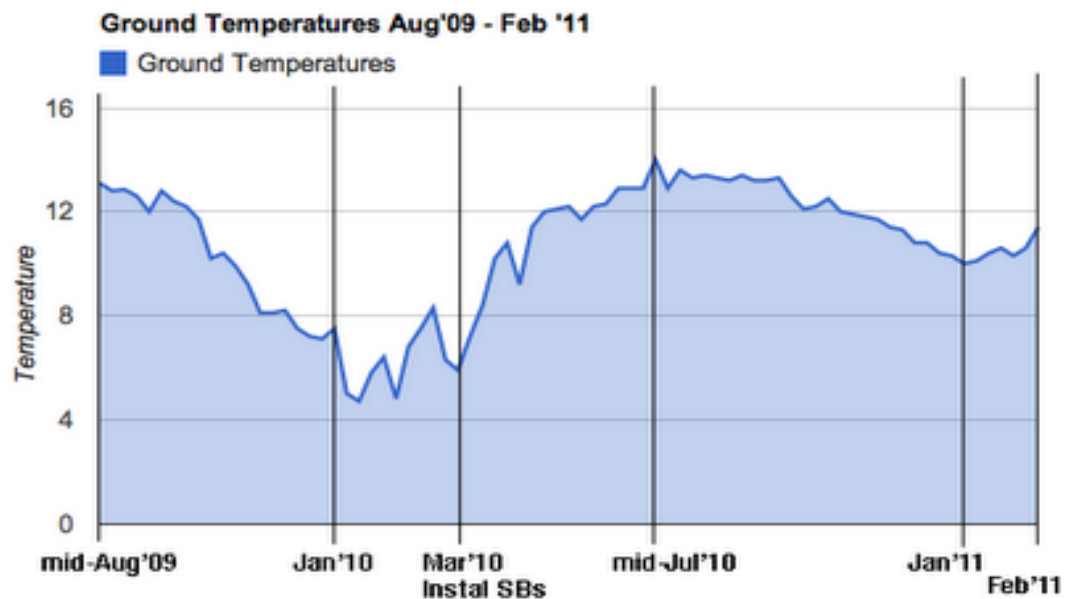


**Figure 7.131:** *The relation between the energy gain at the evaporator, COP and the temperature of glycol /water at the evaporator*

It was informative to compare two years reading using the same method of reading. Last year results (February 2010) as shown in Figure 7.131, the average deep ground temperatures was 6.8°C, and for this year (February 2011) the average deep ground temperatures was 11.4°C. it might because the spring 2010

was cooler than the 2011 one. Also the sunboxes were installed in mid March 2010; these results were useful, because it shown that the ground around the borehole quickly recovered after installed the solar-air collector; and from Figure 7.131 the ground temperature was pretty stable around 12°C between June 2010 and January 2011. These results were informative for the long term vision of the temperature around the boreholes. After the solar-air collector was installed it contributed to maintain a consistent warmest temperature around the boreholes (see Figure 7.131), the temperature of the ground during the heating season in 2011 did not drop significantly compare to 2010; this might be because 2011 winter was warmer compare to 2010, so it caused the temperature around the boreholes to rise, since the rate of heat extraction was reduced. Further thoroughly investigation is needed to confirm these results.

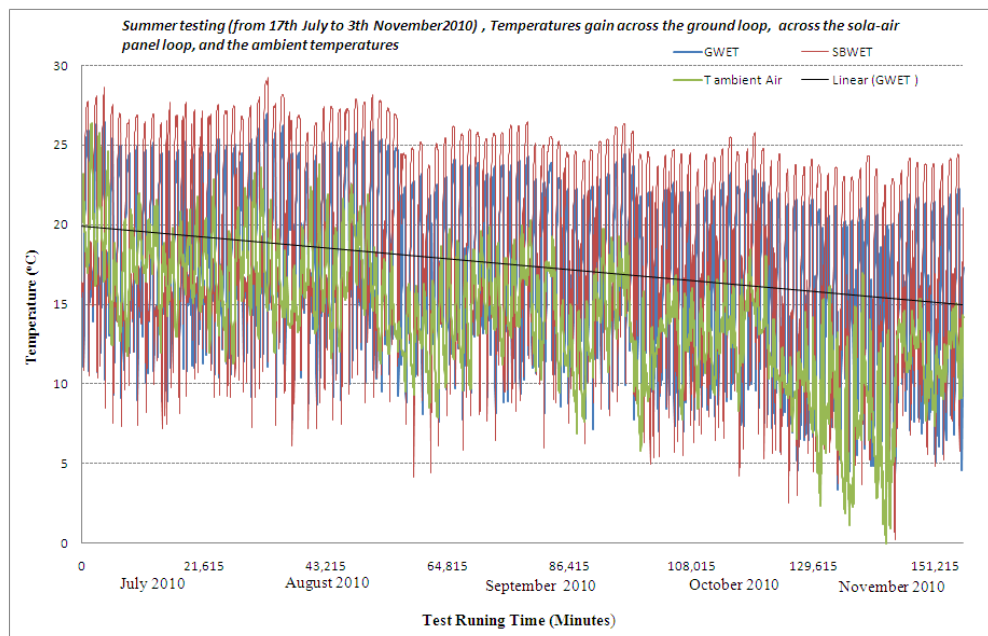


**Figure 7.132:** The relation between the energy gain at the evaporator, COP and the temperature of glycol /water at the evaporator.

Figure 7.132 illustrates how the temperature changes across solar-air collector's circuit (SBWET) and their corresponding GWET, and their relations with the ambient temperature. An initial observation of the *Figure 7.132* reveals that heat gain at the collector was not greater than 10°C, across the testing period. During the night, the heat dissipated in the ground, caused the temperature across the collector to drop below 7°C some days. For comparison reason between the temperature gained at the collector and temperature injected in the ground, both GWET and SBWET were plotted on the *Figure 7.132*, the observation of these graphs shown that the temperature injected in the ground was lower than the generated one, this was due to fact the water/glycol circulated faster than expected so the heat at the ground level did not have the time to dissipate in the ground. The solar collector has displays the greatest change in temperature across the testing period as would be expected, as this is highly influenced by the air temperature and solar radiation, in addition to the heat rejected in the environment during the night.

### **7.3.2.2 In the Case 2, Sunboxes is Off and the heat pump on**

The experimental results obtained for 14 days testing in winter is summarized in the Table 7.27 below, when the Sunboxes were off. The glycol/water temperature is between -6°C and 12°C and the COP reached a value between 3 and 6.4. *Figures 7.133* shows experimental results in Mode 2; Sunboxes and ground loop circulating pumps are all activated; consequently increasing the flow speed of the

Glycol/water passing through the Sunboxes and do not allow the cold glycol to collect enough heat from the Sunboxes. The degree of warm glycol/water at the exit of the solar-air panels was less than 10°C. In all cases of the hybrid of Sunboxes and Ground heat sources the COP was between 1.49 and 5.24. The faster flow was actually an advantage, since it improved performance by increasing turbulence in the panels and clearing ‘dead-spots’ by distributing liquid more widely.

The COP, energy gain at the condenser and evaporator were affected by the outside ambient temperature as expected, consequently, the water/glycol temperature at the evaporator. When the glycol temperature at the evaporator inlet was about 17°C at 10:30, the heat gain respectively at the condenser was 4020Wh and the COP reached a value of about 4.20. In all cases in Mode 1 the variation of the power consumptions (Figure 7.123) and the COP with time and the ambient air temperature were large. COP was between 1.53 and 5.4 (Table 7.27).

**Table 7. 27:** Summary of the experimental results

Date	Running time (hh:mm)	Heat pump Power consumption (W)	T <sub>average ambient air temperature</sub>	COP <sub>ave</sub> range	Comment
24/11/2010	11:54-22:20	1976	4.24	2.57	
25/11/2010	09:00 - 22:08	2050	1.67	2.54	
26/11/2010	09:00-20:48	2004	-0.68	1.34	
27/11/2010	09:00 - 21:16	2037	-1.71	2.30	
28/11/2010	09:00-20:52	2085	-5.45	2.37	
29/11/2010	09:00 - 21:00	2150	0.25	1.71	
30/11/2010	09:00 - 21:00	2185	-1.21	1.96	
01/12/2010	09:00 - 22:05	2089	-1.56	2.12	
02/12/2010	07:54-22:20	2101	-1.68	2.96	
03/12/2010	07:00-23:50	2123	-6.45	4.68	
04/12/2010	09:00 - 22:20	1966	0.78	3.80	
05/12/2010	07:00-20:40	2073	-1.57	4.32	
06/12/2010	09:00-22:32	2177	-7.48	3.97	
07/12/2010	08:12-22:06	2349	-12.10	4.85	Highest COP with the lowest outside ambient temperature
08/12/2010	08:12-21:40	2111	-1.77	1.94	
09/12/2010	08:12-21:00	2285	2.02	3.53	

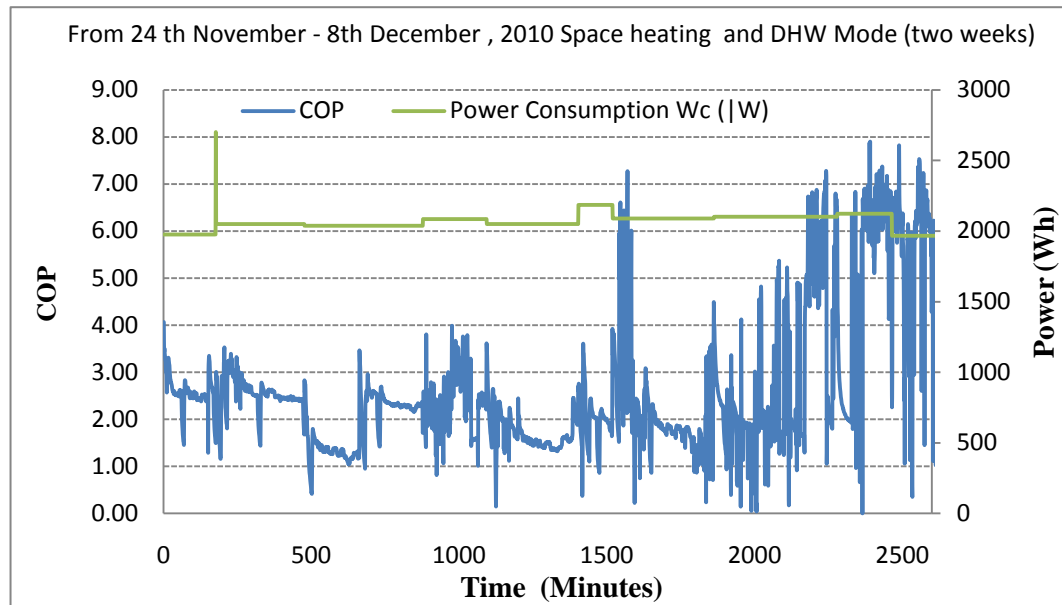


**Figure 7. 133:** The relation between the COP and the compressor power consumption with time in winter.

Spaced boreholes are inefficient because they have reduced surface area to the surroundings. But if the boreholes are charged with external supplied heat, such as it is the case for this experiment, the opposite is the case, as they ‘nurse’ their charge, reducing losses to the surroundings. That could explain the high COP when the outside temperature was at its lowest value.

According to the results in Mode 3, the amount of heat injected in the ground may have some effect in the winter when the ambient temperature is low. However during the summer generation, the amount of heat injected in the ground increased, but this can be allocated to the COP of 4.85, since there are some days in which the COP is relatively low. This required further investigation, with accurate data recording and consistence assessment.

## 7.4 Conclusion Chapter 7

This chapter has summarised the performance monitoring of Solar-Air thermal panels acting as a supplementary source to a Ground Source Heat Pump (GSHP). In the UK, experimental and theoretical data using this type of configuration has not been reported to the best of the author's knowledge. Given a possibility to use shorter boreholes and higher heat extraction from the ground, solar-air thermal panels has been economically combined with the GSHP; an experimental system has been installed on a full size occupied detached two-storey house in the city of Nottingham, UK. The south-facing solar-air panels collected heat on sunny days, bright-sky, and air warmth even during summer nights to warm the glycol/water. The heated glycol/water is sent directly to the borehole then to the GSHP for immediate needs (real-time), and surplus heat is retained the same day (diurnally) during winter and equinox. The solar-air panels continue to work through the summer and are large enough to capture long term warmth to prepare for the following winter season (inter-seasonal). Data were collected in real time. In the initial testing, the real time and diurnal benefits have been immediately realised. The results show that there are advantages with recharging the ground (soil battery); firstly this may increase seasonal performance of the heat pump if the lower soil temperature was maintained at 12°C; this also enables the heat pump to work better at an average coefficient of performance (COP) of 4.0, instead of the annual average of 2.65 predicted by the manufacture.

In this regard after one year ground charging using solar-air collector, the deep temperature was 11.3°C, and was far higher than expected because in 2010, a small amount of sunshine during the year, followed by days of low fog and cloud with periods of drizzle; however the solar-collector was seem to get quite a lot of sun

energy due to sunny days in February and March 2010. The usual springtime drop of ground temperature occur, as presented 7.12, the GWET drop, and when the sun came early enough, this prevent frosting to occur penetrate the ground.

## **CHAPTER 8** - GENERAL DISCUSSION

---

## 8. GENERAL DISCUSSION

Currently, almost half of the UK's carbon emissions come from the use of buildings, even though the application of insulation in new and existing houses has become widespread, energy use in domestic buildings for space and water heating accounts for more than 60% of all primary energy demand of a house. The recent proposals by the UK government which require new housing to become progressively more energy efficient, leading to net zero-carbon dioxide emissions from 2016 and the UK's 2008 Climate Change Act which requires an 80% reduction in CO<sub>2</sub> emissions by 2050 from 1990 level; both have stimulated research for more energy efficient technologies including building envelopes and building services. So there has never been a more important time to encourage the implementation of energy efficient strategies for heating system such as ground and air sources heat pump system.

The ground and air around a development site can be used as a source of heat for new buildings via a heat pump. Heat pumps are available as both heating only or reverse cycle heating/cooling systems and are classified according to the type of heat source and the heat distribution medium used. Typical systems use a refrigeration cycle with electricity as the energy input driving the process. They are generally more suitable for heating applications that use lower temperatures, such as underfloor heating. The efficiency of heat pumps is measured in terms of COP. In addition, the Pile-Water-Equilibrium Temperature (PWET) and Soil Charging Performance Factor (SCPF) were introduced and used to analyse

respectively as a keys indicators of the ground changing temperature and the charging performances of the solar roof/collectors.

The lower the temperature difference (seasonally) between the average source and sink temperature, the greater the efficiency of the system, the higher the COP and the lower the CO<sub>2</sub> emissions.

The European standard EN15450 states that the COP target range for a ground source heat pump installation should lie within the range of 3.5 to 4.5; when used for heating a building, a typical air-source heat pump has a COP of 2.0 to 3.0 at the beginning of the heating season and then decreases gradually as the ambient air becomes cooler, whereas a typical ground source heat pump is in the range of 3.5 –4.0, also at the beginning of the heating season and then decreases gradually as heat is drawn from the ground. For these reasons, in the middle of winter, when the COP drop, the heat pumps can generally only be considered as a ‘pre-heating’ method for producing higher temperature heat such as domestic hot water (as otherwise carbon emission efficiency would be unacceptably low) though technology advances or the application of the novel systems develop from this work may overcome this constraint.

In addition soil presents certain difficulties, due to the high cost of drilling to position coils in the ground compared to air source, although frost formation on the evaporator in winter also limits the use of air source.

In order to maintain high COPs for the heat pumps from the beginning to the end of the heating season; conventional boreholes are spaced at least 5-6m apart and

the depth depends on the ground and building efficiency characteristics, for illustration a detached two storey family house needing 10 kW of heating capacity might need three boreholes of 80 to 110m deep, so in total of 240 – 330m of borehole, from the results of this thesis, this is considerably reduced using a combination of solar-air or solar roof/collectors with the GSHP to a respective total of 96m and 210m for conventional boreholes and the energy piles. So a total of about 70% is reduce on the length of the initial boreholes, and this could be a very attractive option to promote use of the GSHP on low energy buildings to achieve high levels of the low energy homes standards such as the highest Level of Code for Sustainable Homes in the UK.

In Chapter 7 of this report, it has been demonstrated that GSHP system may be combined with solar-air collectors or solar roof/collectors to form a so called Geo-solar system heat pump system with greater efficiency, in this case, when the working conditions was right, the evaporator of the heat pump harvested a combination of geothermal power and heat from sun or warm air for space and domestic hot water heating. In theory, heat can be extracted from any source no matter how cold, but a warmer source allows higher COP. Instead of three boreholes of 110m length, two boreholes of 48m deep was used, therefore contributing towards lowering the drilling cost of the ground source heat pump system and in addition, adding solar-air panels, it assisted to reduce freezing effect around the boreholes.

It has also been observed that the ground exchanger experienced seasonal temperatures cycles mostly at shallow level of the ground said up to 3m deep, due to solar gain and transmissions losses to ambient air. These temperature cycles lag behind the temperature of the season in the far field undisturbed ground, due to the thermal inertia, so during winter, the ground heat exchanger harvested heat deposited by the sun during summer months, these effects was not significant above 8m deep in the ground. However in that level of the ground, heat around the boreholes and energy piles was heavily reliant on migration of heat from surrounding geology. From the literature, the reverse heat pump is not common; therefore unless heats surrounding the ground heat exchange are recharge annually by external heat from the solar-roof/collect, the efficiency of the GSHP or energy pile would considerably reduce after a period of 5 to 10 years heating cycle.

The conventional boreholes for residential GSHP are commonly filled with a betonies grout surrounding soil or rock to improve the heat transfer between the ground and working fluid, in the case of energy piles concrete around the ground heat exchanger loop also enhances the heat transfer from the soil to working fluid water/glycol mixture. One of the advantages of having concrete is that it could protect the ground water from contamination with glycol. This could be a very good option for existing buildings with heat pump systems already installed, which have low COP after years of heating cycle. And for new construction,

foundation piles should definitely be the way to go, if ground source heat pumps have to be considered.

As far as heat distributions are concern in the building, heat pumps including PV/hp-heat pump and Solar-air source heat pumps are especially well matched to underfloor heating and baseboard radiator systems which only require warm temperature (35 - 40°C) to work well. Using large surfaces such as floors, as opposed to radiators, as a heat distribution system allows the heat to be more uniformly distributed in the space to be heated, and also to permit to use lower water temperature; therefore reduce the lift temperature between the heat source and heat distribution system. However the material characteristic of the floor also has an effect on the heat distribution operation temperature; wood or carpet floors have lower thermal efficiency compare to that of masonry floors (tile or concrete).

### **8.1 Seasonal thermal storage**

The earth absorbs a large proportion of incident solar radiation, which keeps the ground/groundwater in the UK at a stable temperature of around 11-12 degrees C throughout the year. This is warmer than the mean winter air temperature. A variant of ground source heating systems is interseasonal heat transfer (IHT). Pipes are placed below tarmac to heat. This can be effective as a tarmac surface in direct sunshine will often be 15° C warmer than the air temperature at the same time. The heat is then transferred to thermal banks below the building for release when needed. This enables transfer of heat between day and night and

summer and winter. IHT may be effective in places where there are large areas of tarmac such as school playgrounds, or retail car parks or roads around the development area.

In the UK residential building, heating only heat pumps are commonly used; compared to reverse heat pump system, which allow heat from the building to be injected to the ground during summer to assist the ground heat recovery. If the heat is only extracted from the ground during winter with no generation during summer, in this case, the efficiency of the system will gradually decreased after let say 5 to 10years heating cycle. The efficiency of the GSHP can be improved by using seasonal thermal storage by injecting heat in the ground using solar-air or solar roof/collectors, during summer. In addition during winter if the heat requirement of the building is relatively low, this means building with high efficiency (The standards EN1283, required a low energy house to be about  $40\text{W}/\text{m}^2$  and an energy house to be use  $10\text{W}/\text{m}^2$ ); in this case the heat extracted from the ground would be sufficiently low, and the amount of heat needed from the solar collectors will also reduce, so small panels could be used to generate the heat for injection into the ground during summer.

In the case of existing heat pumps, the efficiency of existing small heat pump installations can be also improved a lot by adding cheap water filled with water/glycol mixture in collectors. These may be integrated into a wall or roof constructions simply by putting lots of PE pipes into the outer layer; almost free

at SCPF of 3 or 4 into the ground; or when the amount of heat extracted during winter is low; this well also works better when more houses install the GSHP system next to each others.

## **8.2 Environmental Impact**

The USA Environmental Protection Agency, EPA (1993) stated that GSHP systems were the most energy-efficient, environmentally clean and cost-effective space conditioning system available today. In addition, study by the International Energy Agency's Heat Pump Centre finds an 8% contribution potential from heat pumps towards global CO<sub>2</sub> emissions (EHPA, 2010). The European Heat Pump Association (EHPA) vision scenario estimates a 5% reduction potential in final energy demand by 2020. There is clearly untapped potential, but heat pumps need to be used more widely. DX-heat pumps and solar assisted heat pumps investigated in this work have the potential to be used in the residential sector in the UK and Europe; however additional institutional and financial support is necessary.

The efficiency of systems depends on the efficiency of the unit, the quality of installation and the building's energy demand. The higher the system's efficiency can be the lower CO<sub>2</sub> emissions from the heating system. This is also largely influenced by the emission value of the electricity mix / fuel used. Consequently, electrically-driven heat pumps such as DX-heat pumps and solar assisted heat pumps investigated in this work will profit from future improvements in efficiency and carbon footprint of the European power mix. Where the electricity is produced from renewable resources, PV/hp-heat pump

and Solar-air source heat pumps will offer significant emission reduction close to zero. Installed and new units benefit from lower final energy demand and lower Green House Gas (GHG) emissions.

The GHG emissions saving from a heat pump system and conventional boiler can be calculated base of the following formula developed by Honova et al [2]

$$GHG\ Savings = HL \left( \frac{FI}{AFUE \times 1000 \frac{kg}{ton}} - \frac{EI}{COP \times 3600 \frac{sec}{hr}} \right)$$

- HL = seasonal heat load  $\approx 70$  GJ/yr for a modern detached house in the UK
- FI = emissions intensity of fuel = 50 kg(CO<sub>2</sub>)/GJ for natural gas, 73 for heating oil
- AFUE = furnace efficiency  $\approx 95\%$  for a modern condensing boiler
- COP = heat pump coefficient of performance  $\approx 3.2$  seasonally adjusted for UK heat pump
- EI = emissions intensity of electricity  $\approx 200-800$  ton(CO<sub>2</sub>)/GWh, depending on region

For this work, the laboratory test was done for the PV/hp-heat pump, it was difficult to evaluate the CO<sub>2</sub> saving at this stage using the above formula. In addition the energy pile small scale test was also performed on a plot where there was no building on top; however it necessary to know the CO<sub>2</sub> reduction from novel system compared to conventional heating system. Therefore, further work will be needed to investigate, the GHG saving from those two novel systems. The field trial on the Solar-air source pump was under taken in real house, in Nottingham; The GSHP's assumption was that of the 14,600 kWh needed annually by the house, approximately 9,800 kWh were being drawn from the earth, by the heat pump. And the average COP of 3.7 was achieved.

The comparison of heat pump systems using air or ground as energy sources in residential buildings with a gas condensing boiler reveals a possible savings of between 20% and 50% in primary energy, 35% and 80% in final energy, and 49% to 67% in GHG emissions. Heat pumps use between 65% and 78% of renewable energy to meet their total final energy demand.

### **8.3 Economics analysis**

Ground source heat pumps are characterised by high capital costs and low operational costs compared to other conventional space and water heating systems. Their overall economic benefit of air and Ground source heat pumps depends primarily on the relative costs of electricity and fuels. In the UK, the average electricity cost for a standard domestic user is about 12.5p per kWh; if one considered using "green" energy which comes from variable green sources in the UK, and then there is a premium of about 20-30% on top. Based on this research, and the recent prices of electricity, air and ground-source heat pumps could have lower operational costs than any other conventional heating sources. However, natural gas is the only fuel with competitive operational costs, and only in a handful of countries where it is exceptionally cheap, or where electricity is exceptionally expensive [113]. In general, based on the COPs, a homeowner may save anywhere from 20% to 60% annually on utilities by switching from an ordinary system to an air or a ground-source systems. However, many family size installations are reported to use much more electricity, due to the facts that, at the beginning of the heating season the COPs of heat pumps systems are high then decrease gradually as the ambient air

becomes cooler or enough heat is drawn from the ground. These permitted the compressor to consume more electricity than their owners had expected from advertisements. These may partly due to bad design or installation, such in the case of GSHP, the ground heat exchange capacity may be too small, heating pipes in house floors are too thin and too few, or heated floors are covered with wooden panels or carpets. And the case of air source heat pumps it could be because of frost formation on the evaporator or external coils.

By using PV/hp and the combination of the GSHP with additional solar-air panel or solar roof/collectors, the COPs of the heat pumps system could remaining constant all through the heating season, therefore could keep low the electricity consumption of systems. Some electric companies offer special rates to customers who install a ground-source heat pump for heating their building. This is due to the fact that electrical plants have the largest loads during summer months and much of their capacity sits idle during winter months. This allows the electric company to use more of their facility during the winter months and sell more electricity. It also allows them to reduce peak usage during the summer (due to the increased efficiency of heat pumps), thereby avoiding costly construction of new power plants.

For air and ground source heat pump systems, the capital costs and system lifespan have received much less study, and also the return on investment are highly variable. The lifespan of the system is longer than conventional heating

systems. Good data on system lifespan is not yet available because the technology is too recent, but many early heat pumps systems are still operational today after 25–30 years with routine maintenance.

To evaluate the payback period of the novel heat pump system for new built; the Net Present Value (NPV) method could be used. This method could help to compare between the investments made at present. In addition in the UK to generate heat from renewable source as sun could be benefit in the future, the Renewable Heat Incentive (RHI) it has a tariff lifetime of 23 years, and considering interest rates over the same period of time (see appendix **Table A1** - Tariff level). After the results of the novel technologies investigated in this work would be validated the present value of money could be calculated using the following equation:

The net present value analysis was made according to the following equation:

$$NPV = -R_0 + \frac{\sum_{j=1}^{23} R_t}{(1+i)^t}$$

Where:

$t$  - the time of the cash flow

$i$  - the discount rate (the rate of return that could be earned on an investment in the financial markets with similar risk.)

$R_t$  - the net cash flow (the amount of cash, inflow minus outflow) at time  $t$ .

$R_0$  – Initial investment

## **CHAPTER 9 - CONCLUSION AND FURTHER WORKS**

---

## **9 GENERAL CONCLUSIONS**

In this thesis, to reduce the drilling cost of the ground source heat pumps and to maintain high COPs of the heat pumps (air or ground source) systems from beginning to the end of the heating season; four aspects of investigations have been independently carried out.

Two investigations (Chapter 4 and Chapter 5) were focus on the possibilities to reduce the frosting effects on external coil (evaporator) of the ASHP and to enhance the COP of the air source heat pumps. The two systems were investigated under the conditions to provide space and water heating for low carbon homes in the UK and Europe. A series of indoor tests were performed at the laboratory of the school of the Built Environment, University of Nottingham. Experimental results were compared with the theoretical model predictions and despite the fact that they showed some disagreement in some results, the novel evaporators have proven to have the capabilities to reduce the frosting effects on the COP of ASHP. In addition they could perform well at high and constant COP and at different weather conditions in the UK.

Two others investigations (Chapter 6 and Chapter 7) were focused on the concepts to combine of solar collectors with GSHP or Energy piles with shorter ground heat exchangers to charge the ground and to reduce freezing effects around the boreholes after heating cycle.

The heat injection in the ground has the advantage to reduce freezing effect around the boreholes. It has also been illustrated that the majority of heat extracted from the ground was from the heat refill surrounding of energy piles and the deeper ground. Such a heat flow process could be problematic for long term operation of the ground source heat pump in the location of modern high density housing state due to lack of enough surrounding ground, which open directly to the sun to collect enough sun heat during summer for ground heat replenishment to prepare next heating season. It is considered that renewable heat to charge the ground could provide a solution to this problem and additionally provide a sustainable and constant COP for long term.

## **9.1 FURTHER WORKS**

In this thesis, some experimental results were compared with the theoretical model predictions and they showed distinct differences between the ideal and real situations. These provides an opportunity for further investigations to improve and optimise the performance of different methods and materials for direct, indirect and hybrid air or ground source heat pumps. In addition at the end of each chapter (Chapter 4, Chapter 5, Chapter 6, and Chapter 7) a more comprehensive further works related to each aspects of this work have been detailed.

## References

Ashrae. (2003). *Geothermal Energy*. Nayak: Ashrae Application Handbook Bopshetty.

Austin, & W.A.I. (1995). *Development of an in situ system for measuring ground thermal properties*. Oklahoma State University: M Sc. edu Oklahom.

BADC. (2011, April 10). *The British Atmospheric Data Centre*. Retrieved April 14, 2011, from The British Atmospheric Data Centre (BADC) Web site: <http://badc.nerc.ac.uk/home/>

Bellows, A. (2007, 12 08). *The Ethyl-Poisoned Earth*. Retrieved April 10, 2011, from A damn interesting Web site: <http://www.damninteresting.com/the-ethyl-poisoned-earth>

Boardman, B. (2008). *Home Truths: A Low-carbon Strategy to reduce UK housing emissions by 80% by 2020*, University of Oxford's Environmental Change Institute, Co-operative Bank and Friends of the Earth, November 2007, quoted in Department for Communities and Local Government. London: Existing Housing and Climate Change.

BP. (2007, January 7). *What is a Carbon Footprint?* Retrieved December 20, 2009, from BP Web site: [http://www.bp.com/liveassets/bp\\_internet/globalbp/STAGING/global\\_assets/downloads/A/ABP\\_ADV\\_what\\_on\\_earth\\_is\\_a\\_carbon\\_footprint.pdf](http://www.bp.com/liveassets/bp_internet/globalbp/STAGING/global_assets/downloads/A/ABP_ADV_what_on_earth_is_a_carbon_footprint.pdf)

Brandl, H. (2006). Energy foundation and other thermo-active ground structures. *Geotechnique* , 81-122.

Brandl, H. (2006). Energy foundation and other thermo-active ground structures. *Geotechnique* , 56 (2), 81-122.

BRE. (2005). *GIR72: Heat pumps in the UK- a monitoring report*. London: Energy Saving Trust.

Bureau of Energy Efficiency. (2006). *Energy Conservation Building Code*. New Delhi: Bureau of Energy Efficiency.

Carbon Trust . (2007). *Carbon Footprint Measurement Methodology*. London: The Carbon Trust.

Carbon Trust. (2006). *Report Number CTC616: Carbon footprints in the supply chain: the next step for business*. London: the Carbon Trust.

Chaturvedi, S., Chen, D., & Kheireddne, A. (1996). Thermal performance of a variable capacity direct expansion solar-assisted heat pump. *PII* , 196-89.

Chaturvedi, S., Chiang, Y., & Roberts, A. (1982). Analysis of two-phase flow solar collectors with application to heat pumps. *Journal of Solar Energy Engineering* , 104, 358-365.

Chiasson, C. Y. (2003). Assessment of the viability of hybrid geothermal heat pump systems with solar thermal collectors. *ASHRAE Transactions* , 109 (2), 487-500.

Chow, T., He, W., & Ji, J. (2006). Hybrid photovoltaic-thermosyphon water heating system for residential application. *Solar Energy* , 80 (3), 298–306.

Chow, T., He, W., Ji, J., & Chan, A. (2007). Performance evaluation of photovoltaic–thermosyphon system for subtropical climate application. *Solar Energy* , 81 (1), 123–130.

Christian, C., Gilles, N., & Jean, L. (2009). Thermal behavior of a copolymer PV/Th solar system in low flow rate conditions. *Solar Energy* , 83 (8), 1123–1138.

Communities and Local Government. (2006). *Code for Sustainable Homes: A Step-change in Sustainable Home Building Practice*. London: Communities and Local Government.

Communities and Local Government. (2008). *Code for Sustainable Homes: Technical guide*. London: RIBA Publishing .

Communities and Local Government. (2008). *Report: ‘ Code for Sustainable Homes: A Step-change in sustainable home building practice’*. London:

CUBE, H. L., & Fritz, S. (1981). *Heat Pump Technology*. Germany: Butterworth & CO Ltd.

DCLG. (2007). *Building a Greener Future: Policy Statement*. London: Department for Communities and Local Government.

DCLG. (2008). *HC 432-1: Existing Housing and Climate Change*. London: Department for Communities and Local Government (DCLG).

DTI. (2007). *Energy Consumption in the UK*. UK: Association for the Conservation of Energy.

- DTI. (2007). *Energy White Paper – Our Energy Future – Creating a Low Carbon Economy*. London: BIS.
- Dubey, S., & Tiwari, G. (2006). Thermal modeling of a combined system of photovoltaic thermal (PV/T) solar water heater. *Solar Energy*, 82 (7), 602–612.
- Duffi, J., & Beckman, W. (2006). *Solar Engineering of Thermal Process*. (Third, Ed.) New York: Wiley, Inc.
- Edinburg Centre for Carbon Management. (2008). *Report: What is a Carbon Footprint?* Edinburg: Forest Industries.
- EHPA. (2010). *Heat pumps: a gem in renewable*. UK: European Heat Pump Association (EHPA).
- Enerfina. (2008, January 18). *IVT C6 kW Ground Horizontal Heat Pump w/ 185 L Cylinder*. Retrieved April 12, 2011, from Enerfina Web site:  
<http://www.enerfina.com/uk/products/heat-pumps/ground-source-heat-pumps-horizontal/ivt-ground-source-heat-pumps-horizontal/ivt-c6kw/126/30>
- Energetics . (2007). *The Reality of Carbon Neutrality*. London: Energetics Pty Ltd.
- Energy Saving Trust. (2010, June 7). *Home Improvements and Draught proofing*. Retrieved March 23, 2011, from The Energy Saving Trust Web site:  
<http://www.energysavingtrust.org.uk/Home-improvements-and-products/Home-insulation-glazing/Draught-proofing>
- Energy Use in Office. (1998). *Energy Consumption Guide 19*. UK: Energy Use in Office.
- USA: Environmental Protection Agency (EPA).
- EPA. (1993). *Space Conditioning: The Next Frontier - Report 430-R-93-004*. US: Environmental Protection Agency (EPA).
- EPBD. (2003). *DIRECTIVE 2002/91/EC of EUROPEAN PARLIAMENT AND OF THE COUNCIL OF 16 December 2002 on the energy performance of buildings, EPBD Energy Performance of Building Directive*. Bruxelles: Official Journal of the European Communities.
- Eugste, M., & Rybach, L. (2000). Sustainable production from borehole heat exchanger systems. *Proceeding World Geothermal Congress*, 825-830.

- Government memorandum. (2008). *Government memorandum, EV 277-94*. London: Publications parliament.
- Green Building Advisor. (2010, January 1). *Heat Distribution: Forced Air and Hydronic: Ducts, Pipes, and Tubes Should Be Short and Leak-free*. Retrieved April 12, 2011, from Green Building Advisor Web site : <http://www.greenbuildingadvisor.com/green-basics/3b-distribution-systems-choices-incomplete>
- Grubb, & Ellis. (2007). *Meeting the Carbon Challenge: The Role of Commercial Real Estate Owners*. Chicago: Users & Managers.
- Guoying, X., Xiaosong, Z., & Shiming, D. (2006). A simulation study on the operating performance of a solar-air source heat pump water heater. *Applied Thermal Engineering* , 26, 1257–65.
- Hanova, J., & Dowlatabadi, H. (2007). *Strategic GHG reduction through the use of ground source heat pump technology*. UK: Environmental Research Letters (UK: IOP Publishing).
- Hawlader, M., Chou, S., & Ullah, M. (2001). The performance of a solar assisted heat pump water heating system. *Applied Thermal Engineering* , 21, 1049-1065.
- Hawlader, M., Chou, S., Jahangeer, K., Rahman, S., & Eugene Lau, K. (2003). Solar assisted heat-pump dryer and water heater. *Applied Energy* , 74, 185–93.
- Hegazy, A. (2000). Comparative study of the performances of four photovoltaic/thermal solar air collectors. *Energy Conversion and Management* , 41 (8), 861–881.
- Home of Carbon Management. (2011, January 8). *What is a carbon footprint?* Retrieved April 04, 2011, from Carbon Footprint Ltd Web site: <http://www.carbonfootprint.com/carbonfootprint.html>
- IPCC. (2007). *Revised 2007 IPCC Guidelines for National Greenhouse Gas Inventories: Reference Manual*. Intergovernmental Panel on Climate Change. Cambridge: Cambridge University Press.
- Ito, S., & Miura, N. (2000). Studies of a heat pump using water and air heat sources in parallel. *Heat Transfer Asian Research* , 29, 473–90.
- Ji, J., He, H., Chow, T., Pei, G., He, W, et al. (2009). Distributed dynamic modeling and experimental study of PV evaporator in a PV/T solar-assisted heat pump. *International Journal of Heat and Mass Transfer* , 52 (5-6), 1365–1373.

- Kjellson, E. (2004). *Report TVBH 3047: Solar Heating in Dwellings With Analysis of Combined Solar Collectors and Ground Source Heat Pump*. Sweden: Dept. of Buildings Physics, Lund University.
- Kuang, Y., Sumathy, K., & Wang, R. (2003). Study on a direct-expansion solar-assisted heat pump water heating system. *International Journal of Energy Research* , 27, 531–48.
- Li, Y., Wang, R., Wu, J., & Xu, Y. (2007). Experimental performance analysis on a direct expansion solar-assisted heat pump water heater. *Applied Thermal Engineering* , 38, 1477–84.
- Markowitz, G., Rosner, D., Deceit, & Denial. (2002). *The Deadly Politics of Industrial Pollution*. Berkeley, California: University of California Press.
- Mempou, B., Riffat, S., & Nicholson-Cole, D. (2010). Ground-Source Heat Pump Performance Boosted with the Earth Charging by Means of Solar-Air Thermal Collectors. *SET2010 - 9th International Conference on Sustainable Energy Technologies* (p. 24). Shanghai: WSSET.
- Messenger Roger, A., & Ventre, J. (2004). *Photovoltaic system engineering*. Florida: CRC Press.
- Miliband, E. (2008). *United Kingdom Climate Change Act 2008*. UK: Change Committee on Climate .
- Muharomad, Y., Baharudin, Y., Sopian, K., & Muharomad, N. (2007). Performance studies on a finned double-pass photovoltaic-thermal (PV/T) solar collector. *Desalination* , 209 (3), 43–49.
- Niccolo, A., Giancarlo, C., & Francesco, V. (2008). Design, development and performance monitoring of a photovoltaic-thermal (PVT) air collector. *Renewable Energy* , 33 (5), 914–927.
- Nicholls, R. (2006). *The Green Building Bible* (Vol. 2). (3. edition, Ed.) UK: Green Building Press.
- Nicholson-Cole, D., & Wood. (2009, July 22). *Charging the Earth – The Solar Way*. Retrieved August 12, 2009, from Charging the Earth Web site: <http://chargingtheearth.blogspot.com/2009/11/meeting-chris-wood-diurnal.html>
- Ontario Ministry of Energy. (2010, January 1). *Heating and Cooling Your Home - Chapter 4*. Retrieved July 8, 2010, from QUEEN'S PRINTER FOR ONTARIO Web site: [http://www.mei.gov.on.ca/en/energy/conservation/?page=heating-and-cooling-your-home\\_chapter-4](http://www.mei.gov.on.ca/en/energy/conservation/?page=heating-and-cooling-your-home_chapter-4)

- Patel, J. (2006). *Green sky thinking*. London: Environment Business.
- Perez-Lombard, L. O. (2007). A review on buildings energy consumption information. *Energy and Buildings* , 40 (3), 394-398.
- POST . (2006). *POST note 268: Carbon footprint of electricity generation*. London: Parliamentary Office of Science and Technology.
- Roger Bullivant, L. (2008, June 24). Director. (R. B. Ltd, Interviewer)
- Rybach, W. (2000). *SUSTAINABLE PRODUCTION FROM BOREHOLE HEAT EXCHANGER SYSTEMS*. Tohoku, Japan: Geophysics. Kyushu.
- Sumner, J. A. (1976). *Domestic heat pumps*. London: Prism Press.
- Technology Pico. (2001). Improving the accuracy of temperature measurements. *Sensor Review, The international journal of sensing for industry* , 3.
- Tonui, J., & Tripanagnostopoulos, Y. (2007). Improved PV/T solar collectors with heat extraction by forced or natural air circulation. *Renewable Energy* , 32 (4), 861–881.
- Trillat-Berdal, V., & Souyri, B. (2007). Coupling of geothermal heat pumps with thermal solar collectors. *Applied Thermal Engineering* , 27 (10), 1750-1755.
- Trilliant-Berdal, V., Souyri, B., & Fraise, G. (2006). Experimental study of ground-coupled heat pump combined with thermal solar collectors. *Energy and Buildings* , 38, 1477–84.
- Tripanagnostopoulos, Y. (2007). Aspects and improvements of hybrid photovoltaic/thermal solar energy systems. *Solar Energy* , 81 (9), 1117–1131.
- Trust, E. (2004). *Domestic Ground Source Heat Pumps: Design and Installation of closed-loop systems*. London: Carbon Neutral Company.
- US standard categorization. (2009). *DIN8900 part1 Heat Pumps*. UK: Electricity Council Research Centre.
- Wachter, B. (2009). *Nine Systems to heat a home*. Portugal: Leonardo Energy.
- WATMUFFJ, H., WITT, H. T., & JOUBERTP, N. (1985). Developing turbulent boundary layers with in rotating channel flow. *J. Fluid Mech* , 130, 377-395.
- Wiedmann, T., & Minx, J. (2007). *Research Report : A Definition of 'Carbon Footprint'*. London: ISAUK Research & Consulting.

Wood, C. J. (2009). *PhD. Thesis : Investigations of Novel Ground Source Heat Pumps*. Nottingham. UK: The School of the Built Environment, The University of Nottingham, University Park.

Wood, J., Liu, H., & Riffat, S. (2008). *Heat pump performance and ground temperature of a piled foundation heat exchanger system for a residential building*. Nottingham: PhD Thesis.

Wood, J., Liu, H., & Riffat, S. (2009). The use of energy piles in a residential building and the effect upon the ground temperature and heat pump efficiency. *Renewable Energy* , 50-62.

World Resources Institute. (2005). *Safe Climate*. Washington: World Resources Institute (WRI).

WYATT, T. (2004, October 1). *Renewable heat – the era of ground-source heat pumps*. Retrieved December 12, 2010, from Modern Building Services Web site: [http://www.modbs.co.uk/news/fullstory.php/aid/448/Renewable\\_heat\\_\\_96\\_the\\_era\\_of\\_ground-source\\_heat\\_pumps.html](http://www.modbs.co.uk/news/fullstory.php/aid/448/Renewable_heat__96_the_era_of_ground-source_heat_pumps.html)

Yumus, A., Cengel, & Michael, A. (1998). *Thermodynamics: An Engineering Approach*. (3rd, Ed.) Boston: WCB/McGraw-Hill.

Zondag, H., DW, d. V., van Helden, W., van Zolingen, R., & van Steenhoven, A. (2003). The yield of different combined PV-thermal collector designs. *Solar Energy* , 74 (3), 253–269.

## Appendix

### Chapter 5 - EES summary equation

#### Vacuum glass tube (outer)

$$0 = \beta_{og}G * (A_{og}/2) + q_{r,ig-og} * A_{ig} + q_{d,ig-og} * A_{ig} - q_{r,og-sky} * (A_{og}/2) - q_{v,og-a} * A_{og}$$

$$A_{og} = 3.14 * D_{og} * L$$

$$A_{ig} = 3.14 * D_{ig} * L$$

$$q_{r,ig-og} = \frac{\varepsilon_{ig}\sigma}{1 + \frac{\varepsilon_{ig}D_{ig}}{\varepsilon_{og}D_{og}}(1 - \varepsilon_{ig})} (T_{ig}^4 - T_{og}^4)$$

$$q_{d,ig-og} = \alpha_{d,ig-og} (T_{ig} - T_{og})$$

$$q_{r,og-sky} = \varepsilon_{og}\sigma (T_{og}^4 - T_{sky}^4)$$

$$q_{v,og-a} = \alpha_{v,og-a} (T_{og} - T_a)$$

#### Vacuum glass tube (inter)

$$0 = (\beta\tau)_{ig}G * (A_{ig}/2) + q_{r,p-ig} * A_p + q_{d,p-ig} * A_p + q_{r,al-ig} * A_{al} + q_{d,al-ig} * A_{al} - q_{r,ig-og} * A_{ig} - q_{d,ig-og} * A_{ig}$$

$$(\beta\tau)_{ig} = 1.01 * \beta_{ig}\tau_{og}$$

$$q_{r,p-ig} = \varepsilon_p\sigma (T_p^4 - T_{ig}^4)$$

$$q_{d,p-ig} = \alpha_{d,p-ig} (T_p - T_{ig})$$

$$\alpha_{d,p-ig} = \alpha_{d,al-ig} = \frac{\lambda_{gap}}{\delta_{gap}} = \frac{\lambda_{gap}}{\frac{\pi D_{ig}}{8}}$$

$$q_{r,al-ig} = \varepsilon_{al}\sigma (T_{al}^4 - T_{ig}^4)$$

$$q_{d,al-ig} = \alpha_{d,al-ig} (T_{al} - T_{ig})$$

#### PV base plate

$$0 = G(\beta\tau)_c f_c + G(\beta\tau)_p (1 - f_c) - E - q_{d,p-al} - q_{r,p-ig} - q_{d,p-ig}$$

$$(\beta\tau)_c = 1.01 * \beta_c \tau_{og} \tau_{ig}$$

$$(\beta\tau)_p = 1.01 * \beta_p \tau_{og} \tau_{ig}$$

#### Electricity generation:

$$E = \eta_c f_c (\beta\tau)_c G \quad \eta_c = \eta_{rc} [1 - \beta (T_p - T_{rc})]$$

### Heat flux from PV base plate to copper sheet:

$$q_{d,p-al} = \frac{(T_p - T_{al})}{\frac{\delta_p}{2\lambda_p} + \frac{\delta_{al}}{2\lambda_{al}}}$$

$$\text{Effective absorptance of base plate: } (\beta\tau)_p = \frac{\tau_a \tau_\rho \beta_p}{1 - (1 - \beta_p) R_g}$$

$$\text{Effective absorptance of solar cell: } (\beta\tau)_c = \frac{\tau_a \tau_\rho \beta_c}{1 - (1 - \beta_c) R_g}$$

### Aluminium sheet

$$0 = A_p \cdot q_{d,p-al} - A_{al-co} \cdot q_{d,al-co} - A_{al} \cdot q_{r,al-ig} - A_{al} \cdot q_{d,al-ig}$$

$$A_{al-co} = 2 * \left(\frac{3}{4} * \pi d_{o,co} \cdot L_p\right)$$

$$q_{d,al-co} = \frac{(T_{al} - T_{co})}{\frac{\delta_{al}}{2\lambda_{al}} + \frac{\delta_{co}}{2\lambda_{co}}}$$

### Copper tube

$$0 = A_{al-co} \cdot q_{d,al-co} - A_{i,co} \cdot q_{v,co-r}$$

$$q_{v,co-r} = \frac{(T_{co} - T_r)}{\frac{1}{\alpha_r} + \frac{\delta_{co}}{2\lambda_{co}}}$$

$$A_{i,co} = \pi d_{i,co} L_{co}$$

$$\text{For single-phase flow: } \alpha_r = 0.023 \frac{Re^{0.8} Pr^a \lambda_r}{d_i} \quad (a=0.3 \text{ for liquid, } a=0.4 \text{ for vapour})$$

$$\text{For two-phase flow: } \alpha_l = \alpha_l \left[ (1-x)^{0.8} + \frac{3.8x^{0.76}(1-x)^{0.04}}{Pr^{0.38}} \right]$$

$$\text{Where } x \text{ is the average dryness fraction of the refrigerant? } Pr = \frac{\mu_r C_{pr}}{\lambda_r}, Re =$$

$$\frac{\rho_r u_r d_{i,co}}{\mu_r}$$

### Refrigerant

$$0 = 12 * A_{i,co} \cdot q_{v,co-r} - m_r \cdot \Delta h_r$$

**Chapter 8** – data used for the economic analysis of the solar roof/collector energy pile heat pump

**Table A1** - Tariff level tables: Source:

<http://www.rhincenive.co.uk/eligible/levels/>

Technology	Scale	Tariffs (pence/kWh)	Tariff lifetime (years)
<b>Small installations</b>			
Solid biomass	Up to 45kW	9	15
Biodiesel (restricted use)	Up to 45kW	6.5	15
Biogas on-site combustion	Up to 45kW	5.5	10
Ground source heat pumps	Up to 45kW	7	23
Air source heat pumps	Up to 45kW	7.5	18
Solar thermal	Up to 20kW	18	20
<b>Medium installations</b>			
Solid biomass	45kW-500kW	6.5	15
Biogas on-site combustion	45kW-200kW	5.5	10
Ground source heat pumps	45kW-350kW	5.5	20
Air source heat pumps	45kW-350kW	2	20
Solar thermal	20kW-100kW	17	20
<b>Large installations</b>			
Solid biomass	500kW and above	1.6-2.5	15
Ground source heat pumps	350kW and above	1.5	20
Biomethane injection	All scales	4	15

### Fuel price assumptions

Fuel	Gas	Oil	LPG	Coal	Electricity (heating Economy 7)	Electricity (standard rate)
<b>Average price (pence/kWh)</b>	3.67	4.42	6.15	3.53	7.41	12.50
<b>Carbon dioxide factor (kgCO<sub>2</sub>/kWh)</b>	0.185	0.246	0.214	0.296	0.539	0.539

Source : <http://www.energysavingtrust.org.uk/Energy-saving-assumptions>